GEOLOGY AND GEOCHEMISTRY OF MOLYBDENITE SHOWINGS OF THE ACKLEY CITY BATHOLITH FORTUNE; BAY, NEWFOUNDLAND

JOSEPH BRUCE WHALEN

GEOLOGY AND GEOCHEMISTRY OF MOLYBDENITE SHOWINGS OF THE ACKLEY CITY BATHOLITH FORTUNE BAY, NEWFOUNDLAND

by

© Joseph Bruce Whalen, B.Sc. (Hon.)

A Thesis

submitted in partial fulfillment of the

requirements for the degree of

MASTER OF SCIENCE

Department of Geology
Memorial University of Newfoundland

April, 1976

St. John's Newfoundland

ABSTRACT

The Devonian (345±10 my) Ackley City batholith is an oval, approximately 5,400 km^2 granitoid which intrudes Ordovician and Precambrian rocks of the Gander and Avalon zones, respectively, in southeast Newfoundland. It is a composite intrusion consisting of K-feldspar megacrystic granite in the north, east and west, intruded in the southeast by genetically related, more differentiated, alaskitic granite. Spatially related to the southeast contact of the latter are younger, fine grained and pegmatitic intrusive phases, within which are six separate Mo showings. Contacts of the batholith are sharp and characterized by low grade contact metamorphism.

The granitoid phases are composed essentially of quartz, perthite, plagioclase (andesine to albite) and minor biotite, magnetite, sphene, zircon, fluorite, and tourmaline. The pegmatite is composed of large quartz crystals (up to 50 cm diameter) and orthoclase. Myrmekitic texture is common in the megacrystic granite while granophyric texture is rare in the alaskitic granite but common in the aplitic and pegmatitic phases.

The Mo host intrusives are all extreme differentiates and consequently show little variation in major elements. However, fractionation trends of trace elements and elemental ratios indicate they are more highly

differentiated than the alaskitic granite. The latter shows a regional variation in geochemistry, indicating that its degree of differentiation increases gradationally toward the intrusive contact.

The alaskitic and fine grained intrusive phases crystallized between .5 and 1 Kb P_{H_2O} and resemble a hypersolvus granite. The fine grained and pegmatite phases are explicable as erosional remnants of a once extensive roof zone complex possibly formed, by in situ differentiation resulting in concentration of volatile and Mo rich, highly fractionated magma in the roof of the alaskitic granite.

The different showings exhibit variation in lithology of host rocks, mode of mineralization and associated trace metals, although Mo is the only economically important element. They represent a gradation between magmatic (pegmatite) and hydrothermal (porphyry affinity) deposits, resulting essentially from retention and release of volatiles, respectively. The roof zone localization of the granitoid mineralization has important ramifications for exploration on a local and regional scale. The porphyry affinities of some showings indicates that models of absence of porphyry deposits in pre-Mesozoic-Cenozoic orogenic belts due to erosional level may not be valid.

TABLE OF CONTENTS

Page

ABSTRACT i

LIST OF FIGURES vii

LIST OF TABLES x

LIST OF PLATES xii

CHAPTER 1

INTRODUCTION

1.1 General 1

1.2 Previous Work 3

1.2.1 Fortune Bay Region 3

1.2.2 History of Exploration 4

1.3 Present Study 6

1.4 Acknowledgements 7

CHAPTER 2

MOLYBDENUM IN NATURE

2.1 General Geochemistry and Distribution 9

2.2 Behavior of Molybdenum During Magmatic-Hydrothermal Processes 12

2.3 Classification of Molybdenum Deposits 16

2.4 Distribution and Origin of Molybdenum Deposits ... 22

CHAPTER 3

GENERAL GEOLOGY

3.1 General Statement 30

3.2 Long Harbour Series 34

Page

3.2.1 Belle Bay Formation 34

3.2.2 Andersons Cove Formation 34

3.2.3 Mooring Cove Formation 35

3.2.4 Rencontre Formation 36

3.3 Young's Cove Group 36

3.4 Simmons Brook Batholith 37

3.5 Garrison Hills Gneiss 37

3.6 Cinq Isles Formation 37

3.7 Pools Cove Formation 38

3.8 Mafic Intrusions 38

3.9 Great Bay de L'Eau Formation 38

3.10 Belleoram Stock 39

3.11 Dyke Rocks 39

CHAPTER 4

THE ACKLEY CITY BATHOLITH

4.1 Introduction 41

4.2 Structure 42

4.3 Contact Relations and Metamorphic Effects 49

4.4 Geology, Lithology, and Petrology 51

4.5 Geochemistry 59

4.6 The Relationship of the Ackley City Batholith to some other Eastern Newfoundland Granites 68

4.7 Summary 75

Page

CHAPTER 5

THE FORTUNE BAY MOLYBDENITE SHOWINGS

5.1 General 77

5.2 Geology, Lithology and Petrology 79

5.2.1 Introduction 79

5.2.2 Motu Showing 81

5.2.3 Ackley City Showing 87

5.2.4 Dunphey Brook-Crow's Cliff Showing 97

5.2.5 Wylie Hill Showing 106

5.2.6 Frank's Pond Showing 116

5.2.7 Belle Island Showing 118

5.3 Geochemistry 123

5.3.1 Introduction 123

5.3.2 Variation Diagrams 124

5.3.3 Variation Between Showings 132

5.3.4 Variation in the Alaskitic Granite Phase .. 140

5.3.5 Variation Within the Wylie Hill Showing ... 144

5.3.6 Correlation Matrices 147

5.3.7 Economic Geochemistry 152

5.3.8 Geochemistry of Muscovite Alteration 155

5.4 Petrogenesis 158

5.4.1 Introduction 158

5.4.2 Origin of Associated Intrusives 158

5.4.3 Genesis of the Mineralization 168

Page

CHAPTER 6

SUMMARY AND POSSIBLE EXPLORATION APPLICATIONS

6.1 Summary 174

6.2 Possible Exploration Application 179

REFERENCES 181

APPENDIX A SAMPLING AND ANALYTICAL METHODS 196

1.1 Sample Collection and Preparation 197

1.2 Analytical Procedures 197

1.2.1 Major Element Analysis 197

1.2.2 Trace Element Analysis 199

1.2.3 Loss on Ignition 204

1.2.4 Other Analytical Procedures 204

1.2.5 Estimation of Modes 208

1.3 Statistical Procedures and Methods of Data Presentation 208

APPENDIX B MODAL ANALYSES 211

APPENDIX C PLOTS OF ANALYSES OF DIAMOND DRILL CORE, WYLIE HILL SHOWING 220

APPENDIX D GEOCHEMICAL DATA 233

Page

LIST OF FIGURES

Fig. 1	Location of the Ackley City Batholith	2
Fig. 2	Plot of Re (ppm) content of molybdenite versus Mo (wt%) for Mo deposits of different tectonic setting	24
Fig. 3	Plate tectonic model of molybdenite accummulations	29
Fig. 4	Geology of the Belleoram map area	32
Fig. 5	Equal area plot of joints for the alaskitic granite	44
Fig. 6	Strain ellipsoid for the Ackley City batholith	45
Fig. 7	Aeromagnetic map of the Ackley City batholith	47
Fig. 8	Gravity map of the Ackley City batholith ...	48
Fig. 9	Aeromagnetic, gravity and thickness profiles of the Ackley City batholith	50
Fig. 10	Distribution of different intrusive phases of the Ackley City batholith	54
Fig. 11	Classification of the Ackley City batholith on the basis of Streckeisen's (1967) normative classification	60
Fig. 12a	Plot of major elements versus differentiation index for different phases of the Ackley City batholith	63
Fig. 12b	Plot of trace elements versus differentiation index for phases of the Ackley City batholith	65
Fig. 13	Plot of K (wt.%) versus Rb (ppm) for different phases of the Ackley City batholith	67

Page

Fig. 14 Plot of Rb (ppm) versus Sr (ppm) for different phases of the Ackley City batholith 69

Fig. 15 Plot of Wright's (1969) alkalinity index for different phases of the Ackley City batholith 70

Fig. 16 Location of some southeast Newfoundland granitoids 72

Fig. 17 Plot of differentiation index versus Fe_2O_3, SiO_2 and CaO for different southeast Newfoundland granitoids 73

Fig. 18 Geology of the Ackley granite near some of the showings 78

Fig. 19 Modal classification of Ackley plutonic rocks 80

Fig. 20 X-ray diffraction pattern for molybdenite ($2H_1$) from Wylie Hill 82

Fig. 21 Structural states for pegmatite alkali feldspars 83

Fig. 22 Geology of the Motu Showing 84

Fig. 23 Geology of the Ackley City Showing 89

Fig. 24 Geology of the Dunphey Brook-Crow's Cliff Showing 98

Fig. 25 Geology of the Wylie Hill Showing 107

Fig. 26 Geology of the Belle Island Showing 120

Fig. 27a Plot of differentiation index versus Sr, Cu, Ti (ppm) and Fe_2O_3 (total), CaO and MgO (wt.%) for granitoid rocks of Wylie Hill 130

Fig. 27b Plot of differentiation index versus Rb, Pb, Zn, and Ba (ppm) for granitoid rocks of Wylie Hill showing 131

Page

Fig. 28a Plot of Zn, Pb, Ti, Zr, Y and Ba (ppm) versus normative quartz for average intrusive unit compositions of the showings 134

Fig. 28b Plot of K/Rb, Ba/Rb, Rb/Sr, Ca/Sr, Ba/Sr, and Rb (ppm) versus normative quartz for average intrusive unit compositions of the showings 135

Fig. 29 AFM diagram for the different molybdenite showings 139

Fig. 30 Contoured differentiation index data for the alaskitic granite intrusive phase 141

Fig. 31 Contoured Ba/Rb X 10 data for the alaskitic granite intrusive phase 142

Fig. 32 Contoured Rb/Sr data for the alaskitic granite intrusive phase 143

Fig. 33a Plot of major element and trace element data for diamond drill hole NLX-69-11 at Wylie Hill showing versus depth and rock type 145

Fig. 33b Plot of trace element data for diamond drill hole NLX-69-11 at Wylie Hill showing versus depth and rock type 146

Fig. 34 Qtz-Ab-Or plot of average intrusive unit compositions of the showings 160

Fig. 35 Ab-Or-An plot of average intrusive unit compositions of the showings 161

Fig. 36 Diagrammatic section across the Tregonning-Godolphin granite 169

Fig. 37 Comparison of modes by XRD and point counting methods with norms 209

Fig. 38 Format of computer cards for trace and major element data 210

Page

LIST OF TABLES

Table 1 Average values for molybdenum of common rocks 10

Table 2 Classification of molybdenum deposits 17

Table 3 Stratigraphic succession in Belleoram map-area 31

Table 4 Comparison of the chemistry of Belle Bay Formation rhyolite near the Ackley City batholith with average regional rhyolite composition 52

Table 5 Composition of different intrusive phases of the Ackley batholith 61

Table 6 Composition of different intrusive phases at the Motu showing 125

Table 7 Composition of different intrusive phases at the Ackley City showing 126

Table 8 Composition of different intrusive phases at the Crow's Cliff-Dunphey Brook showing .. 127

Table 9 Composition of different intrusive phases at the Wylie Hill showing 128

Table 10 Composition of different intrusive phases at the Belle Island and Frank's Pond showing 129

Table 11 Correlation matrix for data of all samples (206) 148

Table 12 Correlation matrix for the alaskitic granite near the showings (40) 149

Table 13 Correlation matrix for data on samples (80) from the Mo showings 150

Table 14 Correlation matrix for diamond drill core samples (86) from the Wylie Hill showing ... 151

Page

Table 15 Ackley City showing, increasing degree of muscovite alteration of medium grained granite 156

Table 16 Some characteristics of the mineralogy, chemistry, texture, and rock associations of hypersolvus and subsolvus granite 163

Table 17 Classification of Ackley molybdenite showings 171

Table 18 Precision of atomic absorption spectrophotometry analysis for major elements 200

Table 19 2θ positions and count time for trace elements by X-ray fluorescence spectrometry . 201

Table 20 Information on element parameters and corrections required for operation of computer program "Tratio" 203

Table 21a Precision data for standard JG-1 205

Table 21b Precision data for standard BCR-1 206

Table 21c Precision data for standard JB-1 207

Page

LIST OF PLATES

Plate 1	Myrmekitic intergrowth of plagioclase and vermicular quartz, in K-feldspar megacrystic granite	56
Plate 2	Zoned subhedral radioactive tourmaline, in K-feldspar megacrystic granite	56
Plate 3	Alaskitic granite phase of the Ackley batholith	58
Plate 4	Stringlet perthite in alaskitic granite	58
Plate 5	Coarse grained granophyric intergrowth of string perthite and quartz in medium grained granite	86
Plate 6	Coarse grained molybdenite rosettes in drusy medium grained granite	86
Plate 7	View of Ackley City showing from northeast ..	88
Plate 8	Quartz segregation, Ackley City showing	88
Plate 9	Hypidiomorphic granular aplite, Ackley City showing	92
Plate 10	Pegmatitic aplite which contains numerous pegmatitic miarolitic segregations, Ackley City showing	92
Plate 11	Coarse grained graphic intergrowth from fringe of a pegmatitic segregation, Ackley City showing	93
Plate 12	Intensive purple fluorite mineralization within medium grained granite, Ackley City showing	93
Plate 13	Secondary biotite containing numerous inclusions characterized by radioactive halos, Ackley City showing	96
Plate 14	Sharp contact between coarse grained alaskitic granite and medium grained porphyritic granite, near Dunphey Brook	96

Page

Plate 15 Embayed bipyramidal quartz phenocrysts, in quartz-feldspar porphyry, Dunphey Brook-Crow's Cliff showing 100

Plate 16 Pegmatite consisting of milky large quartz crystals surrounded by perthitic orthoclase and aplite, the Dunphey Brook showing 100

Plate 17 Plagioclase phenocryst with a perthite and graphic quartz overgrowth rim, in porphyritic granite, Dunphey Brook-Crow's Cliff showing 102

Plate 18 Breccia dyke (tuffisite) consisting of alaskitic granite fragments in a fine grained matrix, in Dunphey Brook 102

Plate 19 Matrix of tuffisite in Plate 18 104

Plate 20 Zone of molybdenite mineralization orientated parallel to the direction of growth of a quartz crystal, in pegmatite, at Crow's Cliff showing 104

Plate 21 Cross section of a large quartz crystal with concentric zones of molybdenite and K-feldspar, Crow's Cliff 105

Plate 22 Intrusive contact between quartz aplite and aplite, Wylie Hill 105

Plate 23 Bent strained albite within a pegmatite segregation, Wylie Hill 109

Plate 24 Elongated strongly strained quartz within the innermost zone of a pegmatite segregation, Wylie Hill 109

Plate 25 Quartz aplite showing anorthoclase, altered plagioclase and amoeboid quartz, Wylie Hill . 111

Plate 26 Stained K-feldspar which contain numerous small sodic blebs which resist staining, Wylie Hill 111

Plate 27 Tuffisite vein, Wylie Hill showing 112

Plate 28 Weathered mineralized fine grained porphyritic granite, Wylie Hill showing 112

Page

Plate 29 Part of pyrite nodule showing the dendritic nature of the pyrite, Wylie Hill 114

Plate 30 Fine grained platey aggregate of molybdenite disseminated in fine grained porphyritic granite, Wylie Hill 114

Plate 31 Coarse grained muscovite alteration of perthite, Wylie Hill 115

Plate 32 Grains of pitchblende with minute inclusions of gold in mineralized porphyritic fine grained granite, Wylie Hill 115

Plate 33 Autoradiograph of the pitchblende grains in Plate 32 117

Plate 34 Quartz veins with quartz-sericite alteration fringes, cutting alaskitic granite, Frank's Pond showing 117

Plate 35 Alaskitic granite plug exposed on the eastern side of Belle Island 119

Plate 36 Fracture related quartz-sericite-clay mineral alteration of porphyritic fine grained granite, Belle Island 119

Plate 37 Coarse grained sericite replacing plagioclase phenocryst in medium grained porphyritic granite, Belle Island 122

Plate 38 Biotite replaced by sericite-calcite-sphene-rutile-pyrite in porphyritic aplite, Belle Island 122

CHAPTER 1

INTRODUCTION

1.1 General

The Ackley City batholith occupies an area of approximately 5,400 sq. km. between latitudes 55°28' to 54°27' and longitudes 48°18' to 47°39' in south-east Newfoundland (Fig. 1). The molybdenite showings occur on the south-west border of the intrusive, the nearest settlement being Rencontre East on Fortune Bay. The village is serviced only by scheduled C.N.R. steamer service twice weekly from Argentia and Port aux Basques. An unpaved road to English Harbour East from the paved Burin Peninsula road reaches to within 23 km. from the east, while a road to Pool's Cove from the Bay D'Espoir highway reaches to within 17 km. from the west. Surface access to five of the showings is via Rencontre Lake which is reached by a trail (1 km.) from the village. Float planes can land on the lake while helicopters can land readily at all the showings. The Belle Island showing, located 38 km. east of Rencontre East, is accessible only by boat.

The general area displays two somewhat contrasting types of topography reflecting the different rock units. The granite areas in the north are barren and of local relief with elevations averaging 180 meters in contrast to the slightly higher elevations and much greater

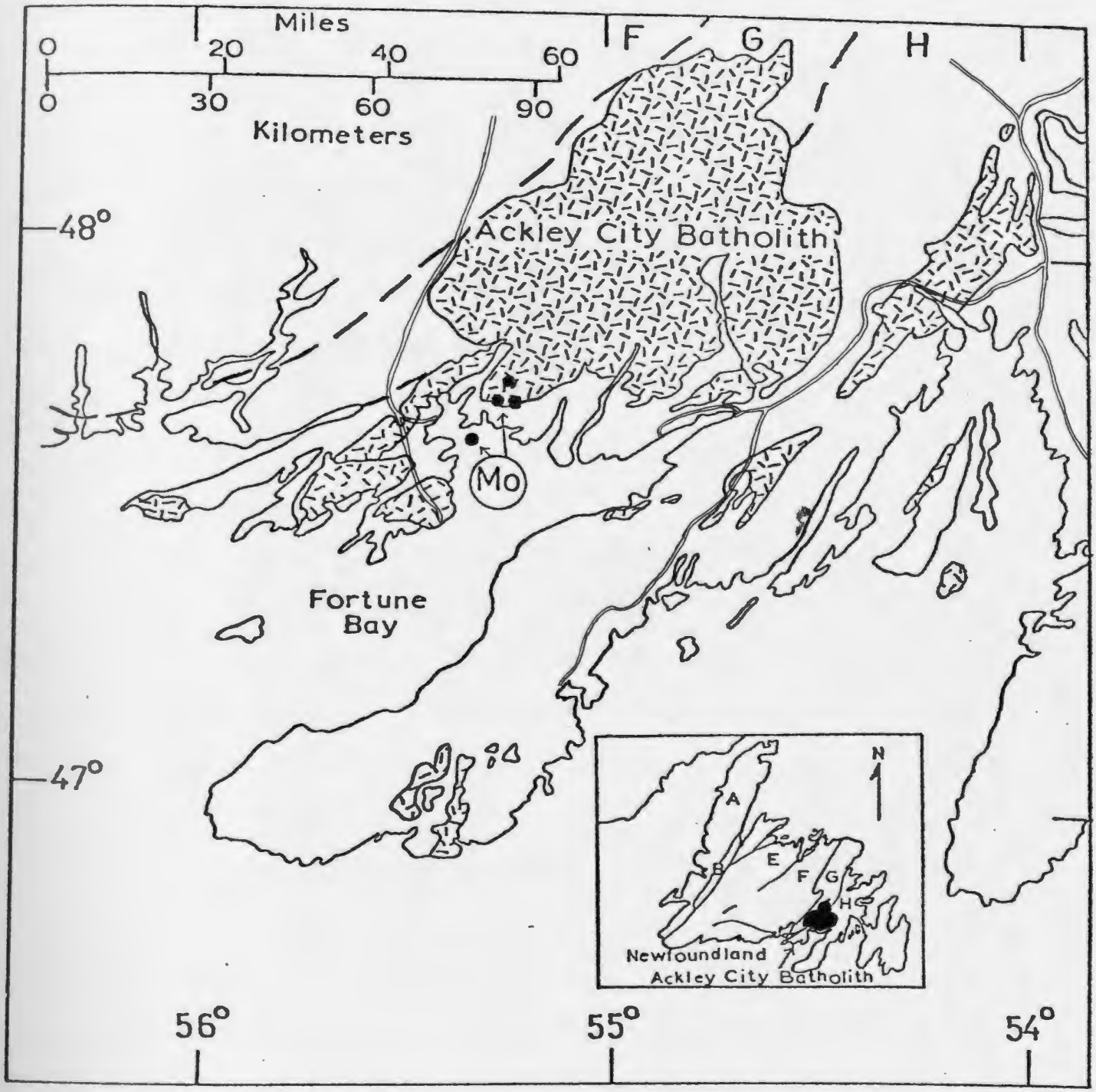

Figure 1. Location of the Ackley City batholith and the molybdenite mineralization along its southwest margin, Fortune Bay, Newfoundland. Different zones (F,G and H) of the Appalachian structural province (Williams et al., 1972) indicated on top of figure and boundaries by dashed lines. Granites are hatched and roads indicated as thin double solid lines.

irregular local relief of the volcanics and sediments to the south. Rencontre Lake is a deep glacial valley with high and very steep sides. Exposure in the area is excellent with bush occurring only in protected valleys.

1.2 Previous Work

1.2.1 Fortune Bay Region

The earliest work in the area was done by Howley (1888) who made a hurried reconnaissance of a part of the area near the settlement of Bay Du Nord. Little subsequent work was done until White (1939) mapped the Belleoram (Rencontre East) area. Widmar (1950) mapped the Hermitage Bay area. Smith (1953) studied the fluorite occurrences of Long Harbour, and with White, compiled a report on the regional geology of the Belleoram area (Smith and White, 1954). The Rencontre East area between Pool's Cove and Long Harbour was mapped in 1955 for Newfoundland and Labrador Corporation Ltd. (NALCO) by D.A. Bradley. Bradley (1962) also mapped the Terrenceville area, which adjoins the Belleoram map-area to the east. The whole of the Fortune Bay area was investigated by Anderson (1965) as part of a geological reconnaissance study. The latest regional geological mapping in the area was Williams' (1971) map of the Belleoram map-area.

Special aspects of the geology of the map-area were studied by the following: Twenhofel (1947), who described the sedimentology and stratigraphy of the Rencontre Formation in connection with a regional study of the Silurian rocks of

Newfoundland; Hutchinson (1962) who studied the Cambrian faunas and stratigraphy as part of a general investigation of the Cambrian rocks and trilobite faunas of southeastern Newfoundland; Ermanovics et al. (1967) who investigated the petrogenesis of the Belleoram Stock; and Williams (1967) who summarized the stratigraphy and relationships of the late Precambrian Long Harbour Group as possibly representing Silurian deposits of southeastern Newfoundland.

1.2.2 History of Exploration

A molybdenite discovery was recorded in the vicinity of Rencontre Lake about 1882 (Smith, 1936). This prospect, or a similar one in the immediate area was explored by the Van Allen Mining Company for a four month period commencing October, 1900. The prospects were examined in 1915 on behalf of U.S. interests and on several occasions in the period from 1926 to 1934 by geologists on behalf of the Newfoundland Geological Survey.

The first serious exploratory program appears to have been conducted by Dana and Company Incorporated of New York who investigated the prospects between 1935 and 1937 (Smith, 1936). Subsequently, the claims covering the prospects were incorporated as Newfoundland Molybdenum Limited and examined by McKinstry (1938). In 1937 the area was surveyed by D.E. White for the Geological Survey of Newfoundland and the mineral deposits were studied in extensive detail (White, 1939, 1940). To the end of 1938,

development work on the Ackley deposit included extensive surface trenching, probably over 305 meters, and underground work which included 76 meters of tunnelling, an 18 meter shaft, and approximately 122 meters of drifting and cross-cutting from the 18 meter level. Over 122 meters of surface trenching had been completed on the Motu showing. On the Wylie Hill showing over 305 meters of surface trenching had been completed, largely on the eastern orebody and a pit 2.6 meters deep had been sunk near the southwest shore of Wylie Pond. In 1944 six diamond drill holes were put down on the Ackley prospect by the Newfoundland Department of Mines (Quinn, 1944).

Little further interest was expressed in the showings until 1953 when the prospects formed a portion of a territory of some 4,662 sq. kms. granted to the Newfoundland and Labrador Corporation Limited (NALCO) by the Newfoundland Government under the terms of Act 64. In 1955 a compilation of data on the prospects was made for NALCO (Dunlop, 1955) and the area was mapped and examined for NALCO by Bradley (1955). The following year an evaluation of the Ackley City molybdenite deposit was made by Cooper and Steward (1956) for NALCO. Between 1958 and 1959 Caledon Minerals Co. Ltd. drilled eleven shallow diamond drill holes at Wylie Hill, three at Ackley City and five at Motu (Ellgring, 1959; McNeil, 1959), also an induced potential, resistivity, and

biogeochemical survey was completed at Wylie Hill while a resistivity survey and metallurgical tests were made at Ackley City.

Between 1965 and 1967 the showings were visited a number of times by Fogwill for Canadian Javelin Ltd. (Fogwill, 1965) and for NALCO (Fogwill, 1966, 1967). The claims were subsequently optioned by Norlex Mines Ltd. for whom the prospects were examined by consultants (Knight, 1968; Zurowski, 1968) to determine what further development work should be done. The diamond drilling program outlined and recommended by Fogwill (1968 a, b) was carried out with a total of eleven holes being drilled, totalling 120 meters at the Ackley showing in 1968 to 1969 and subsequently twelve holes totalling 1,228 meters were drilled at the Wylie Hill showing in 1969. Results were considered discouraging and since no further work was undertaken, the claims were dropped by NALCO in early 1975.

1.3 Present Study

One of the unifying geologic characteristics which is displayed by porphyry copper and/or molybdenum deposits is a young age ranging from 210 m.y. to 5 m.y. (Lowell and Guilbert, 1970; De Geoffroy and Wignall, 1972), a feature attributed by Sillitoe (1972b) to the effects of erosion in pre-Mesozoic-Cenozoic orogenic belts. However, older porphyry type deposits have been documented in the Canadian Shield (Kirkham, 1971b) and the Appalachians

(Hollister et al., 1974; Allcock, 1974; Kirkham and Soregorali, 1975; Whalen and Hodder, in prep.). One cited example is the Devonian Ackley Mo deposits. This thesis examines these deposits with the object of arriving at a better understanding of their nature and origin, such information being important in terms of metallogenic models of the Appalachians (Strong, 1974), in relation to genesis of Mo deposits in general, and in exploration for Mo on both a local and regional scale.

The approach taken was to do detailed mapping, bulk chemistry, petrography and mineralogy on the individual showings. An attempt to answer questions of petrogenesis was made using data from the showings and by trying to relate them to the Ackley City Batholith in general.

1.4 Acknowledgements

The writer would like to thank Dr. D.F. Strong for supervising the project, for helpful discussions and assistance in various other matters.

The writer would like also to thank Dr. R.W. Hodder, Dr. R.W. Henley, Dr. C.J. Hughes and D.G. Minatidis for helpful discussions, A.M. Frew of Newfoundland and Labrador Corporation Limited for drill core samples and access to unpublished reports and maps, Dr. M.E. Fleet and Dr. R.C.O. Gill of the University of Western Ontario for help and advice in trace element analysis, G.L. Andrews for similar assistance

in major element analysis, J. Vahtra for assistance in X-ray diffraction work, and D. Press for assistance in data processing. The study was financed by a Memorial University Fellowship to the writer and N.R.C. operating grant A-7975 to Dr. D.F. Strong.

CHAPTER 2

MOLYBDENUM IN NATURE

2.1 General Geochemistry and Distribution

The element molybdenum is a heavy metal with a specific gravity of 10.2 at 20° C, atomic weight of 95.94, atomic number of 42 and atomic radius of 1.36 A. The most common valence state is 6+, less common oxidation states range from 5+ through 4+, 3+ to 2+, the least common. At high temperatures molybdenum has a high affinity for iron, and to a lesser extent for Ni, Mn and Mg, which suggests it would tend to accumulate in the iron-nickel core of the earth. The fact that molybdenum ions tend to be fixed by FeO and MnO_2 radicals indicates that Mo could be preferentially carried upward from the interior of the earth. This could mean that the mantle of the earth may be depleted in Mo as compared with the core and the near surface volumes of the planet (Goldschmidt, 1954), a suggestion which is partly supported by the low Mo content of ultramafic in comparison to other rock types. Average values of Mo for common igneous and sedimentary rock types and estimates of the abundance of the element in the lithosphere are presented in Table 1. The only significant high values are in sediments of strongly reducing environments, other variations are only in the order of 1 ppm.

The most common Mo mineral, molybdenite (MoS_2), is known to have two naturally occurring polytypes, hexagonal

Table 1

Average Values for Molybdenum of Common Rocks (in ppm)

	Rock Type	1	2	3	4	5
Igneous Rocks	Ultramafic	.4	.3	.2		
	Mafic	.8	1.5	1.4		
	Intermediate	—	1.0	.9		
	Granitic	1.1	1.3	1		
	Syenitic	—	.6	—		
Sedimentary Rocks	Slate	1	2.6	2	24	
	Sandstone		.2		2	
	Carbonates	.5	.4			
	Deep Sea Carbonates		3			
	Deep Sea Clays		27			
	Manganese Nodules	up to 100			1000-3000	
	Black Shales				5-10	
	Pelite				50-200	
	Average Abundance in Lithosphere (Clarke Value)	1±.5		1.1		1.5

(1) Sandell & Kurada (1954)
(2) Turekian & Wedepohl (1961)
(3) Vinogradov (1962)
(4) Enzmann (1972)
(5) Taylor (1964)

(2H) and rhombohedral (3R), which differ only in the way the MoS_2 layers are stacked (Takeuchi and Nowachi, 1964). Although there are 112 theoretically possible polytypes of molybdenite (Wickman and Smith, 1970) in numerous investigations throughout the world (Vorma et al., 1966; Chukrovet et al., 1970; Khurshudyar et al., 1969; Ayres, 1974) only two polytypes $2H_1$ and 3 R have been found, which can be present in varying proportions in any one specimen or deposit. Limited studies by Somina (1966) suggest that natural 3R MoS_2 contains an unusually high amount of trace metals, suggesting that reduced 3R symmetry is the result of impurity-induced stress effects on the mineral structure during growth. Zelikman et al. (1970) conclude from studies of synthetic polytypes that (1) at high sulfur pressure 2H MoS_2 is stable, relative to the 3R variety and (2) the proportion of the 3R form in mixed crystal molybdenites increases proportionally to the Re content. Other minerals of molybdenum are secondary in origin and include wulfenite ($PbMoO_4$), powellite ($Ca(MoW)O_4$), ferrimolybdite ($Fe_2(MoO_4)_3$ $8H_2O$ (?)), ilsemannite ($Mo_3O_8 \cdot nH_2O$), koechlinite ($(BiO)_2(MoO_4)$) and lindgrenite ($Cu_3(MoO_4)_2(OH)$).

Molybdenum is found in association with minerals of other elements such as Cu, Sn, W, and also accommodates substitution of economic impurities in the structure of molybdenite. Rhenium (Re) is one of the rarest, but most

widely dispersed metals in the earth's crust, its average abundance in igneous rocks being of the order of 0.05 ppb (Morris and Short, 1969). Although Re occurs in minor amounts in a variety of minerals, molybdenite is the only known significant concentrator of Re in the crust. Giles and Schilling (1972) have shown that the Re content of molybdenite from porphyry Cu deposits has a mean value of 720 ppm, that from Cu-poor stockwork molybdenum deposits averages 50 ppm, and molybdenite from greisens, pegmatites, and skarns has a range of 7-129 ppm. Terada et al. (1971) have shown that the Re content of molybdenite from Japanese deposits decreases in the order: volcanic sublimates, porphyry Cu deposits, contact metasomatic deposits, disseminated deposits and quartz veins.

2.2 Behavior of Molybdenum During Magmatic-Hydrothermal Processes

The rather uniform distribution of Mo among the common igneous rocks (Table 1) is attributed by Sandell and Kurada (1954) to its ability to replace a number of elements in the lattices of rock-forming minerals. It is present in the feldspars, in biotite, amphiboles and pyroxenes and especially in magnetite and ilmenite. Substitution of Mo for Fe^{3+}, Ti, Al, and possibly Si is indicated. Mo exists both in the 4^+ and 6^+ states and the high value of ionic potential for Mo^{6+} tends to the formation of $(MoO_4)^{2-}$

complexes which are concentrated in residual magmas (Taylor, 1965). The Mo^{4+} ion maintains an equilibrium between existence as the free ion and as $(MoO_4)^{4-}$ complexes. There will thus be a general concentration of these elements in residual or volatile-rich magmas, due to the large size of the complexes compared with $(SiO_4)^{4-}$, and in the case of the hexavalent complexes, a charge discordency as well (Ringwood, 1955).

The close association in time and space of granitic rocks and large economic concentrations of Mo is convincing evidence of a close genetic relationship. The fact that the association is not a simple case of the concentration of an incompatible element is apparent in a summary by Barsukov (1966) of the numerous studies of the distribution of Mo in granitic intrusives by Russian workers. Granitoids to which Mo mineralization is related paragenetically and probably also genetically were found not to be distinquishable by high contents of the elements. In some cases it was possible to establish that there is an increase in the Mo contents from older to younger granites within each separate intrusive complex. Several papers by Pokalov (1961, 1962) and Kazitsin (1962) mention the manifestations of metallogenic specialization of granitoids with respect to Mo in certain areas in Kazakhstan and Transbaikalia, where the Mo content in metalliferous granitoids is two or three times higher than the clarke value for the element.

Tauson and Petrovskaya (1971) attribute such accumulations to be due to secondary enrichment by gaseous emanations. They suggest that the Mo content of the granitoids was 1 to 1.5 ppm. before being enriched by an influx of Mo into zones of high permeability unaccompanied by any other alteration of the rock.

The composition and volume of volatile components in a magma and the sequence of their separation from the magma chamber during cooling and crystallization are apparently much more important factors in Mo ore formation than the processes of differentiation or derivation from Mo-enriched parental magmas. The effect of removal of a Mo-enriched fluid phase from a magma would not significantly alter the Mo concentration in the melt, for only amounts in the order of a few percent of the total Mo content would be removed, thus large volumes of magma would be required for production of economic concentrations of Mo (Kitarovetal et al., 1967). Burnham's (1967) discussion of hydrothermal fluids at the magmatic stage reveals the great complexity of the subject. Separation of a water-rich phase would result whenever the equilibrium pressure of water in the melt exceeds the total confining pressure. Upon separation the composition of an aqueous phase is dependent upon the temperature, pressure, bulk composition and nature of co-existing phases. If the Mo is deposited in close association with the crystallization of its genetically related intrusive

such as in pegmatites, a syngenetic magmatic molybdenite deposit results. If, however, the magmatic fluid phase migrates vertically through structurally controlled permeable zones, reacting with wall rocks and depositing its metal content, then a epigenetic hydrothermal deposit is formed.

The orthomagmatic model described by Burnham (1967), Nielsen (1968) and Whitney (1975) is the genetic model most preferred in literature for the generation of porphyry deposits, the major type of Mo epigenetic deposit, since the classic papers of Bowen (1933), Emmons (1933) and Lindgren (1937). The sequence of events, as described by Nielsen (1968) can be paraphrased as: intrusion, early marginal crystallization which produces a solid shell, and rupture of that shell to produce porphyritic-aphanitic textures in subsequently crystallized rocks. If the build up of volatiles is great enough, breccia pipes may be formed when they are released (Norton and Cathles, 1973). Alteration and mineralization follow in the crackle, stockwork, and brecciated zones. Evidence for the close genetic relationship between magmatic activity and the alteration-mineralization process is the presence of intermineral intrusions (intrusions that were emplaced between or during periods of mineralization) in many porphyry deposits (Kirkham, 1971 a).

Isotope studies on porphyry Cu-Mo deposits have shown that the outer alteration zones are mainly formed by

meteoric water at temperatures of 390° to 285° C, while the inner alteration zone (potassic) was formed by mainly magmatic water at temperatures of 580° to 390° C. (Sheppard et al., 1971). Similar results were obtained from studies at the Climax orebody, a major porphyry Mo deposit (Hall et al., 1974). This suggests that magmatic-hydrothermal solutions which formed during late stages of crystallization of a porphyry stock interact with an extensive meteoric water convection system which is driven by the heat of the magma (Taylor, 1974). The main focus of mineralization is at the interface between the two hydrothermal convection systems, possibly because of temperature, salinity, Eh, pH or pressure differences at this interface.

2.3 Classification of Molybdenum Deposits

The different types of molybdenite deposits have been classified in somewhat different ways by different authors. A classification based on economic aspects was proposed by Creasey (1957) while genetic considerations have been used by Stevensen (1940), Vandervilt (1953), Vokes (1963) and Sutherland Brown (1969). The classification presented in Table 2, which is based mainly on information obtained in the above mentioned publications, subdivides the deposits into three major classes, syngenetic, epigenetic and secondary, with further subdivision within these groups.

The term syngenetic is used to describe deposits in which there is apparently a very close genetic relationship

Table 2

Classification of Molybdenum Deposits

I Syngenetic	A.	In Acidic and Alkalic Igneous Rocks	
	B.	Pegmatitic and Aplitic Type	
	A.	Vein Type	1. Pegmatitic Quartz Veins 2. Quartz Veins 3. Gold Veins 4. Base Metal Sulphide Veins
II Epigenetic	B.	Porphyry	1. Porphyry Mo Type 2. Porphyry Cu Deposits (i) Continental Margin Type (ii) Arizona Type (iii) Island Arc Type
	C.	U-Mo Type	
	D.	Metasomatic Type	
III Secondary	A.	Sedimentary Accumulations	
	B.	Weathering Enrichments	

between mineralization and host rocks in space and time. Molybdenite is a sparse but relatively common constituent of granites and other igneous rocks occurring sparsely disseminated in a manner strongly suggesting it has crystallized in situ as an ordinary accessory mineral. Such deposits are widespread but tenor is generally so low that they are not of commercial interest. Molybdenite is the most common sulphide mineral in pegmatites and related aplitic rocks. These rock types usually form later than the main intrusive mass and tenor of molybdenite mineralization, which tends to occur in lenses or pods, is erratic. The grade in the pods may be high but small size and wide spacing mean that the grade of the pegmatite and/or aplite body, as a whole, is generally not economic. Molybdenite in pegmatite occurs in large crystals or flakes and in aplites as radial or rossette-like aggregates.

The group of deposits termed epigenetic are deposits formed by igneous and metamorphic processes in which mineralization is younger than its host rocks. A widespread type of occurrence, but uneconomic in Mo content is in veins. Pegmatitic quartz veins contain various amounts of feldspar and mica with associated Mo and Bi, and represent a transition from pegmatite to simple quartz veins. Quartz veins vary in width from a fraction of a centimeter to several meters, and in mineralogy of associated sulphides, for pyrite is common and chalcopyrite, sphalerite and galena may, or may not be

present. Molybdenite is a common accessory mineral in gold veins, especially in Precambrian areas. There is a transition between molybdenite-bearing quartz veins with few accessory base-metal sulphides, and veins which are dominantly composed of the later minerals. Molybdenite is recovered from a few deposits, but as a whole no significant quantity of molybdenite has come from such deposits.

Porphyry deposits, the second type of epigenetic deposit, account for over 90% of Free World Mo production, approximately 65% from porphyry Mo deposits and 25% as a by-product from porphyry Cu deposits, and the trend is toward an even greater growth in the percentage of world production from these deposits (Clark, 1972). Recent publications (Lowell and Guilbert, 1970; Rose, 1970; James, 1971; DeGeoffroy and Wignell, 1972) have developed the concept that there are unifying geologic characteristics which are displayed to varying degrees by porphyry Cu and/or Mo sulphide deposits, consisting of disseminated and stockwork veinlet sulphide mineralization emplaced in various host rocks that have been altered by hydrothermal solutions into roughly concentric zonal patterns. Porphyry copper deposits contain pyrite, chalcopyrite, and molybdenite in that order of abundance and contain ore values in Cu, Mo, Au, Ag, and Re. They are generally associated with porphyritic quartz-monzonite intrusives. Clark (1972) documented the

concept of porphyry Mo deposits as a type to be distinguished from porphyry Cu-Mo deposits, for with the exception of Climax, Colorado which recovers by-product Sn, Mo is the only element of economic importance in porphyry Mo deposits. The deposits are related to siliceous oversaturated stocks which have a petrological composition ranging from granodiorite through quartz-monzonite to granite. Pyrite is the most abundant sulphide while other sulphides (chalcopyrite, sphalerite, galena, pyrrhotite) in addition to molybdenite occur in minor quantities.

Heinrich (1958) has described an association between U and Mo in a number of deposits which are chiefly uraninite-molybdenite tactite deposits. The U-Mo association has been reported in a wide variety of deposit types which include pegmatites, base metal veins, skarns, pyroxenite, metamorphic rocks, Colorado Plateau U deposits and porphyry deposits (Soregaroli, 1975). This association is manifest in many different types of Mo deposits, however, in most reported occurrences either Mo or U is the dominant metal with the other element occurring in trace or very minor amounts. Some deposits contain recoverable quantities of both metals and according to Tugarurov et al. (1973) constitute an independent type of ore deposits which is most often related to continental volcanic formations, predominately of lithophilic composition.

Many replacement bodies of lime-silicate minerals or skarn carry low erratic values in molybdenite which is recovered as a by-product. This type of deposit is common in the Cordillera of Canada where limestones have been metasomatically altered near granitic intrusions. These deposits have a variable ore mineralogy, some carrying only molybdenite while in others Au or W or Cu are the principle economic metals with accessory molybdenite. In the Grenville province there are numerous occurrences of possibly metasomatic deposits consisting of diopside with or without feldspar, mica, and calcite heavily mineralized with pyrite and/or pyrrhotite and molybdenite.

The last group, those molybdenite occurrences of secondary origin, are not significant in quantity or economically. They can be divided into two types, sedimentary accumulations and weathering enrichments. Sedimentary accumulations occur in manganese nodules, saprolites and pelites. Precipitates as ferromanganese nodules and encrustations are found abundantly spread over certain areas of the ocean floor and contain up to 3,000 ppm Mo. Saprolites (mud rich in organic matter) in the Dead Sea asphalts contain 100-1,000 ppm Mo. Silts and muds (pelites) of the slightly metamorphosed Kupferschiefer of Mansfeld, Germany, contain 50-200 ppm Mo, apparently precipitated from sea water by the hydrogen sulphide-rich reducing

environment, which is recovered as a by-product. The sandstones of Colorado which contain carnotite (U-V) deposits contain Mo in the form of ilsemannite. Weathering enrichments of Mo occur in the oxidized parts of some Pb-Zn deposits in arid and semi-arid regions of the world (McInnis, 1957). They contain wulfenite, minerals such as vanadinite and descloizite. The origin of the Mo and V is obscure, but they were apparently introduced after oxidation of the deposit, possibly having been leached from adjacent V-Mo bearing shales.

2.4 Distribution and Origin of Molybdenum Deposits

Molybdenum mineralization is widespread in both space and time, with numerous occurrences in Paleozoic orogens and Precambrian shield areas, although economic concentrations are almost solely restricted to Cenozoic-Mesozoic orogenic belts. The distribution and origin of these deposits is probably best considered in the context of the theory of lithospheric plate tectonics, an extension of which proposes that certain types of economic mineral deposits are uniquely formed in specific plate regimes. Guild (1971), Sawkins (1972), Pereira and Dixon (1971), Sillitoe (1972 a, b, and c), Mitchell and Garson (1971), and Godwin (1975) have all pointed out the general relation between porphyry deposits and consuming plate margins. Because of the economic importance and resultant attention given to them in literature the implications of porphyry type deposits will be considered first.

The majority of the world's porphyry deposits are distributed around the Pacific and in the central portion of the Alpine orogenic belt. They range in age from less than 5 to 200 m.y., although Precambrian shield deposits (Kirkham, 1971b) and Appalachian deposits (Hollister et al., 1974; Kirkham and Soregoroli, 1975; Allcock, 1975; Whalen and Hodder, in prep.) have also been documented. Kesler (1972) has subdivided these consuming plate margin deposits according to Cu-Mo-Au abundances into: (1) a Cu-Mo type which occurs mainly in continental or cratonic areas, and (2) a Cu-Au type which occurs mainly in island arc areas. Hodder (1974) has proposed a more detailed subdivision by subdividing the first type into cratonic and continental margin types. Sutolov (1963, 1970, 1974) and Giles and Schilling (1972) have drawn attention to the Re content of molybdenite in porphyry deposits, indicating that Re content of porphyry Cu-Mo deposits is exceptionally high whereas in stockwork Mo deposits it is very low. A Plot of Re versus Mo (Fig. 2) suggests a subdivision of porphyry deposits into a Mo type, Cu Mo type, continental margin Cu-Mo type, Arizona Cu-Mo type and island arc Cu-Au type, in order of increasing Re content. The Re content may, therefore, be related to the conditions of formation of the deposits in different plate tectonic settings. These types are discussed in the preceeding order:

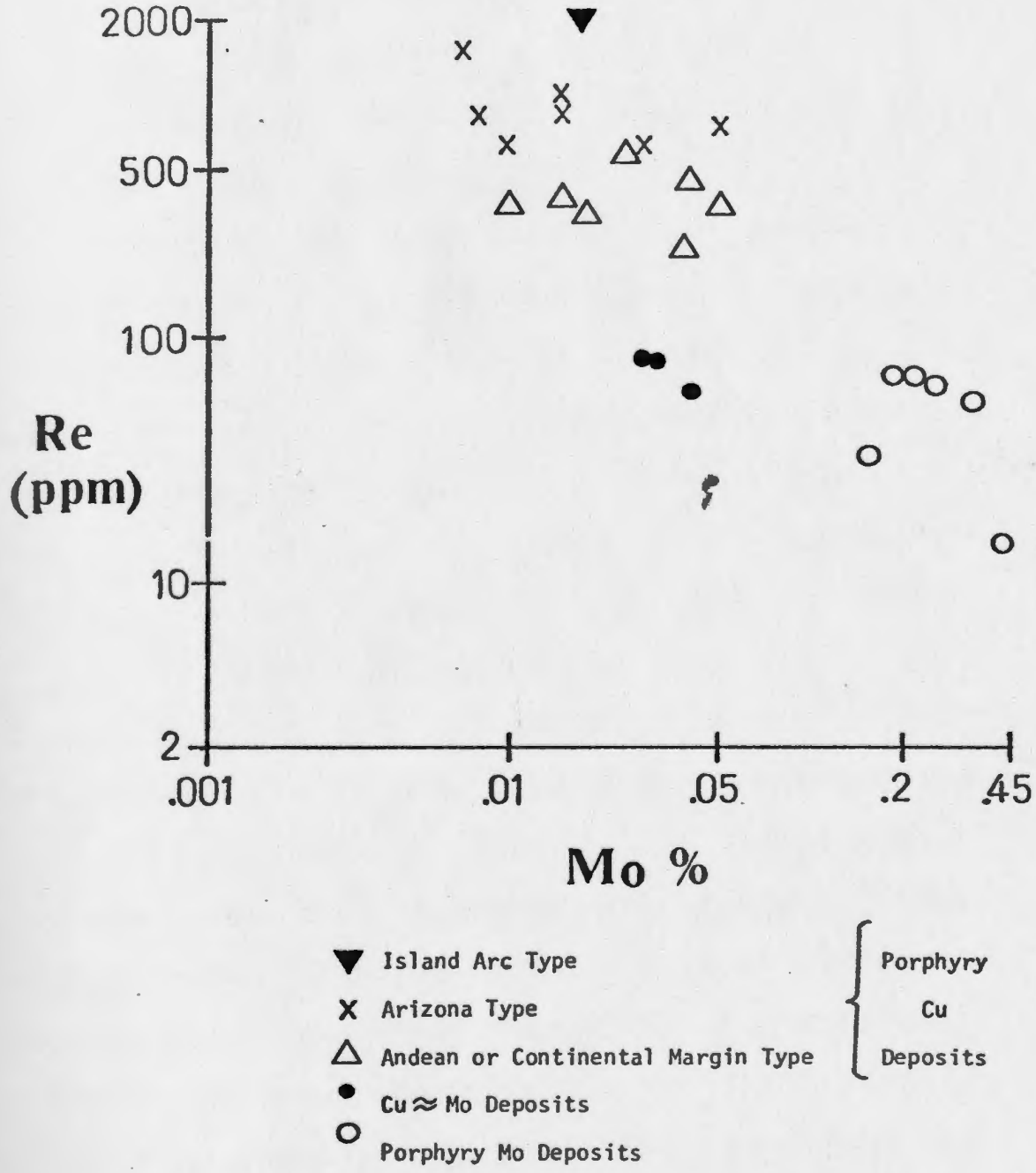

Figure 2. Plot of Re (ppm) content of molybdenite versus Mo (wt.%) content of ore for porphyry deposits of different tectonic settings (data from Sutulov, 1974; Giles and Schilling, 1972).

(a) The major economic porphyry Mo deposits are located in Western North America, are cratonic in setting, and generally occur continent-ward of porphyry Cu-Mo type deposits in metal zoning models.

(b) The well exposed and intensely mineralized central section of the post-Paleozoic Andean orogen has emerged as a model for the generation of ore deposits at a convergent plate margin (Clark et al., 1976; Sillitoe, 1976). The porphyry deposits of this orogen can, therefore, be considered as the type examples of this tectonic setting. These continental margin deposits are Paleocene or younger in age, higher grade in Cu and lower in Re content then Arizona deposits. Their emplacement is apparently related to deep crustal weaknesses resulting from vertical tectonics (Hollister, 1974; Sillitoe, 1976). Origin of the deposits is best explained in terms of Sillitoe's 1972 and 1973 models of emplacement of magma derived from an underlying subduction zone, with resultant formation of porphyry deposits beneath stratovolcanos during the final stages of calc-alkaline volcanism. If the Andes represents a realistic model then older deposits of this type may not be numerous. The Andes is underlain by an extensively thick (70 km) crust (James, 1971), the existance of which may be the result of a long lasting period of subduction suppressing the mantle isotherms beneath the area. Cessation of subduction probably would be followed by mantle homogenization, extensive basal crustal anatexis and voluminous

granite emplacement accompanied by uplift and erosion of overlying porphyry type deposits. The large poorly mineralized coastal batholiths of the Western U.S.A. and Canada may be the result of such a process.

(c) The southwestern part of the United States and adjacent Mexico has long been considered as an excellent example of a Cu metallogenic province (Spurr, 1923) for it contains an anomalous number of porphyry deposits which formed at 170 m.y. and between 65 and 55 m.y., and which contain high Re content. The deposits are within the Basin and Range structural province which is usually taken to constitute the last 30 m.y. but Lowell (1973) points out that this is probably not the case and that structural deformation and extensive igneous activity were somewhat episodic but more or less continuous from Jurassic through Late Tertiary time. The area has been the object of many plate tectonic interpretations (McKenzie and Morgan, 1969; Atwater, 1970; McKee et al., 1970; Scholz et al., 1971; Christiansen and Lipman, 1972; Lowell, 1974; Churckin and McKee, 1974), which make it plain that the thin layered subcontinental crust of the area may be inherited from Palaeozoic marginal ocean basins. Formation of deposits in such a crust would be facilitated, for extension would form zones of weakness to tap deep magma sources and the resulting deposits would not be readily uplifted and eroded.

(d) Porphyry deposits in island arc areas have high Re and Au, minor uneconomic accessory molybdenite, lower tonnage, younger age and less extensive alteration of host rocks. They represent a part of the subaerial comagmatic-volcanic history of island arcs.

Other Mo deposits formed in an Andean type convergent plate margin are vein, metasomatic, aplite-pegmatite and U-Mo types. According to Sillitoe (1973) deep levels of porphyry deposits are characterized by pegmatite which suggests that such showings represent deeper levels of erosion. Significant Mo mineralization is minor or absent in island arcs constructed on oceanic crust while Japan, which is constructed on a detached segment of continental crust, has numerous vein and skarn type Mo mineral occurrences located in the portion of Japan distal from the trench (Ishihara, 1973). Rifts are another type of plate environment in which Mo mineralization is sparse, except possibly for the Kupfershiefer sedimentary Cu deposits from which by-product molybdenite is recovered. Precambrian shields contain numerous, generally uneconomic occurrences of most types. The relation of this mineralization to plate tectonic processes is not readily apparent but it is usually related to granitic rocks distributed within or near the margins of greenstone belts, rather than to the large Precambrian gneiss-granitic terrains. The ferromanganese

nodules and encrustations from the ocean floors are an intra-plate type deposit which are variably enriched in Ni, Cu, Co, Ti, Pb, U, Ag, As, Zn, and Mo, depending upon both proximity to potential magmatic sources, the environment of deposition and redox potential in particular (Cronan, 1972).

It is apparent from these patterns of distribution of molybdenite deposits, summarized in Fig. 3, that the most significant concentrations are related to destructive plate margins, occur in areas underlain by a continental crustal basement, show a close genetic relationship to granitic intrusions and occur more continentward than other important mineralization. An empirical relationship to subduction can be suggested, but the actual origin and the mechanism of Mo deposition could be the result of one or a combination of factors. These include crustal contamination, deeper down-dip melts off a subduction zone, difference in dip of a subduction zone, variation in metal content of subducted oceanic crust and greater distance of rise of a melt off a subduction zone with attendent greater time of fractionation and differentiation. It appears, however, that the presence and involvement of continental crust may be the most important factor in the formation of Mo deposits.

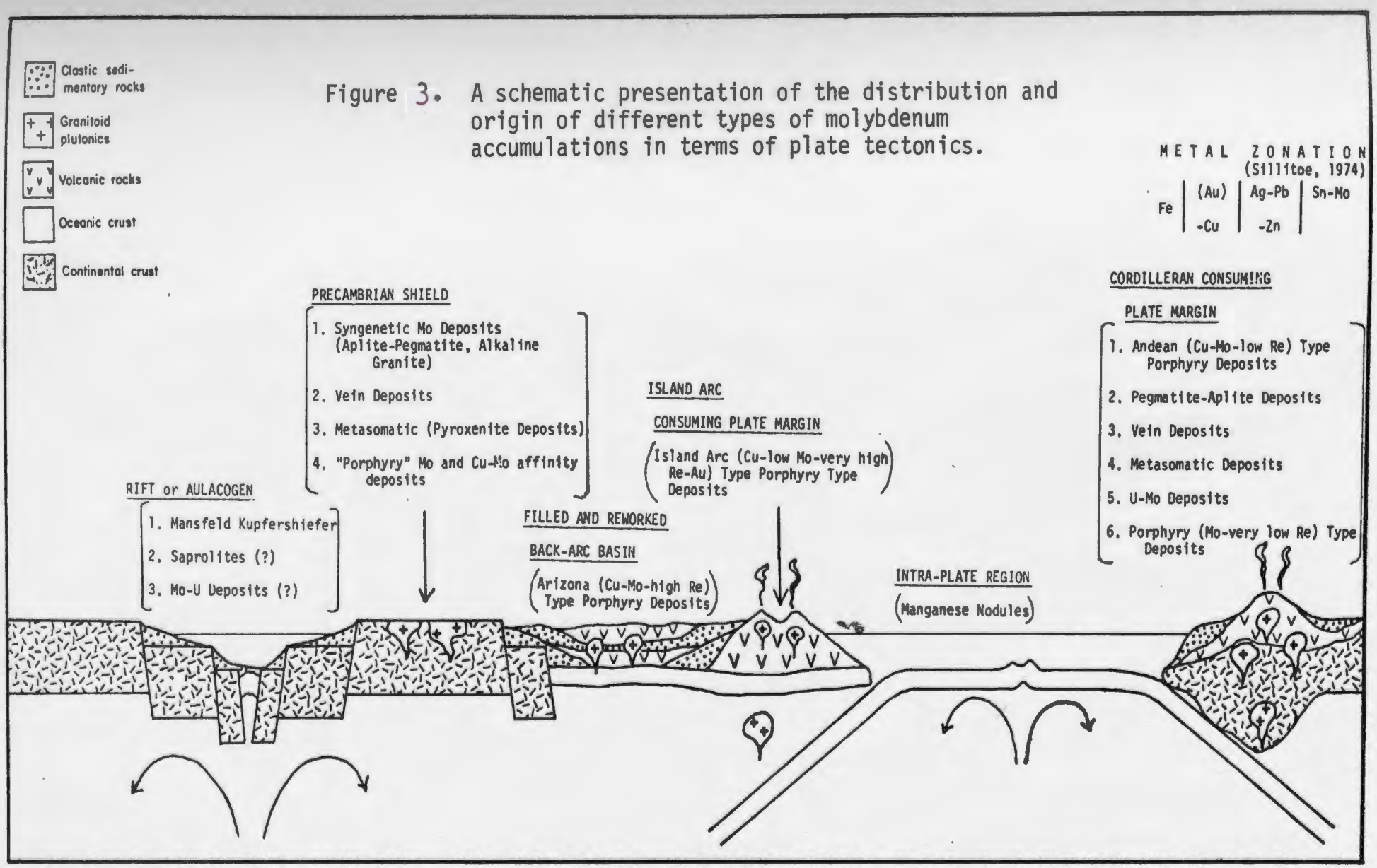

Figure 3. A schematic presentation of the distribution and origin of different types of molybdenum accumulations in terms of plate tectonics.

CHAPTER 3

GENERAL GEOLOGY

3.1 General Statement

The Canadian Appalachian structural province has been subdivided into nine zones based on different "Ordovician and earlier depositional and/or structural histories" (Williams et al., 1972 and 1974). The study area lies in the western portion of the Avalon Zone or Zone H (Fig. 1). The main work of the present study was concerned with the Ackley City granite and its associated mineralization with reconnaissance observations and sampling of the country rocks. Examination of the geochemistry and petrology of the volcanics is being undertaken as part of a separate study (Whalen and Strong, in prep.), but the following chapter is based mainly on the work of White (1939) and Williams (1971).

The two main opposing interpretations of the stratigraphy of the area are given in Table 3, and the geology according to Williams (1971) is given in Fig. 4. The eastern part of the map-sheet is underlain mainly by a thick succession of silicic and minor mafic volcanic rocks (Belle Bay Formation), overlain by grey sedimentary rocks (Anderson Cove Formation), mixed basic volcanic and red sedimentary rocks (Mooring Cove Formation) and thick purple to red clastic sediments (Rencontre Formation).

TABLE 3

Stratigraphic Succession in Belleoram Map Area

Period	White (1939)	Williams (1971)
Pleistocene	glacial outwash	glacial outwash
Devonian	Acid & Basic Dykes Ackley Batholith	Acid Dykes Basic Dykes ____intrusive contact____ Belleoram Stock ____intrusive contact____ Great Bay de l'Eau Formation ____unconformity____ Ackley Batholith
Devonian or Earlier (?)	Rencontre Formation ____unconformity____	Pyroxenite , gabbro, diorite ____intrusive contact____ Pools Cove Formation ____regional disconformity____ Cinq Isles Formation
Ordovician	Long Harbour Series: Mooring Cove volcanics; Anderson Cove slates; Belle Bay volcanics	
Ordovician or Earlier	Youngs Cove Group Doten Cove Formation	Garrison Hills Gneiss ____Hermitage Fault____ Simmons Brook Batholith not in contact
Cambrian or Late Precambrian	Bay du Nord Series: Spyglass Cove Formation; Tilt Point Formation; Poole's Cove Formation; Bay d'Est Formation; Spoon Cove Formation	Young's Cove Group
Late Precambrian	Gneissic granites Gneisses	Long Harbour Series: Rencontre Formation; Mooring Cove Formation; Anderson Cove Formation; Belle Bay Formation

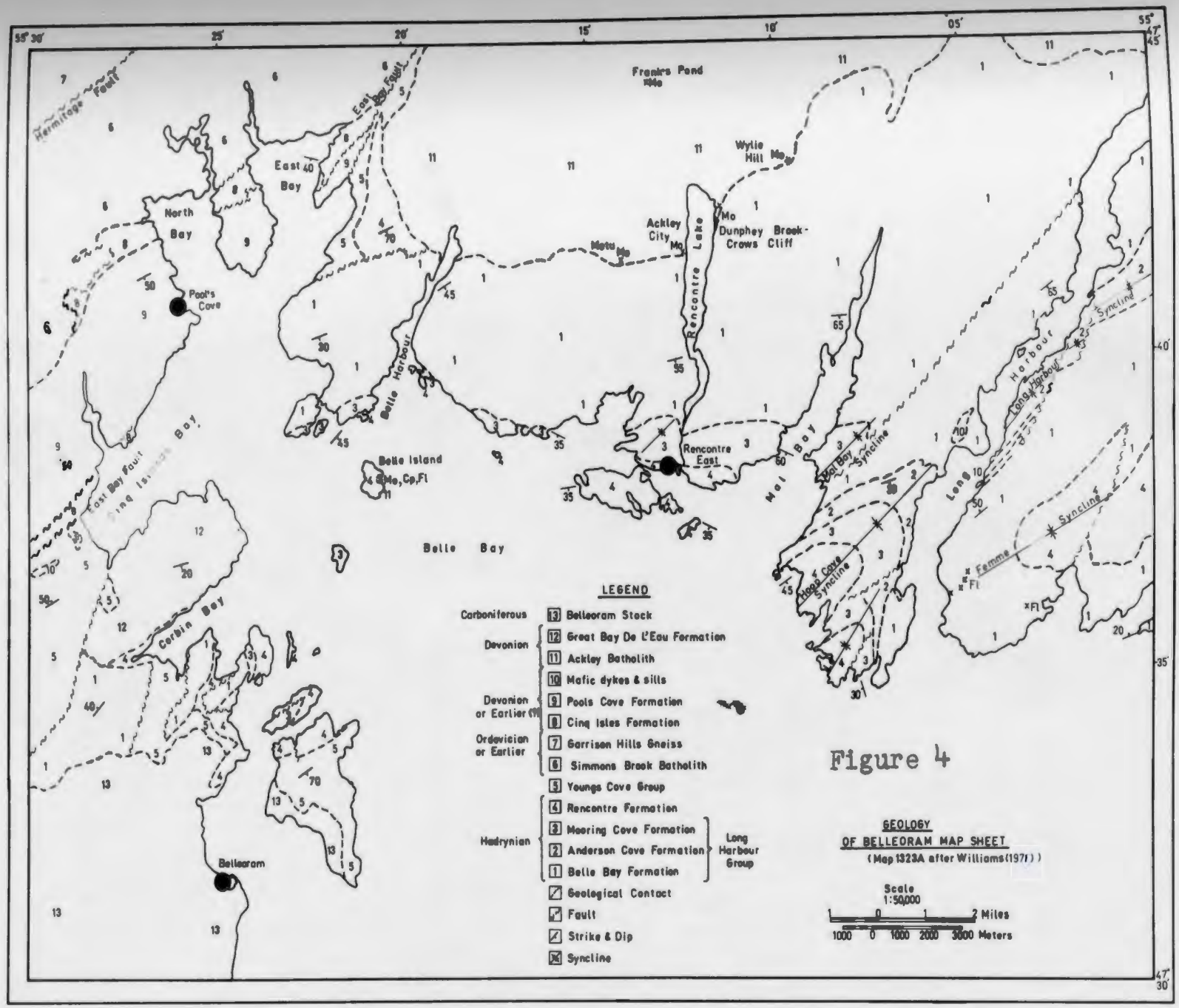
Hermitage Fault
East Bay Fault
East Bay
North Bay
Pool's Cove
Cinq Isles Bay
East Bay Fault
Belle Harbour
Belle Island
Mo,Cp,Fl
Belle Bay
Corbin Bay
Bellearam
Frank's Pond
Wylie Hill
Ackley City
Motu
Rencontre Lake
Dunphey Brook-Crows Cliff
Rencontre East
Mal Bay
Pool Bay Syncline
Hogg Cove Syncline
Long Harbour
Long Harbour Syncline
Femme Syncline
Fl
LEGEND
Carboniferous
13 Bellearam Stock
Devonian
12 Great Bay De L'Eau Formation
11 Ackley Batholith
10 Mafic dykes & sills
Devonian or Earlier (?)
9 Pools Cove Formation
8 Cinq Isles Formation
Ordovician or Earlier
7 Garrison Hills Gneiss
6 Simmons Brook Batholith
5 Youngs Cove Group
Hadrynian
4 Rencontre Formation
3 Mooring Cove Formation
2 Anderson Cove Formation
1 Belle Bay Formation
Long Harbour Group
Geological Contact
Fault
Strike & Dip
Syncline
Figure 4
GEOLOGY
OF BELLEORAM MAP SHEET
(Map 1323A after Williams (1971))
Scale
1:50,000
1 0 1 2 Miles
1000 0 1000 2000 3000 Meters

These four formations, the Long Harbour Group, are overlain in local areas by Cambrian or Late Precambrian rocks of the Youngs Cove Group. All these rocks are folded about northeast trending axes and cut by batholithic intrusions of pre-Devonian, Devonian and post-Devonian age. Between Cinq Islands Bay and Corbin Bay, Upper Devonian conglomerates of the Great Bay de L'Eau Formation unconformably overlie Cambrian and Late Precambrian rocks. The area between the East Bay Fault and the Hermitage Fault is mainly underlain by the Simmons Brook Batholith which is unconformably overlain by red sandstone and limey shale of the Cinq Isles Formation in turn overlain by red clastic sediments of the Pools Cove Formation.

The main difference between the above interpretation of Williams (1971) and that of earlier workers (White, 1939; Widmar, 1950; Smith and White, 1954 and Bradley, 1962) is the age of the Long Harbour Group (Table 3). Earlier workers interpreted the Belle Bay Formation to overlie Cambrian strata unconformably while Williams indicated that the boundaries are faults, an interpretation which is supported by a whole rock Rb/Sr age of the volcanics of 500 m.y. The following sections give brief descriptions of the different formations except for the Ackley City Batholith which is examined in detail in the next chapter.

3.2 Long Harbour Series

3.2.1 Belle Bay Formation

The base of the Belle Bay formation is truncated by the younger granites while the top of the formation is marked by the overlying grey sedimentary rocks of the Anderson Cove Formation or where the dominantly volcanic assemblage is succeeded by the alternating sedimentary and volcanic units of the Mooring Cove Formation. This formation, which constitutes the major part of the Long Harbour Group, forms a southward-facing succession between East Bay and Mal Bay with thickness estimated to be at least 5,000 feet.

The Belle Bay Formation consists of mainly silicic volcanics with lesser mafic volcanics in alternating units from 300 meters or less to 1,000 meters or more thick and minor tuffaceous sedimentary rocks and purple sandstone. The silicic volcanics are mainly pink to purple and red rhyolite flows, ignimbrites, lithic tuff, crystal lithic tuff, agglomerate and spherulitic rhyolite. The mafic volcanics are mainly green to purple amygdaloidal basalt. Rare tuffaceous sediments occur mainly in irregular bands and lenses among the volcanics.

3.2.2 Andersons Cove Formation

The Andersons Cove Formation is a distinct sedimentary assemblage of finely laminated grey argillite or shale with wavy irregular bedding, grey siltstone and grey sandstone that overlies the Belle Bay Formation. The formation is probably 300 to 450 meters thick.

The base of the formation is marked in most places by a purple to red volcanic boulder conglomerate, purple sandstone and pebble-conglomerate or red crystal tuff and agglomerate. The overlying coarser clastic rocks occur in beds a few inches to a foot or more thick. The argillites commonly display 10 to 15 laminae in a 2.5 centimeter stratigraphic thickness. The grey clastic sedimentary rocks are monotonous except at the base of the formation where purple argillite and sandstone interlayers are present.

3.2.3 Mooring Cove Formation

The Mooring Cove Formation is dominantly a mixed volcanic assemblage that overlies the Andersons Cove Formation and is succeeded by sandstone of the Rencontre Formation in Hoop's Cove and Long Point Synclines. Similar rocks between Mal Bay and East Bay directly overlie the Rencontre Formation. The thickness of the formation varies from 450 meters to a maximum of 750 meters.

The Mooring Cove Formation consists of minor red to pink rhyolite, amygdaloidal and porphyritic basalt and associated purple to grey sedimentary rocks. Fifteen to forty-five meters thick individual mafic flows are easily distinguishable by means of brecciated and more highly amygdaloidal flow tops. Purple to red sandstone, conglomerate, and argillite occur interlayered with the volcanics.

3.2.4 Rencontre Formation

The Rencontre Formation overlies the Mooring Cove Formation, its base being drawn at the top of the highest volcanic unit in the Mooring Cove Formation. The formation is present in the axial zones of the Femme, Hoop Cove, Long Point and Mal Bay Synclines. The thickest section of 1,500 meters is exposed across Rencontre Island.

The Rencontre Formation consists of pale purple and deep purple, grey and red, crossbedded sandstone, red micaceous sandstone, and pebble-conglomerate, with thin interlayers of bright red siltstone, sandstone, and argillite. The formation apparently thickens and coarsens from west to east suggesting derivation from the east, a relationship which is supported by the direction of cross-bedding and cut and fill structures (Twenhofel, 1947).

3.3 Young's Cove Group

The Young's Cove Group is a sequence of shales, siltstones, and sandstones that form a thin northeast trending belt in the type area along the east shore of East Bay. It appears to conformably overlie redbeds of the Rencontre Formation and has an estimated thickness of 600 meters in the type area (White, 1939). The Young's Cove Group consists of grey to green micaceous siltstone, light to dark grey shale and argillite, and grey to green micaceous sandstone. Trilobite fragments of early Middle Cambrian age are present in the Young's Cove Group.

3.4 Simmons Brook Batholith

The Simmons Brook Batholith is considered to be Ordovician or earlier, as it is unconformably overlain by the Cinq Isles Formation of Devonian or earlier age. The batholith is a composite, elongate intrusion which is composed of pink to grey, medium- to coarse- grained granite and granodiorite with locally predominant dark green mafic intrusive rocks. The mixed acid to mafic lithology and foliation of the batholith distinguishes it from the homogeneous and undeformed Ackley and Belleoram intrusives.

3.5 Garrison Hills Gneiss

The Garrison Hills Gneisses are coarse-grained, foliated and porphyroblastic biotite gneiss, muscovite-biotite gneiss, and fine grained, pink foliated gneiss that is interpreted as mylonite. Everywhere along their southeastern margin the gneisses are bounded by faults, which were interpreted to represent part of the fundamental break which in Newfoundland separates the Avalon zone from the Central Moble Belt (Williams, 1969).

3.6 Cinq Isles Formation

The Cinq Isles Formation forms a northeast trending, steeply southeast-dipping succession approximately 0.8 km wide that extends from Parsons Cove in East Bay southwesterly to Salmon River, and is missing or preserved only in local patches elsewhere. It is

approximately 300 meters thick. The formation is composed of red micaceous siltstone and shale, grey and reddish crossbedded sandstone, grey micritic limestone and quartz-pebble conglomorate (Calcutt, 1974).

3.7 Pools Cove Formation

The Pools Cove Formation forms a northeast trending, southeast-dipping succession which has a thickness estimated at between 1,200 and 1,500 meters. The formation is separated into three mappable units, a basal unit approximately 150 meters thick consisting of coarse red conglomerate, a central unit about 400 feet thick consisting mainly of coarse arkosic sandstone and arkosic conglomerate, and an upper unit of boulder conglomerate and coarse arkosic sandstone interbeds.

3.8 Mafic Intrusions

A wide variety of small mafic intrusions occur throughout the area, some of which are northwest trending dykes of Devonian age, however another group of intrusions occur as northeast trending dykes and sills, and as small plugs, and cut only Cambrian and older rocks. They include dioritic, gabbroic, and ultramafic rocks.

3.9 Great Bay de L'Eau Formation

The Great Bay de L'Eau Formation occurs only at Corbin Head Promontory and consists of relatively undeformed layered conglomerates which strike parallel to the shoreline and dip gently to moderately inland, forming an open synclinal

structure. At least 500 to 1,000 feet of strata are exposed. The formation consist of poorly bedded purple to red, grey and buff cobble and boulder conglomerate. Clasts within the rock are in most cases similar to immediately underlying rocks and therefore pebble or clast lithology changes markedly where it overlies contrasting rock types.

3.10 Belleoram Stock

The Belleoram Stock occupies the southwest corner of the area and intrudes the Long Harbour and Youngs Cove Groups toward the north, and to the southwest it intrudes the Upper Devonian Great Bay de L'Eau Formation. It is composed of uniform grey to pink massive granite which is medium grained and equigranular, with potash feldspar and plagioclase in roughly equal amounts. It has between 10 and 20 percent mafic constituents, chiefly amphibole with lesser biotite, and usually not more than 10 percent quartz. The Belleoram granite has been dated isotopically at 400 and 342 million years (Wanless et al., 1965, 1967) but because it intrudes the Upper Devonian Great Bay de L'Eau Formation a Late Devonian or Early Carboniferous age is probable.

3.11 Dyke Rocks

A variety of dykes of unknown affinity and age occur throughout the map area. Almost all trend north-northwest and are steeply dipping or vertical. They vary

in width from a meter to a few tens of meters, rarely exceeding 15 meters and range in composition from basic to intermediate to acid with the more acid varieties being most abundant.

CHAPTER 4

THE ACKLEY CITY BATHOLITH

4.1 Introduction

The Ackley City Batholith intrudes Precambrian rocks of the Long Harbour Group, the Love Cove Group and the Musgravetown Group, Cambrian rocks of the Young's Cove Group, all in the Avalon Zone, and Middle Ordovician (Jenness, 1963) or Middle Ordovician and Pre-Ordovician (Kennedy and McGonigal, 1972) rocks of the Gander and Davidsville Groups in the Gander Zone (Williams et al., 1972). The name 'Ackley', first used by White (1939, 1940) for the granite that constitutes the northern part of the Belleoram (Rencontre East) map area, was subsequently used by Bradley (1962) for the eastward extension of the batholith and by Jenness (1963) and Williams (1968) for the northward extension of the batholith. Workers on the southern (White, 1939; Bradley, 1962; Anderson, 1965; Williams, 1971) and northern (Jenness, 1963; Williams, 1968) parts of the Ackley City Batholith have considered it to be Devonian earlier on the basis of correlation with known Devonian granites and more recently on the basis of geochronological evidence. The Ackley granite has been dated by the K/Ar method as 350, 368, 365 and 352 m.y. giving an average age of 365 ± 15 m.y. (Jenness, 1963) and by whole rock Rb/Sr as 345 ± 10 m.y. (Bell and Blenkinsop, 1975).

4.2 Structure

The overall concordancy of the Ackley City Batholith with regional structural trends indicates that the emplacement of the pluton was largely controlled by the pre-existing structural framework. However, the way in which the granitic rocks often cross-cut large scale anticlinal and synclinal structures, the sharp intrusive nature of the observed intrusive contacts, and the lack of any pronounced internal structures indicates that the intrusion was post-tectonic and relatively passive. The post-tectonic emplacement is supported by the presence of roof pendents in the southeast part of the intrusion which contain pre-emplacement large scale fold structures. Moreover, as shear zones and faults were rarely observed within the batholith it appears the pluton has not undergone any major deformation since its intrusion.

Internal structures within the granite are not present or only of local extent, for no alignment of constituent minerals, such as biotite or feldspars, was observed in the study area or in samples collected on a regional scale from the intrusive by Strong et al. (1974). There are samples, however, which display a strong foliation consisting of quartz-feldspar and biotite-epidote-calcite-hornblende rich bands (CD 472, 496, 497, 498). The deformed-metamorphic fabric and the fact that

geochemically they are more mafic (higher in Fe, Mg, Ca and Ti and lower in Si and K) than other Ackley samples suggests that these rocks probably represent older gneissic material which has been mapped as part of the Ackley City batholith.

A stereogram plot of poles to joint planes from the Ackley granite in the study area (Fig. 5) suggests that there are three nearly vertical sets along with a fourth set which is approximately horizontal. Orientation of the joints in the country rocks in the vicinity of the granite is similar to those within the granite, but much more variable in detail. The major trend is NW-SE with less important sets striking E-W and NE-SW. The sub-horizontal joints, which dip very gently and have variable strikes, forming sheeting structures, were probably produced as a result of tension perpendicular to the roof of the batholith during cooling and later accentuated during removal by erosion of the superincumbent load of host rocks. The other joint directions may be interpreted in terms of the concept of the strain ellipsoid described by Ramsey (1967). The direction of greatest compression (P) could be interpreted as being orientated midway between the NW-SE and NE-SW striking joints at 010° while the direction of greatest release is perpendicular to it and approximately parallel to the E-W striking joints (Fig. 6). With such

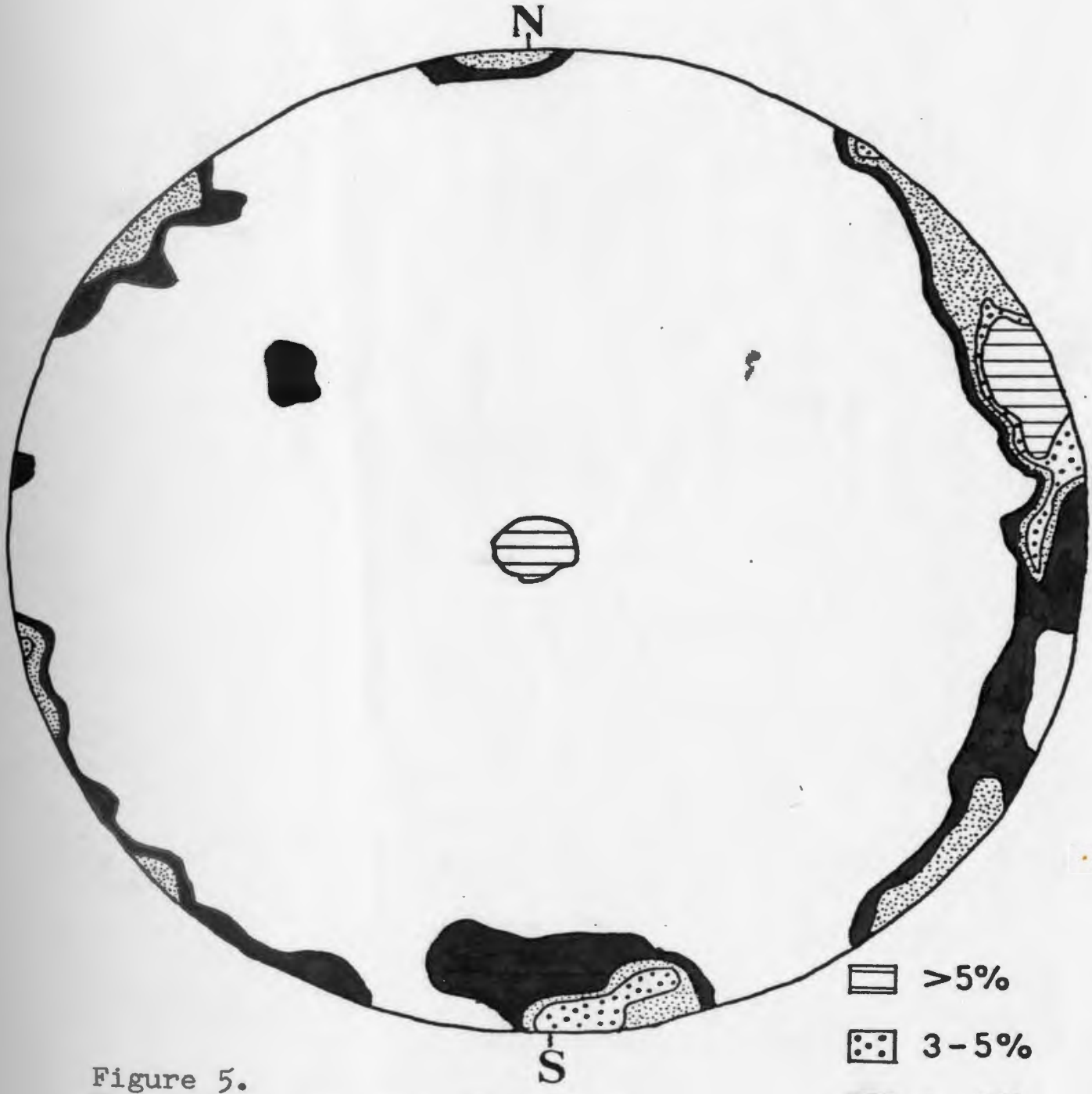

>5%
3-5%
2-3%
1-2%
0-1%

Figure 5.
Equal area net plot of poles to joints for the alaskite granite near and at the molybdenite showings. Contoured data for 360 joint readings.

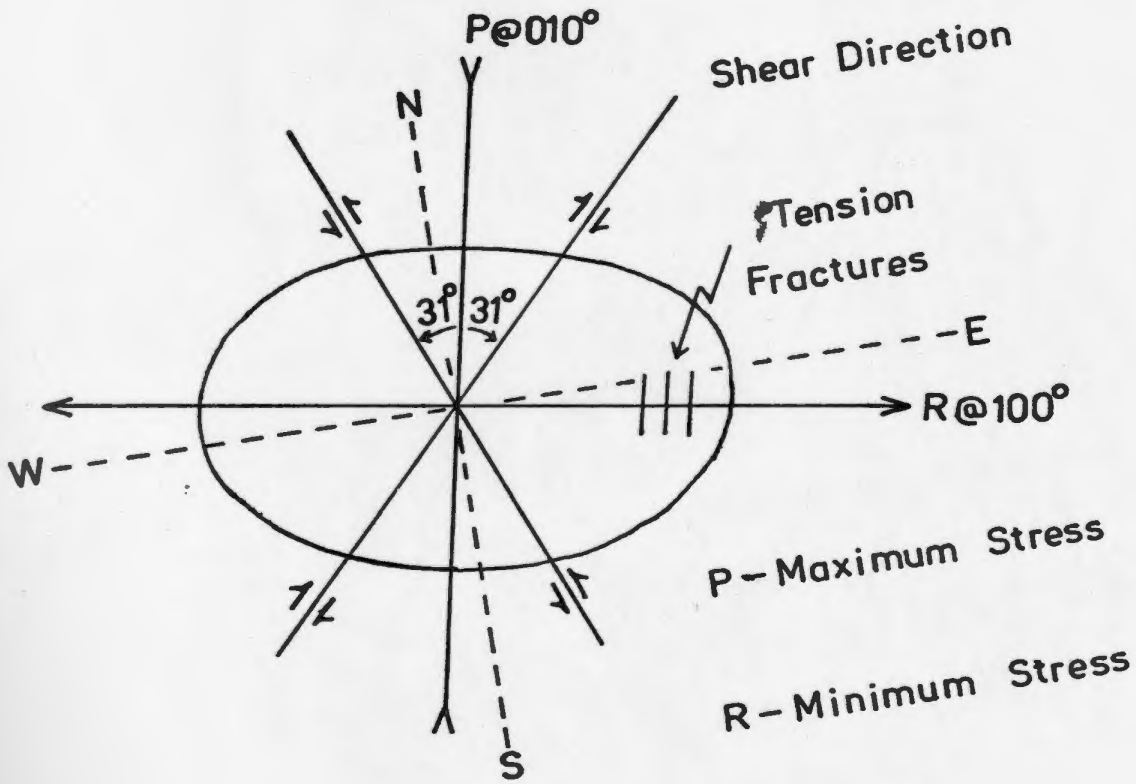

Figure 6. Strain elipsoid for the Ackley City batholith near the molybdenite showings based on joint data.

an orientation of stress the NW-SE and NE-SW joints represent a conjugate set of shear fractures developed at 31° to the principle stress while the E-W joints set are tension factures developed parallel to the direction of minimum stress. This direction of maximum stress is at variance with that suggested by known regional structural features (mainly NW-SE), and since it represents analysis of joint data from such a small area no major regional implications can be inferred.

Magnetic measurements which have been made over the Ackley City batholith (Fig. 7) indicate that there is a magnetic high over the central part of the intrusive of the order of 1,400 to greater than 1,600 gammas, while it is bordered to the east and west by magnetic lows of the order of 800 to 1,000 gammas. The basic volcanics of the Long Harbour series and the roof pendents in the Batholith in the south and the metamorphic and granitic rocks to the north are reflected by magnetic highs. Gravity measurements which have been made over the Ackley City batholith (Fig. 8) indicate that there is a gravity low over the intrusive averaging approximately -80 milligals and varying between 0 and -115 milligals. The host rocks to the west have low positive values while the rocks to the south and east are characterized by quite strongly positive values. The granitic and metamorphic rocks to the north of the intrusive are reflected by negative gravity values.

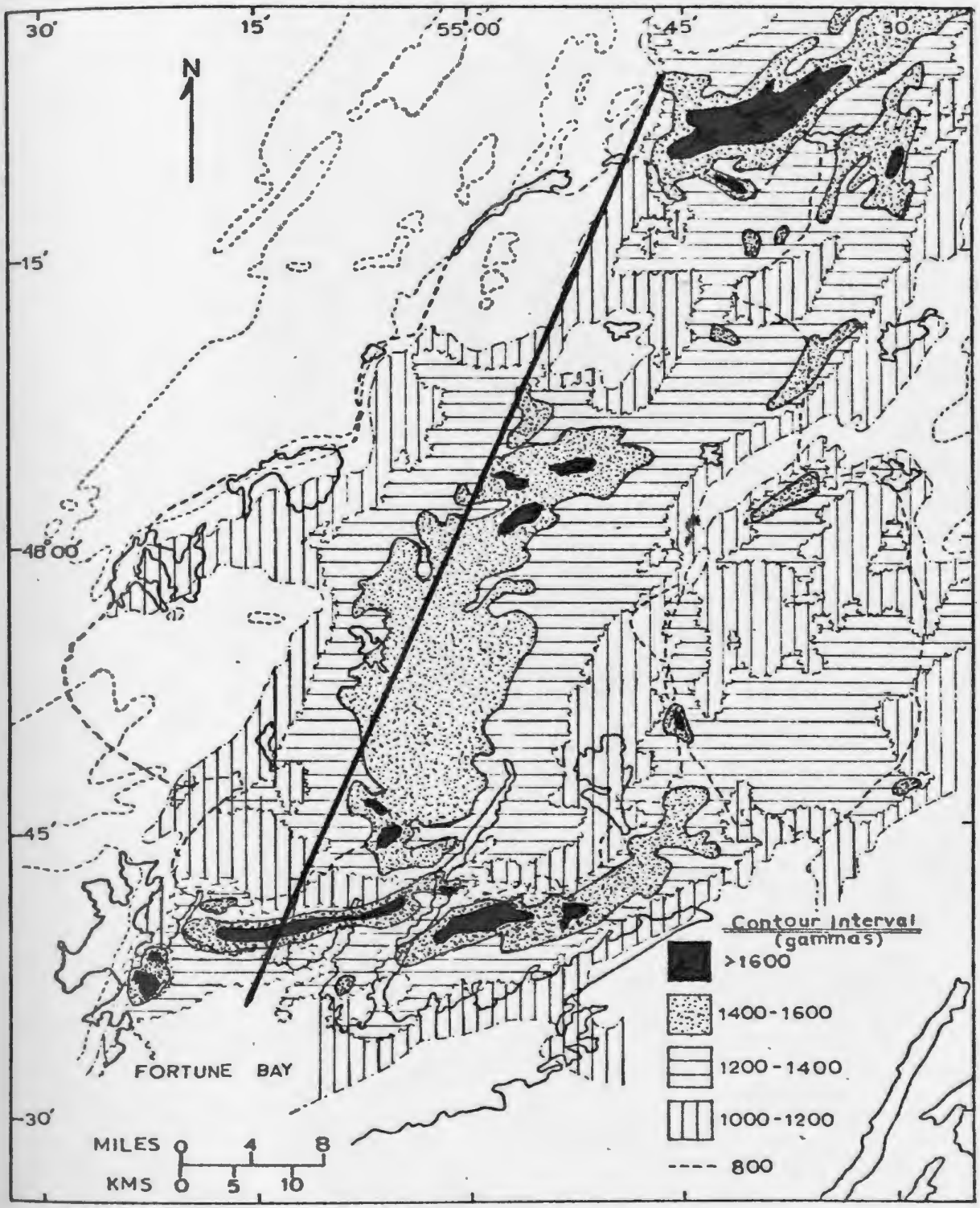

Figure 7. Aeromagnetic map of the Ackley City batholith, solid NE-SW line is the location of the aeromagnetic cross-section in Fig. 9a. Aeromagnetic data from Map 7048G (1968) - Gander Lake, Map 7326G (1971) - St. Lawrence, and Map 7330G (1971) - Belleoram.

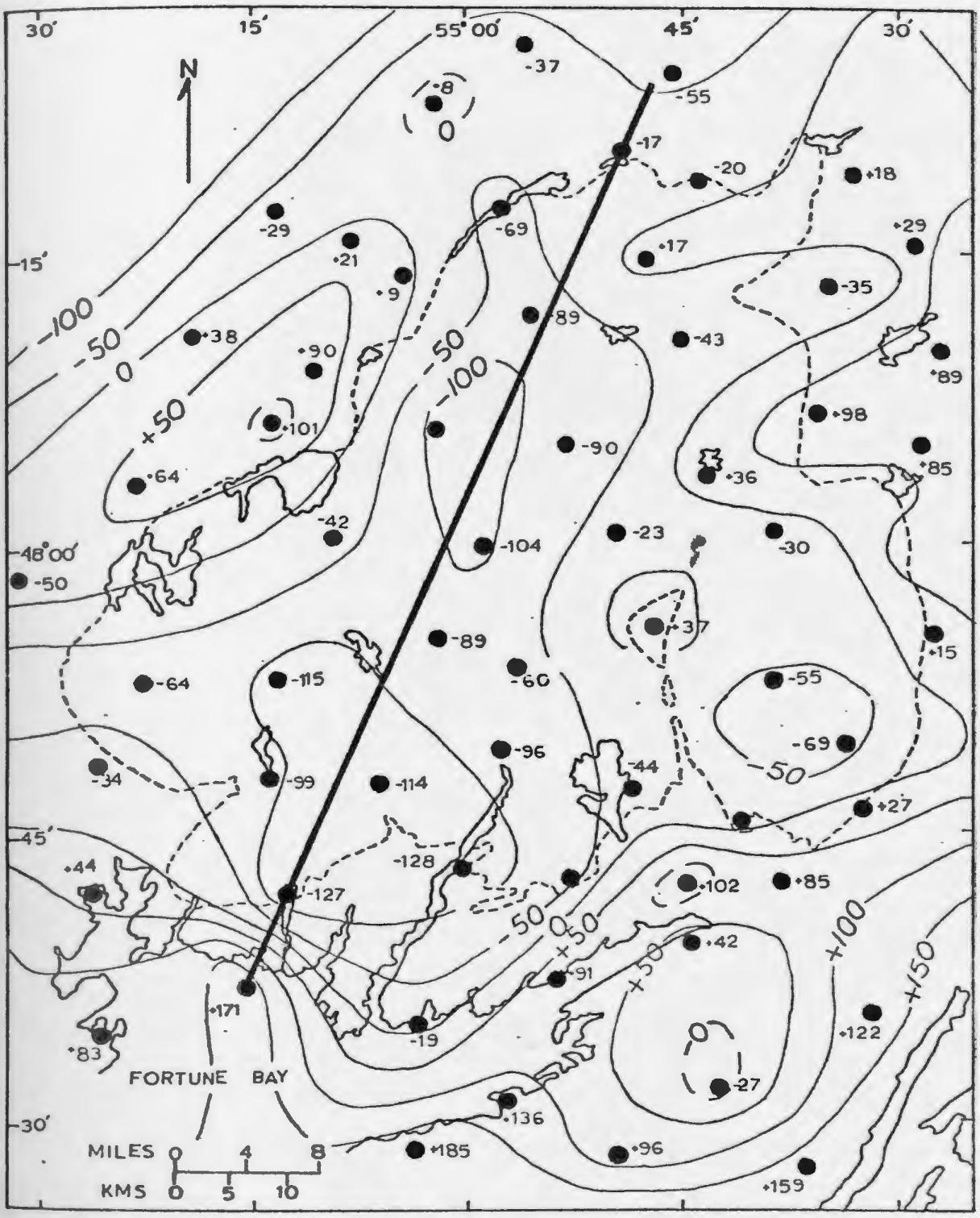

Figure 8. Bouger anomaly gravity map of the Ackley City batholith (in milligals) after Dominion Observatory Branch, Department of Energy, Mines and Resources Gravity Map Series No. 53. Thick solid NE-SW line is the location of the gravity cross-section in Fig. 9b.

The Ackley City batholith in cross-section is reflected by a magnetic high (Fig. 9a), a fact which can be explained by a high magnetite content within the granite, an explanation which is supported by petrological studies (see 4.4). The higher values over the centre of the intrusive could be the result of a higher content of magnetite in these areas or by greater thicknesses of granite of the same magnetite content. The second explanation is supported by the close correspondence between the areas of magnetite highs and gravity lows in the granite. The granite is characterized by a Bouger anomaly low in cross-section (Fig. 9b). A cross-section constructed using the gravity data and the rock densities of Weaver (1967) (Fig. 9c) suggests that the Ackley City batholith is a relatively thin flat sheet approximately 2 km thick.

4.3 Contact Relationships and Metamorphic Effects

The observed contacts of the Ackley City batholith in the study area are sharp, and similar contacts were reported by other workers at the other margins of the intrusive (Bradley, 1962; Jenness, 1963; Anderson and Williams, 1970; Williams, 1971) except at the north-east margin where Jenness (1963) found it to be gradational. The batholith has a thin thermal metamorphic aureole which rarely exceeds 400 m, except in the north-east margin where the metasomatism of schists and paragneiss over many square kilometers with addition of large quantities of potash, soda and silica makes drawing of contacts difficult (Jenness, 1963). On the southern

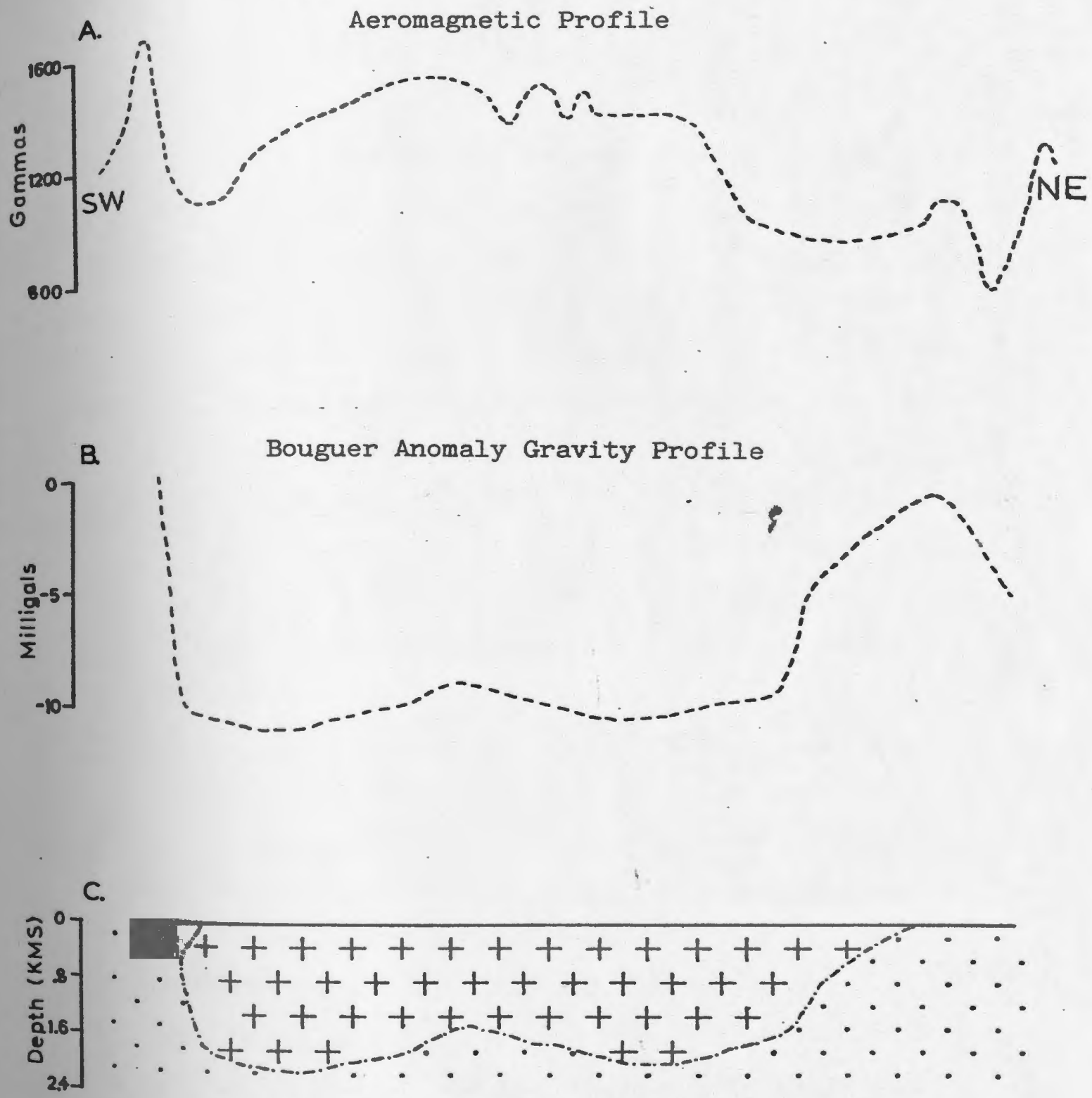

Figure 9. Northeast to southwest aeromagnetic (a), and gravity (B) profiles through the Ackley City batholith. Based on the gravity data and a density contrast of -.09 (from use of Weaver (1967) density data) the thickness of the intrusive was calculated (c).

margin thermal metamorphic effects are most apparent in the sedimentary rocks of the Rencontre Formation and Young's Cove Groups where original purplish red and grey sandstone, siltstone, and shale have been converted to dark grey to pale purplish, hard cherty hornfels (Williams, 1971). At Isle à Glu Pond, just west of the Motu Mo showing, mafic volcanic rocks of the Belle Bay Formation have been converted to black hard hornfels near the granite contact. In the silicic volcanic rocks thermal effects are less noticeable. They are characterized by the development of white mica on fracture surfaces and pinkish red, irregularly circular alteration spots which have dark green chlorite centers within 20 meters of the granite contact. At all observed contacts, however, there appears to be very little evidence for anything but thermal metamorphism of the host rock. A lack of metasomatism of host rhyolite, at least on a major scale, is compatible with the analysis of rhyolites near the contact of the granite in comparison with the average composition of rhyolitic rocks of the Belle Bay Formation (Table 4), there being complete overlap of the compositions and no systematic variation in relation to distance from the contact.

4.4 Geology, Lithology, and Petrology

The Ackley City batholith is, as would be expected for a body of such size, a composite intrusion. This was suggested by Bradley (1962) for the Terrenceville map-area,

Table 4

COMPARISON OF THE CHEMISTRY OF BELLE BAY FORMATION RHYOLITE NEAR THE ACKLEY CITY BATHOLITH

WITH THE AVERAGE REGIONAL RHYOLITE COMPOSITION

Element	Rhyolites at Motu Showing			Rhyolites at Wylie Hill Showing				Composition of Rhyolite at Contact		Average Composition of Belle Bay Formation Rhyolites*	
Distance from Contact	30.5 m	10 cm	20 cm	21.4 m	117.4 m	2 cm	.17 m				
	75-91	75-92	75-97	69-2-110	69-11-441	69-12-135	69-12-135	$\bar{x}$	σ	$\bar{x}$	σ
SiO_2	78.40	77.30	78.40	75.45	75.13	76.24	75.25	76.94	1.02	76.00	2.23
TiO_2	.15	.13	.13	.05	.11	.12	.05	.11	.03	.22	.08
Al_2O_3	9.20	11.40	10.30	12.17	11.37	12.71	11.60	11.25	1.02	11.76	1.39
Fe_2O_3	1.10	1.00	1.62	2.40	2.76	2.09	3.70	2.10	.83	2.12	1.05
FeO	.87	.95	.54	N.A.	N.A.	N.A.	N.A.	.79	.20	.58	.36
MnO	.02	.02	.01	.04	.11	.06	.02	.04	.03	.06	.04
MgO	.07	.02	.02	.02	.18	.02	.25	.08	.08	.08	.07
CaO	.00	.00	.00	.27	2.57	.17	.19	.46	.81	.14	.21
Na_2O	1.20	2.61	3.90	4.85	2.76	4.24	3.57	3.30	1.05	3.64	1.13
K_2O	6.60	5.19	4.91	4.95	5.06	4.68	.68	5.15	.58	4.55	.92
H_2O	.40	.24	.27	.10	.77	.06	1.23	.44	.36	.59	.42
Total	98.01	98.86	100.10	100.35	100.82	100.39	100.54	100.66		99.74	
Zr	882	783	845	534	628	767	665	649	173	945	334
Sr	1	ND	ND	10	19	6	8	13	12	24	40
Rb	262	219	208	213	193	187	216	213	22	174	48
Zn	24	37	25	61	40	105	239	87	67	112	105
Cu	9	2	20	36	40	31	138	30	42	7	6
Ba	28	24	19	461	475	446	420	359	283	191	218
Nb	43	40	42	34	41	34	27	39	5	50	25
Pb	22	25	39	29	28	37	57	29	13	41	29
Ni	21	13	13	6	9	10	45	22	9	14	5
Y	186	77	95	118	124	126	112	115	29	145	45
Cr	5	11	3	10	3	9	88	18	27	7	4
Ti	769	836	854	1081	972	1097	1074	965	120	1360	419
n	1	1	1	1	1	1	1	7		44	

$\bar{x}$ = mean σ = standard deviation n = number of samples

* = analyses from Whalen and Strong , in prep.

and is further supported by Jenness' (1963) description of the northern part of the batholith. However, no previous attempt has been made to determine the nature, number, extent and intrusive relationships of the different phases. On the basis of examination of a limited number of samples collected by Strong et al. (1974) from the Ackley City batholith (Fig. 10) it is possible to recognize a number of phases. There appears to be two major intrusive types, megacrystic granite and alaskitic granite, but there are also some minor leucocratic granitic phases and gneissic granites in the batholith area. The extent and the location of the contacts of the different phases is difficult to determine on the basis of sample density, although the geophysical data is of some assistance. The megacrystic granites of the northern Gander zone are characteristized by highly irregular magnetic contours, a relationship which is true of the known area of that type of granite in the northern part of the intrusive (Fig. 7). On this basis and using the extent of a gravity low over the alaskite phase (Fig. 8) an approximate contact is suggested between the alastite and megacrystic granite (Fig. 10). The other leucocratic granite phases are of unknown extent, but can probably be assumed to cover only small local areas. The amount of area covered by older gneissic granite in the northern part of the intrusive is unknown. Descriptions by Jenness (1963) and examination of similar areas further north (Kennedy and McGonigal, 1972; Jayasinghe and Berger,

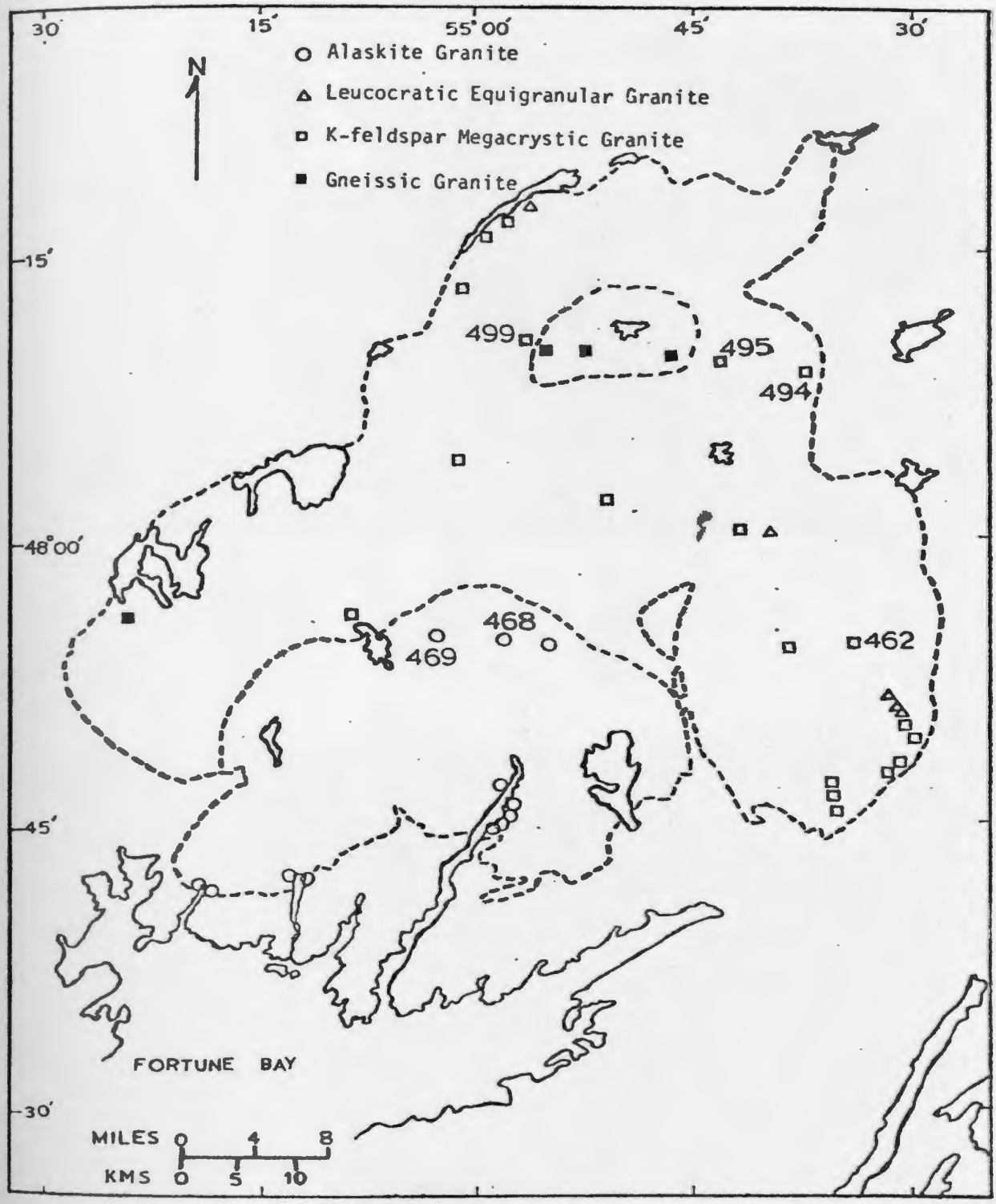

Figure 10. Different intrusive phases of the Ackley City batholith, based on indicated samples from Strong et al. (1974) and boundaries inferred from differences in aeromagnetic patterns (irregular in the north and smoother in south (Fig. 7) and gravity patterns (Fig. 8). The samples with numbers (CD prefix omitted) are those employed for whole rock Rb/Sr dating of the batholith by Bell and Blenkinsop (1975).

in prep.) suggest there may be complex deformation-intrusive relationships in the area, but recent whole-rock Rb/Sr age dating in that area (Bell and Blenkinsop, 1975) suggest that such processes did not occupy a particularly long time span.

The megacrystic granite consists of subhedral to euhedral light pink K-feldspar megacrysts (2-5 cm) in a relatively equigranular, medium grained, white to grey matrix of interlocking anhedral quartz, subhedral feldspar and small variable amounts of ragged biotite. Twenty thin sections of the megacrystic granite were examined. Quartz forms compositely grained anhedral strained aggregates (1-12mm). Plagioclase is subhedral to anhedral, 2-13 mm in size, oligoclase in composition, normally zoned, usually dusted with sericite and occurs rarely in myrmekitic intergrowth with quartz (Plate 1). K-feldspar is poikilitic, subhedral to anhedral perthite. Some of the perthite megacrysts have plagioclase rims while other megacrysts have inclusions which suggest discontinuous stages of growth. The biotite is ragged, .5-5 mm in size and generally has chlorite alteration along cleavages. Accessory minerals include abundant magnetite, lesser sphene, zircon, apatite, muscovite, and a couple of sections contain radioactive tourmaline (Plate 2). The samples of megacrystic granite exhibit such great variability in appearance in terms of colour, amounts of different minerals present, idiomorphism of megacrysts and grain size that it may be

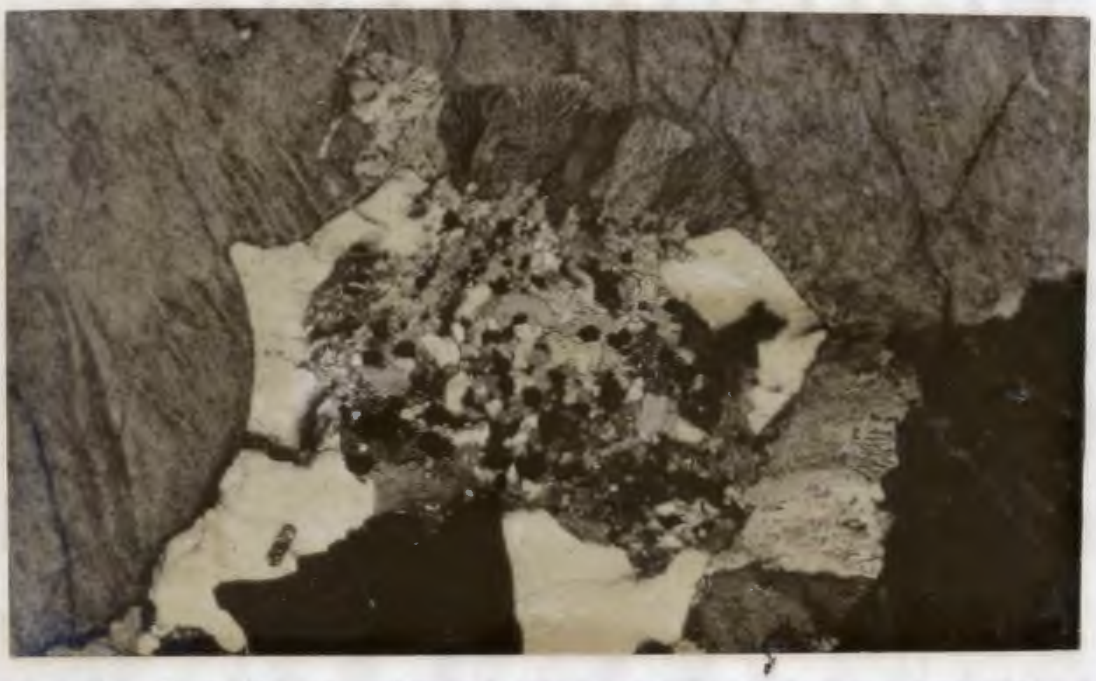

Plate 1: Perthite rimmed and replaced by myrmekitic intergrowth of plagioclase and vermicular quartz, K-feldspar megacrystic granite, crossed nicols, X60, T.S. CD-462.

Plate 2: Zoned subhedral tourmaline which has a radioactive halo when in contact with biotite (circled), K-feldspar megacrystic granite, crossed nicols, X45, T.S. CD-179.

reasonable to conclude there are a number of different megacrystic intrusive phases.

The alaskitic granite is a medium to coarse grained, equigranular, pinkish red rock consisting of interlocking aggregates of anhedral quartz and pinkish red feldspar, with rare scattered biotite (Plate 3). Twenty-two thin sections of the alaskite were examined. The quartz is strained, 2 to 8 mm in size and present as compositely grained, rounded aggregates. The plagioclase is 1-7 mm in size, oligoclase in composition and dusted with fine sericite. K-feldspar is perthitic (Plate 4), 2-9 mm in size, anhedral, and poikiolitic. The rare biotite is present as ragged, .5-2 mm, partly chloritized flakes. The main accessory is magnetite but there are also minor sphene, zircon and rare fluorite. Granophyric textures are present in some samples collected from within a km of the southern contact. Modal analyses indicate a variable composition, possibly due to the coarse grained nature of thin sections examined, of quartz 25-50%, plagioclase 14-26%, pethite 26-46%, biotite .6-3% and other less than 1%.

The other leucocratic phases are either similar to the alaskite phase or are porphyritic, fine grained granites or aplites, many of which exhibit granophyric textures. A number of such intrusive phases of the later

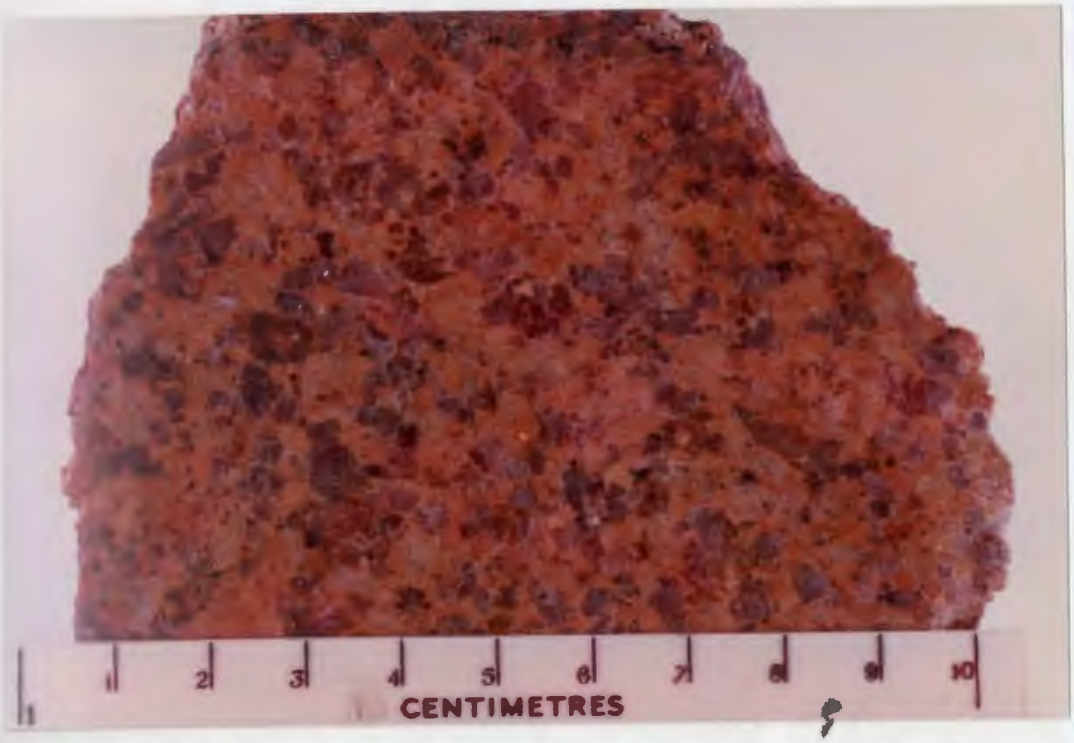

Plate 3: Alaskitic granite phase of the Ackley Batholith composed of red feldspar, quartz aggregates, and rare ragged biotite, Sample CD-334.

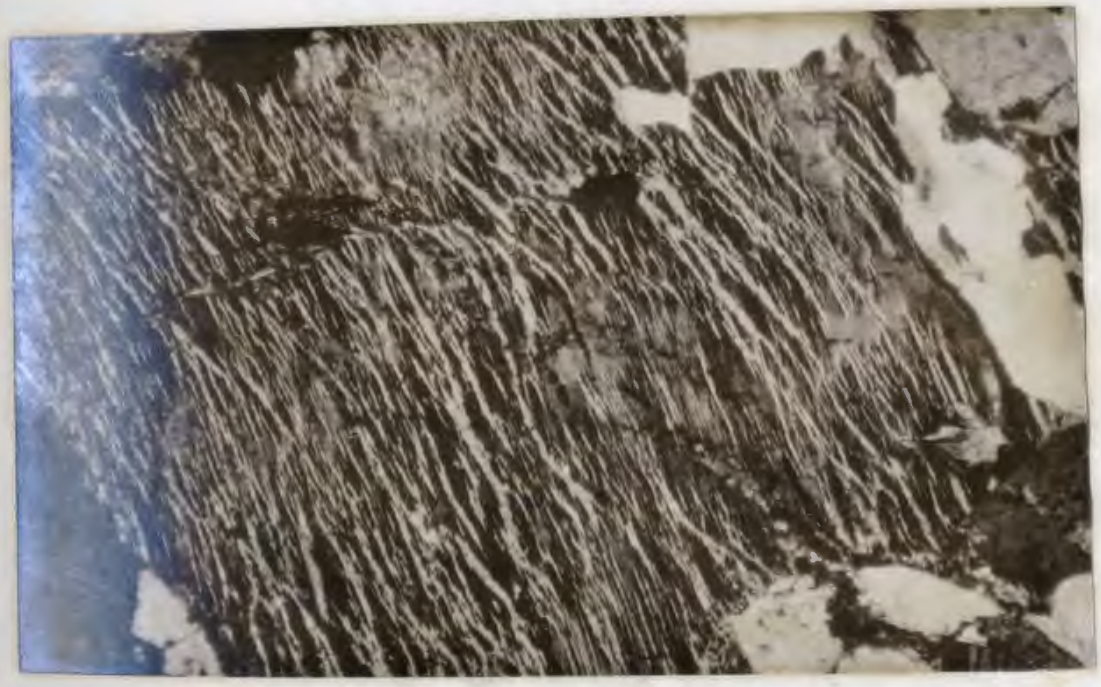

Plate 4: Strongly ribbed stringlet perthite, alaskitic granite phase, crossed nicols, X30, T.S. JW-143.

type are the host rocks of the Ackley molybdenite deposits and will be discussed in the next chapter.

The above described phases of the Ackley City batholith, the megacrystic phase which is composed chiefly of quartz, perthite, plagioclase, and biotite, and the more leurocratic phase composed essentially of quartz, perthite and lesser plagioclase can be readily classified as granite and alaskite granite, respectively (Moorhouse, 1957). They are clearly classified as mainly granite on a chemical basis, (Fig. 11), but some of the megacrystic samples are quartz monzonites and kaligranites and some of the alaskite samples are kaligranites.

4.5 Geochemistry

This section attempts to explain the causes of chemical variation within the Ackley City batholith and to provide evidence for the different phases of the intrusive constituting a plutonic series, employing data from Strong et al. (1974) and the author's own analyses of samples near the showings.

Means and standard deviations of the different intrusive phases are presented in Table 5. Some of the elements have been plotted against Thornton's and Tuttles' (1960) differentiation index (normative Q+Ab+Or+Ne+Lc+Kp) (Fig. 12 a, b). There is a tendency in some plots, notably Ba, Ba/Rb and total Fe (as Fe_2O_3) for the alaskite

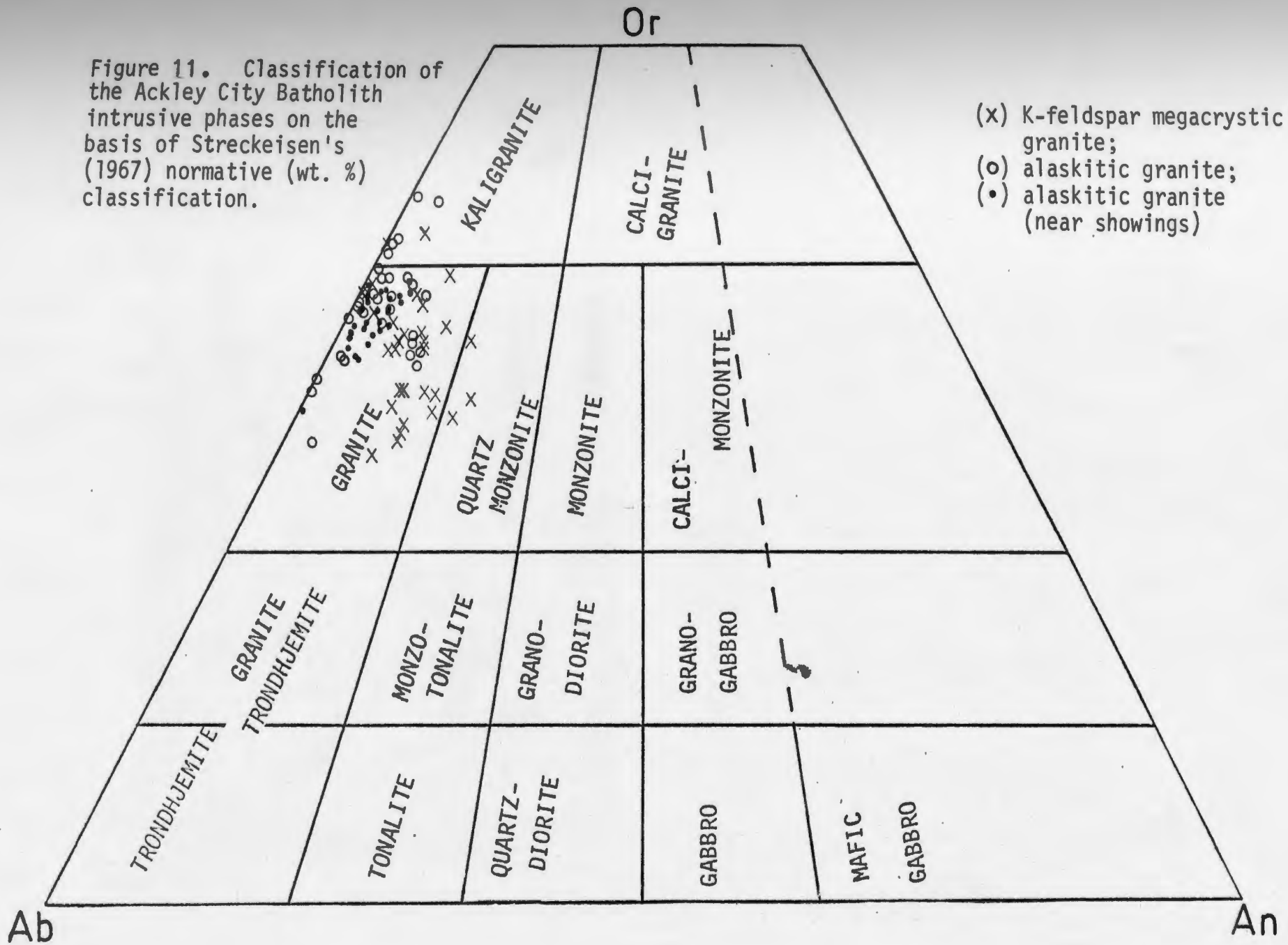

Figure 11. Classification of the Ackley City Batholith intrusive phases on the basis of Streckeisen's (1967) normative (wt. %) classification.

Table 5

COMPOSITION OF DIFFERENT INTRUSIVE PHASES OF THE ACKLEY BATHOLITH

	K-feldspar -Biotite Megacrystic Granite		Leucocratic Mg. Granite		Mg-Cg Alaskite * Granite		Mg. Alaskite Granite **	
Element	$\bar{x}$	σ	$\bar{x}$	σ	$\bar{x}$	σ	$\bar{x}$	σ
SiO_2	73.42	3.13	76.73	3.49	79.00	2.68	76.50	1.91
TiO_2	.29	.13	.21	.15	.07	.05	.22	.12
Al_2O_3	13.65	.68	12.90	1.31	12.60	.97	12.25	.67
Fe_2O_3	1.67	.64	1.27	.69	.70	.18	1.17	.42
MnO	.06	.02	.04	.02	.04	.01	.05	.02
MgO	.93	.37	.74	.55	.80	.12	.20	.13
CaO	1.06	.70	.60	.30	.09	.10	.43	.19
Na_2O	3.51	.22	3.46	.39	3.29	.49	3.44	.44
K_2O	5.13	.58	5.17	.58	5.26	.58	4.80	.16
H_2O							.64	.11
Total	99.72		101.09		101.85		99.68	
Zr	262	314	185	144	142	44	176	52
Sr	131	154	22	33	0	2	60	40
Rb	230	56	316	78	470	170	313	61
Zn	43	10	36	13	52	71	25	37
Cu	1	3	1	3	5	6	4	11
Ba	328	178	151	167	11	29	138	86
Q	29.8	4.56	34.1	6.71	37.6	5.96	38.2	4.06
Or	30.2	2.46	28.9	3.05	27.4	4.25	28.5	.93
Ab	29.6	3.35	30.3	3.47	30.6	3.39	29.7	3.88
An	4.3	2.40	2.59	1.51	.4	.48	1.4	.72
DI	89.6		93.3		95.6		96.4	
K/Rb	15.83		11.61		7.94		10.88	
Ba/Rb	1.43		.48		.023		.44	
Ca/Sr	5.79		19.48		64.33		5.12	
Ba/Sr	2.50		6.86		11.00		2.30	
Rb/Sr	1.76		14.36		13.82		5.22	
n	32		14		19		31	

$\bar{x}$ - mean
σ - standard deviation
n - number of samples

* - samples and analysis (Strong et. al., 1974)
** - statistical sampling of granite near showings

phase samples collected by the author to plot differently from similar samples of Strong et al. (1974). This is most likely the result of different analytical methods, since for major elements analysis was done by AAS and XRF, respectively, while trace elements were done using different calibrations, count processing methods, and XRF units.

The variation diagrams for the major elements (Fig. 12a) show that CaO, Fe_2O_3 (total), and Al_2O_3 have a negative correlation with differentiation index. SiO_2 has a positive correlation, while K_2O increases then decreases. Na_2O remains essentially unchanged. CaO, and Fe_2O_3 (total) decrease to much less than half their initial values, as would be expected from differentiation, since these oxides are concentrated in low silica minerals. The decrease of Al_2O_3 especially when the differentiation index is greater than 95 can be attributed to the dilution effect of a greater free quartz content, an explanation which can also be used to explain the unexpected decrease of K_2O at the same point. Na_2O remains essentially unchanged, for as plagioclase feldspar content decreases with increasing quartz content, the feldspar becomes increasingly sodic. The increase of SiO_2 with differentiation index is expected as free quartz content increases. No variation diagrams were drawn for MnO, TiO_2 and MgO because their concentrations were generally so low that differences due to differing analytical methods become dominant.

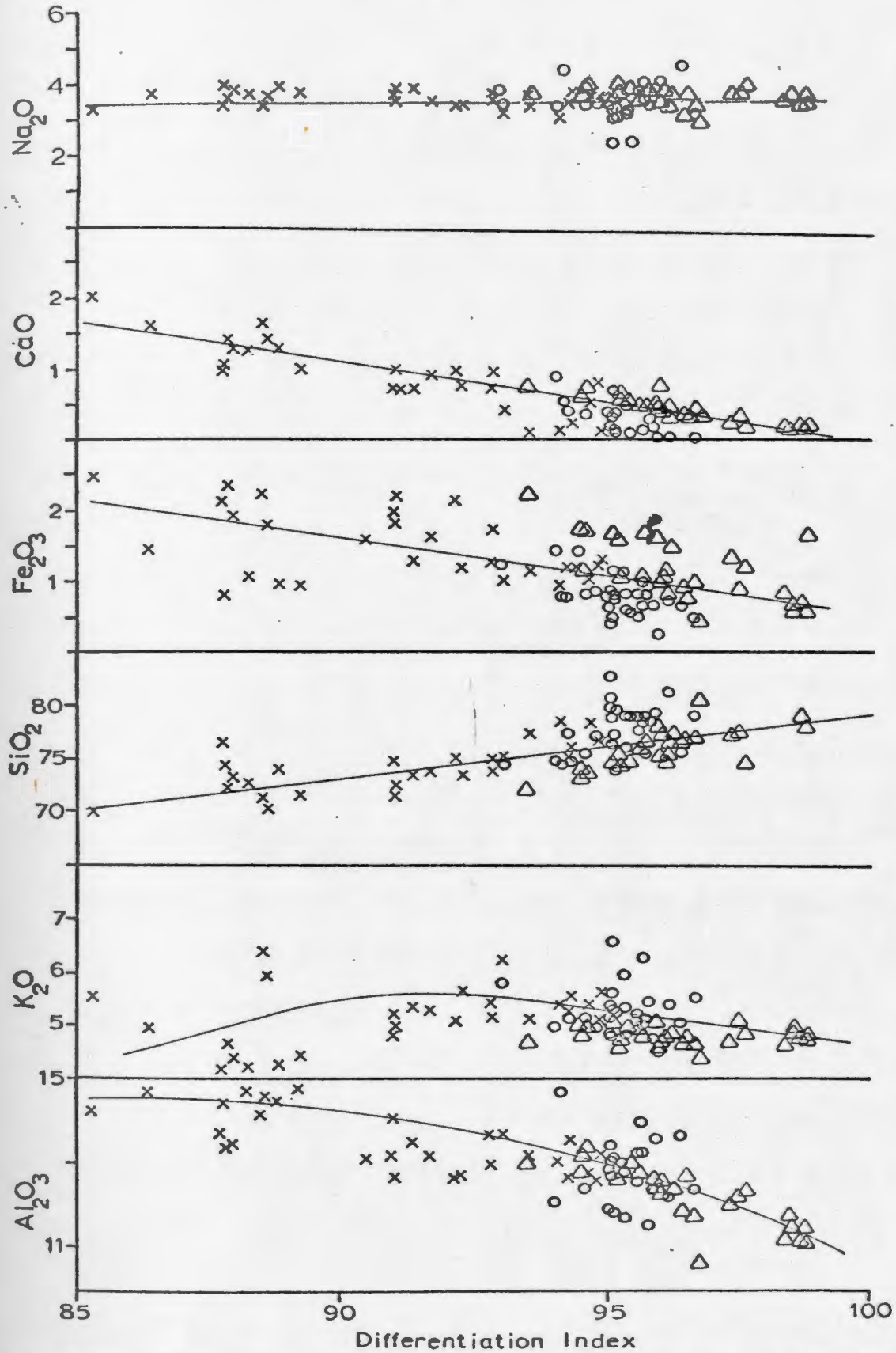

Figure 12a. Plot of major elements versus Thornton and Tuttle's (1960) differentiation index for different intrusive phases of the Ackley City batholith; (x) K-feldspar megacrystic granite; (o) alaskitic granite, (△) alaskitic granite near the showings.

The trace element distributions are somewhat erratic, especially in the case of Sr and Cu in which concentrations are generally near or below detection limits. Ba, Zn and Zr have negative correlations while Rb has a positive correlation with differentiation index (Fig. 12b). The negative correlation of Ba is consistent with the general trend of a differentiating magma (Nockolds and Allen, 1953; Taylor, 1965) for Ba enters early formed K minerals and becomes depleted in late differentiates of a magma. The trend of Zn is as expected, for it mainly substitutes for Fe^{+2} in the biotites of granites and therefore decreases as the proportion of this mineral decreases with differentiation. Although Zr (Chao and Fleischer, 1960), would be expected to increase in concentration with fractionation, the reverse occurs, reflecting a decrease in zircon as determined by petrological studies. The trend of Rb would be expected to closely follow that of K, the only major element of comparable ionic radius and ionization potential. Rb exhibits a positive correlation but does not follow K in its decrease at high values of differentiation index. This may be the result of the fact that the slightly greater size of Rb^{+} (1.47A°) compared to K^{+}(1.33A°) becomes effective under conditions of extreme fractionation, with Rb being slightly concentrated in later fractions (Taylor, 1965). Thus, later K-feldspars, though lower in abundance, may cause a higher Rb content.

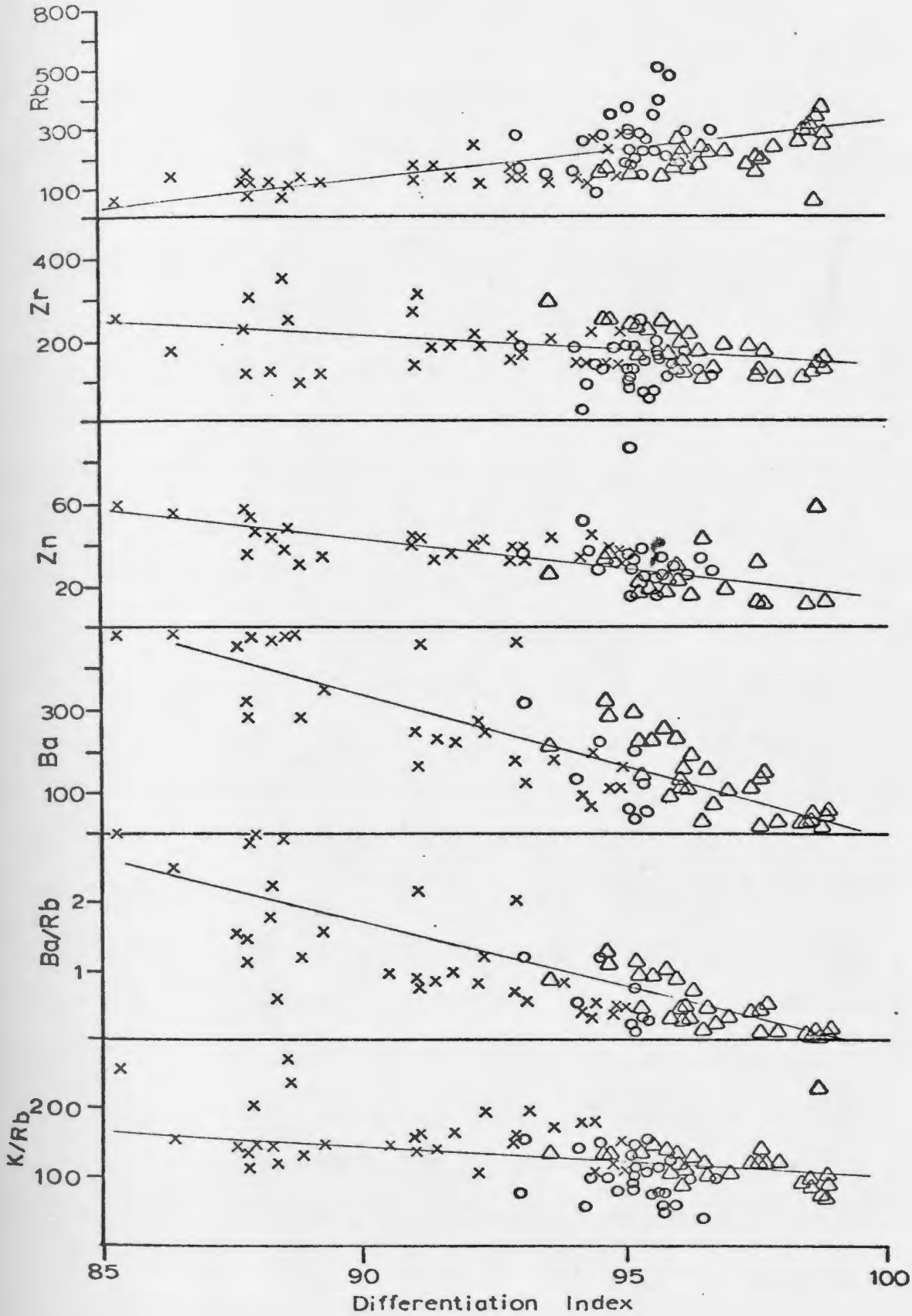

Figure 12b. Plot of trace elements and Ba/Rb, K/Rb versus differentiation index for the Ackley City batholith.

The major and trace elements exhibit uniform, petrologically explicable trends for the different intrusive phases of the Ackley City batholith. These trends are compatible with the different phases representing a plutonic series with the megacrystic granite representing the earliest intrusive phase and the alaskite granite being a later more highly differentiated phase. A relationship which supports this suggestion is the negative correlation of the K/Rb ratio with differentiation index (Fig. 12b). The ratio is expected to decrease with differentiation and sequence of intrusion (Taylor, 1965), a relationship which has been documented by Butler et al. (1962); Teng, (1974) and others. The ratio separates and constitutes evidence for different stages of differentiation of granites as they approach major element uniformity with approach to the ternary minimum (see Section 5.4.2). The plot of K versus Rb (Fig. 13) shows a trend toward the zone of Rb enrichment and indicated the alaskitic phase is a late stage granite. The negative correlation of Ba/Rb with differentiation index (Fig. 12b) is as expected, since Ba has a tendency to concentrate in early K minerals, while Rb exhibits the reverse trend (Taylor, 1965). For this reason Ba/Rb ratios, like K/Rb ratios, provide a critical index of fractionation, decreasing with differentiation. The plot further substantiates the sequence of related intrusive phases,

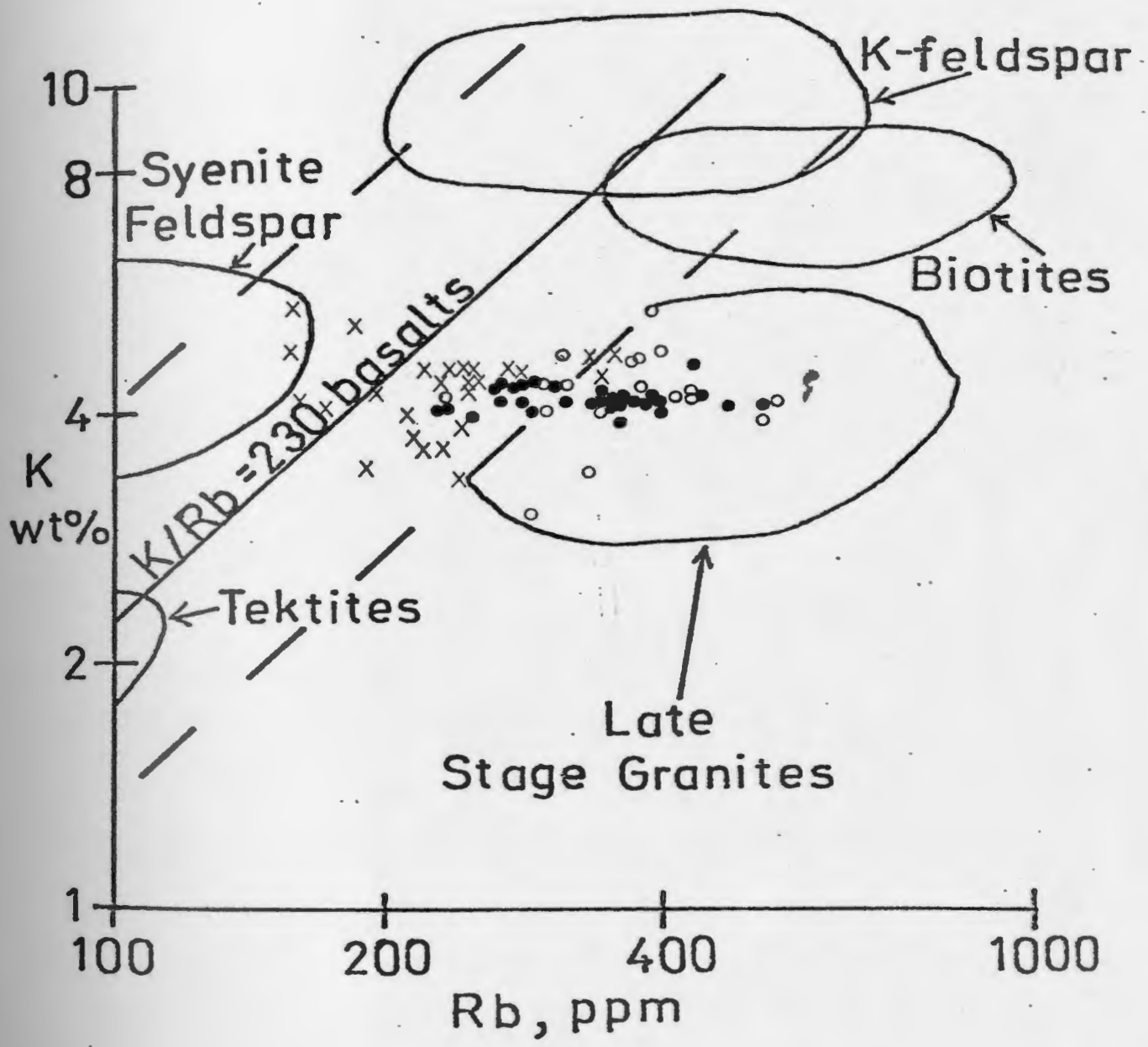

Figure 13. Plot of K (wt. %) versus Rb (ppm) for different phases of the Ackley City batholith, (x) K-feldspar megacrystic granite; (o) alaskitic granite; (•) alaskitic granite (near showings) (diagram adapted from Taylor, 1965).

A plot of Rb versus Sr (Fig. 14) indicates that all phases plot in a similar area forming a trend toward greater Sr depletion and Rb enrichment. The batholith is, as a whole, more Rb enriched than rocks of the Sierra Nevada Batholith as indicated by the samples plotting outside fields for those rocks. The different phases of the intrusive also trend toward increasing alkalinity with increasing SiO_2, in terms of Wright's (1969) alkalinity ratio (Fig. 15). Not only does this suggest a genetic relationship between the different intrusive phases but it also classifies the granite as alkaline to extremely alkaline, as distinguishable from the peralkaline St. Lawrence granite (Teng, 1974). A final point of evidence for a relationship between the different phases of the Ackley City batholith is the fact that the whole rock Rb/Sr age date for the intrusive by Bell and Blenkinsop (1975) was obtained using samples of both the megacrystic and alaskite intrusive phases (see Fig. 10).

In summary, the geochemistry supports or is at least consistent with there being a genetic relationship between the different intrusive phases of the Ackley City batholith.

4.6 The Relationship of the Ackley City Batholith To Some Other Eastern Newfoundland Granites

This section attempts to compare and to investigate the genetic relationship between various granite

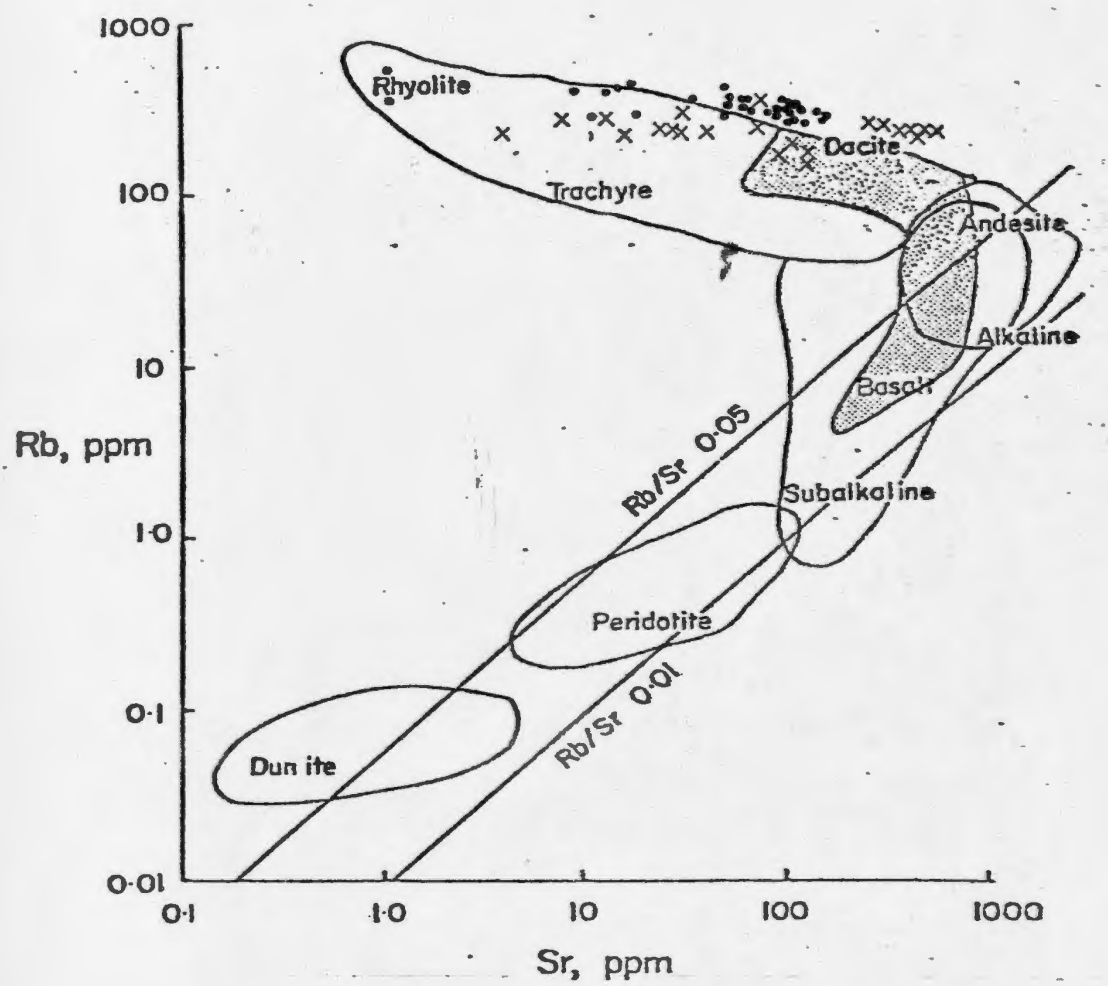

Figure 14. Plot of Rb (ppm versus Sr (ppm) for the different intrusive phases of the Ackley City batholith, (x) K-feldspar megacrystic granite, (•) alaskitic granite (diagram after Kistler and Peterman, 1973).

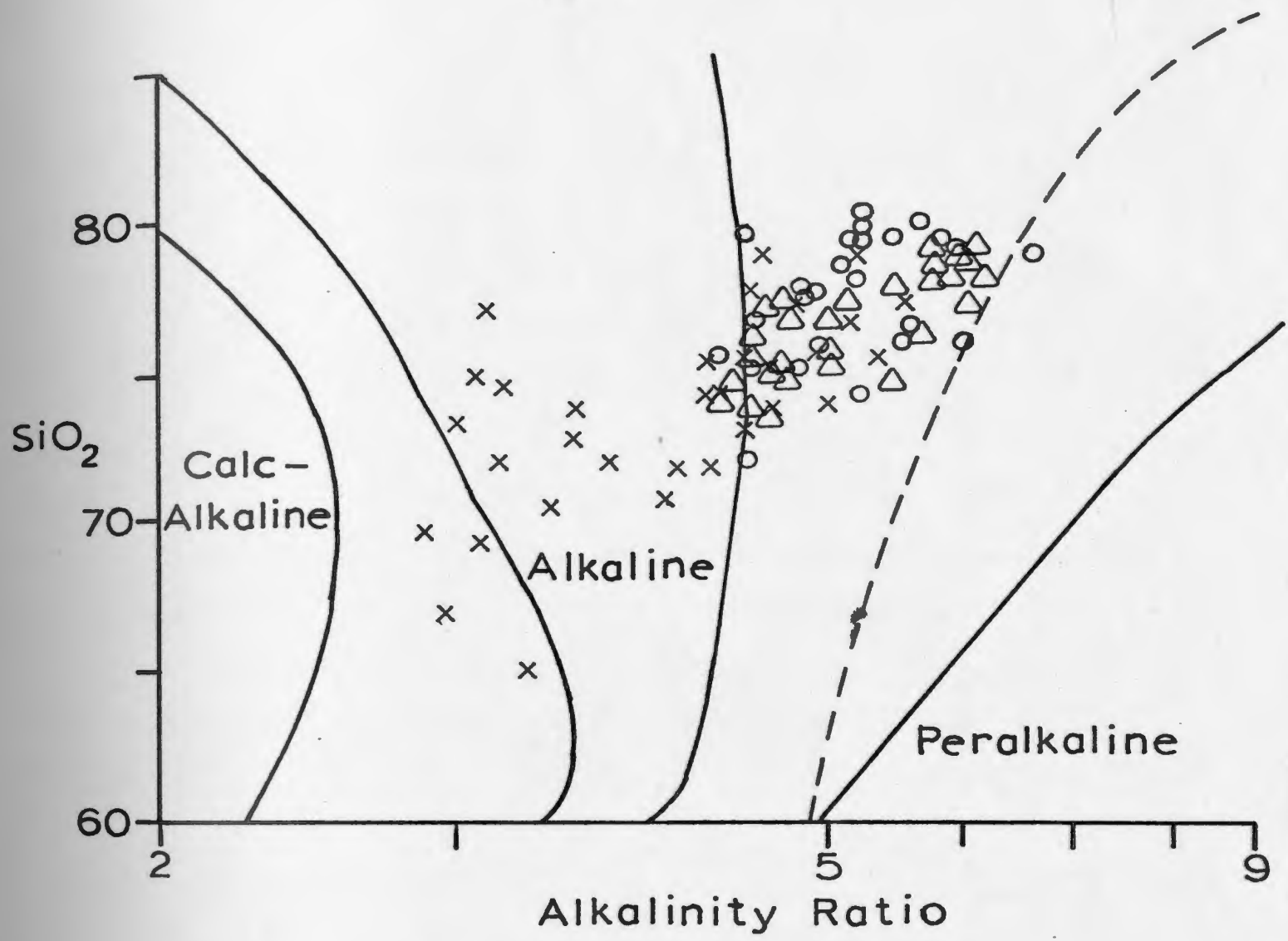

△ Alaskite Granite (near Mo showings)

O Alaskite Granite

X K-feldspar Megacrystic Granite

Figure 15. Plot of Wright's (1969) alkalinity index ((Al$_2$O$_3$+ CaO + total alkalis)/(Al$_2$O$_3$+ CaO - total alkalis) (wt.%)) for different intrusive phases of the Ackley City Batholith. Dashed line is shift of boundary between alkaline and peralkaline suggested by Teng (1974).

plutons of the Fortune Bay-Burin Peninsula region and the Ackley City batholith (Fig. 16). A geochemical comparison was carried out by plotting some major oxide percentages versus the Thornton and Tuttle (1960) differentiation index (Fig. 17). The data for the various plutons is that of Strong et al. (1974).

The trends of the Cape Roger Mountain and Swift Current granites are similar, while field evidence shows that both have a similar geologic setting, both are foliated, and are texturally and chemically very similar (O'Driscoll, 1973; Strong et al., 1974; Teng, 1974). Recent age dating of the Swift Current at 510±20 m.y. (Bell and Blenkinsop, 1975) indicates the trend may represent that of an older group of granites. The Jacques Fontaine granite plots close to the field of the Swift Current and Cape Roger Mountain granites, a fact which supports Bradley's (1962) suggestion of it being genetically related to them. The more acid phases of the composite, acid to basic, Cross Hills intrusive overlap with both trends, a fact which could be explained by the sampling of offshots of the nearby Ackley granite in the area of the Cross Hills intrusive. This pluton may also, therefore, be genetically related to the Swift Current and Cape Roger Mountain intrusives, although Bradley (1962) considered it to be intermediate in age between the Cape Roger Mountain

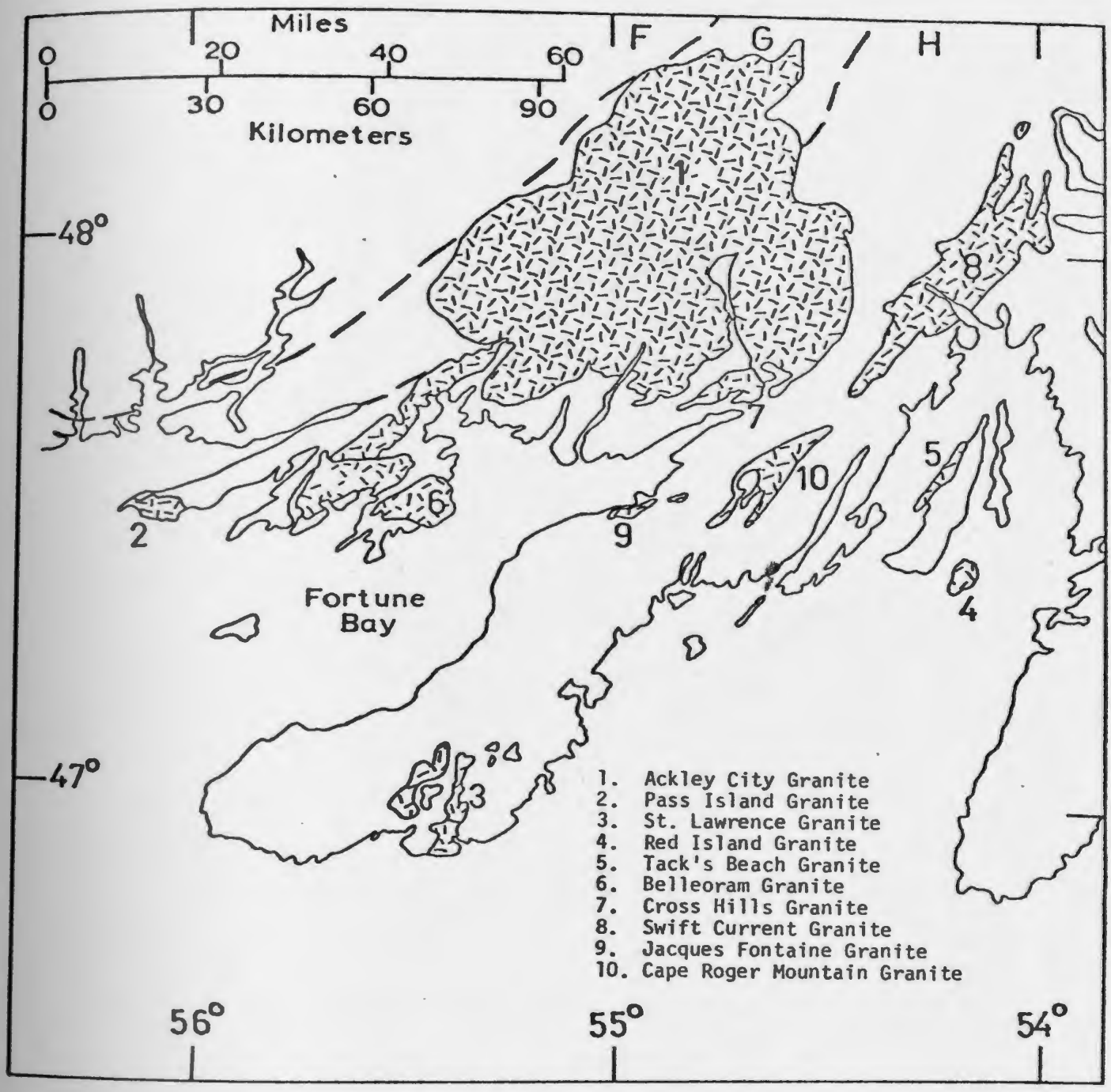

Figure 16. Location of some different southeast Newfoundland granitoids (hatched pattern).

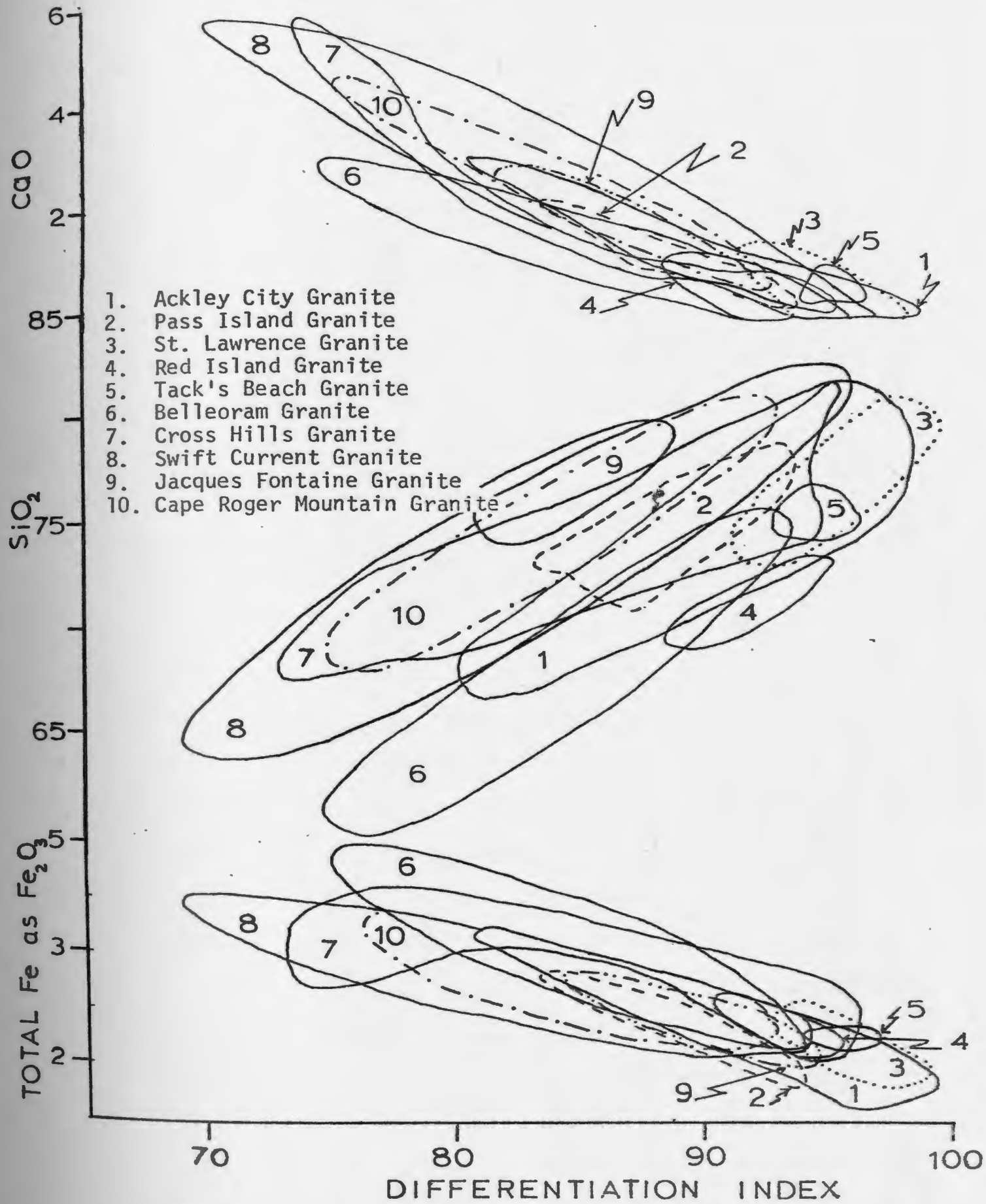

Figure 17. Plot of Thornton and Tuttle's differentiation index versus total Fe as Fe_2O_3, SiO_2, CaO for different south-east Newfoundland granitoids.

and Ackley City plutons. The Simmons Brook Batholith (see Section 3.4) although not indicated on Fig. 16 or plotted in Fig. 17 probably belongs to this trend also due to its textural similarity and foliated nature (Greene and O'Driscoll, 1976).

The Ackley City batholith lies on a second trend occupied also by the St. Lawrence, Red Island, Tack's Beach, and Belleoram granites. The St. Lawrence and Belleoram granites are both known to be of Carboniferous age, 315±10 m.y. (Bell and Blenkinsop, 1975) and 400,342 m.y. (Wanless et al., 1965, 1967) respectively, while the Ackley City granite is known (345±10 m.y.) (Bell and Blenkinsop, 1975) and the Red Island and Tack's Beach considered to be of Devonian age. The Harbour Breton granite, although omitted in Figures 16 and 17 is similar texturally and probably in age to the Ackley City batholith. The St. Lawrence granite appears to be a late differentiate of a magma similar to the Belleoram granite, a suggestion which is supported by the similar age, and it appears that there is a fractionation trend from Belleoram granite-Tack's Beach granite-St. Lawrence granite (Teng, 1974). The Ackley City batholith plots in a field which overlaps with the fields of the Belleoram to St. Lawrence granites, the megacrystic phase occupying the area on the plot from the Belleoram to the Tack's Beach granites while

the alaskite phase overlaps almost completely with the St. Lawrence granite. The youngest phases of the alaskite granite which are associated with the molybdenite deposits (see Chapter 5) are more or as highly differentiated as the St. Lawrence granite.

4.7 Summary

The Ackley City batholith is Devonian in age (354±10) (Bell and Blenkinsop, 1975) and intrudes Precambrian and Ordovician rocks of the Avalon and Gander zones of the Newfoundland structural province. The batholith is passive, post-tectonic, has the form of an approximately 2 km thick sheet, and is characterized by very low grade contact thermal metamorphism without associated metasomatism. It is a composite body consisting of K-feldspar megacrystic granite in the north, east and west and alaskitic granite in the southwest. Both these intrusive phases are composed mainly of perthite, quartz, plagioclase and biotite with accessory sphene, zircon, apatite, tourmaline and fluorite. Geochemical data is compatible with the different phases being related, the alaskitic granite being the younger, more differentiated phase. This phase, according to K/Rb ratios is a "late stage" granite. The intrusive phases trend towards increasing alkalinity, the K-feldspar megacrystic granite being alkaline while the alaskitic granite is extremely alkaline. The Ackley City batholith is of a

composition with geochemical affinities to the Pass Island, Red Island, Tack's Beach, Belleoram and St. Lawrence granites, although the later two are apparently younger.

CHAPTER 5

THE FORTUNE BAY MOLYBDENITE SHOWINGS

5.1 General

The four main molybdenite showings (Motu, Ackley City, Crow's Cliff - Dunphey Brook, and Wylie Hill) are located at the southwest contact of the Ackley City batholith with acid volcanic rocks of the Belle Bay Formation (Fig. 18). Another showing, Frank's Pond, is located 5 km within the Ackley City granite and another within a small granite plug on Belle Island in Fortune Bay (Fig. 4). These showings, which have been the object of a limited amount of assessment work (see Chapter 1.2), were examined in detail and the surrounding granite was also mapped.

The geology of the granite to the north of the showings (Fig. 18) is generally monotonous alaskitic granite, as described in Chapter 4. It has sharp contacts with rhyolite except in the area of the showings where there are marginal medium grained granite, fine grained porphyritic granite, aplite and pegmatite phases. These phases, which are described in the following sections, are not, however, restricted to near the contact for they extend well within the alaskitic granite phase northwest of the Motu showing and north of the Dunphey Brook - Crow's Cliff showing (Fig. 18). The rarely observed intrusive contacts indicate that the finer grained phases are younger.

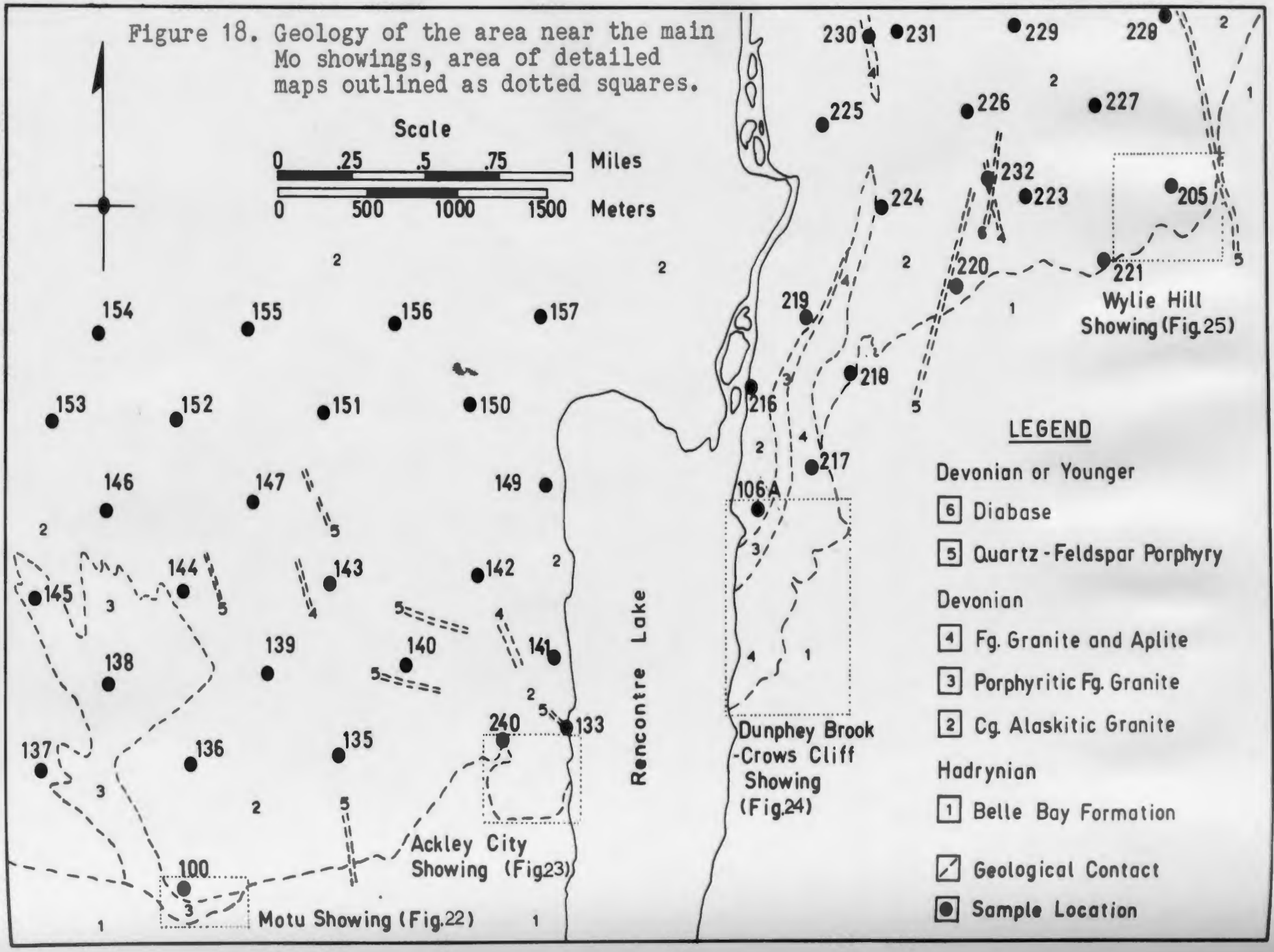

Figure 18. Geology of the area near the main Mo showings, area of detailed maps outlined as dotted squares.

The granite was sampled at 800 meter intervals on traverses spaced 450 meters apart in an attempt to obtain a statistical geochemical sampling of the granite, these samples being those used in Chapter 4 as the alaskitic granite near the showings.

5.2 Geology, Lithology and Petrology

5.2.1 Introduction

The geology, petrology of the different mapped intrusive units and the mode of mineralization for each showing are described separately. Although this is somewhat repetitious, especially in regard to some of the petrographic descriptions, it was considered to be the best method to emphasize what are considered to be significant differences between the showings.

The different intrusive phases associated with the molybdenite showings are modally classifiable as granites (Fig. 19), as determined by point counts and XRD methods. There is no apparent systematic variation in the modal compositions of the different intrusive units. A couple of mineralogical characteristics also common to the showings are one type of molybdenite polytype, and pegmatite alkali feldspar structural state. As all the showings have molybdenite as the only economic sulphide, polytypism of four concentrates from each showing were studied by the method of Frondel and Wickman (1970). Only the expected

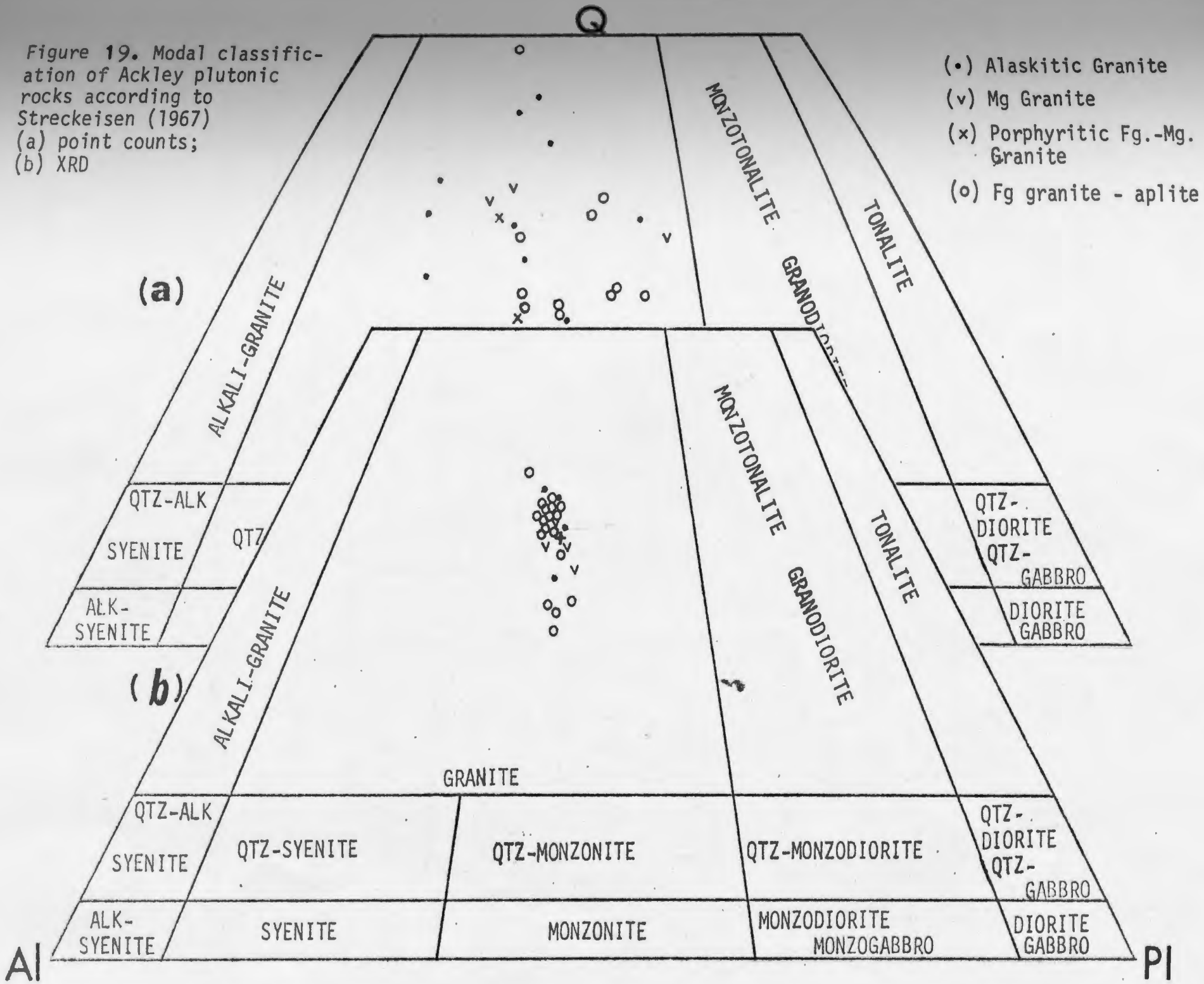

Figure 19. Modal classification of Ackley plutonic rocks according to Streckeisen (1967) (a) point counts; (b) XRD

common $2H_1$ polytype was found (Fig. 20). Pegmatite alkali feldspar were examined using the method of Wright and Steward (1968) to determine structural state (Fig. 21). The feldspars were all found to have anomalous cell parameters, indicated by their having higher predicted 2θ values for $\bar{2}01$ then the measured values, however, they form a trend which indicates they have a similar orthoclase structural state. Anomalous unit cell parameters would be expected of pegmatite feldspar which would likely accommodate large residual elements in its crystal lattice.

5.2.2 Motu Showing

The Motu Showing is located just east of Isle a Glu Pond, and 2.3 km west of Rencontre Lake at the contact between the Ackley City batholith and the Belle Bay Formation (Fig. 18). Mapping of the showing (Fig. 22) has outlined two other intrusive units, medium grained granite and porphyritic aplite. Sharp contacts have been observed between these and alaskitic granite but not between each other, which indicates that they may be mutually gradational. The intrusive-rhyolite contact varies in strike and dips approximately 30° south, while sheeted joints have the same dip, and strike 085°.

The porphyritic aplite is a miarolitic, fine grained (average .2 mm), light pink rock which has scattered anhedral quartz phenocrysts (2-4 mm). It is composed of anhedral perthite, anhedral to subhedral

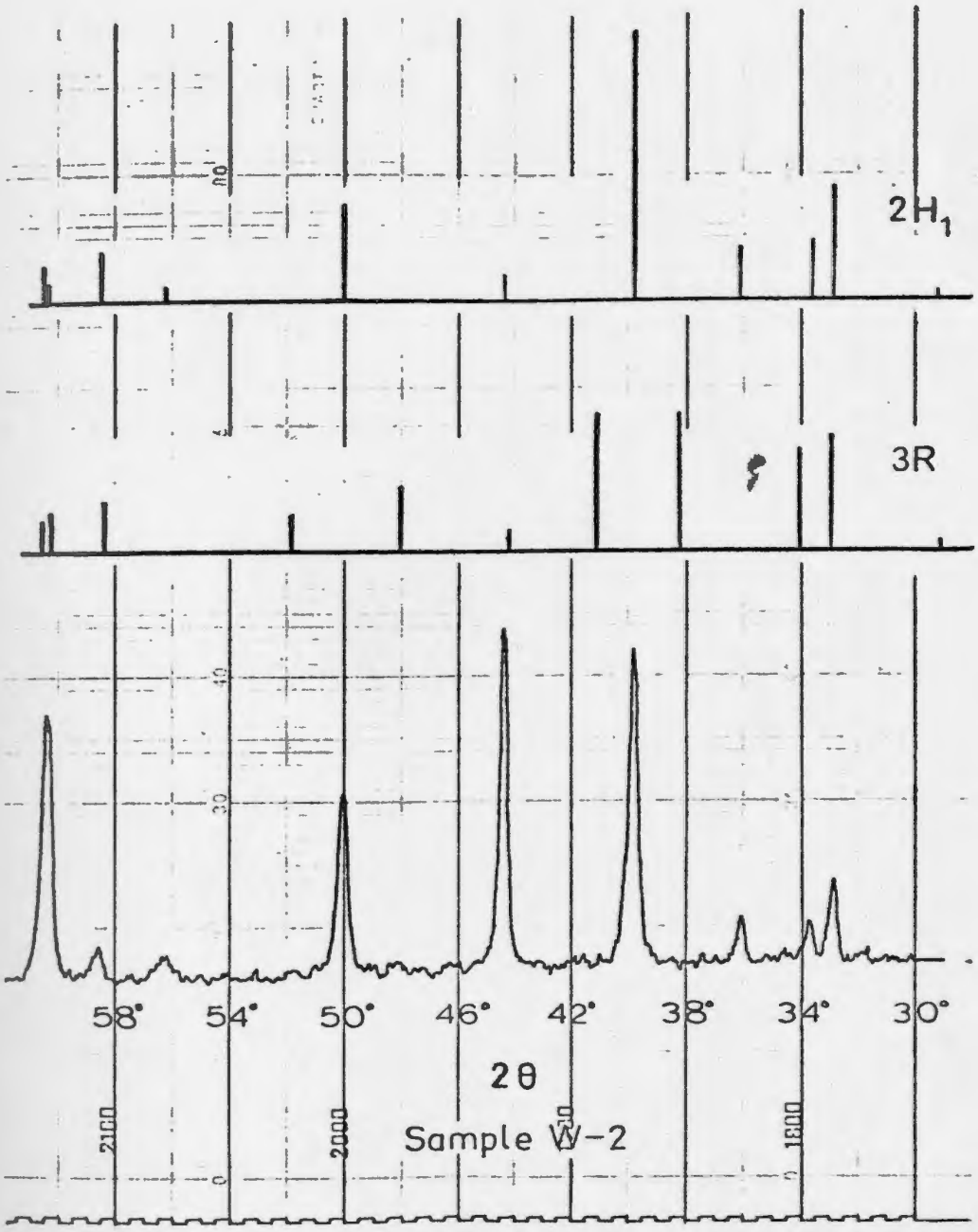

Figure 20. X-ray diffraction pattern for molybdenite ($2H_1$) from Wylie Hill (bottom), and predicted patterns for $2H_1$ and 3R molybdenite polytypes (from Wickham and Smith, 1970).

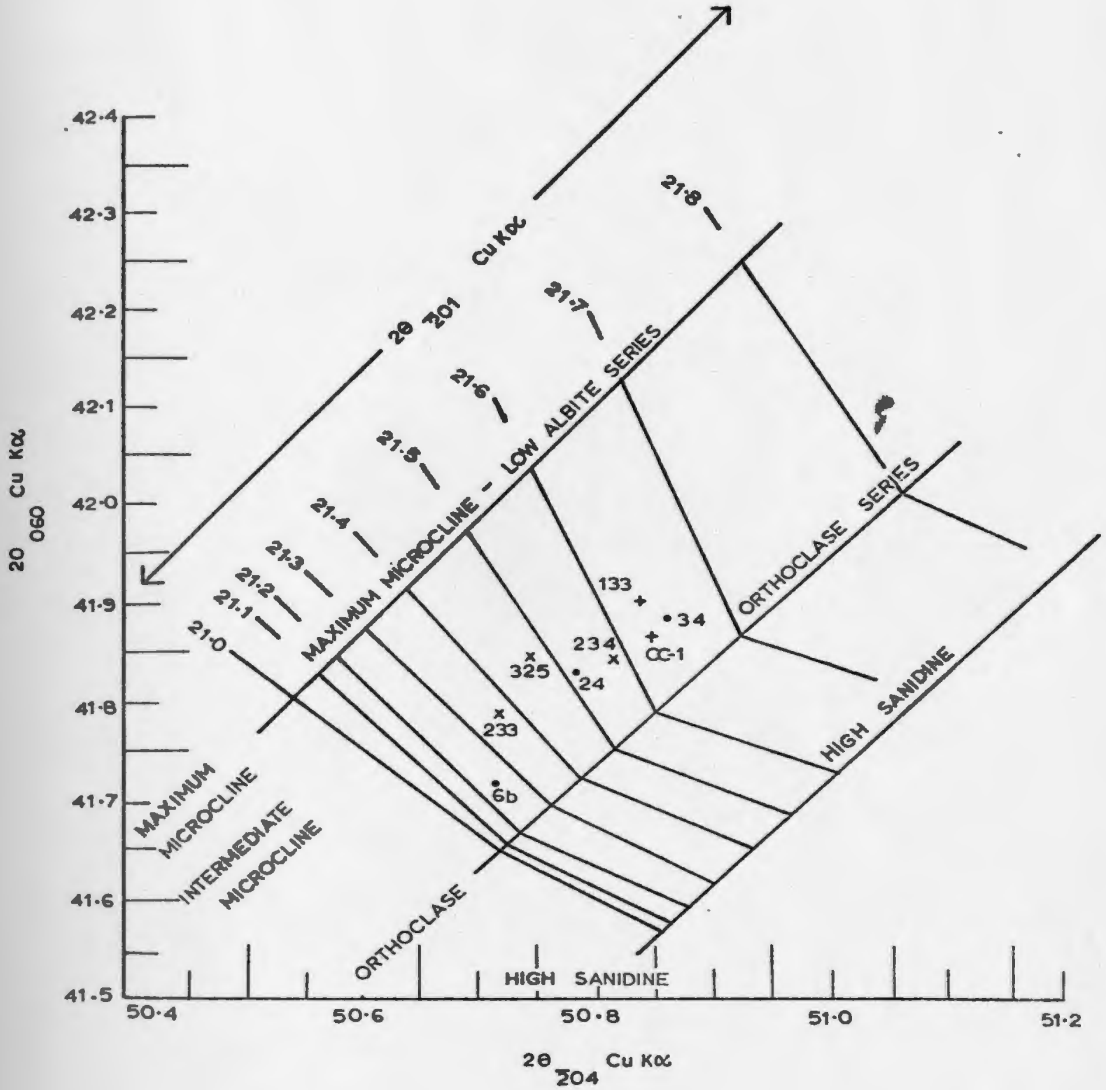

Figure 21. Structural states for pegmatite alkali feldspars from (+) Crows Cliff-Dunphey Brook, (x) Wylie Hill and (·) Ackley City Showings.

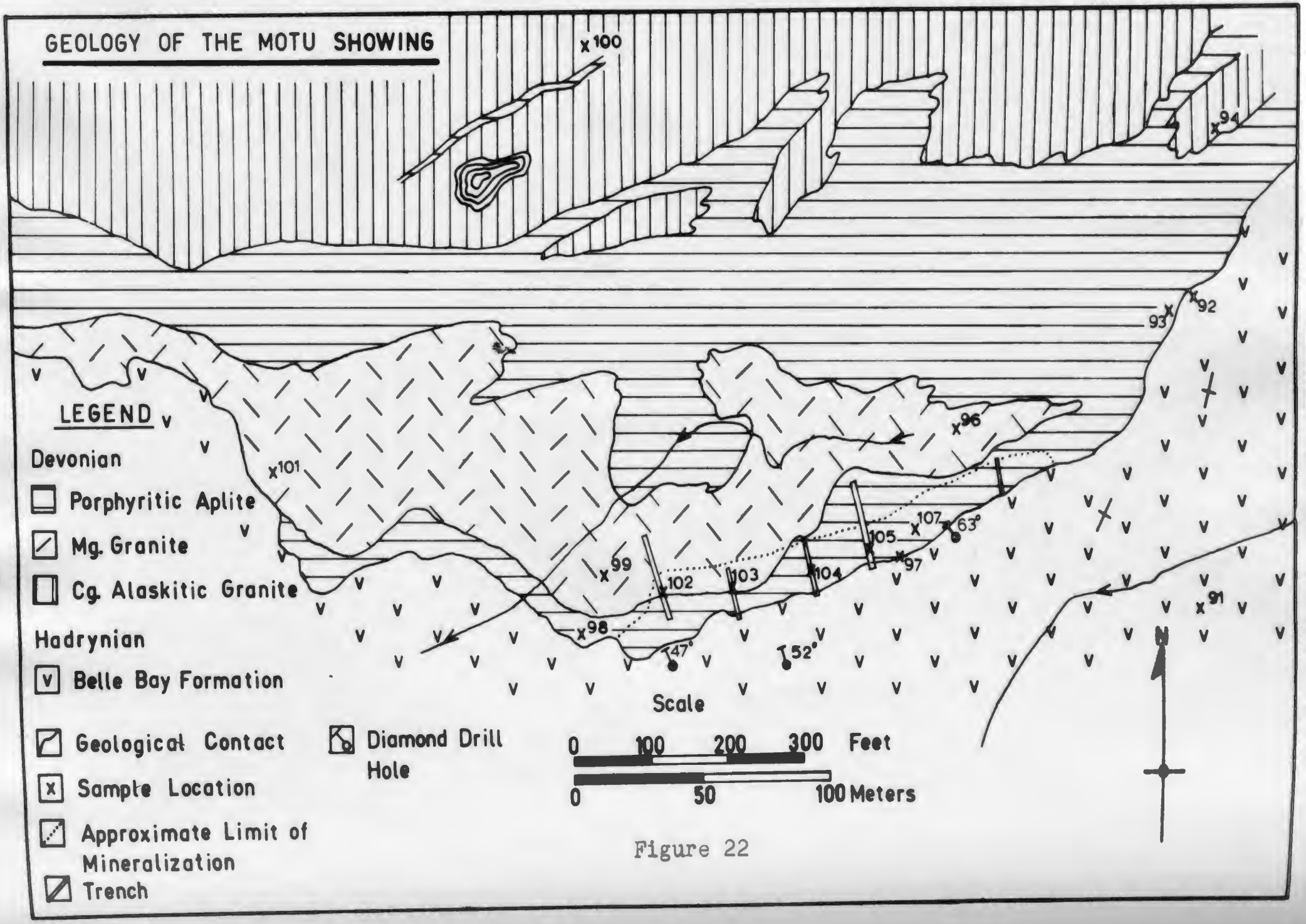
GEOLOGY OF THE MOTU SHOWING
LEGEND
Devonian
Porphyritic Aplite
Mg. Granite
Cg. Alaskitic Granite
Hadrynian
Belle Bay Formation
Geological Contact
Sample Location
Approximate Limit of Mineralization
Trench
Diamond Drill Hole
Scale
0 100 200 300 Feet
0 50 100 Meters
N
x100
x94
x92
93
x96
x101
x99
102
103
104
105
x107
63°
x97
x98
47°
52°
x91

Figure 22

albite, and embayed anhedral to euhedral quartz as phenocrysts with stippled overgrowth rims and as an anhedral strained matrix component. The medium grained granite is a pale pink, miarolitic, semi-equigranular rock composed of anhedral to subhedral, normally zoned (oligoclase to albite) plagioclase (1-6 mm), strained anhedral quartz (1-4 mm) in the form of composite grained aggregates (4 mm), and poikiolitic string and bead perthite (1-6 mm). Plagioclase is dusted with sericite and in some cases altered to pale green, fine grained clay minerals and granophyric intergrowths of perthite and quartz (Plate 5) are common. Scattered fine grained (1 mm) fibrous biotite aggregates are often ribbed with chlorite. The Belle Bay Formation consists of highly fractured, dark grey, flow banded rhyolite at 035°/55 NW characterized by contact metamorphic development of sericite parallel to this banding near the granite contact.

Molybdenite mineralization occurs within the intrusion along a length of approximately 175 meters and a width of 25 meters adjacent to the granite-rhyolite contact (Fig. 22). Diamond drill core data suggests the mineralization is in the form of a sheet, with a true thickness not greater than 10 meters, which plunges down the contact at 30° south. It does not, however, continue

Plate 5: Coarse grained granophyric intergrowth of string perthite and quartz in medium grained granite, Motu, crossed nicols, X30, T.S. JW-99.

Plate 6: Coarse grained molybdenite rosettes in drusy medium grained granite, Motu, scale in cm., Sample JW-107.

down dip for a distance greater than 30 meters except in the central part of the mineralized zone. The molybdenite mineralization generally occurs as erratically distributed coarse grained rosettes (Plate 6). There is no alteration associated with the mineralization, although some of the associated quartz may be secondary.

5.2.3 Ackley City Showing

The Ackley City Showing is located on the east side of Rencontre Lake in an embayment of the granite into the rhyolite (Plate 7). Mapping of the area (Fig. 23) outlined a number of intrusive types (pegmatite, fine grained granite, aplite and medium grained granite) as well as a major alteration unit (quartz segregation) other than the normal alaskitic granite. The fine grained granite and aplite on the main map (Fig. 23) includes medium grained granite which was separated only in the more detailed mapping of the mineralized zone. The fine grained granite, aplite and medium grained granite appear to be gradational in many locations, although rare sharp intrusive contacts have been observed. A similar relationship may exist in some areas between mg. granite and cg. alaskitic granite, but sharp contacts were more commonly observed, with the finer grained phases invariably cutting the coarser grained phase. The largest area of pegmatite occurs west of the mineralized zone, but small pods were observed near the intrusive-rhyolite contact in many locations.

Plate 7: View to southwest, Rencontre Lake in foreground, rhyolite to south, granite to north, with contact outlined, Ackley City Showing is within the embayment beside the lake.

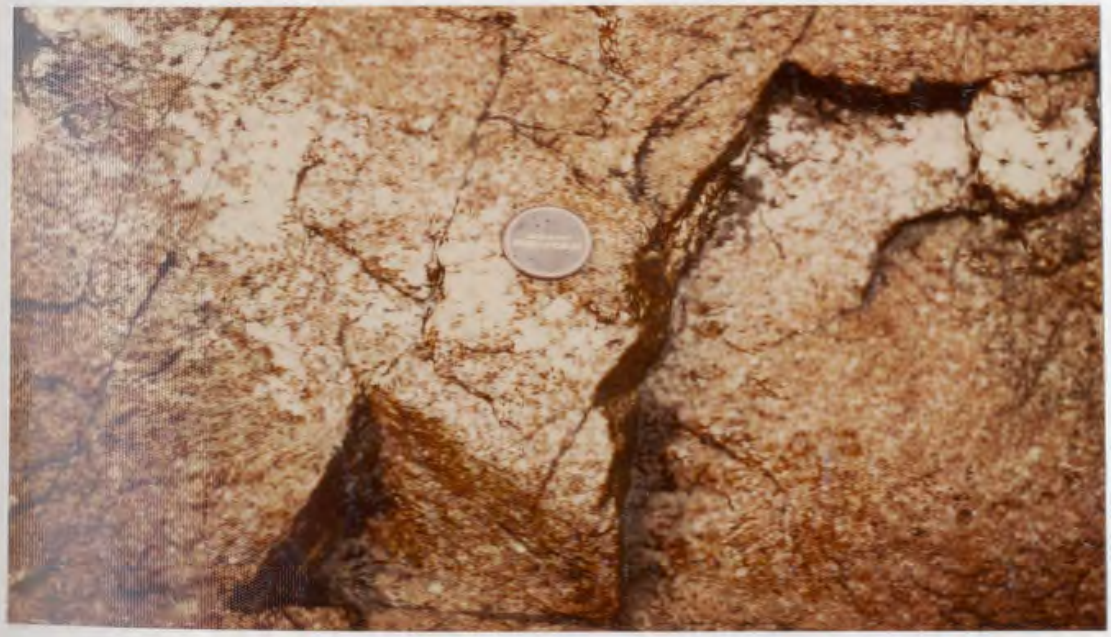

Plate 8: Quartz segregation at the Ackley City Showing, massive milky quartz grades into granite with augmented primary quartz.

Figure 23

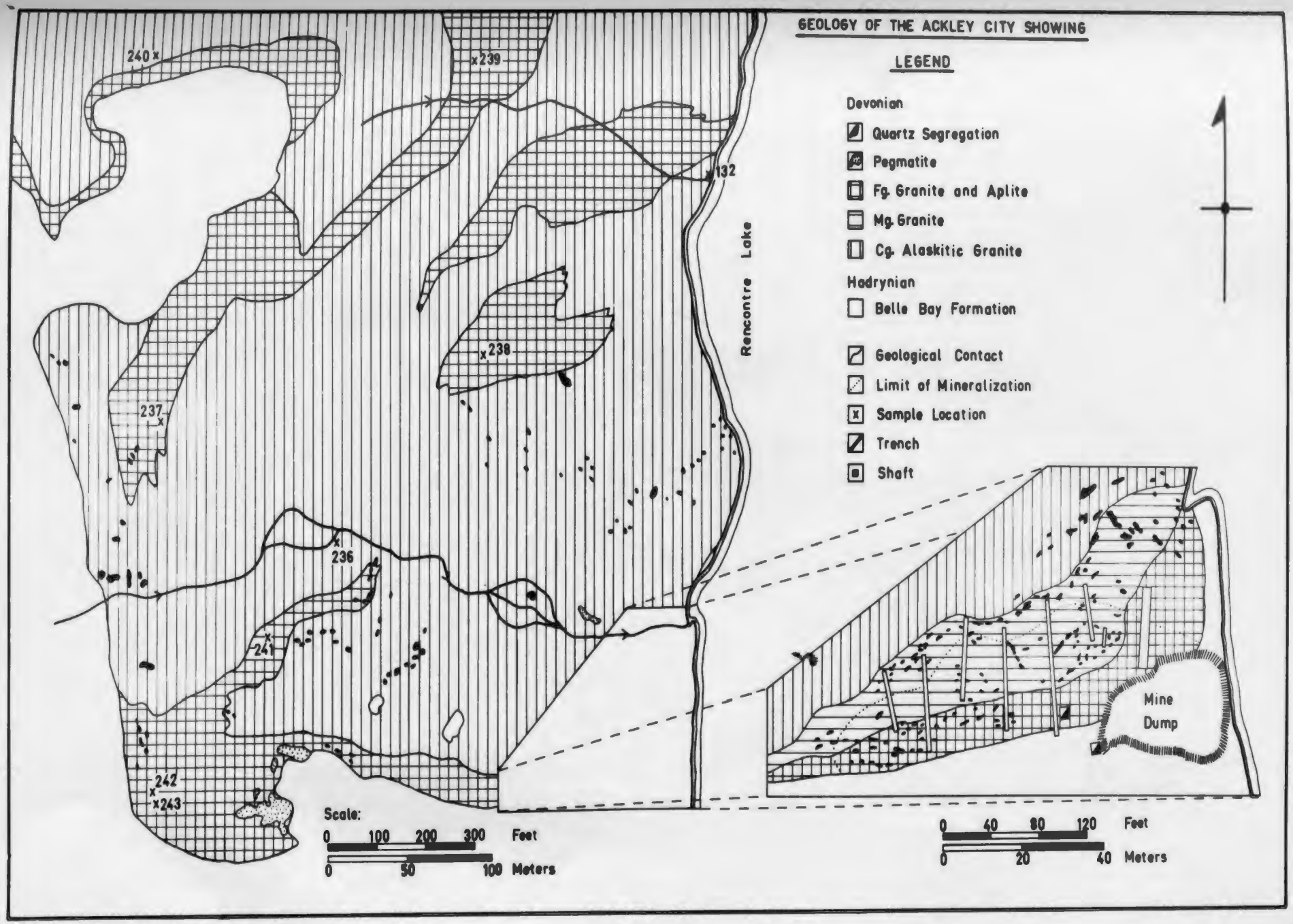
GEOLOGY OF THE ACKLEY CITY SHOWING
LEGEND
Devonian
Quartz Segregation
Pegmatite
Fg. Granite and Aplite
Mg. Granite
Cg. Alaskitic Granite
Hadrynian
Belle Bay Formation
Geological Contact
Limit of Mineralization
Sample Location
Trench
Shaft
Rencontre Lake
240
239
132
238
237
236
241
242
243
Mine Dump
Scale:
0 100 200 300 Feet
0 50 100 Meters
0 40 80 120 Feet
0 20 40 Meters

This contact strikes at 075° and dips 45° to 50° S to form the hanging wall of the orebody. Toward the east the contact becomes much steeper as it approaches the lake and proceeds north along the side of the lake.

The quartz segregations consist of irregular pods or patches of milky white quartz which vary in size from a few centimeters to more than a meter. They appear to form large "belts" which contain a high density of quartz segregations separated by granite with extensive augmentation of primary quartz. The pods are characterized by massive quartz centres grading outwards into granite with specks of pink feldspar, then into granite with augmented primary quartz (Plate 8).

Pegmatite, distinguishable from the quartz segregations only by the presence of coarse grained K-feldspar, is similar to that which will be described in detail for the Dunphey Brook-Crow's Cliff Showing, though not as coarse grained or extensive. From mine dump material it was recognized that some primary pegmatite clots or segregations consist of milky white massive quartz surrounded by a zone of feathery intergrown K-feldspar and quartz. Since such fine detail was not recognizable in weathered outcrop, primary pegmatitic segregations of this nature would have been mapped as quartz segregations.

The fine grained granite and aplite is similar to that described from Motu, for it is a red, fine grained, hypidiomorphic granular rock consisting of quartz, albite and perthite (Plate 9). An unusual feature, however, is the pronounced inversion to microcline of the perthite, particularly in the ore zone. Areas of pegmatitic aplite are common. It consists of fine grained red aplite with abundant small (2-20 mm), irregular, lenticular pods of a pegmatitic nature (Plate 10). These have an outer fringe of coarse grained graphically intergrown string perthite and quartz (Plate 11) radiating toward the centre of the segregation, succeeded by a zone of euhedral orthoclase with lesser quartz, and the centre of the pod being massive milky quartz, or a miarolitic cavity lined with chlorite. The medium grained granite includes porphyritic granite, equigranular granite and pegmatitic granite, all of which are apparently gradational. The Belle Bay Formation consists of medium brown, flow banded, highly fractured rhyolite which is cut by numerous tongues and veins of aplite and granophyric aplite.

The orebody is approximately 42 meters long by a maximum of 12 meters wide, bounded by rhyolite (south), Rencontre Lake (east) and assay values (west and north), and has a proved tonnage of 65,000 tons of .38% MoS_2 (Smith, 1938). Molybdenite mineralization occurs in a number of different modes; disseminated, podiform and

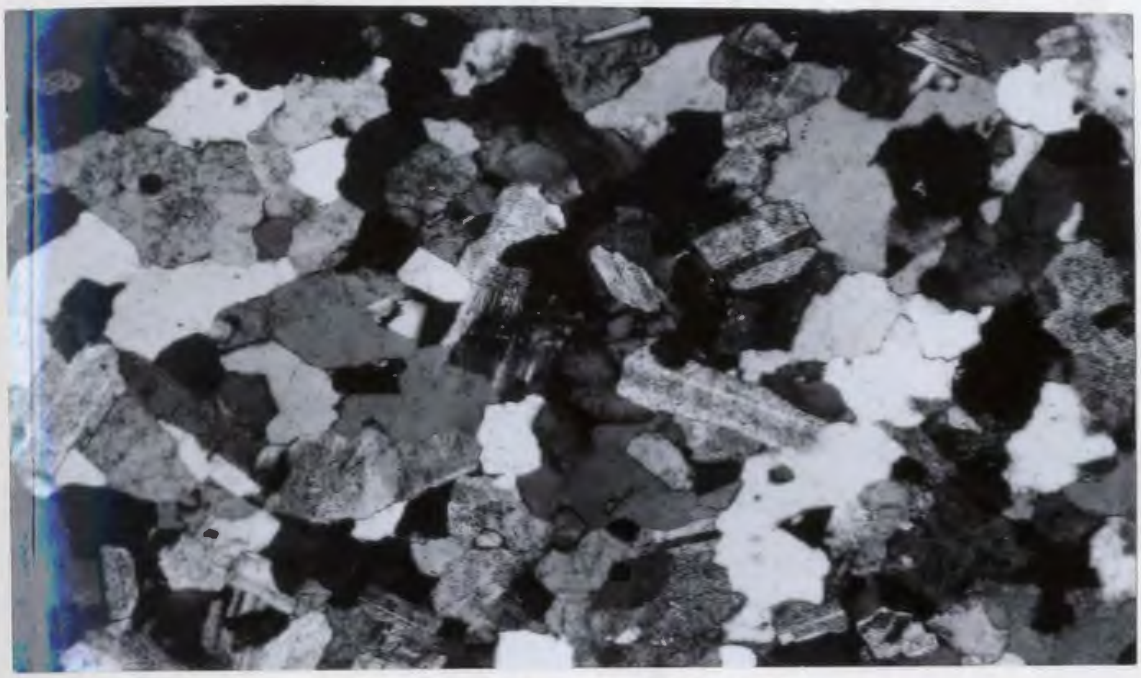

Plate 9: Hypidiomorphic granular aplite composed of anhedral perthite, subhedral albite and quartz, Ackley City Showing, crossed nicols, X30, T.S. JW-238.

Plate 10: Pegmatitic aplite which contains numerous pegmatitic miarolitic segregations, Ackley City Showing, Sample ACD-22.

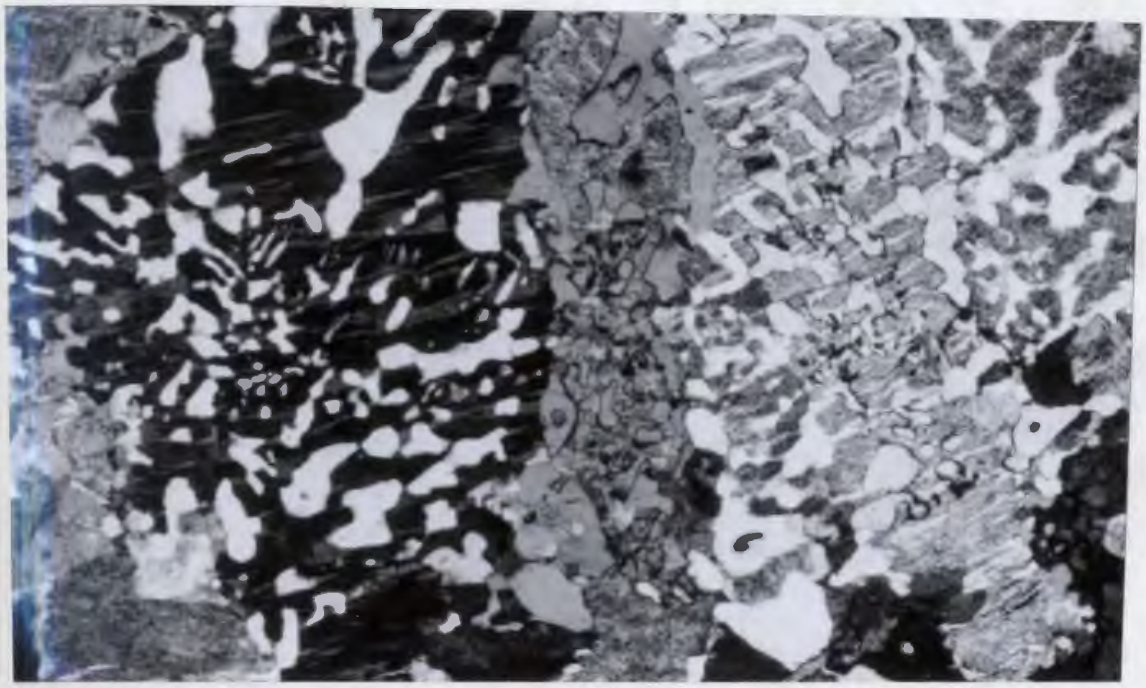

Plate 11: Coarse grained graphic intergrowth of string perthite and quartz from the fringe of a pegmatitic segregation in Plate 10, crossed nicols, X30.

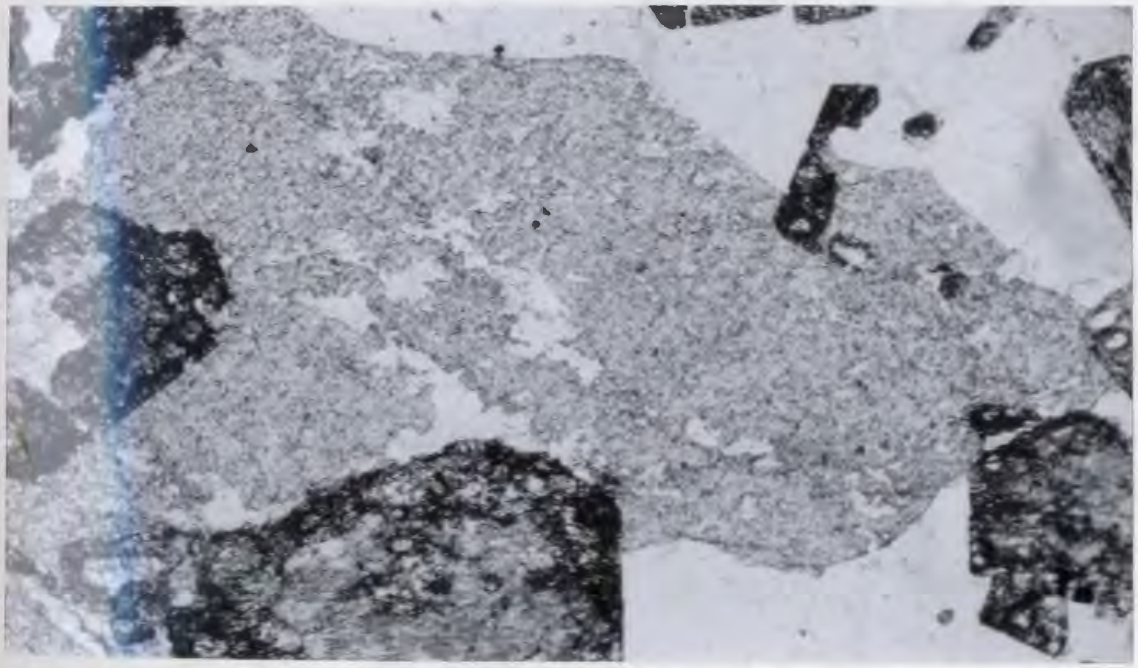

Plate 12: Intensive fluorite mineralization within medium grained granite, occupying quartz sites, Ackley City Showing, uncrossed nicols, X30, T.S. A.C.C.-43.

fracture filling. The disseminated mineralization consists of medium grained (2 to 5 mm) anhedral flakes of molybdenite sparsely to strongly disseminated throughout dark red, medium to fine grained granite. Such molybdenite occupies quartz or plagioclase sites, but there is little indication of replacement other than the association of fluorite and interleafing of molybdenite with muscovite and chlorite. Molybdenite also occurs as large (2-3 cm) rosettes associated with quartz, barite and calcite in secondary quartz segregations and primary pegmatitic pods. Quartz and medium grained molybdenite (.5 cm) fill fractures of varying widths (.2-20 mm). Some disseminated molybdenite mineralization is closely associated with muscovite alteration. There is not, however, a definite correlation between the two, for there are barren muscovite alteration patches and also the intensity of such alteration has no bearing on the degree of mineralization. There are also small areas of fluorite mineralization occurring as intense disseminated purple fluorite occupying original quartz sites (Plate 12), and as fracture fillings with calcite and barite. Fracture filling quartz, pyrite and bismuth mineralization is present west of the orebody, the presence of bismuth being indicated by geochemical analyses. Sphalerite, chalcopyrite and pyrrhotite are other minor associated ore minerals (White, 1939).

Alteration associated with mineralization is quite extensive and variable. A major alteration type is the abundant addition of quartz in the form of quartz segregations especially in the area of the orebody (Fig. 23). Irregularly shaped and distributed medium to coarse grained patches of muscovite alteration are also closely associated with mineralization. Intensity of alteration varies from replacement of all K-feldspar and plagioclase by muscovite and augmentation of primary quartz, to complete coarse grained muscovite (up to 1 cm) replacement of the intrusive. Muscovite and quartz alteration fringing quartz veins is present within and outside the orebody. Quartz veins with secondary biotite surrounding or within the veins occur within the mineralized zone. The biotite is poikilitic, many of the inclusions of zircon and other unidentified minerals being surrounded by radioactive halos (Plate 13). Anastomosing pegmatite veins are common and there are also late quartz veins with K-feldspar alteration halos cutting fracture related quartz-muscovite alteration veins. The rhyolite, for a couple of hundred meters beyond its contact with the mineralized zone, is characterized by stockwork, hairline fracture filling, fine grained pyrite and chlorite. This is especially notable in view of the fact that pyrite was almost absent from the orebody, magnetite being the most common iron mineral.

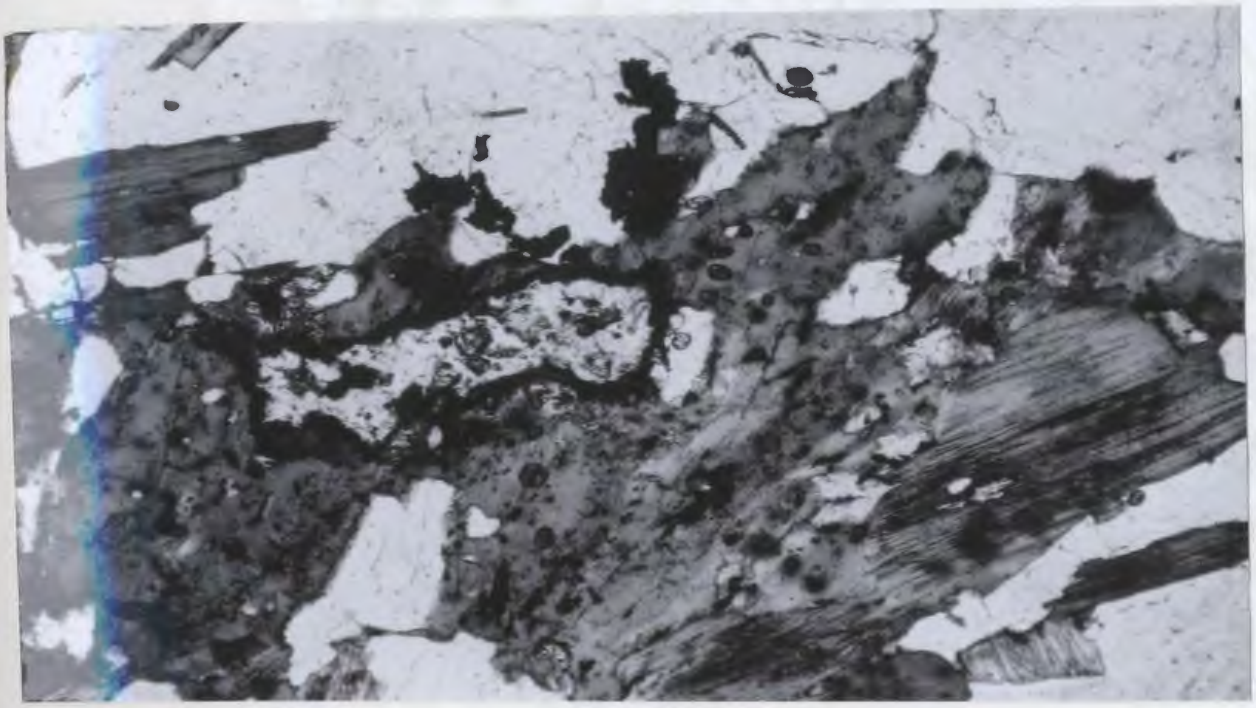

Plate 13: Secondary biotite containing numerous inclusions characterized by radioactive halos, Ackley City Showing, uncrossed nicols, X30, T.S. ACD-5.

Plate 14: Sharp contact between coarse grained, alaskitic granite to the north (top) and medium grained porphyritic granite to the south (bottom), contact dips gently (20°) to the south, Dunphey Brook-Crow's Cliff.

5.2.4 Dunphey Brook-Crow's Cliff Showing

The Dunphey Brook-Crow's Cliff Showing is located on the north-east side of Rencontre Lake (Fig. 18) adjacent to the granite-Belle Bay Formation contact. Mapping of the area (Fig. 24) has outlined a number of intrusive types (quartz-feldspar porphyry, pegmatite, fine grained granite and aplite, and porphyritic fine grained granite) other than the coarse grained alaskitic phase which borders these phases to the northwest. The quartz-feldspar porphyry occurs as dykes cutting the rhyolite and also the granite, but figure 24 shows two dykes cutting only the rhyolite due to the poor exposure in that area. Sharp contacts between the alaskitic granite and porphyritic fine grained granite (Plate 14) were observed in a number of locations in Dunphey Brook. In this same area there are breccia dykes and veins, which probably represent degassing breccias (tuffisites). The porphyritic granite varies in grain size of matrix and abundance of phenocrysts, both of which are greatest near the alaskitic granite contact. The latter contact was not observed and may be gradational, the mapped contact representing the disappearance of phenocrysts. The fine grained granite and aplite cover a large area within which there are variations in the presence or absence of fine grained biotite, pegmatite segregations (2-5 cm) and colour (light pink to dark pinkish

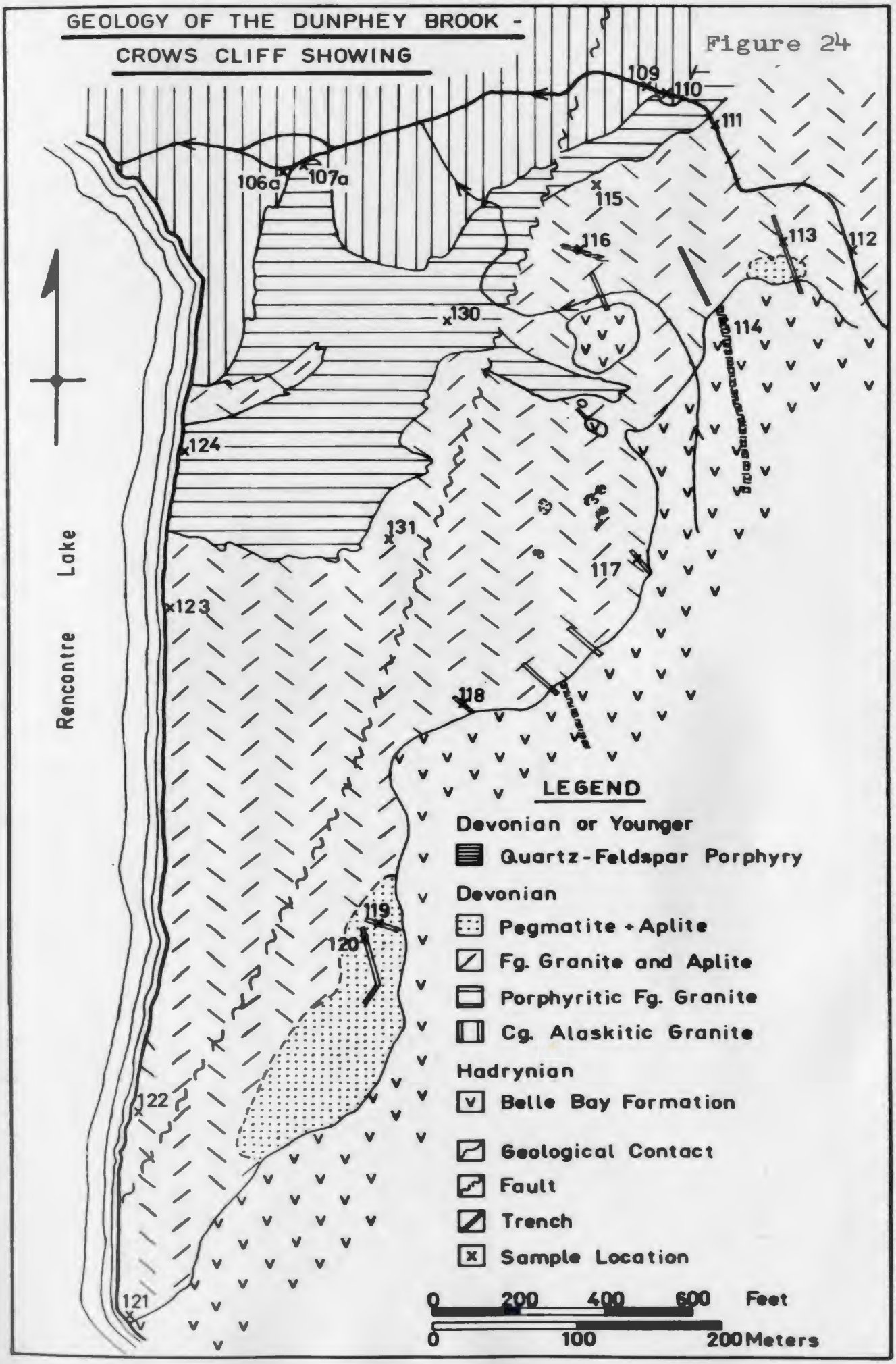
GEOLOGY OF THE DUNPHEY BROOK -
CROWS CLIFF SHOWING
Figure 24
Rencontre Lake
109
110
111
106a
107a
115
116
113
112
130
114
124
131
117
123
118
119
120
122
121
LEGEND
Devonian or Younger
Quartz-Feldspar Porphyry
Devonian
Pegmatite + Aplite
Fg. Granite and Aplite
Porphyritic Fg. Granite
Cg. Alaskitic Granite
Hadrynian
Belle Bay Formation
Geological Contact
Fault
Trench
Sample Location
0 200 400 600 Feet
0 100 200 Meters

red). The pegmatite bodies occur adjacent to the rhyolite contact, one major body in the north (Dunphey Brook), one in the south (Crow's Cliff) and a number of smaller bodies between the two. The pegmatite is in the form of sills which dip parallel to the rhyolite contact, a fact which is readily apparent due to topographic relief. The rhyolite-granite contact has a general strike of 020° and varies in dip from 60° S at Crow's Cliff to 15° S at Dunphey Brook. Flow banding in the rhyolite has a similar strike. The showing is cut by a major fault which strikes at 025° and is marked by a major escarpment the east side being approximately 200 meters higher then the west.

The quartz-feldspar porphyry is a medium reddish brown, porphyritic rock. It consists of anhedral to euhedral, embayed, bipyramidal quartz phenocrysts (2-6 mm) with radiating, fine grained quartz overgrowth rims (Plate 15) and medium pink, subhedral to euhedral perthite phenocrysts (3-8 mm) in a very fine grained devitrified glass matrix. Strong dusting with very fine grained hematite occurs throughout.

The pegmatite consists of large (maximum 50 cm diameter) milky white quartz crystals which are surrounded by medium grained (1-2 cm) anhedral, perthitic orthoclase (Plate 16). The quartz crystals exhibit prismatic as well as pyramidal faces, the presence of the former indicates that

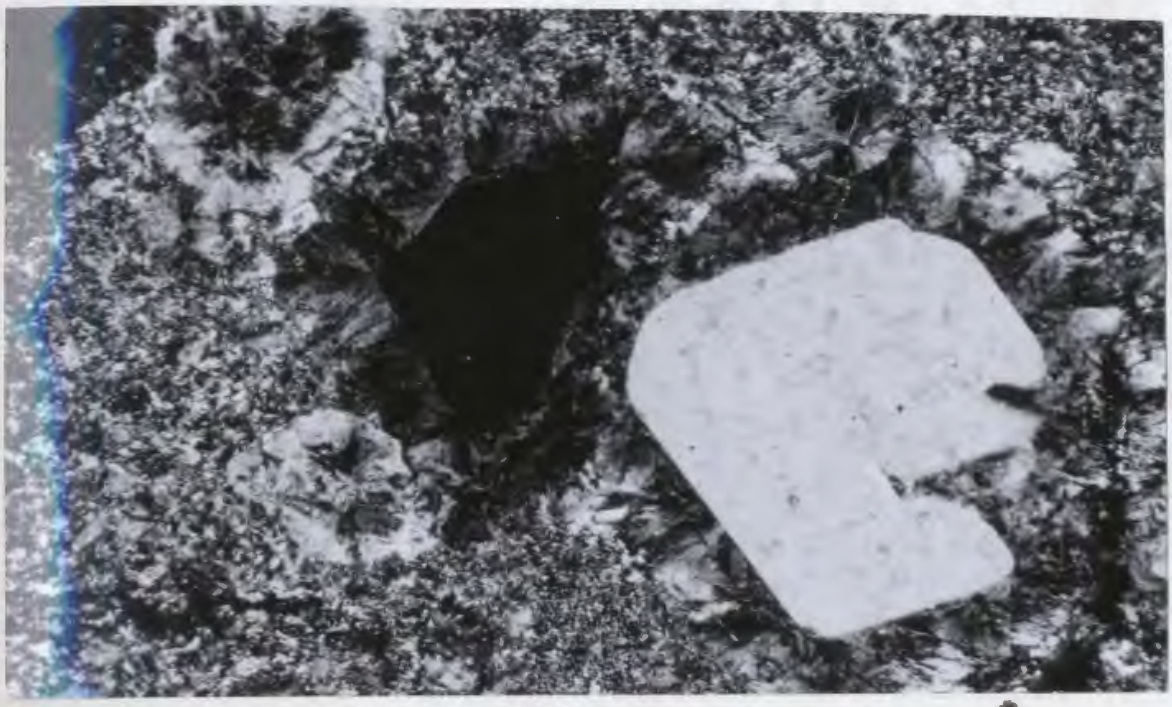

Plate 15: Embayed bipyramidal quartz phenocrysts with radiating fibrous overgrowth rims, quartz-feldspar porphyry, Dunphey Brook-Crow's Cliff Showing, crossed nicols, X45, T.S. JW-116.

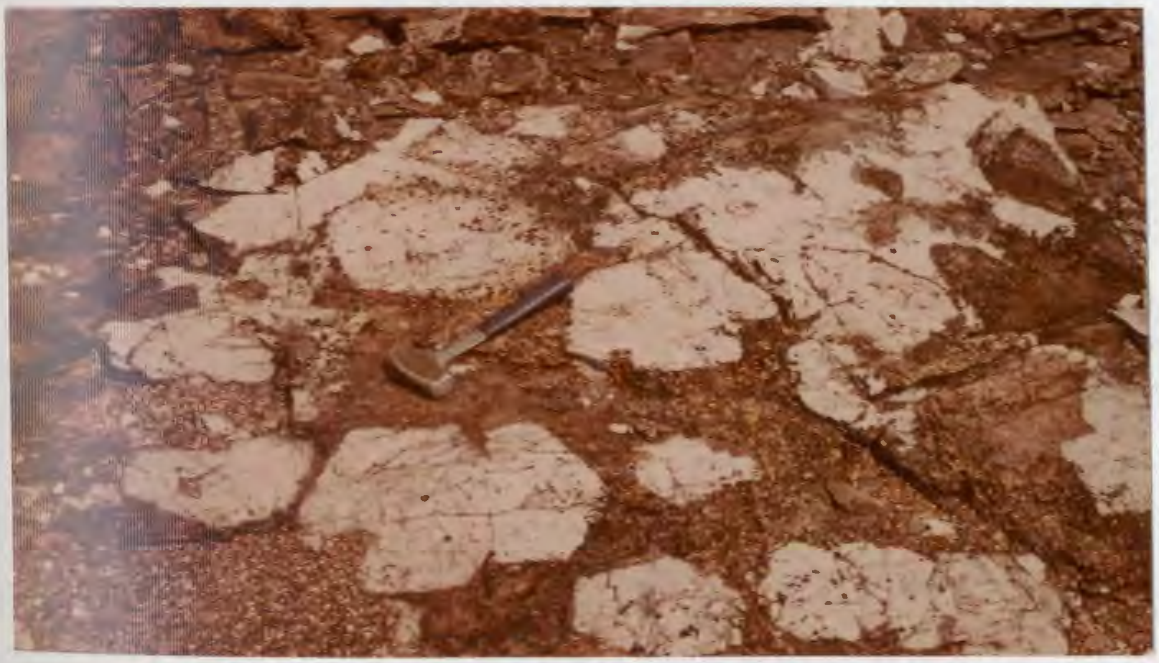

Plate 16: Pegmatite consisting of milky white, large quartz crystals surrounded by perthitic orthoclase and aplite, Dunphey Brook Showing.

they crystallized as the low (alpha) variety of quartz. Many of the quartz crystals contain one or more thin zones of pink perthite or granophyric quartz and perthite that indicate the crystal outline of the quartz crystal at different stages of growth. Variation in the size and density of distribution of quartz crystals exists from dense coarse grained patches to smaller pegmatitic pods (4 cm to 45 cm) separated by granophyric and pegmatitic aplite. The pegmatite quartz crystals have a vertical orientation with terminations pointing downward, which indicates they may have grown from the rhyolite roof (now eroded) downwards.

The fine grained granite and aplite is a hypidiomorphic granular, medium to dark pink rock composed of stringlet perthite (average .3 mm), albite (.3 mm), amoeboid or graphic quartz (.5 mm) and green ragged biotite (.2 mm). Areas which are strongly miarolitic and others of pegmatitic aplite are common. The porphyritic fine grained granite is similar to the fine grained granite except that it contains subhedral, slightly sericitically altered, normally zoned (oligoclase to albite) plagioclase (3-8 mm) and anhedral quartz (2-5 mm) phenocrysts. Pegmatitic segregations are rare or absent and many of the plagioclase phenocrysts have graphic quartz and perthite overgrowth rims (Plate 17). The

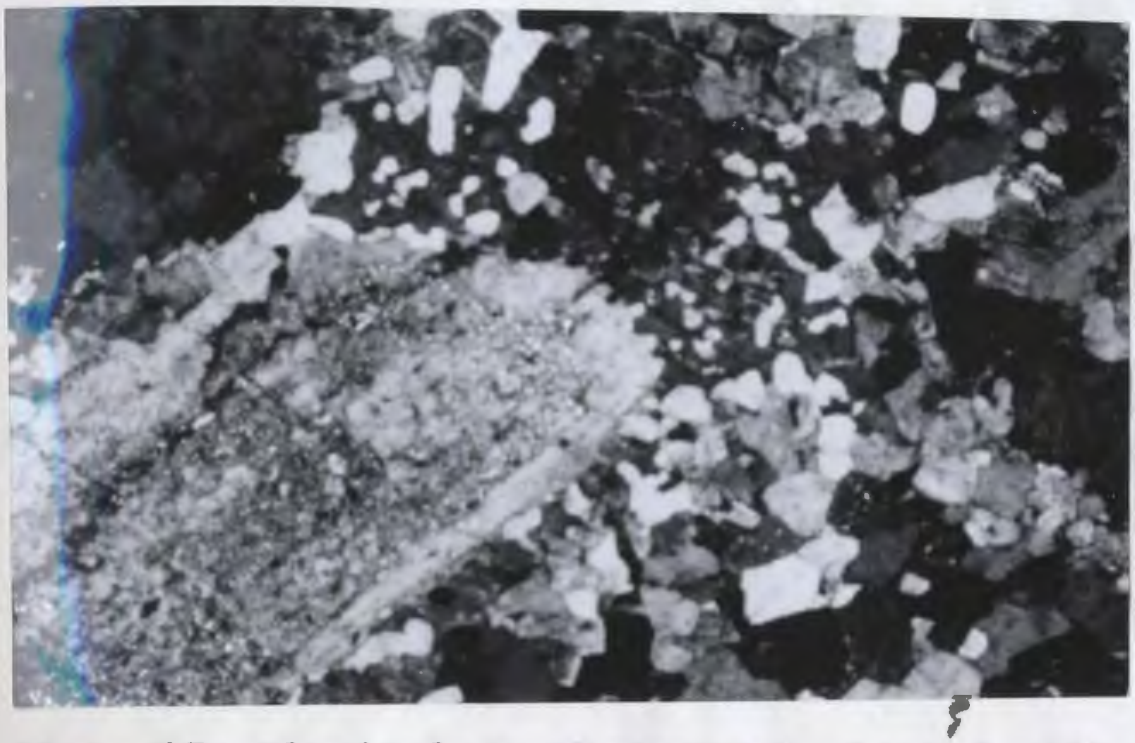

Plate 17: Plagioclase phenocryst, dusted with sericite, with a perthite and graphic quartz overgrowth rim, Dunphey Brook-Crow's Cliff, crossed nicols, X30, T.S. JW-124.

Plate 18: Brecia dyke (tuffisite) consisting of alaskitic granite fragments in a fine grained matrix, in Dunphey Brook.

tuffisites occur in dykes up to 50 cm. wide, but usually are .5 to 2 cm wide and consist of angular to subrounded fragments of red alaskitic granite in a brownish red matrix (Plate 18). The matrix consists of granulated rock flour, small angular rock fragments, calcite and clay minerals (Plate 19). Tuffisites are most abundant cutting alaskitic granite near the alaskitic-porphyritic granite contact and have highly irregular strike and dip directions.

Mineralization at the Dunphey Brook-Crow's Cliff showing occurs mainly as coarse grained molybdenite within the large quartz crystals of the pegmatite. Two types of occurrence were noted: (1) as irregularly continuous zones of molybdenite orientated parallel to the growth direction of the quartz crystals (Plate 20), and (2) as molybdenite flakes with K-feldspar distributed in concentric zones within the quartz crystals (Plate 21). The first mode of mineralization can be interpreted as a migrating nucleus of precipitation in the same area throughout the growth of the quartz crystals, while the second type can be interpreted as reflecting periods of molybdenite deposition during the growth of the quartz crystals. There is also scattered very fine grained molybdenite mineralization within the aplite between the major pegmatite bodies. In Dunphey Brook, cutting fine grained granite near

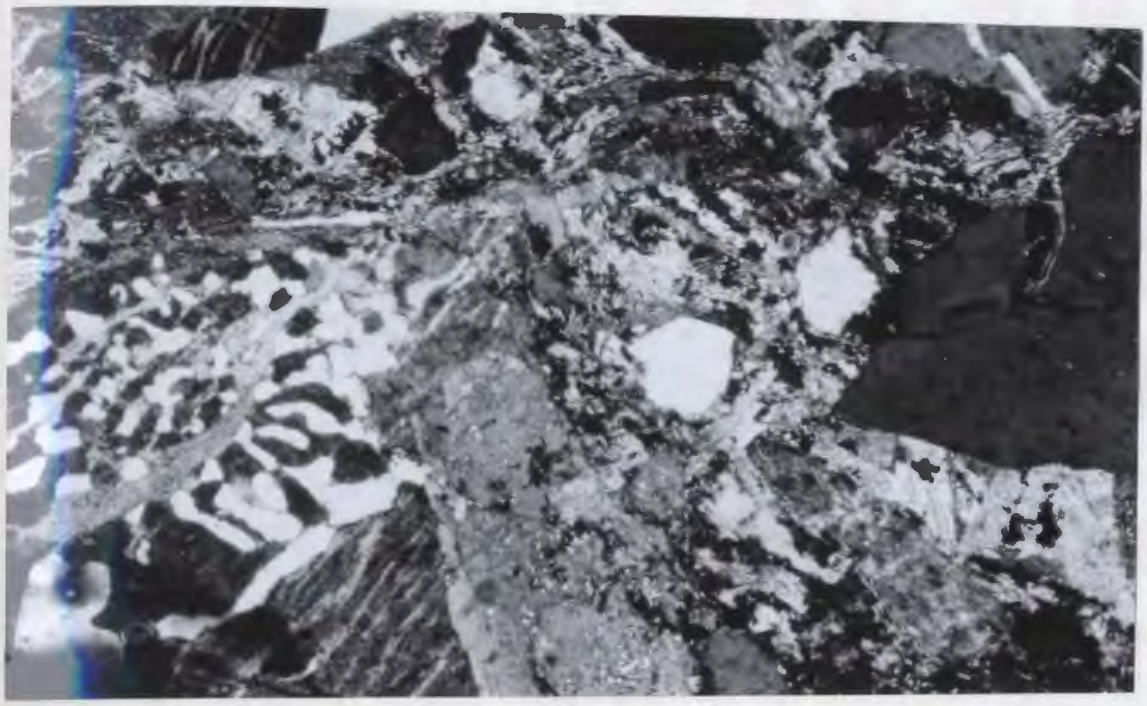

Plate 19: Matrix of tuffisite in Plate 18 composed of angular rock fragments, including granophyric fragment, clay minerals and calcite.

Plate 20: Zone of coarse grained molybdenite mineralization orientated parallel to the direction of growth (from left to right) of the quartz crystal, Crow's Cliff.

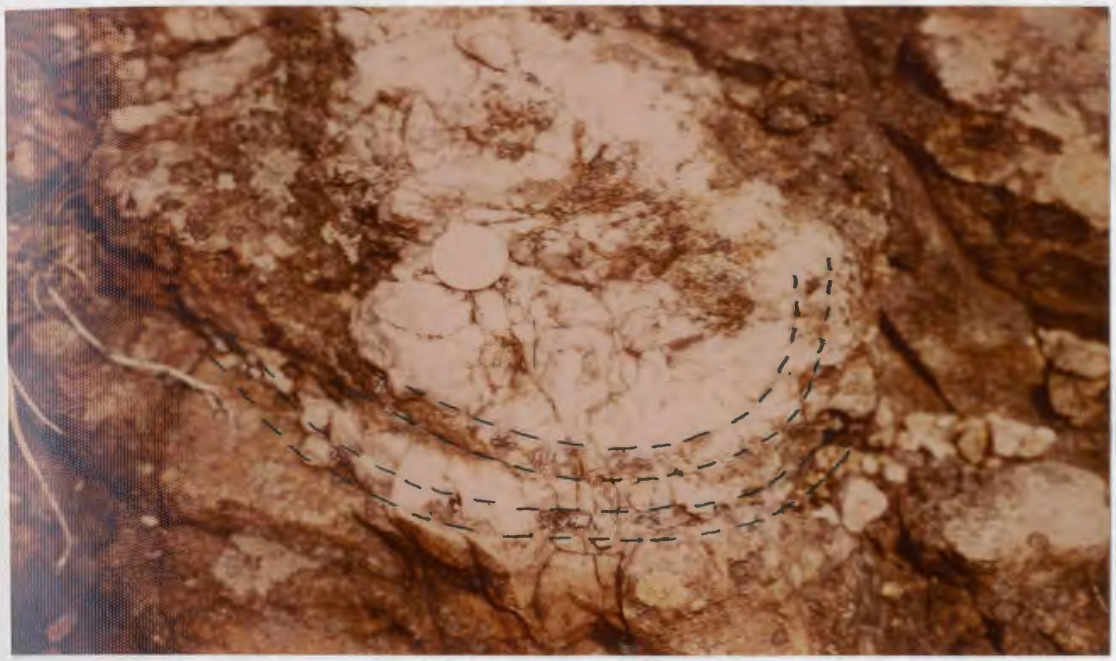

Plate 21: Cross section of a large quartz crystal with concentric zones of molybdenite and K-feldspar, Crow's Cliff.

Plate 22: Intrusive contact between quartz aplite and aplite, Wylie Hill. Note alteration within the aplite which indicates that it is older. Sample JW-211.

the intrusive-rhyolite contact, there are fractures at 000°/90° which have associated quartz- sericite alteration halos up to 25 cm on either side and which contain sparse chalcopyrite, galena and fluorite mineralization.

5.2.5 Wylie Hill Showing

The Wylie Hill Showing, the furthest east of the showings, is located 2.5 km east of the north end of Rencontre Lake within an embayment of the rhyolite-granite contact. It consists of two low grade orebodies approximately 370 by 120 meters separated by faults. The eastern orebody averages 0.15% Mo, the western 0.5% Mo. Mapping of the area in detail (Fig. 25) outlined six intrusive rock units, quartz-feldspar porphyry, pegmatite, quartz aplite, porphyritic fine grained granite and aplite, porphyritic medium grained granite and coarse grained alaskitic granite. The quartz-feldspar porphyry occurs as a dyke which cuts the rhyolite in the east part of the map area, and that continues to the north cutting the alaskitic granite (Fig. 18). A number of areas of pegmatite occur adjacent to the intrusive-rhyolite contact. Quartz aplite occurs as small bodies in the eastern and western orebodies and has sharp intrusive contacts with adjacent fine grained aplite (Plate 22). The porphyritic fine grained granite and aplite covers a large area within which the mineralization is mainly restricted. It is bordered on the north by porphyritic medium grained

Figure 25

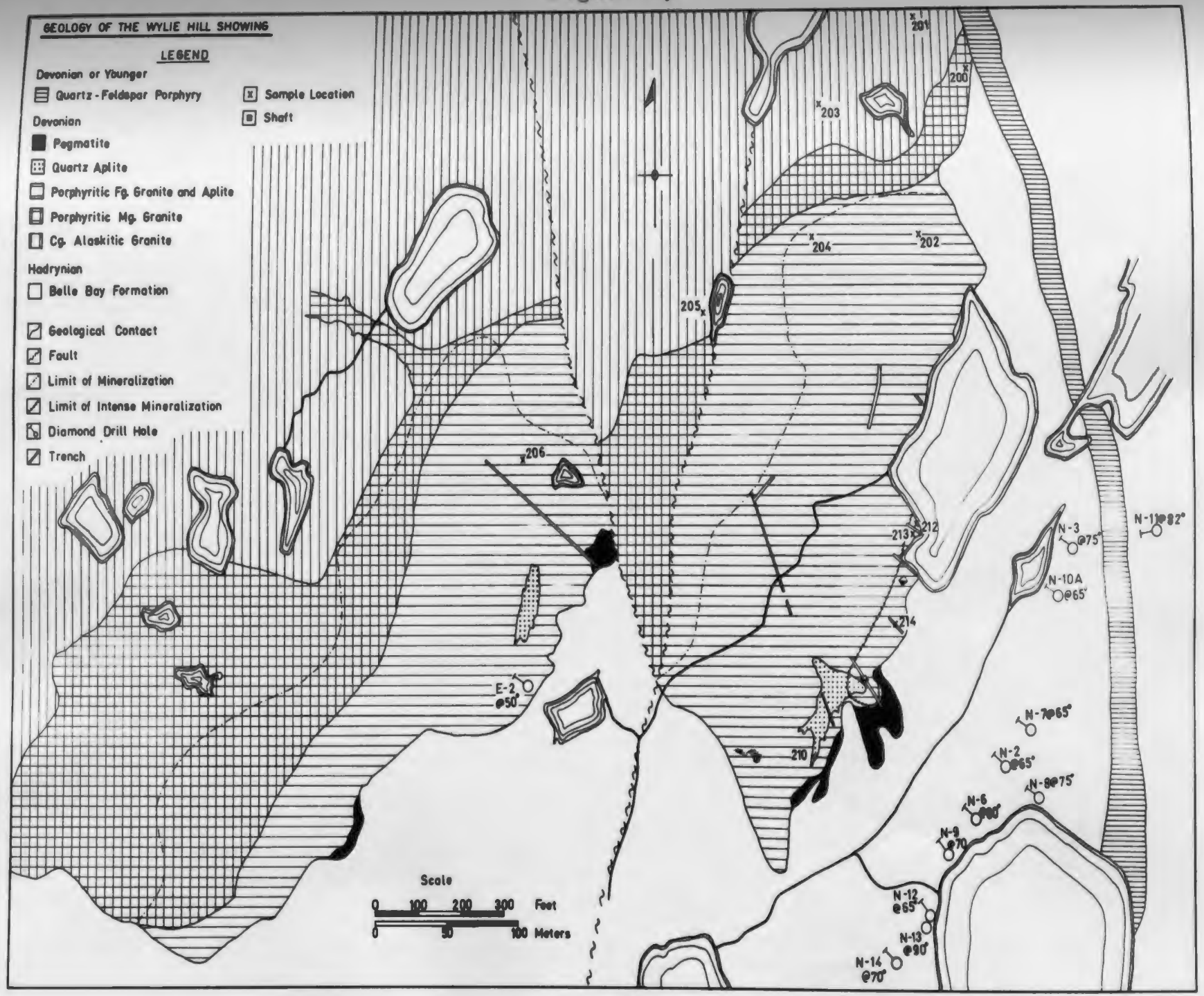
GEOLOGY OF THE WYLIE HILL SHOWING
LEGEND
Devonian or Younger
Quartz-Feldspar Porphyry
Sample Location
Shaft
Devonian
Pegmatite
Quartz Aplite
Porphyritic Fg. Granite and Aplite
Porphyritic Mg. Granite
Cg. Alaskitic Granite
Hadrynian
Belle Bay Formation
Geological Contact
Fault
Limit of Mineralization
Limit of Intense Mineralization
Diamond Drill Hole
Trench
Scale
0 100 200 300 Feet
0 50 100 Meters
201
200
203
204
202
205
206
212
213
214
210
E-2 @50°
N-3 @75°
N-10A @65°
N-1 @82°
N-7 @65°
N-2 @65°
N-8 @75°
N-6 @90°
N-9 @70
N-12 @65°
N-13 @90°
N-14 @70°

granite with which it is apparently gradational. This phase is in turn bordered to the north by coarse grained alaskitic granite with which it may also be gradational. Drill hole data suggests the orebody and these phases represent a sill underlain by coarse grained alaskitic granite. The Belle Bay Formation strikes at 075° south of the showing while the intrusive-acid volcanic contact dips 30°E at the centre of the eastern orebody and is slightly steeper to the east and west.

The quartz-feldspar porphyry is a dark brown, aphanitic rock with subhedral to euhedral, bipyramidal quartz (2-6 mm) and light pink perthite (2-9 mm) phenocrysts. The large areas of pegmatite and also the quartz-feldspar porphyry dyke rock are lithologically similar to these units at the Crow's Cliff-Dunphey Brook showing. There are also rare disconnected ellipsoidal bodies of granophyric pegmatite (up to 5 cm) which consists of an outer rim of aplite, succeeded by a layer of granophyric quartz and perthite, succeeded by a layer of quartz albite, and perthite (in order of decreasing abundance) (Plate 23), and an inner zone of elongated highly strained quartz (Plate 24). The quartz aplite is a fine grained, medium pink granite with large amoeboid quartz bodies (Plate 22), some of which are over a couple cm long but usually no more than 0.5 cm wide. It is composed of euhedral to anhedral anorthoclase (0.2 - 1.5 mm), easily

Plate 23: Bent strained albite within a pegmatitic segregation, Wylie Hill, centre is toward the left, crossed nicols, X30, T.S. 13-325.

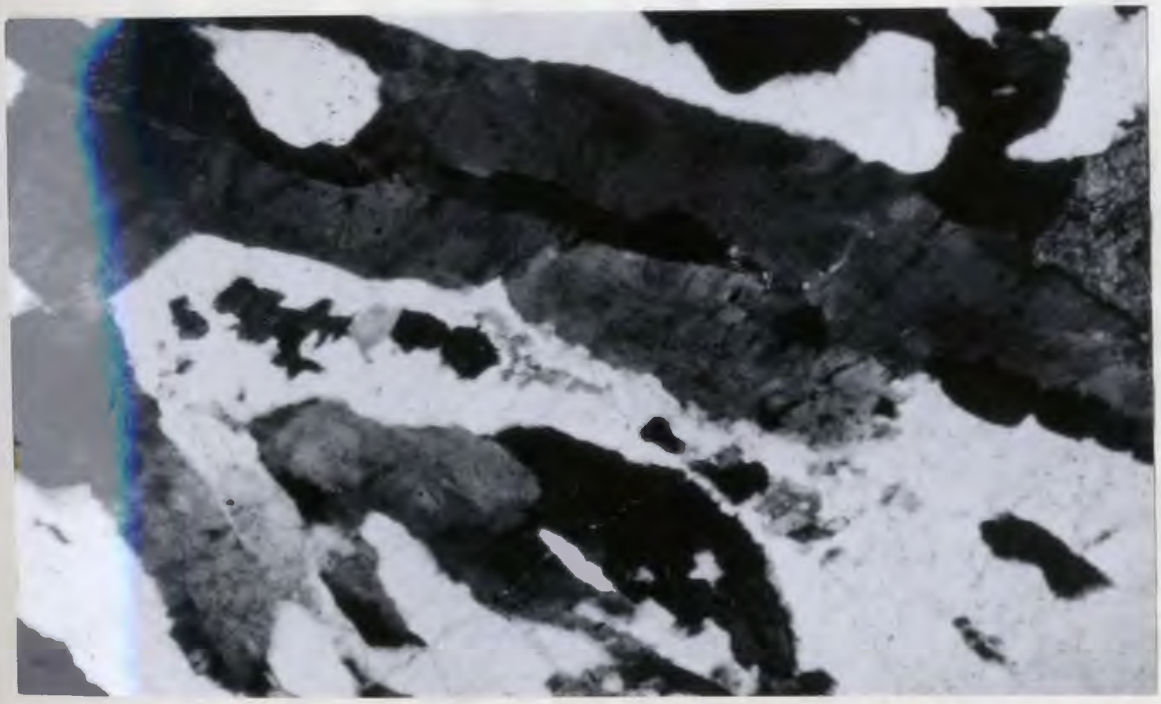

Plate 24: Elongated strongly strained quartz within the innermost zone of the same pegmatite segregation in Plate 23, centre is toward the left, crossed nicols, X30, T.S. 13-325.

distinguishable by its poor reaction with potassium stain, (Plate 25), anhedral to subhedral albite which is slightly to strongly dusted with sericite and clay minerals, and strongly strained masses of quartz. The porphyritic fine grained granite is a rock with a white to pale pinkish grey, saccharoidal matrix enclosing anhedral quartz (3-6 mm) and subhedral pink feldspar (2-6 mm) phenocrysts. It is composed of anhedral orthoclase (.2-1.5 mm) which has sodium-rich blebs revealed by staining (Plate 26), strained quartz (.2-2 mm) with serated boundaries, rare biotite (.4-1.5 mm) altered to an assemblage of chlorite, sericite, and sphene, and accessory apatite, zircon, sphere, and clinozoisite. The aplite which is included within this intrusive unit is the same but lacks phenocrysts. An unusual feature noted in drill core was the presence of compositionally and grain size banded aplite. The bands, which are approximately 5 mm wide, vary in composition from bands composed of equal amounts of quartz and albite, or of albite and perthite, or of albite, perthite, and quartz. The fine grained porphyritic granite and aplite is cut by rare thin (.2-1.5 mm) tuffisite veins composed of angular quartz and feldspar fragments in a more finely granulated rock flour matrix (Plate 27). The porphyritic, medium grained granite is a medium pink rock with phenocrysts (.5-1.5 cm) of anhedral quartz, subhedral strongly normally zoned (oligoclase to albite) plagioclase and

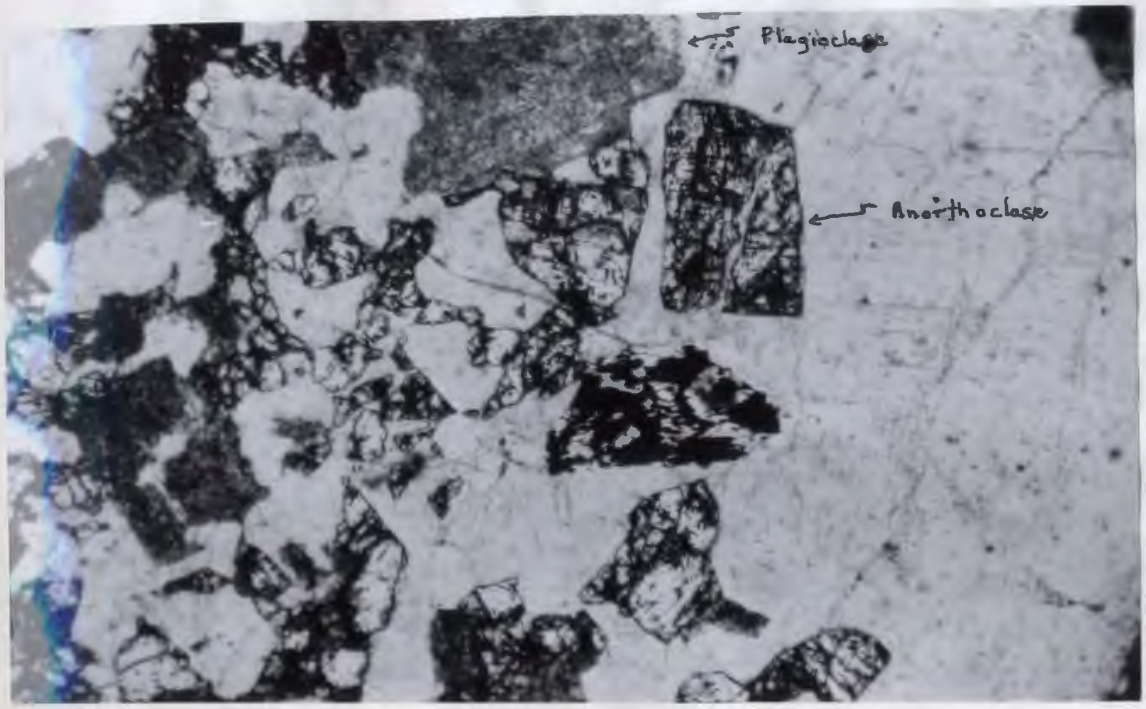

Plate 25: Quartz aplite showing partially stained (mainly on cleavages) anorthoclase and sericitically altered plagioclase bordering an amoeboid quartz to the right, Wylie Hill, uncrossed nicols, X30, T.S. JW-211.

Plate 26: Stained K-feldspar containing numerous small sodium-rich blebs that are not visible without staining, and coarse grained albite exsolution patches, Wylie Hill, crossed nicols, X30, T.S. JW-211.

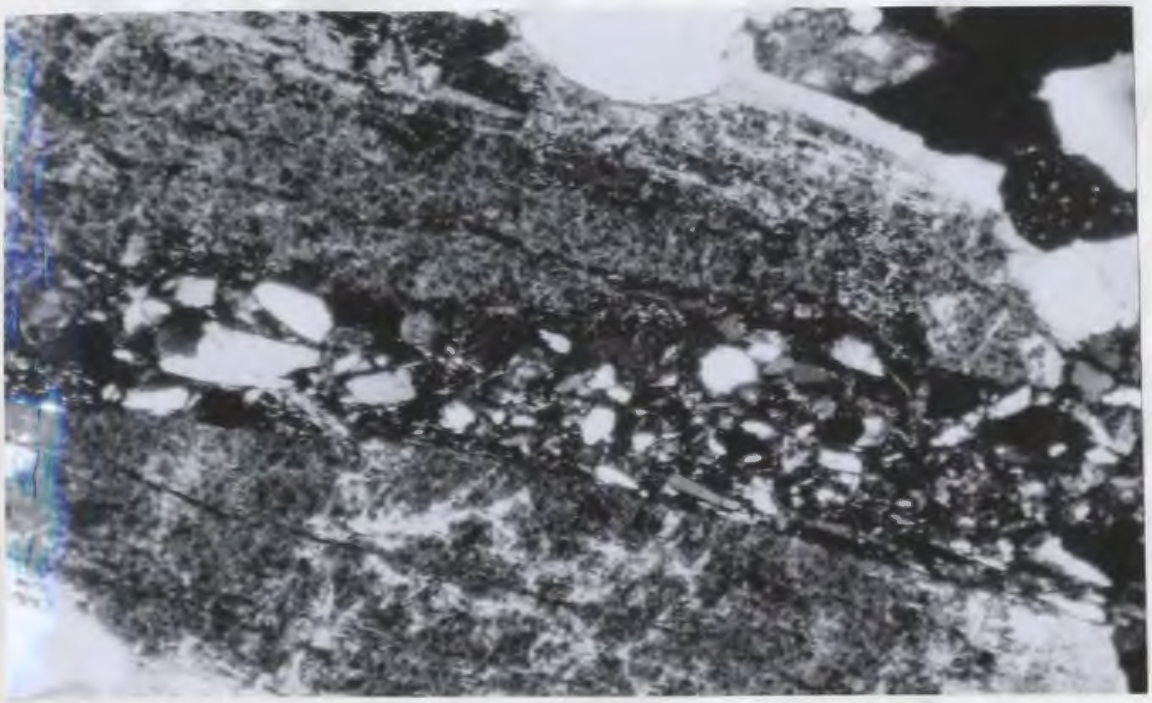

Plate 27: Tuffisite vein composed of angular fragments of quartz and feldspar cutting a plagioclase which has a sericite altered centre and an albite overgrowth rim, Wylie Hill, crossed nicols, X30, T.S. WH-14-158.

Plate 28: Weathered mineralized fine grained porphyritic granite, Wylie Hill, pyrite aggregates and molybdenite rosettes give a nodular appearance, similar to a concretion bearing weathered sandstone, Wylie Hill.

subhedral stringlet perthite. The Belle Bay Formation consists of flow banded, dark grey and medium brown rhyolite in the southwest and mixed rhyolite and acid fragmental units composed of angular rhyolite and porphyritic tuff fragments (1-6 cm) in a fine grained tuffaceous matrix in the southeast.

Mineralization at the Wylie Hill showing consists of fracture filling and disseminated molybdenite with extensive associated pyrite. Joints orientated at 160°/90° and 135°/60° SW are closely spaced, averaging 4 to 12 cm. between joints, and mineralized with molybdenite (2-4 mm), pyrite (2-6 mm) and quartz. Disseminated sulphides are extensive in the large mineralized area with pyrite occurring as nodules (Plate 28) within which the pyrite forms anhedral dentritic growths (Plate 29) occupying original quartz sites. Molybdenite occurs either as inclusions within the pyrite, a relationship indicating it is earlier than pyrite, or as fibrous platey aggregates (Plate 30). There are rare small scattered patches of muscovite replacing plagioclase or perthite (Plate 31). The white colour of the aplite and fine grained porphyritic granite associated with mineralized areas is apparently due to alteration. White (1939) attributed this to a leaching of all iron from feldspars to form the abundant pyrite. However, this seems to be an unreasonable explanation,

Plate 29: Part of pyrite nodule showing the dendritic nature of the pyrite which occupies quartz sites in the granite, Wylie Hill, reflected light, uncrossed nicols, X60, P.S. WH-249.

Plate 30: Fine grained platy aggregate of molybdenite disseminated in fine grained, porphyritic granite, Wylie Hill, crossed nicols, X60, P.S. WH-69-7-150.

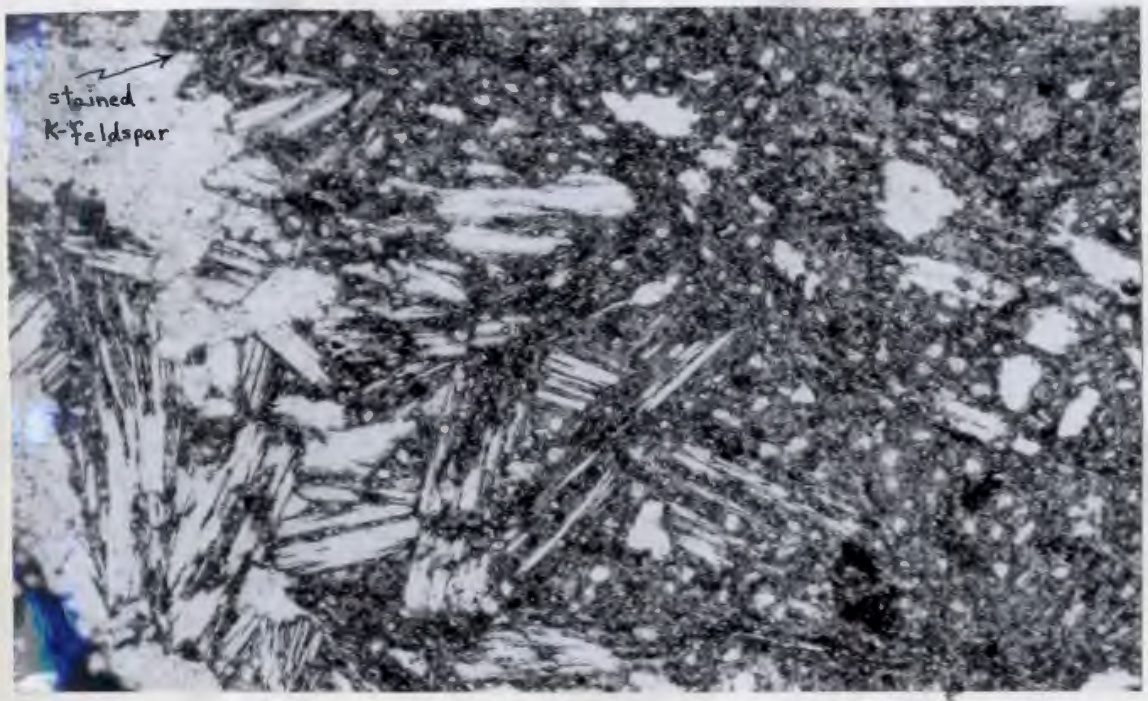

Plate 31: Coarse grained muscovite alteration of perthite in a small dense aggregate, Wylie Hill, uncrossed nicols, X30, T.S. WH-7-148.

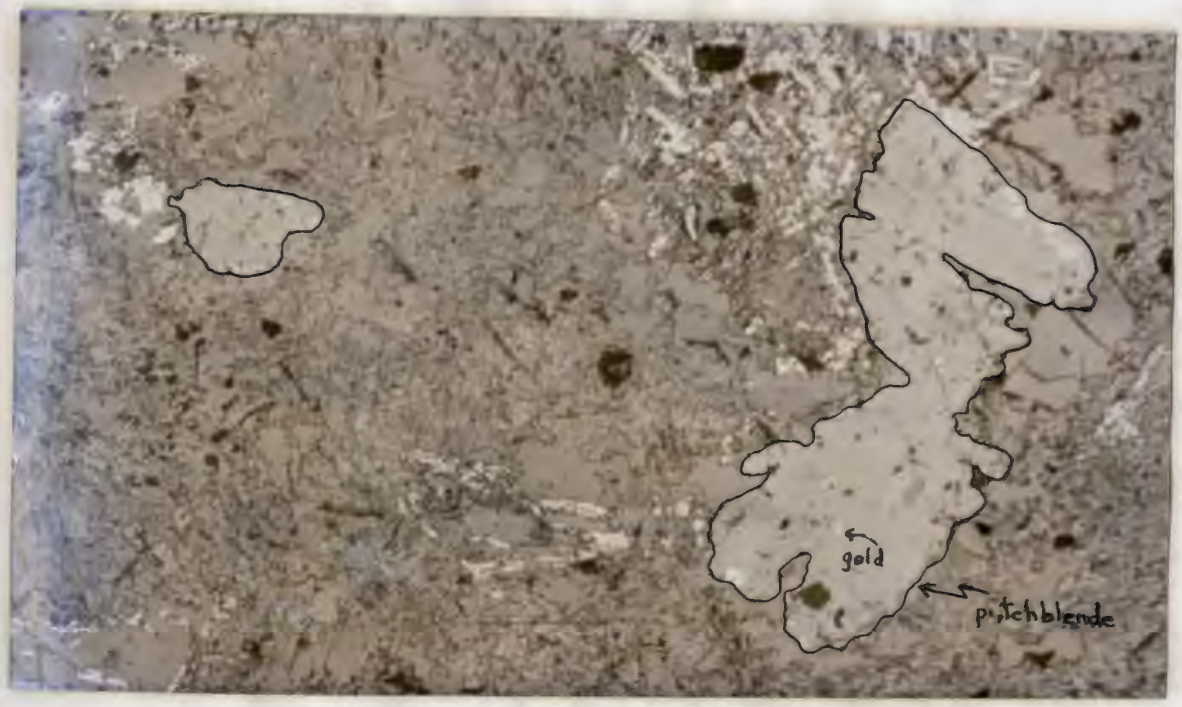

Plate 32: Grains of pitchblende with minute inclusions of gold in mineralized porphyritic fine grained granite, Wylie Hill, reflected light, crossed nicols, X60, P.S. WH-69-7-150.

the phenomenon being easier explained as reduction of all iron from the 3+ to 2+ state by the addition of sulphur to the rock. Minor accessory sphalerite and galena were noted in the mineralized granite as well as pitchblende with minute inclusions of gold (Plate 32), identification of the former being aided by the use of an autoradiograph (Plate 33). A major feature of the rhyolite bordering the extensive mineralized zone of the eastern orebody is the presence of abundant barren quartz veins. These pinch and swell up to half a meter wide, contain angular rhyolite fragments, have highly variable attitudes and do not extend far laterally away from the contact. Fracture filling quartz, molybdenite, and pyrite mineralization within the rhyolite is not extensive, but it is the only mineralized rhyolite observed in all the showings.

5.2.6 Frank's Pond Showing

The Frank's Pond Showing is located 3.5 km north northwest of the north end of Rencontre Lake, 5 km within the alaskitic phase of the Ackley batholith (Fig. 4). There are numerous lithologically different types of granite in the area, medium grained granite to aplite, and porphyritic granite, which may be mutually gradational, all cutting normal coarse grained alaskitic granite. These intrusive phases, which are characterized by miarolitic cavities and pegmatitic patches (up to ½ meter) are megascopically identical to those associated with molybdenite

Plate 33: Autoradiograph of the pitchblende grains in Plate 32 (one month plate exposure), X14.

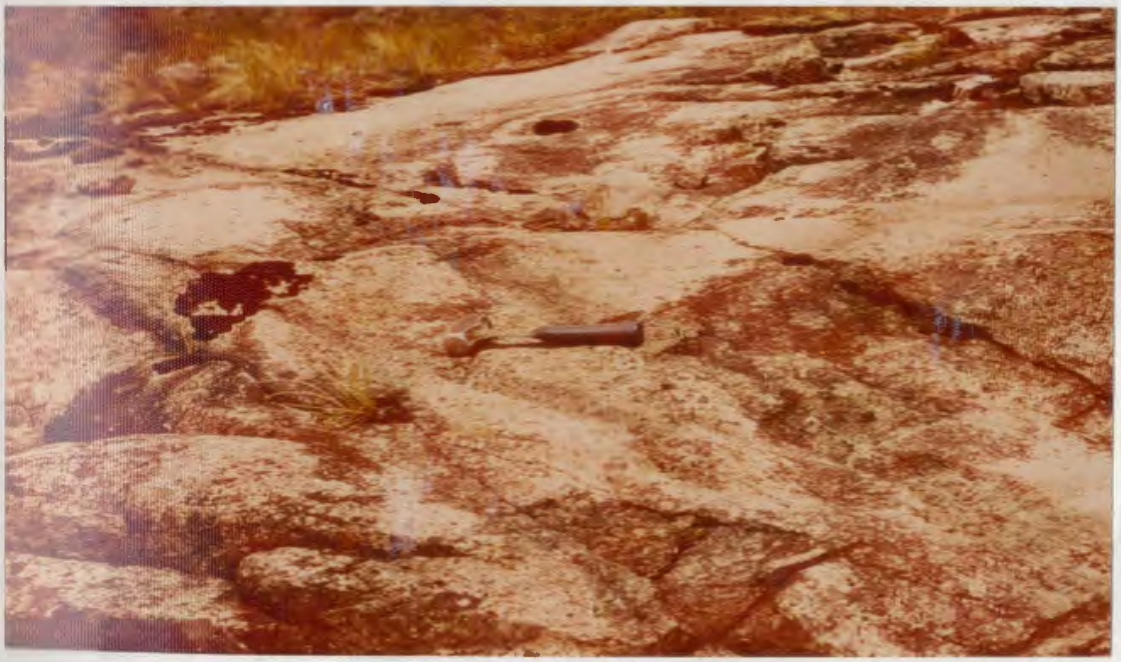

Plate 34: Quartz veins striking at 308° which have fringes of quartz-sericite alteration cutting alaskitic granite, Frank's Pond.

mineralization to the south. Cutting the alaskitic granite are numerous aplite veins and dykes and rare quartz veins striking at 308°/90° with associated quartz-sericite alteration (Plate 34). Quartz veins lacking alteration are common, striking at 163°/90° and 072°/90°. These veins, which are rarely over 5 cm wide, locally carry molybdenite flakes (2-3 mm) lining their borders. Extent and tenor of mineralization is, however, very sparse.

5.2.7 Belle Island Showing

The Belle Island Showing is located in Fortune Bay, approximately 10 km southeast of Rencontre East (Fig. 4), and is within an approximately 305 by 150 meters granitic plug exposed on the cliff face of the eastern side of the island (Plate 35). This granite, which intrudes sandstone of the Precambrian Rencontre Formation, has been subdivided into a number of phases, aplite, porphyritic aplite, porphyritic medium grained granite and coarse grained alaskitic granite, all of which appear to be gradational into each other (Fig. 26). A Devonian age for the body has been assumed on the basis of lithological and geochemical similarity to the Ackley alaskitic granite.

The intrusive breccia consists of numerous angular 2 to 6 cm fragments of the sandstone host rock in a matrix of pale pink saccharoidal aplite. Similar miarolitic aplite also occurs in dykes or tongues and as a marginal chilled zone approximately 1 meter wide adjacent to host

Plate 35: Alaskitic granite plug, approximately 305 by 150 meters, exposed on the eastern side of Belle Island.

Plate 36: Fracture related quartz-sericite-clay mineral alteration of porphyritic fine grained granite, Belle Island.

Figure 26

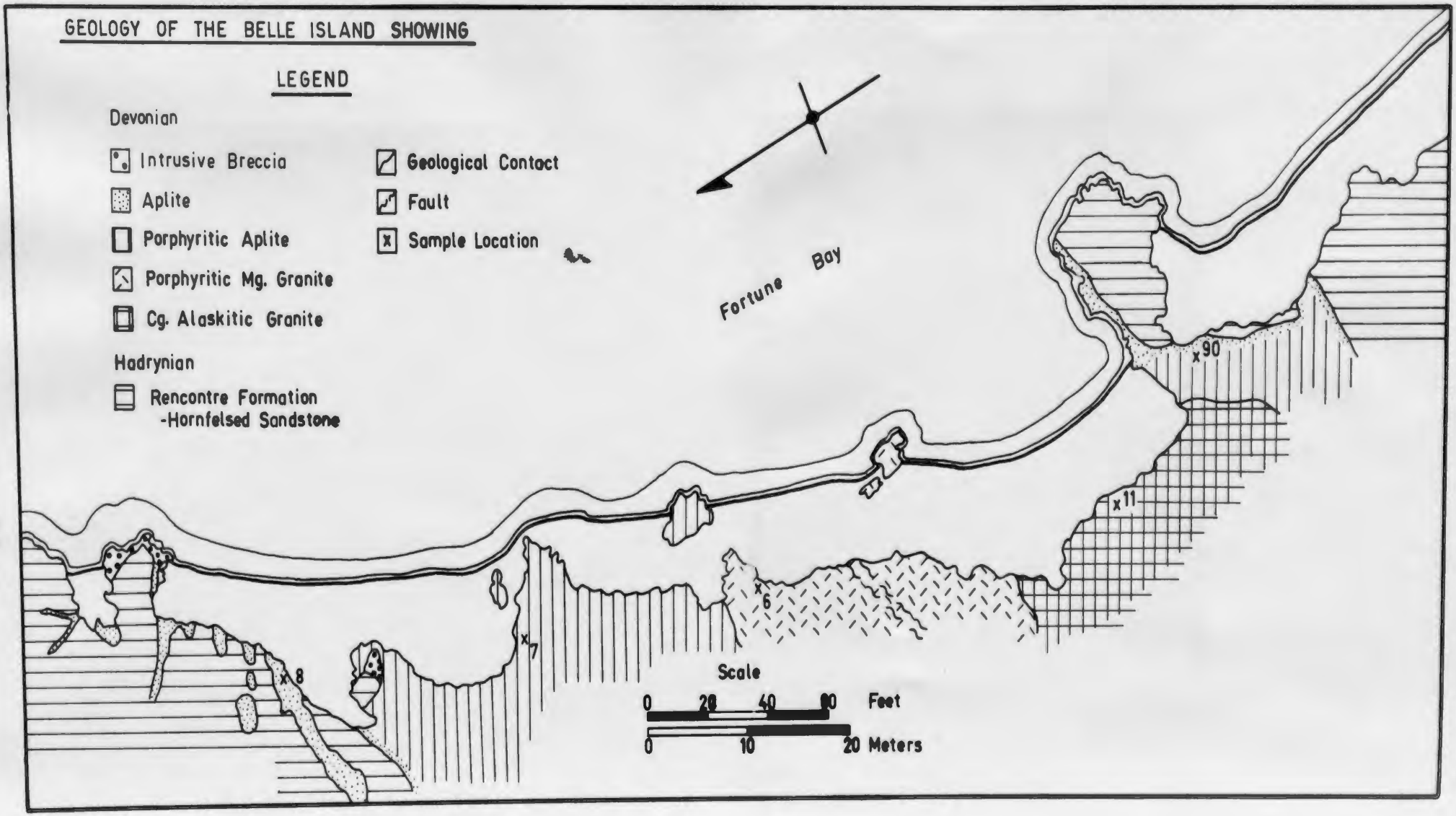
GEOLOGY OF THE BELLE ISLAND SHOWING
LEGEND
Devonian
Intrusive Breccia
Aplite
Porphyritic Aplite
Porphyritic Mg. Granite
Cg. Alaskitic Granite
Hadrynian
Rencontre Formation
-Hornfelsed Sandstone
Geological Contact
Fault
Sample Location
Fortune Bay
x90
x11
x6
x7
x8
Scale
0 20 40 60 Feet
0 10 20 Meters

sandstone. It is a hypidiomorphic equigranular (.5 mm) rock composed of normally zoned albite, strained anhedral quartz, and perthitic K-feldspar. The porphyritic aplite is similar but contains less miarolitic cavities and has rare to abundant anhedral to subhedral bipyrimidal quartz (2-3 mm), pale pink perthite (2-20 mm) and plagioclase (2-10 mm) phenocrysts. K-feldspar mottled, euhedral, strongly normally zoned (oligoclase to albite) plagioclase phenocrysts are common. An increase of the grain size of the matrix to an average 2 mm characterizes the porphyritic medium grained granite while the alaskitic granite is an hypidiomorphic equigranular (5 mm), rock of similar mineralogy. The intruded Rencontre Formation consists of fine grained (1-2 mm), dark brown to grey, argillaceous, commonly cross-bedded sandstone.

Both intrusive and host rock are highly fractured, a feature which has localized alteration and mineralization. Although mild alteration is pervasive, intense alteration is closely fracture controlled (Plate 36), while similar fractures cutting the sandstone are lined with fine grained sericite. Alteration is mainly sericitic with plagioclase (Plate 37) and K-feldspar being strongly altered to fine to coarse grained felted masses of sericite with minor associated calcite, while biotite is replaced by aggregates of sericite, rutile calcite, and sphene (Plate 38). Widely spaced fractures in both the intrusive

Plate 37: Coarse grained radiating felted masses of sericite completely replacing a plagioclase phenocryst in porphyritic medium grained granite, Belle Island, crossed nicols, X30, T.S. JW-10.

Plate 38: Biotite completely replaced by sericite-calcite-sphene-rutile-pyrite in porphyritic aplite, Belle Island, crossed nicols, X60, T.S. JW-90.

and sandstone are mineralized with flakes (2 mm) of molybdenite, rare chalcopyrite and more abundant pyrite along with quartz and calcite. Within the aplite some of the miarolitic cavities are similarly mineralized. A late narrow (4 cm) fault breccia cemented by vuggy purple fluorite, calcite and barite cuts the centre of the intrusive.

5.3 Geochemistry

5.3.1 Introduction

Two hundred and six samples of mineralized and unmineralized intrusive rocks of the showings and the nearby barren alaskitic granite were analyzed for major elements and trace elements and 120 of these were also analyzed for U and Bi. All this analytical data as well as corresponding Barth (1962) molecular norms are presented in Appendix D.

This analytical data was obtained to aid in the understanding of: (1) the relationship between the different mapped intrusive units of the showings and the surrounding alaskitic granite; (2) the difference between mineralized and unmineralized intrusives and the different elements associated with molybdenum in the deposits; (3) the similarities and differences between the different showings; and (4) the petrogenesis of the showings and their host intrusives. To aid in comparison between different intrusive units of individual showings and

between the different showings, the geochemical data has been summarized in tables 6, 7, 8, 9 and 10 which present the means and standard deviations for the compositions of different intrusive units described in the previous section. The following sections will examine the geochemical data with respect to the problems outlined above.

5.3.2 Variation Diagrams

A comparison of the data of tables 6, 7, 8, 9 and 10 reveals that the mean compositions of the different mapped intrusive units within and between different showings, especially in major elements are very similar, generally overlapping when standard deviations are taken into consideration. Not only are they similar in composition but silica content (75 - 80%) and differentiation index (generally 95 - 100) indicate they are all extremely differentiated and very little further fractionation with attendent elemental variation could be expected. During the very final stages of differentiation only trace elements and possibly a few major elements might be expected to fractionate slightly, and this is the type of behavior exhibited by the data. Plots of data from the Wylie Hill showing (Figure 27 a, b) are representative examples of the behavior of the data from all the showings.

Most major elements (SiO_2, Al_2O_3, MnO, Na_2O and K_2O) show no variation or trend when plotted versus differentiation index or silica, however, Fe_2O_3 total,

Table 6

COMPOSITION OF DIFFERENT INTRUSIVE PHASES AT THE MOTU SHOWING

Element	Mg. Granite		Porphyritic Aplite		Mineralized Fg. Granite	
	$\bar{x}$	σ	$\bar{x}$	σ	$\bar{x}$	σ
SiO_2	77.46	.77	77.91	.58	82.58	1.26
TiO_2	.08	.03	.12	.00	.08	.03
Al_2O_3	12.33	.36	12.09	.10	8.47	1.14
Fe_2O_3*	.57	.07	.32	.00	.45	.16
MnO	.03	.00	.02	.02	.02	.01
MgO	.04	.00	.00	.00	.03	.02
CaO	.23	.04	.18	.00	.22	.12
Na_2O	3.50	.20	3.54	.09	2.22	.46
K_2O	5.07	.29	4.92	.09	3.27	.68
H_2O	1.16	.75	.57	.07	1.88	1.51
Total	100.47		99.67		99.22	
Zr	109	7	140	2	100	18
Sr	5	3	6	4	3	2
Rb	447	21	457	2	333	66
Zn	41	39	24	20	42	36
Cu	8	3	12	6	12	8
Ba	30	3	20	9	11	5
U	8	2	8	0	8	1
Mo	12	4	12	1	3270	1469
Nb	38	4	44	3	57	20
Bi	19	7	12	2	25	20
Pb	68	11	84	29	39	6
Ni	11	1	10	2	6	2
Y	58	17	80	18	37	16
Cr	10	2	6	0	18	8
Ti	725	57	725	76	712	69
S	190	50	405	94	11436	1203
Q	37.8	.9	38.7	1.29	58.7	6.1
Or	30.2	2.0	29.4	.69	19.8	3.9
Ab	30.0	1.4	30.3	.92	19.3	3.8
An	.9	.2	.50	.02	.9	.6
D.I.	98.0		98.4		97.8	
K/Rb	9.42		8.94		8.15	
Ba/Rb	.07		.04		.03	
Ca/Sr	32.88		21.44		52.41	
Ba/Sr	6.00		3.33		3.67	
Rb/Sr	89.40		76.17		111.00	
n	3		2		5	

$\bar{x}$ = mean

σ = standard deviation

n = number of samples

* = total Fe as Fe_2O_3

Table 7

COMPOSITION OF DIFFERENT INTRUSIVE PHASES AT THE ACKLEY CITY SHOWING

Element	Mg.-Cg. Alaskitic Granite		Mg. Granite		Aplite		Mineralized Granite	
	$\bar{x}$	σ	$\bar{x}$	σ	$\bar{x}$	σ	$\bar{x}$	σ
SiO_2	76.22	1.06	78.55	1.46	77.15	1.83	73.41	7.71
TiO_2	.15	.03	.11	.03	.12	.07	.10	.01
Al_2O_3	11.72	.43	10.75	.73	11.65	.73	8.08	.77
Fe_2O_3 *	.78	.07	.74	.08	.62	.11	2.39	1.67
MnO	.05	.03	.05	.01	.02	.01	.10	.07
MgO	.09	.03	.08	.02	.03	.01	.14	.06
CaO	.29	.06	.42	.08	.29	.10	.74	.21
Na_2O	3.30	.35	2.37	.22	3.19	.59	1.04	.27
K_2O	4.86	.10	5.11	.69	4.82	.42	4.65	.70
H_2O	.61	.06	.65	.10	.76	.30	4.08	2.10
Total	98.07		98.18		98.65		94.73	
Zr	125	10	108	20	112	28	84	24
Sr	17	7	14	4	6	6	4	2
Rb	433	27	484	62	445	63	395	75
Zn	65	100	249	146	123	116	283	87
Cu	12	13	33	14	23	18	51	5
Ba	44	9	54	6	29	11	32	6
U	8	2	12	0	10	3	18	2
Mo	56	62	27	6	31	16	8657	2329
Nb	30	1	30	4	32	7	86	27
Bi	20	1	17	5	17	4	36	15
Pb	52	14	54	7	64	13	59	8
Ni	8	3	9	2	9	2	8	2
Y	60	15	38	5	46	12	61	8
Cr	18	5	6	5	18	18	12	6
Ti	861	101	766	135	592	164	759	258
S	428	210	723	427	389	182	37893	2264
Q	39.2	2.6	45.6	4.2	40.7	4.2	54.4	6.2
Or	29.4	.5	30.7	4.3	29.2	2.4	30.9	4.4
Ab	28.9	3.1	20.6	1.8	27.8	5.1	10.3	3.6
An	.9	.2	1.8	.3	1.1	.6	3.6	1.8
D.I.	97.5		96.9		97.7		95.6	
K/Rb	9.32		8.76		8.99		9.77	
Ba/Rb	.10		.11		.07		.08	
Ca/Sr	12.19		21.44		34.54		132.22	
Ba/Sr	2.59		3.86		4.83		8.00	
Rb/Sr	25.47		34.57		74.17		98.75	
n	4		4		7		3	

$\bar{x}$ = mean
σ = standard deviation
n = number of samples
* = total Fe as Fe_2O_3

Table 8

COMPOSITION OF DIFFERENT INTRUSIVE PHASES AT THE CROWS CLIFF-DUNPHEY BROOK SHOWING

Element	Cg. Alaskitic Granite		Fg. - Mg. Granite		Aplite		Porphyritic Mg. Granite		Quartz-Feldspar Porphyry	
	$\bar{x}$	σ	$\bar{x}$	σ	$\bar{x}$	σ	$\bar{x}$	σ	$\bar{x}$	σ
SiO_2	78.19	.58	75.82	.58	77.48	1.02	76.59	.96	76.59	1.37
TiO_2	.07	.02	.05	.01	.07	.04	.13	.06	.08	.04
Al_2O_3	11.70	.27	12.37	.33	11.94	.73	12.28	.19	12.23	.18
Fe_2O_3*	.81	.04	.72	.03	.62	.14	.87	.10	1.12	.09
MnO	.03	.00	.02	.00	.02	.00	.04	.01	.03	.00
MgO	.07	.02	.02	.01	.02	.02	.08	.05	.06	.02
CaO	.34	.05	.13	.02	.18	.03	.23	.12	.11	.00
Na_2O	3.44	.02	3.31	.08	3.38	.22	3.61	.12	1.21	.79
K_2O	4.97	.13	5.43	.12	4.99	.47	4.69	.56	6.17	.09
H_2O	.76	.03	.45	.08	.55	.19	.62	.09	1.35	.01
Total	100.38		98.32		99.25		99.14		98.95	
Zr	134	15	205	50	124	10	157	13	196	3
Sr	23	6	55	44	4	2	16	10	36	0
Rb	354	6	312	55	377	37	390	27	566	91
Zn	18	15	42	16	4	7	11	14	56	23
Cu	4	1	15	12	10	6	8	8	ND	—
Ba	78	0	150	98	29	19	63	26	60	6
U	8	0	8	2	7	1	9	2	7	0
Mo	12	0	21	2	51	62	17	4	12	3
Nb	31	3	31	7	19	14	28	4	52	2
Bi	12	5	12	0	11	6	14	1	18	0
Pb	29	7	83	41	36	18	50	14	61	9
Ni	14	0	9	3	6	4	11	1	16	1
Y	82	1	76	9	69	31	87	22	112	5
Cr	10	2	16	3	7	6	4	4	6	4
Ti	1024	156	1417	562	674	112	879	169	618	51
S	350	180	335	45	165	98	203	36	175	12
Q	39.3	1.3	36.6	.6	39.2	3.6	38.2	2.5	47.4	5.4
Or	29.7	.8	33.0	.7	30.0	2.8	28.2	3.4	37.6	.2
Ab	29.5	.2	28.8	.8	29.2	1.8	31.2	1.0	10.7	7.0
An	1.3	.2	.5	.1	.7	.3	1.0	.4	.3	.2
DI	98.5		98.4		98.4		97.6		95.7	
K/Rb	11.65		14.45		10.99		9.98		9.05	
Ba/Rb	.22		.48		.08		.16		.11	
Ca/Sr	10.57		1.69		32.16		10.27		2.18	
Ba/Sr	3.39		2.73		7.25		3.94		1.67	
Rb/Sr	15.39		5.67		94.25		24.38		15.72	
n	2		2		4		6		2	

* - total Fe as Fe_2O_3 σ - standard deviation

$\bar{x}$ - mean n - number of samples

Table 9

COMPOSITION OF DIFFERENT INTRUSIVE PHASES AT Wylie Hill Showing

Element	Cg. Alaskitic Granite		Fg.-Mg. Granite		Porphyritic Mg. Granite		Mineralized Fg. Granite		Quartz Aplite	Quartz-Feldspar Porphyry
	$\bar{x}$	σ	$\bar{x}$	σ	$\bar{x}$	σ	$\bar{x}$	σ		
SiO_2	76.44	2.72	77.28	1.60	76.97	1.23	78.14	2.06	84.00	76.06
TiO_2	.07	.06	.07	.04	.09	.06	.06	.02	.04	.05
Al_2O_3	12.22	1.66	11.81	.69	11.67	.75	10.73	.53	8.30	12.00
Fe_2O_3*	1.31	.36	1.03	.45	1.38	.55	1.19	1.24	.27	1.39
MnO	.03	.02	.02	.01	.03	.02	.01	.01	.00	.02
MgO	.21	.08	.19	.24	.25	.09	.10	.08	.01	.07
CaO	.43	.16	.46	.15	.44	.29	.41	.09	.10	.47
Na_2O	3.50	.70	3.30	.53	3.12	.34	2.81	.35	2.41	5.02
K_2O	4.78	.71	5.04	.61	4.69	.23	4.51	.68	3.39	5.01
H_2O	.59	.48	1.27	.55	.54	.38	1.56	.77	.54	.53
Total	99.58		100.47		99.18		99.52		99.10	100.62
Zr	135	19	151	23	141	14	138	17	82	247
Sr	34	28	23	12	38	24	13	8	7	14
Rb	353	31	375	34	350	20	354	49	295	271
Zn	182	142	123	108	75	52	104	163	117	22
Cu	40	19	33	23	35	18	12	9	ND	27
Ba	103	67	81	29	119	73	55	17	25	97
U	5	0	7	1	7	1	7	2	4	8
Mo	81	105	264	289	75	46	2530	1632	72	23
Nb	28	4	31	5	30	3	34	5	22	42
Bi	16	1	15	0	16	5	25	5	3	14
Pb	137	104	102	70	88	42	77	42	121	32
Ni	32	15	23	22	37	22	13	14	ND	8
Y	34	8	38	6	34	4	35	7	21	103
Cr	36	18	48	38	28	11	40	21	30	ND
Ti	746	193	780	146	901	208	625	169	500	812
S	3510	2365	3957	2264	2744	2521	12333	4926	220	320
Q	37.8	8.9	38.6	5.7	43.4	7.3	45.2	3.1	57.8	22.5
Or	28.4	4.2	29.9	3.4	27.9	1.4	27.4	3.9	20.4	28.1
Ab	30.3	5.9	28.1	4.3	27.1	2.9	24.6	3.3	20.8	30.7
An	2.0	.6	1.7	.8	1.8	.9	1.7	.5	.4	0.0
D.I.	96.5		96.6		98.4		97.2		99.0	81.1
K/Rb	11.24		11.66		11.12		10.58		9.54	15.35
Ba/Rb	.29		.22		.34		.16		.08	.36
Ca/Sr	9.04		14.29		8.28		22.54		10.21	23.99
Ba/Sr	3.03		3.52		3.13		4.23		3.57	6.93
Rb/Sr	10.38		16.30		9.21		27.23		42.14	19.36
n	17		52		13		11		1	1

$\bar{x}$ = mean
σ = standard deviation
n = number of samples
* = total Fe as Fe_2O_3

Table 10

COMPOSITION OF DIFFERENT INTRUSIVE PHASES AT THE BELLE ISLAND AND FRANK'S POND SHOWINGS

Element	Belle Island Showing					Frank's Pond Showing		
	Cg. Alaskitic Granite	Porphyritic Mg. Granite	Porphyritic Aplite	Aplite	Mineralized Porphyritic Granite	Porphyritic Mg. Granite	Fg. Granite	Mineralized Alaskitic Granite
SiO_2	72.91	73.00	75.03	69.71	75.03	77.56	75.64	85.00
TiO_2	.22	.13	.14	.21	.14	.07	.04	.03
Al_2O_3	13.60	13.14	13.03	13.65	13.03	11.84	12.17	6.98
Fe_2O_3*	1.36	1.00	1.00	1.56	1.00	1.03	.90	1.17
MnO	.04	.03	.02	.05	.02	.03	.04	.03
MgO	.53	.30	.00	.48	.00	.01	.00	.10
CaO	.76	.76	.74	2.13	.74	.20	.17	.62
Na_2O	3.56	3.02	2.97	2.90	2.97	3.59	3.78	1.86
K_2O	4.88	5.12	4.77	4.53	4.77	4.67	4.80	2.48
H_2O	2.26	2.14	2.29	3.74	2.29	.61	.59	.81
Total	100.14	98.65	100.02	98.99	100.02	99.63	98.15	99.37
Zr	125	235	220	254	218	171	179	141
Sr	3	209	203	422	208	7	ND	8
Rb	398	253	251	259	244	357	441	192
Zn	ND	ND	ND	4	ND	19	27	10
Cu	15	26	17	132	84	1	ND	6
Ba	22	501	501	748	628	32	24	53
U	8	4	7	5	4	7	11	4
Mo	12	25	28	19	143	19	16	3275
Nb	36	32	23	18	22	37	49	35
Bi	18	15	18	19	19	15	16	18
Pb	41	25	26	23	41	36	57	35
Ni	4	12	12	14	13	8	15	10
Y	33	53	49	33	42	111	137	123
Cr	6	19	18	20	9	9	8	22
Ti	745	1689	1684	2083	1714	647	305	878
S	150	60	300	300	290	210	160	2940
Q	33.20	35.23	39.32	33.18	35.50	39.23	35.96	65.27
Ab	31.20	27.03	25.99	26.19	26.57	31.01	32.92	16.12
Or	28.55	31.24	29.13	27.32	28.04	28.11	29.14	14.82
An	3.11	3.51	3.29	10.50	5.94	.76	.72	3.06
D.I.	92.95	93.50	94.44	86.89	90.11	98.35	98.02	96.30
K/Rb	10.26	16.80	15.78	14.52	16.23	10.86	9.04	10.72
Ba/Rb	.06	1.98	2.00	2.89	2.57	.09	.05	.02
Ca/Sr	181.06	2.60	2.61	3.61	2.54	20.42	—	55.39
Ba/Sr	7.33	2.40	2.47	1.73	3.02	4.57	—	6.62
Rb/Sr	132.67	1.21	1.24	.61	1.17	51.00	—	24.00
n	1	1	1	1	1	1	1	1

n = number of samples

* = total Fe as Fe_2O_3

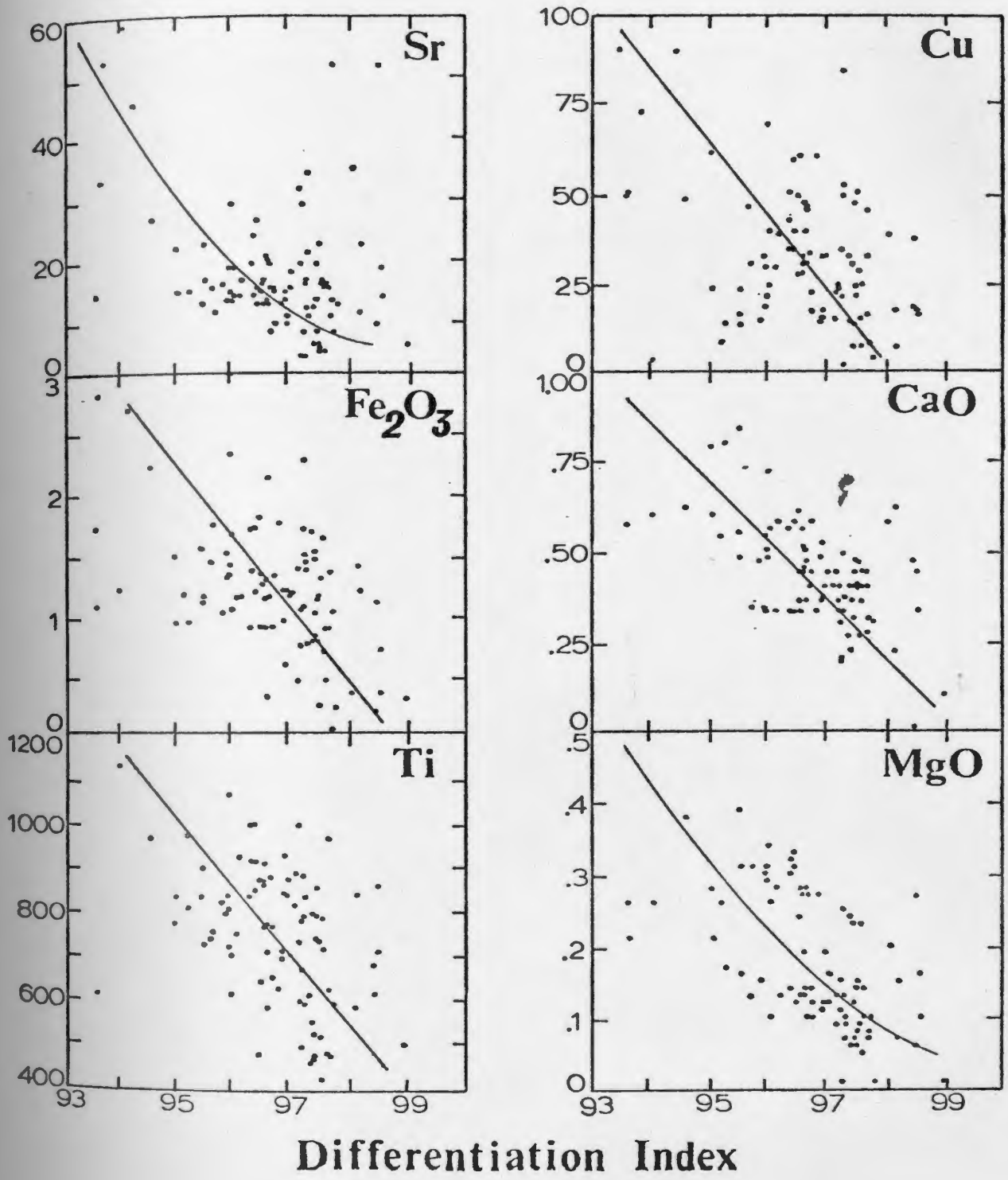

Figure 27 a. Plot of Thornton and Tuttle's (1960) differentiation index versus Sr, Cu, Ti in ppm and Fe_2O_3 total, CaO and MgO in wt. percent for granitoid rocks of the Wylie Hill showing. Lines are visually estimated approximate fit to data.

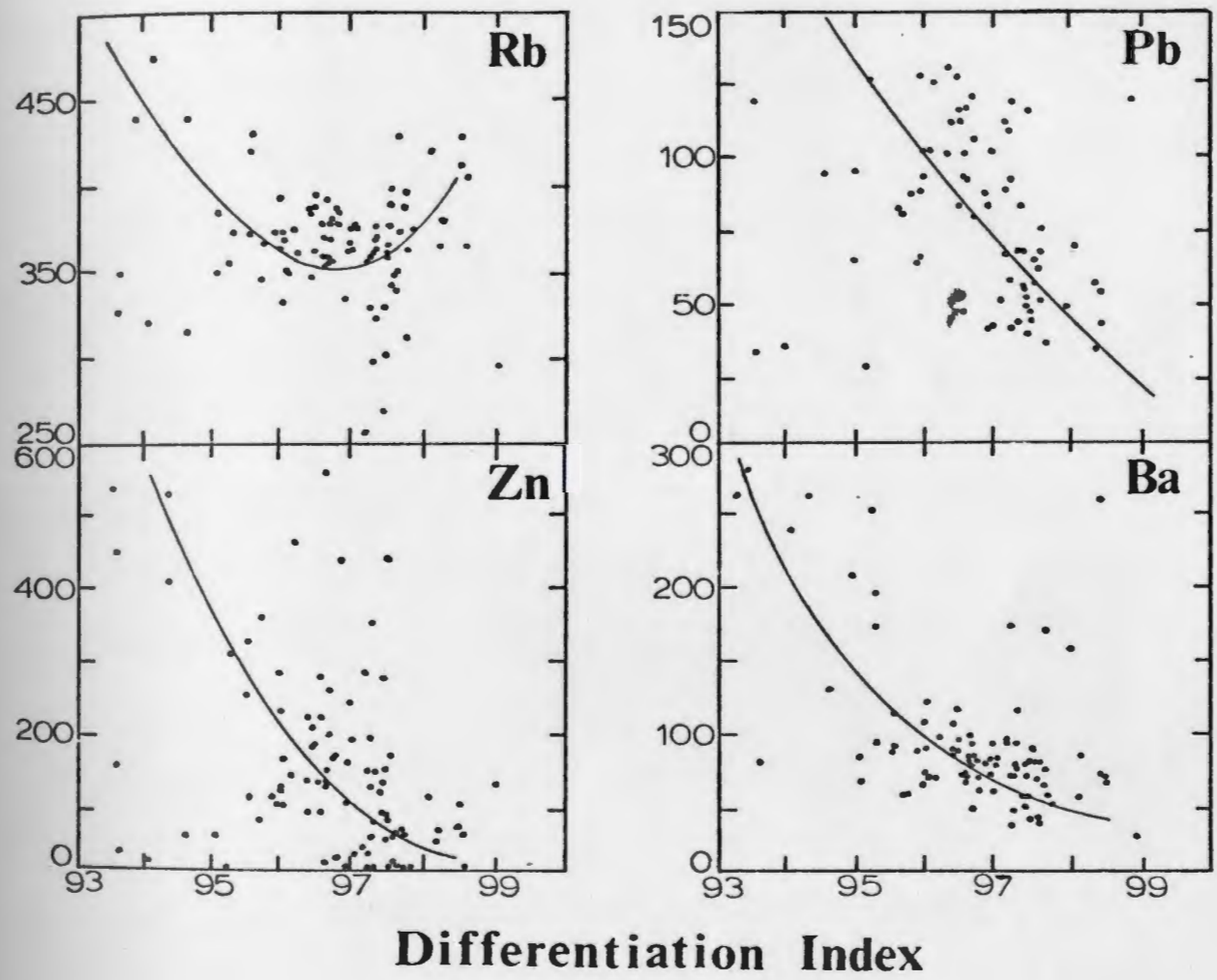

Figure 27b. Plot of Thornton and Tuttle's (1960) differentiation index versus Rb, Pb, Zn, and Ba in ppm for granitoid rocks of the Wylie Hill showings.

CaO and MgO have a negative correlation with differentiation index (Figure 27 a). Most of the trace elements (Zr, Mo, Nb, Ni, Y, Cr, S, U, and Bi) either show no variation or irregular scatter, but Sr, Cu, Ti, Pb, Zn, Ba and Rb have a negative correlation with differentiation index (Figure 27 a, b).

The sharp drop in the trends of Fe_2O_3 total, Ti, MgO, Cu, and Zn can all be explained by the virtual disappearance of biotite, the only mafic mineral, in the most differentiated granite. The negative correlation trends of CaO and Sr can both be explained by change of the composition of the finally formed plagioclase feldspar to almost pure albite. The behavior of Ba, Pb, and Rb are all related to K-feldspar, the major potassic mineral in granites, even though K_2O shows essentially no variation. Ba exhibits capture behavior and is thus deficient in late formed K-feldspar, and similar behavior may be shown by Pb, although its strong tendency to exist as a sulphide phase complicates this picture. Rb apparently decreases, then increases, behavior which has been explained by the slightly larger radius of Rb^+ (1.47A°) versus that of K^+ (1.33A°) resulting in its concentration under conditions of extreme fractionation (Taylor, 1965).

5.3.3 Variation Between Showings

In examining the data it became obvious that the usual parameters used as indices of differentiation such

as silica and Thornton and Tuttle's differentiation index were not very useful. The granitoids are so highly differentiated that differentiation index did not vary greatly, for although quartz, orthoclase and albite contents vary in proportion the total remains essentially the same. The normative quartz content was considered as a helpful index to plot the variation of other elements against since it increases at the expense of other minerals in late differentiation and it is also a helpful indicator of late stage silicification, possibly resulting from separation of a Si rich fluid phase, as discussed by Burnham (1967). Comparison of the geochemical data tabulated in tables 6, 7, 8, 9 and 10 for intrusive units within and between the different showings reveals that some trace elements and element ratios show significant variations. Values of these for the different mapped intrusive units of the different showings have been plotted against normative quartz with units for the same showing joined by numbered dashed tie lines (Figure 28 a and b). Second order regression lines have been calculated and drawn through the data to show the combined trend of variation. The average composition of the statistically sampled alaskitic granite phase (Figure 18) has been plotted in each diagram as a reference to which variation in the intrusives associated with the showings may be compared. Sr is present in very low concentrations, generally

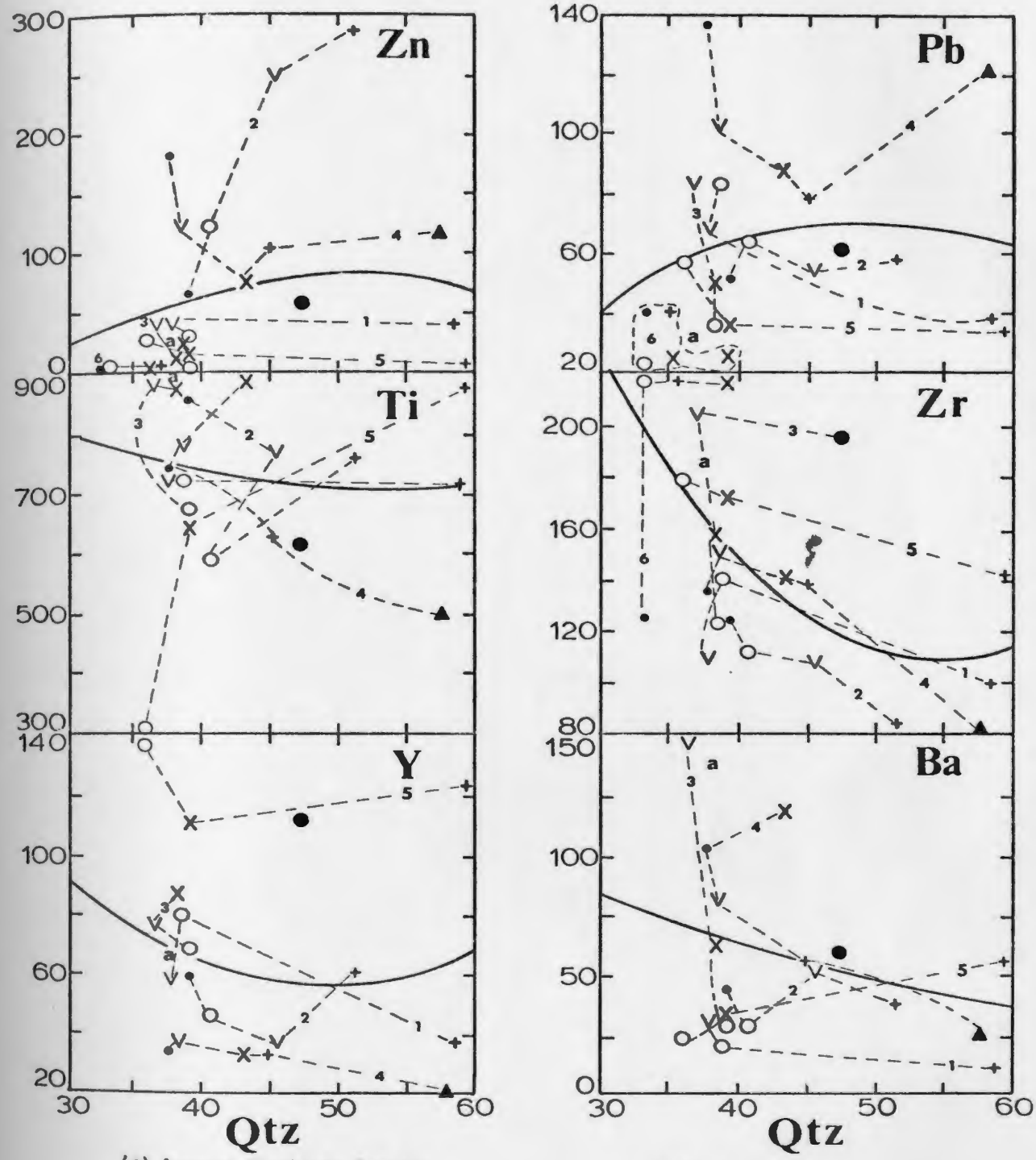

Figure 28 a. Plot of Zn, Pb, Ti, Zr, Y and Ba in ppm versus normative quartz for average intrusive unit compositions of the showings; points for the same showing joined by numbered dashed tie lines, solid lines are second order regression lines through all data.

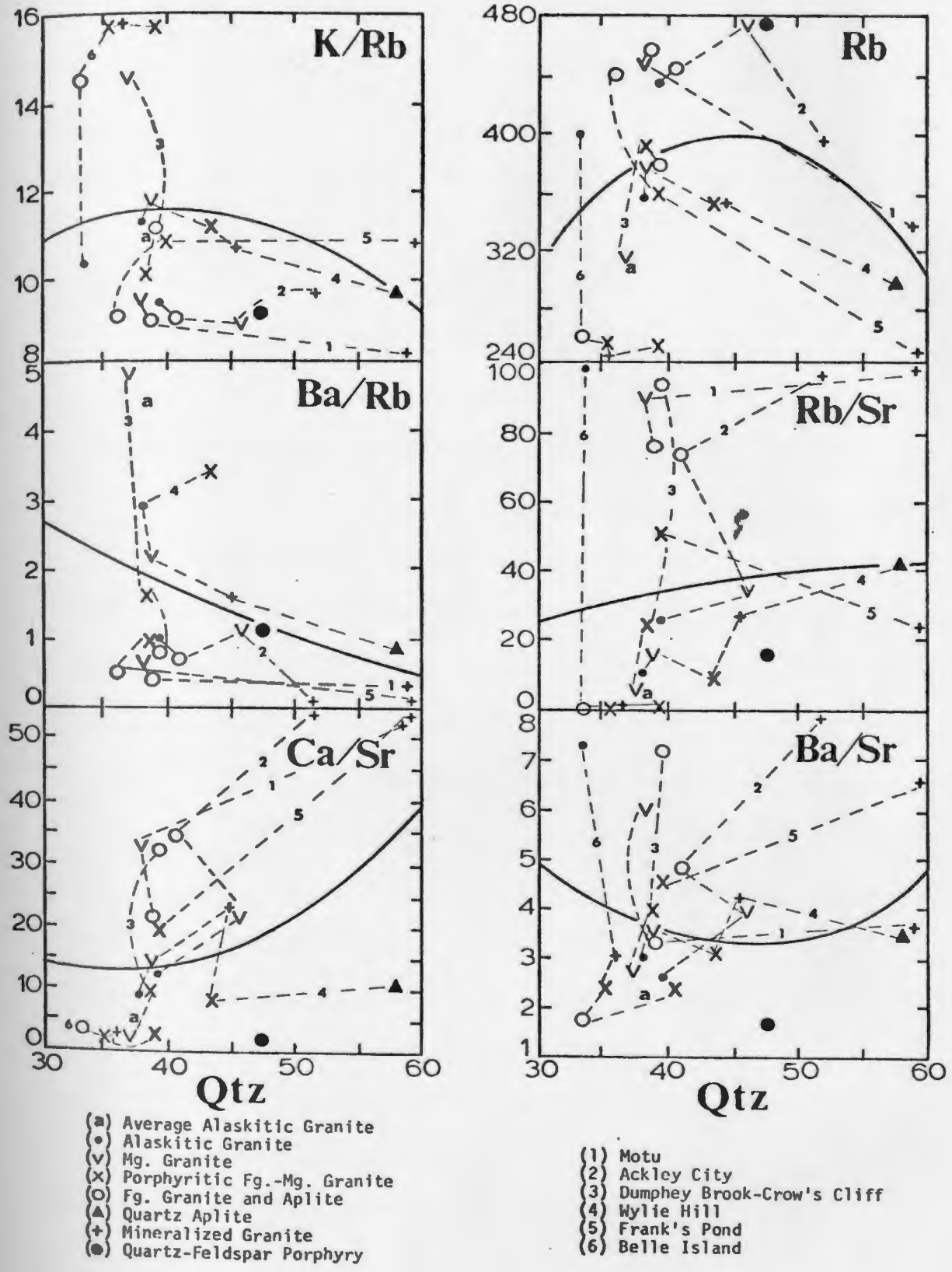

Figure 28 b. Plot of K/Rb, Ba/Rb, Rb/Sr, Ca/Sr, Ba/Sr and Rb (ppm) versus normative quartz for average intrusive unit compositions; points for the same showing joined by numbered dashed tie lines, solid lines are second order regression lines through all data.

within the limits analytical precision, however, the ratios with other elements exhibit trends of variation similar to that of other elements, and therefore the values are considered useful. The actual variation of the elements and ratios will be first described and then their possible significance will be discussed.

Zinc is strongly enriched in the Ackley and Wylie Hill showings while the other showings all have low values close to that of the average alaskite composition, and the Belle Island showing is markedly depleted in the element. Lead is strongly enriched in the Wylie Hill showing while the other showings are fairly similar with there being quite a bit of variation within individual showings. All showings except Belle Island are more enriched in Pb then the average alaskitic granite. Titanium shows little change at Motu, and decreases in the order alaskite, mg granite, aplite, mineralized granite at the Ackley City showing. There is similar variation in the other showings, all having lower Ti values then the average alaskitic granite. Zirconium also exhibits variation within showings as well as there being a general trend of decrease in average Zr contents of showings from a high in the Belle Island showing, and a slightly lower content in the average alaskite granite to lower values in the Ackley City showing. Y is enriched in the Frank's Pond showing relative to the average alaskitic granite and some other showings, while the Wylie Hill showing

is similarly depleted in the element. Ba is depleted in all showings, except Belle Island (500-750 ppm), relative to the average alaskitic granite and there is also extensive variation within and between the different showings. Rb shows extensive variation, all showings except Belle Island being more enriched then the average alaskitic granite, this trend being most pronounced in the Ackley City and Motu showings. K/Rb and Ba/Rb show similar features of lower ratios in all showings, other then Belle Island, then the average alaskitic granite and general trends to lower values in finer grained or higher quartz normative intrusive units. Opposite trends toward higher ratio values than that of the average alaskitic granite is exhibited by the showings for the ratios Rb/Sr, Ca/Sr, and Ba/Sr, the highest values of individual showings being in the mineralized equivalents.

The variations in Pb, Zn and Y apparently represent relative enrichments of these trace elements in certain showings. A secondary origin for the high Pb and Zn seems unlikely in view of the consistent high values for all intrusive units. Some of the variations, such as those of the mineralized granite are probably the result of secondary alterations, however, the differences of the other intrusive units must be primary. The overall trends of variation, namely decreases in Zr, Ba, Ti, K/Rb and Ba/Rb and increases in Rb, Rb/Sr, Ca/Sr, and Ba/Sr in the showings compared to the average

alaskitic granite are, according to Taylor (1965), those which would result from crystal fractionation. It is quite obvious from field evidence and the geochemistry that the alaskitic granite and the intrusive phases associated with mineralization are closely related. The indications that the fine grained intrusive units are younger than the coarse grained alaskitic granite given by field relations is supported by the trace elements and especially the elemental ratios. Within the individual showings the sequence of variation of these generally suggests a decreasing age and an increasing degree of fractionation sequence of alaskite granite, medium grained granite, porphyritic fine grained granite and aplite. Belle Island, however, is a notable exception, the coarsest grained intrusive being the most highly fractionated and all samples being generally less than or equally fractionated as the average alaskitic granite.

A sequence of AFM diagrams for the different showings (Figure 29) has been plotted to illustrate the variation of major element mafic components. All the showings plot similarly, as being less mafic than the average alaskitic granite. Mineralized equivalents are generally more "mafic" than the other intrusive units of a showing, possibly as a result of secondary addition of Fe as pyrite or magnetite. Generally the sequence of variation within individual showings is

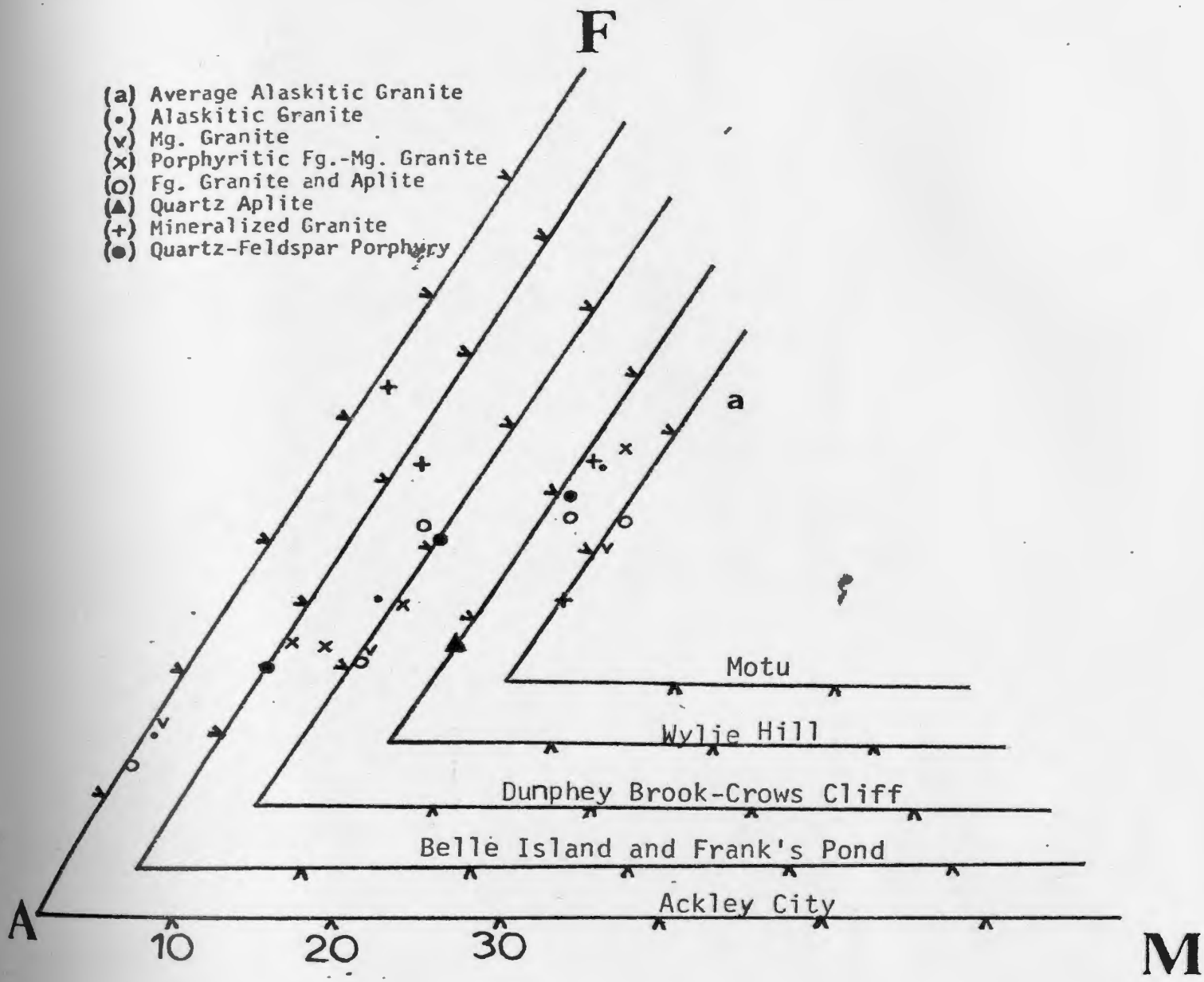

Figure 29. A F M diagram ($A=K_2O + Na_2O$; $F=FeO_t + MnO$; $M=MgO$) for the different molybdenite showings. The corners of 5 AFM diagrams have been combined in one diagram, the lower corner of the triangle for each showing is labeled.

similar to that illustrated in Figures 29 a and b, the finer grained intrusive units being the least mafic or most differentiated.

5.3.4 Variation in the Alaskitic Granite Phase

The alaskitic granite north of the rhyolite contact was systematically sampled (Figure 18), these samples were subsequently analyzed for the same elements as the intrusives associated with the showings. These samples vary slightly in major and trace element contents, a fact which is apparent in Figure 12 a and b. When the spatial distribution of this variation was considered it was found to be systematic, although no corresponding variation in lithology of the alaskitic granite is apparent.

The apparent degree of differentiation of the alaskitic granite phase, as measured by Thornton and Tuttle's (1960) differentiation index increases toward the intrusive contact (Figure 30). This systematic variation is mirrored by a decrease in Zr, Ti, Ni, Cu, Sr, Zn, and Ba and an increase in Nb, Pb, Rb and Y toward the contact. The Ba/Rb ratio decreases and Rb/Sr increases toward the contact (Figure 31 and 32). Other elements of interest, notably Mo, do not exhibit regular spatial variation. The alaskitic granite phase, therefore, exhibits a sequence of variation of increasing fractionation of trace elements and major elements toward the contact,

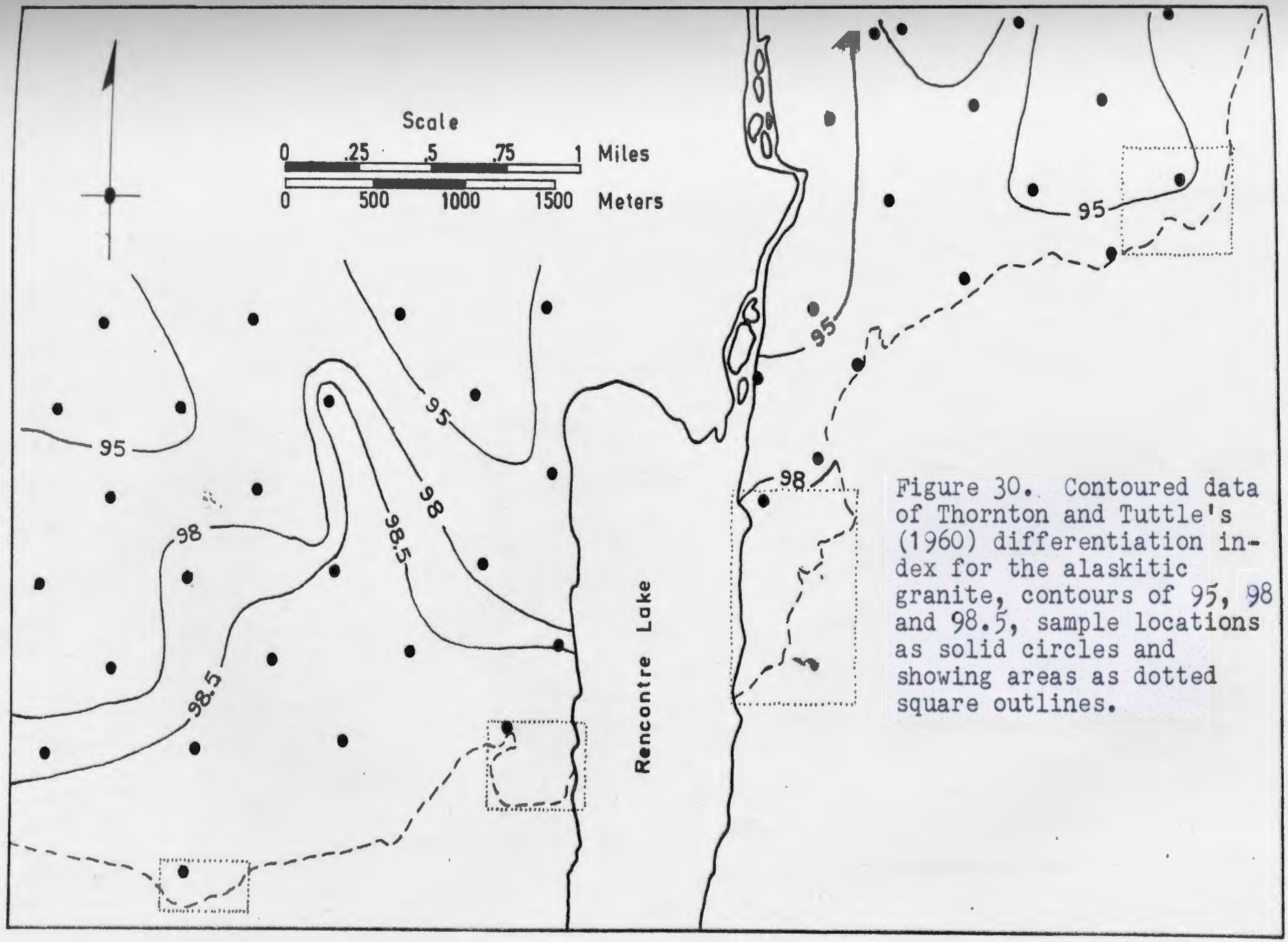

Figure 30. Contoured data of Thornton and Tuttle's (1960) differentiation index for the alaskitic granite, contours of 95, 98 and 98.5, sample locations as solid circles and showing areas as dotted square outlines.

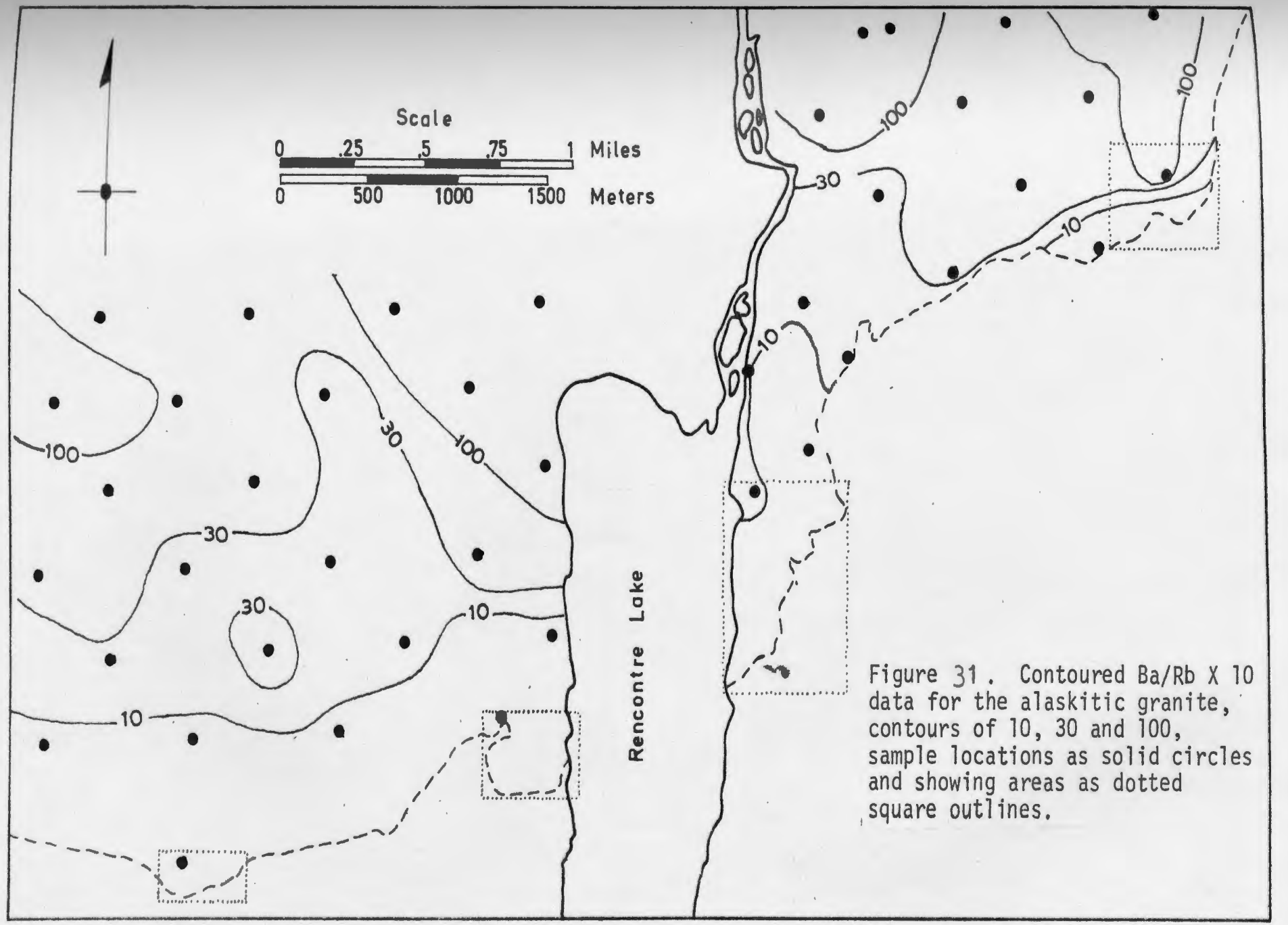

Figure 31. Contoured Ba/Rb X 10 data for the alaskitic granite, contours of 10, 30 and 100, sample locations as solid circles and showing areas as dotted square outlines.

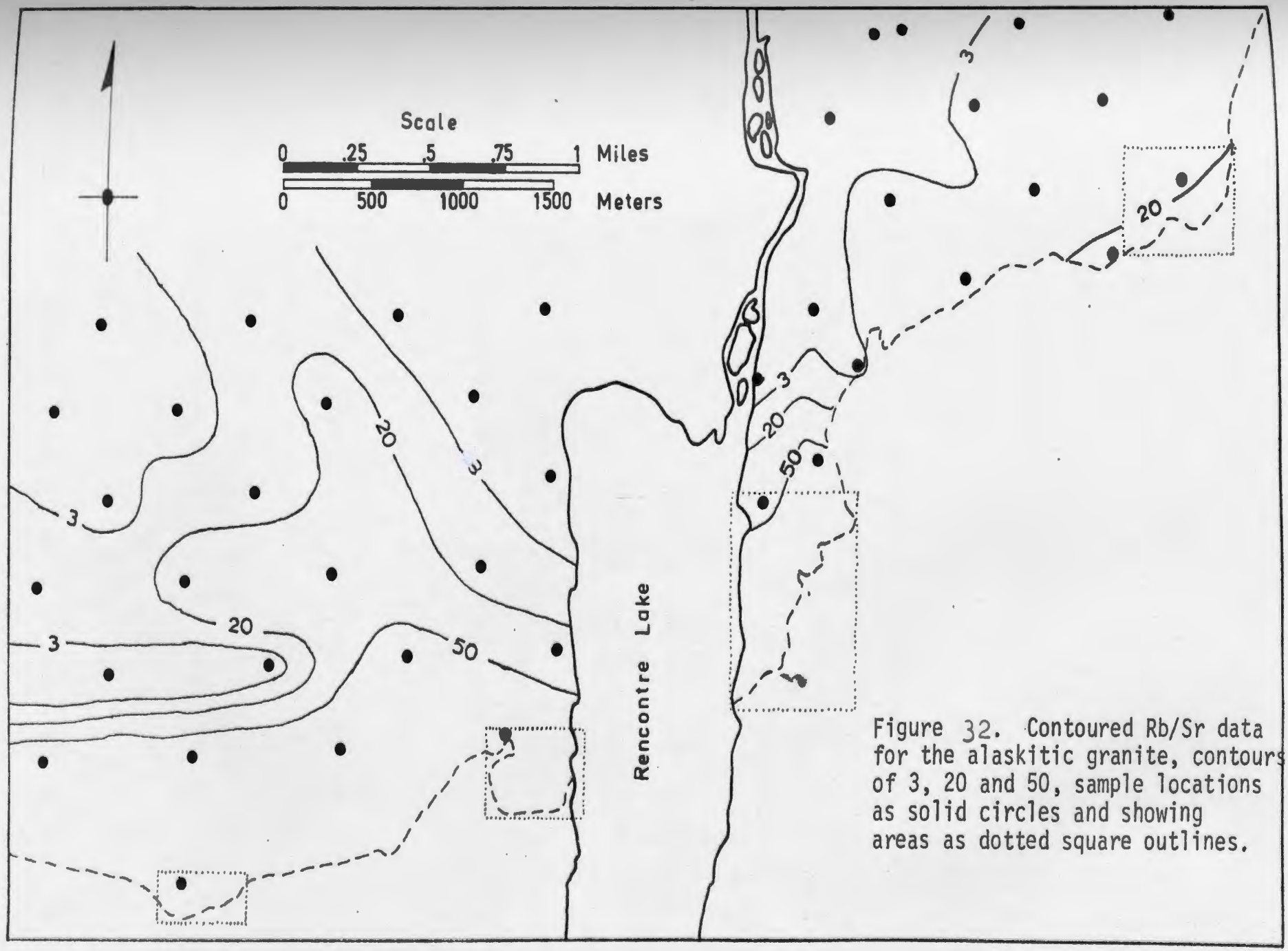

Figure 32. Contoured Rb/Sr data for the alaskitic granite, contours of 3, 20 and 50, sample locations as solid circles and showing areas as dotted square outlines.

the element and ratio trends being the same as those exhibited by the molybdenite showings' intrusive units in comparison to the average alaskitic granite.

5.3.5 Variation Within The Wylie Hill Showing

The actual variation of elements within a showing, Wylie Hill, has been investigated by the analysis of drill core samples which usually represent crushed split core of 3 to 6 meter lengths. The results have been plotted against depth and rock type to graphically present the variations, an example being presented in the text (Figure 33 a and b), the rest of the sections being in Appendix C.

The drill hole sections show a number of important features which are best listed in point form:

(1) Major elements exhibit normal covariant behavior.

(2) There is a major difference in composition between the rhyolite and intrusive, there being no suggestion of contamination of the intrusive near the contact.

(3) There is an indication that the mafic nature of the intrusive increases and degree of differentiation decreases with depth away from the contact.

(4) Mineralization generally reaches a peak somewhat on the intrusive side of the contact and decreases quickly thereafter.

(5) There is a fairly close apparent relationship between Cr, Ni, and S. The high Ni and Cr values in drill core samples had been considered to be due to

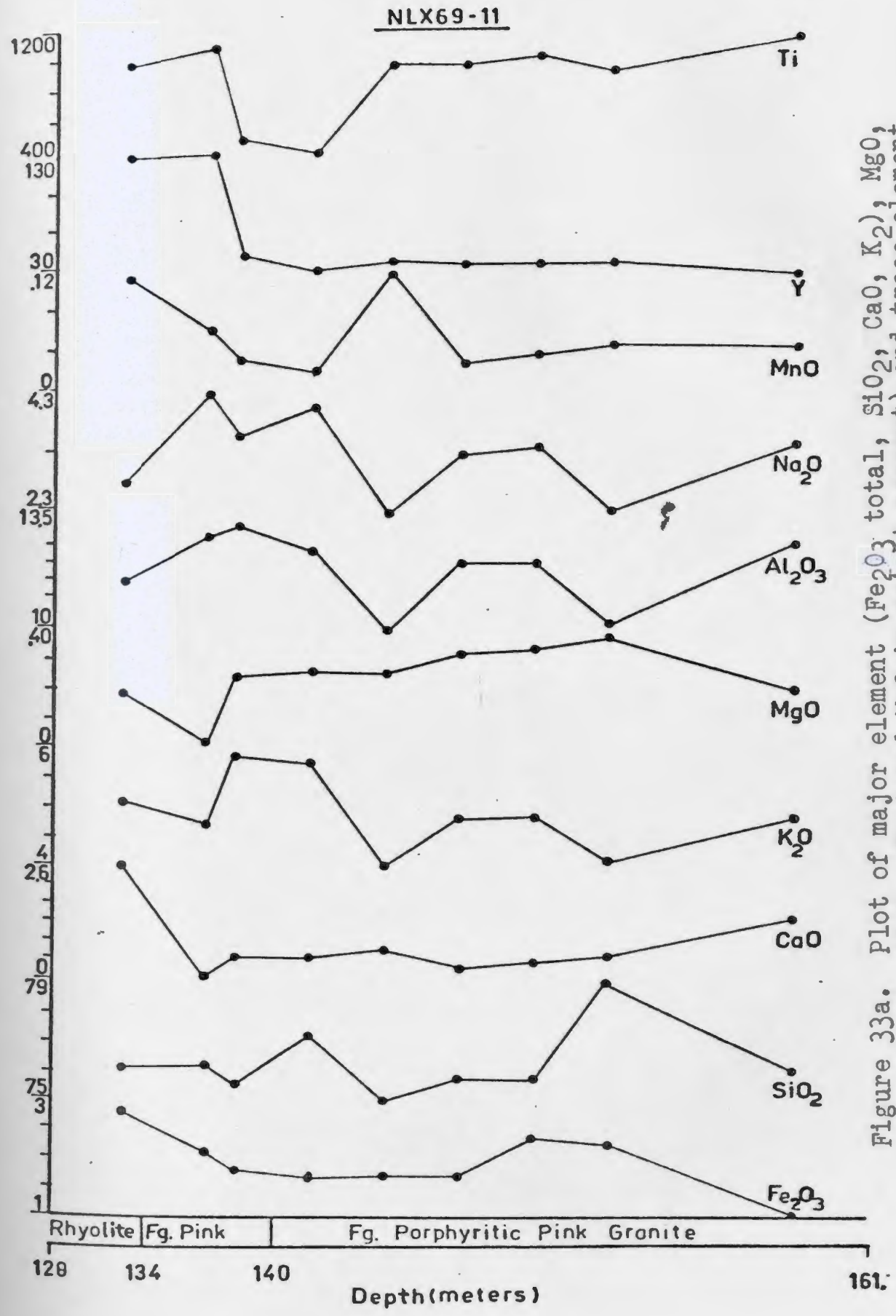

Figure 33a. Plot of major element (Fe_2O_3 total, SiO_2, CaO, K_2), MgO, Al_2O_3, Na_2O and MnO in weight percent) and trace element (Ti and Y in ppm.) data for diamond drill hole NLX-69-11 at Wylie Hill showing versus depth in meters and rock type.

Figure 33b. Plot of trace element (Zr, Sr, Rb, Zn, Cu, Ba, Mo, Nb, Pb, Ni, Cr and S in ppm.) data for diamond drill hole NLX-69-11 at Wylie Hill showing versus depth in meters and rock type.

contamination from the drill bit, but this correspondence suggests that Ni and Cr may be accommodated in the abundant pyrite of the showing.

(6) In some of the sections there is a suggestion of metal zonation, a high of Mo being rimmed by highs of Pb, Zn, Cu or Nb. Such variations are not always present but are quite marked in some sections.

5.3.6 Correlation Matrices

To aid in an understanding of the large amount of geochemical data a number of correlation matrices were calculated. The first (Table 11) is for all of the geochemical data and is therefore not valid for U and Bi, since these elements were not analyzed for 86 of these samples. The second (Table 12) is for the samples of alaskitic granite, the third (Table 13) being for all the samples from the different showings, and the fourth (Table 14) is for the diamond drill core samples from Wylie Hill which were not analyzed for U and Bi. Presented with each table are critical values of the correlation coefficient (r) for different levels of significance (.05, .02, .01 and .001) or confidence (95%, 98%, 99% and 99.9%) for the number of samples used in each correlation matrix. For 99% confidence based on 200 samples the critical value of r is shown to be .181. In other words, a value of ± greater than .181 would indicate a correlation between variables that could be predicted with 99% confidence.

Table 11. Correlation Matrix For Data of All Samples (206)

	Fe_2O_3	TiO_2	SiO_2	CaO	K_2O	MgO	Al_2O_3	Na_2O	H_2O	MnO	Zr	Sr	Rb	Zn	Cu	Ba	U	Mo	Nb	Bi	Pb	Ni	Y	Cr	Ti	S
S	0.25	-0.18	-0.17	0.16	-0.18	0.02	-0.26	-0.26	0.67	0.10	-0.13	-0.14	-0.04	0.35	0.10	-0.13	-0.00	0.62	0.50	-0.02	0.02	0.11	-0.14	0.07	-0.15	1.00
Ti	0.10	0.54	-0.18	0.29	-0.03	0.30	0.19	0.07	-0.01	0.28	0.52	0.73	-0.08	-0.11	0.02	0.72	0.13	-0.12	-0.03	-0.00	-0.03	-0.08	0.21	-0.08	1.00	
Cr	0.60	-0.18	0.12	-0.01	-0.21	0.00	-0.27	-0.26	0.13	-0.07	-0.03	-0.10	-0.01	0.08	0.52	-0.08	-0.33	0.01	-0.10	0.80	0.12	0.11	-0.20	1.00		
Y	-0.04	0.12	0.02	-0.09	0.07	-0.17	0.02	0.10	-0.16	0.09	0.54	0.02	0.13	-0.18	-0.22	0.16	0.35	-0.05	0.47	-0.10	-0.12	-0.10	1.00			
Ni	0.09	-0.28	-0.04	0.01	0.01	0.20	0.04	0.03	-0.07	-0.20	0.01	-0.06	0.11	0.37	0.27	-0.03	-0.41	-0.11	-0.00	-0.08	0.04	1.00				
Pb	0.04	-0.14	0.22	0.08	-0.25	0.02	-0.28	-0.17	0.01	0.17	-0.07	-0.05	-0.12	0.23	0.47	-0.08	-0.10	-0.03	-0.08	0.06	1.00					
Bi	0.68	-0.01	0.05	-0.06	-0.19	-0.04	-0.26	-0.27	0.08	0.07	-0.03	-0.04	-0.06	-0.06	0.49	-0.04	-0.05	-0.01	-0.11	1.00						
Nb	0.02	-0.04	-0.07	-0.03	-0.06	-0.12	-0.17	-0.23	0.44	0.16	0.10	-0.16	0.34	0.10	-0.09	-0.13	0.35	0.45	1.00							
Mo	0.10	-0.13	0.09	0.07	-0.22	-0.09	-0.40	-0.37	0.48	0.05	-0.14	-0.15	-0.03	0.07	-0.03	-0.16	0.21	1.00								
U	-0.09	0.40	-0.09	-0.12	0.01	-0.20	0.01	-0.15	0.07	0.34	-0.11	0.02	0.26	-0.17	-0.24	-0.08	1.00									
Ba	0.11	0.31	-0.26	0.46	0.06	0.24	0.24	0.19	0.04	0.16	0.66	0.85	-0.24	-0.10	0.15	1.00										
Cu	0.50	-0.18	-0.05	0.23	-0.17	0.20	-0.16	-0.22	0.26	0.16	0.09	0.10	0.01	0.30	1.00											
Zn	0.07	-0.23	-0.01	0.09	-0.01	0.06	-0.08	-0.17	0.15	0.01	-0.04	-0.16	0.18	1.00												
Rb	0.05	-0.01	-0.37	-0.18	0.52	0.06	0.43	-0.21	0.22	0.18	-0.15	-0.21	1.00													
Sr	0.02	0.43	-0.25	0.45	0.02	0.28	0.22	0.12	0.09	0.16	0.31	1.00														
Zr	0.14	0.16	-0.05	0.24	0.02	0.09	0.08	0.17	-0.13	0.07	1.00															
MnO	0.45	0.52	-0.45	0.25	0.05	0.29	0.25	-0.26	0.30	1.00																
H_2O	0.27	-0.01	-0.40	0.26	0.01	0.15	0.00	-0.38	1.00																	
Na_2O	-0.35	0.10	-0.17	-0.04	0.09	-0.00	0.43	1.00																		
Al_2O_3	-0.04	0.34	-0.79	0.02	0.69	0.28	1.00																			
MgO	0.16	0.27	-0.31	0.35	0.08	1.00																				
K_2O	-0.02	0.07	-0.62	-0.10	1.00																					
CaO	0.08	0.18	-0.16	1.00																						
SiO_2	-0.30	-0.34	1.00																							
TiO_2	0.12	1.00																								
Fe_2O_3	1.00																									

Values of the Correlation Coefficient (r) for
n = 200 samples

Significance Level	.05	.02	.01	.001
r value	.138	.150	.181	.204
Confidence Level	95%	98%	99%	99.9%

from Snedecor and Cochran (1967)

Table 12. Correlation matrix for the alaskitic granite samples (40) near the showings.

	Fe_2O_3	TiO_2	SiO_2	CaO	K_2O	MgO	Al_2O_3	Na_2O	H_2O	MnO	Zr	Sr	Rb	Zn	Cu	Ba	U	Mo	Nb	Bi	Pb	Ni	Y	Cr	Ti	S
S	0.07	0.32	-0.21	0.19	-0.13	0.10	0.19	0.08	0.18	0.25	0.08	0.19	0.07	-0.00	-0.07	0.05	-0.01	0.17	-0.01	0.32	0.11	-0.12	-0.05	0.27	0.11	1.00
Ti	0.47	0.48	-0.31	0.33	0.06	0.33	0.40	0.15	-0.09	0.19	0.97	0.86	-0.17	0.36	0.11	0.91	-0.07	0.20	0.10	0.47	-0.01	0.10	0.36	0.03	1.00	
Cr	0.10	0.05	-0.05	0.01	-0.07	-0.02	0.13	0.03	0.09	0.11	0.05	0.13	0.18	0.13	-0.01	0.03	0.28	0.25	0.05	0.31	0.41	0.03	0.11	1.00		
Y	0.05	-0.09	0.17	-0.18	0.09	-0.26	-0.18	0.15	-0.39	-0.41	0.49	0.09	0.54	-0.12	0.01	0.22	0.30	0.04	0.76	0.40	0.31	0.85	1.00			
Ni	-0.07	-0.18	0.24	-0.22	0.11	-0.34	-0.23	0.18	-0.42	-0.45	0.26	-0.10	0.67	-0.24	0.19	-0.02	0.31	0.11	0.73	0.27	0.40	1.00				
Pb	-0.08	-0.08	0.08	-0.23	0.19	-0.36	0.08	0.15	-0.28	-0.17	0.07	0.03	0.74	0.18	0.09	-0.02	0.53	0.40	0.53	0.37	1.00					
Bi	0.24	0.32	-0.14	0.13	0.06	0.09	0.23	0.05	-0.05	0.04	0.46	0.40	0.25	0.14	0.07	0.41	0.24	0.37	0.38	1.00						
Nb	-0.02	-0.15	0.27	-0.35	0.04	-0.41	-0.30	0.06	-0.42	-0.42	0.21	-0.09	0.79	-0.21	0.06	-0.02	0.59	0.08	1.00							
Mo	0.12	0.32	-0.38	0.04	-0.02	0.01	0.36	0.24	0.02	0.17	0.18	0.26	0.27	0.13	0.62	0.13	0.24	1.00								
U	-0.05	-0.16	0.09	-0.14	-0.08	-0.33	-0.05	0.00	-0.20	-0.13	-0.01	-0.16	0.67	-0.15	0.01	-0.19	1.00									
Ba	0.35	0.39	-0.21	0.33	0.07	0.32	0.39	0.14	-0.06	0.20	0.89	0.95	-0.30	0.43	0.14	1.00										
Cu	0.01	0.13	-0.13	-0.01	0.04	-0.02	0.08	0.13	0.05	-0.02	0.13	0.18	0.06	-0.08	1.00											
Zn	0.07	0.14	-0.25	0.18	0.09	0.13	0.30	0.08	0.01	0.13	0.29	0.44	-0.08	1.00												
Rb	-0.21	-0.28	0.24	-0.41	0.11	-0.57	-0.25	0.11	-0.33	-0.40	-0.06	-0.30	1.00													
Sr	0.45	0.54	-0.33	0.46	-0.02	0.46	0.52	0.21	0.06	0.39	0.82	1.00														
Zr	0.39	0.36	-0.19	0.23	0.06	0.18	0.29	0.17	-0.24	0.06	1.00															
MnO	0.58	0.72	-0.72	0.69	-0.11	0.83	0.72	0.27	0.63	1.00																
H_2O	0.20	0.51	-0.45	0.55	-0.02	0.63	0.46	0.02	1.00																	
Na_2O	0.12	0.17	-0.43	-0.01	0.03	0.18	0.19	1.00																		
Al_2O_3	0.55	0.71	-0.81	0.70	0.23	0.74	1.00																			
MgO	0.69	0.79	-0.71	0.82	-0.11	1.00																				
K_2O	-0.12	-0.09	-0.16	-0.25	1.00																					
CaO	0.62	0.71	-0.57	1.00																						
SiO_2	-0.58	-0.69	1.00																							
TiO_2	0.75	1.00																								
Fe_2O_3	1.00																									

Values of the Correlation Coefficient (r) for n = 40 samples

Significance Level	.05	.02	.01	.001
r value	.304	.358	.393	.490
Confidence Level	95%	98%	99%	99.9%

from Fisher and Yates (1963)

Table 13. Correlation Matrix For Data on Samples (80) From the Showings(Excluding D.D. Core Data From Wylie Hill Showing)

	Fe_2O_3	TiO_2	SiO_2	CaO	K_2O	MgO	Al_2O_3	Na_2O	H_2O	MnO	Zr	Sr	Rb	Zn	Cu	Ba	U	Mo	Nb	Bi	Pb	Ni	Y	Cr	Ti	S
S	0.31	-0.08	-0.24	0.23	-0.18	0.01	-0.26	-0.30	0.74	0.26	-0.22	-0.10	-0.11	0.32	0.03	-0.11	0.24	0.70	0.67	-0.02	-0.02	-0.18	-0.08	0.02	-0.13	1.00
Ti	0.09	0.40	-0.18	0.48	-0.05	0.55	0.17	-0.11	0.20	0.22	0.79	0.73	0.15	-0.05	0.24	0.76	0.05	-0.09	0.03	0.01	0.02	0.40	0.16	0.05	1.00	
Cr	0.75	-0.03	0.06	-0.05	-0.25	-0.01	-0.29	-0.38	0.12	0.08	0.01	-0.03	-0.07	-0.07	0.66	-0.04	-0.23	0.00	-0.10	0.99	0.10	-0.23	-0.18	1.00		
Y	-0.19	-0.10	0.08	-0.09	-0.03	-0.11	0.02	0.20	-0.19	-0.05	0.47	-0.06	0.20	-0.16	-0.25	-0.05	0.36	0.00	0.33	-0.18	-0.09	0.62	1.00			
Ni	-0.15	0.27	-0.31	0.17	0.32	0.25	0.43	0.12	0.03	0.13	0.51	0.27	0.56	0.02	-0.08	0.31	0.47	-0.16	0.20	-0.23	-0.24	1.00				
Pb	0.04	-0.12	0.27	0.12	-0.31	0.05	-0.31	-0.23	-0.01	0.26	-0.05	-0.02	-0.20	0.14	0.54	-0.07	-0.07	-0.04	-0.08	0.06	1.00					
Bi	0.74	-0.06	0.06	-0.07	-0.21	-0.03	-0.28	-0.36	0.08	0.06	-0.01	-0.05	-0.08	-0.06	0.65	-0.05	-0.23	-0.04	-0.14	1.00						
Nb	0.03	0.03	-0.13	0.11	-0.16	0.08	-0.16	-0.27	0.58	0.28	-0.00	-0.17	0.26	0.29	-0.07	-0.18	0.57	0.58	1.00							
Mo	0.16	-0.13	0.08	0.19	-0.28	-0.02	-0.41	-0.43	0.51	0.14	-0.16	-0.15	-0.12	0.21	-0.02	-0.15	0.29	1.00								
U	-0.14	0.21	-0.07	0.09	0.06	0.07	0.01	-0.17	0.20	0.23	0.09	-0.22	0.49	0.50	-0.04	-0.21	1.00									
Ba	0.01	0.28	-0.26	0.64	0.05	0.45	0.21	0.07	0.20	0.02	0.67	0.97	-0.14	-0.17	0.20	1.00										
Cu	0.57	0.08	-0.04	0.39	-0.22	0.34	-0.23	-0.53	0.34	0.40	0.06	0.24	0.00	0.26	1.00											
Zn	0.06	0.05	-0.05	0.14	0.02	0.06	-0.13	-0.44	0.30	0.36	-0.22	-0.16	0.28	1.00												
Rb	0.14	0.41	-0.51	-0.16	0.56	0.33	0.59	-0.19	0.17	0.41	0.07	-0.19	1.00													
Sr	0.00	0.27	-0.22	0.72	0.01	0.43	0.15	0.05	0.21	0.02	0.64	1.00														
Zr	-0.08	0.21	-0.01	0.34	-0.07	0.24	0.09	0.16	-0.08	-0.11	1.00															
MnO	0.49	0.40	-0.47	0.22	0.06	0.58	0.24	-0.48	0.54	1.00																
H_2O	0.44	0.19	-0.52	0.48	-0.01	0.50	0.08	-0.46	1.00																	
Na_2O	-0.58	0.02	-0.05	-0.09	0.10	-0.17	0.39	1.00																		
Al_2O_3	-0.06	0.45	-0.80	0.02	0.74	0.46	1.00																			
MgO	0.24	0.61	-0.56	0.62	0.14	1.00																				
K_2O	0.00	0.20	-0.67	-0.14	1.00																					
CaO	0.05	0.30	-0.24	1.00																						
SiO_2	-0.33	-0.42	1.00																							
TiO_2	0.14	1.00																								
Fe_2O_3	1.00																									

Values of the Correlation Coefficient (r) for
n = 80 samples

Significance Level	.05	.02	.01	.001
r value	.217	.256	.283	.357
Confidence Level	95%	98%	99%	99.9%

from Fisher and Yates (1963)

Table 14. Correlation Matrix For Diamond Drill Core Samples (86) From Wylie Hill Showing (U-Bi not analyzed)

	Fe_2O_3	TiO_2	SiO_2	CaO	K_2O	MgO	Al_2O_3	Na_2O	H_2O	MnO	Zr	Sr	Rb	Zn	Cu	Ba	U	Mo	Nb	Bi	Pb	Ni	Y	Cr	Ti	S
S	-0.16	-0.20	0.06	-0.02	-0.20	-0.02	-0.22	-0.33	0.38	-0.28	-0.16	-0.18	0.08	0.41	-0.00	-0.21	0.12	0.27	0.02	0.09	0.08	0.13	-0.16	-0.03	-0.13	1.00
Ti	0.17	0.38	-0.20	0.26	0.15	0.24	0.18	0.16	-0.15	0.45	0.46	0.46	-0.12	0.05	0.18	0.57	0.13	-0.21	0.01	0.17	0.06	-0.08	0.40	-0.34	1.00	
Cr	0.10	-0.19	0.32	-0.14	-0.15	-0.15	-0.22	-0.23	0.10	-0.22	-0.14	-0.24	0.03	-0.01	-0.05	-0.22	-0.14	0.02	-0.07	-0.14	0.01	-0.06	-0.06	1.00		
Y	0.49	0.22	-0.05	0.27	0.05	-0.09	-0.01	0.13	-0.10	0.53	0.95	-0.20	-0.65	-0.12	0.16	0.83	-0.05	-0.04	0.28	-0.06	-0.18	-0.22	1.00			
Ni	0.36	-0.16	-0.14	-0.18	-0.21	0.13	-0.01	-0.08	-0.25	-0.08	-0.15	-0.03	-0.12	0.28	0.28	-0.13	-0.15	-0.20	-0.19	-0.15	0.10	1.00				
Pb	0.03	0.01	-0.14	-0.06	0.16	-0.04	0.10	-0.00	-0.03	0.05	-0.18	0.06	0.19	0.56	0.18	-0.14	-0.13	-0.15	-0.19	-0.13	1.00					
Bi	-0.09	0.37	-0.04	0.23	0.10	-0.03	-0.04	-0.10	-0.00	0.05	-0.01	0.43	0.05	-0.15	-0.01	0.18	0.98	0.53	0.06	1.00						
Nb	-0.11	-0.07	0.23	0.03	0.04	-0.31	-0.28	-0.18	0.17	0.05	0.14	-0.21	-0.03	-0.19	-0.21	0.08	0.11	0.32	1.00							
Mo	-0.24	-0.14	0.17	-0.08	0.06	-0.13	-0.32	-0.33	0.28	-0.31	-0.09	-0.16	0.14	-0.16	-0.24	-0.18	0.63	1.00								
U	-0.10	0.29	-0.03	0.18	0.12	-0.04	-0.07	-0.13	0.03	0.01	-0.02	0.35	0.06	-0.15	-0.03	0.13	1.00									
Ba	0.50	0.43	-0.34	0.33	0.18	-0.01	0.32	0.40	-0.25	0.63	0.88	0.27	-0.58	-0.06	0.26	1.00										
Cu	0.50	0.00	-0.26	-0.05	-0.06	0.08	0.15	0.22	-0.05	0.15	0.20	0.18	-0.34	0.16	1.00											
Zn	0.12	-0.14	-0.04	0.05	-0.15	-0.02	0.05	-0.03	-0.10	-0.09	-0.06	-0.11	-0.03	1.00												
Rb	-0.64	-0.13	-0.15	-0.20	0.54	0.10	0.20	-0.13	0.32	-0.41	-0.68	0.18	1.00													
Sr	-0.07	0.50	-0.45	0.19	0.26	0.20	0.52	0.43	-0.12	0.24	-0.12	1.00														
Zr	0.49	0.27	-0.13	0.24	0.02	-0.03	0.08	0.22	-0.14	0.51	1.00															
MnO	0.51	0.40	-0.20	0.61	0.18	0.08	0.17	0.13	-0.33	1.00																
H_2O	-0.51	-0.05	-0.01	0.01	0.09	-0.12	-0.21	-0.19	1.00																	
Na_2O	0.08	0.26	-0.61	-0.17	0.29	-0.05	0.83	1.00																		
Al_2O_3	0.04	0.27	-0.79	-0.08	0.58	0.07	1.00																			
MgO	0.06	0.08	-0.07	0.02	0.05	1.00																				
K_2O	-0.14	0.15	-0.56	0.02	1.00																					
CaO	0.09	0.29	-0.00	1.00																						
SiO_2	-0.08	-0.25	1.00																							
TiO_2	0.05	1.00																								
Fe_2O_3	1.00																									

Values of the Correlation Coefficient (r) for n = 86 samples

Significance Level	.05	.02	.01	.001
r value	.210	.248	.274	.345
Confidence Level	95%	98%	99%	99.9%

from Fisher and Yates (1963)

The elements in the correlation matrices generally show correlations at the 99% confidence level, these correlations being mainly ones which could be predicted on standard petrological grounds, as for example the negative correlation of almost all elements with silica. Variations in element correlations between the different groups of samples used in the correlation matrices is apparently not major, as would be expected if all the samples are of closely genetically related intrusive phases. A detailed discussion of the different positive and negative correlations with petrological explanations seems unnecessary, except for the behavior of the different metals which would be expected to be associated with mineralization. These are discussed in the next section (5.3.7) on economic geochemistry.

5.3.7 Economic Geochemistry

Analyses of mineralized intrusive material from the different showings, other then the Dunphey Brook-Crow's Cliff, was made to aid in understanding the nature of mineralization. To determine metal associations trace element analysis was made for a large number of elements, such as Pb, Bi, Ni, Cr, U, Cu and Zn which might be expected to show some association with molybdenite mineralization. Also, since there is a common association of W and Sn with Mo, six mineralized samples from the

different showings were commercially assayed for W and Sn, but neither were detected (less then .00%) in the samples. The average composition of mineralized intrusives from the different showings are presented in Tables 6, 7, 9 and 10.

The enrichments and depletions associated with mineralization are minor, many of the major element changes being probably the result of increases of SiO_2 due to silicification resulting in a corresponding decrease in other elements such as Al_2O_3, K_2O and Na_2O. Trace element variations in the form of decreases may also be the result of silica dilution, while the increases in some other elements, Cu, Pb, Bi, Zn, U, Nb and Y indicate additions of these elements. There are also variations in enrichment between showings. These increases, however, are generally slight, indicating that Mo is the only economically interesting element and that enrichment of this element in the showings is not characterized by major addition of the other elements which it generally shows an association with. Increases in Cu, Pb, Zn and Bi are probably the result of minute quantities of sulphides of these elements, but the increases in U, Nb and Y are less easily explained. The identification of pitchblende in one ore sample from Wylie Hill suggests the presence of rare radioactive minerals which would also be expected to be enriched in Y and Nb.

The correlation matrices (Tables 11, 12, 13 and 14) are useful in understanding the behavior of different elements of economic interest, Mo, Pb, Zn, Cu, Bi and U. They indicate that there are differences in the associations of these elements in rocks of the showings as opposed to the unmineralized alaskite granite. Mo apparently shows no relationship to the other metals in the showings, but correlates closely with U and Nb. The correlation of Mo with Cu and Pb in the alaskite granite suggests that it may be accommodated in biotites. The correlations of Pb suggest that it has a simple distribution, possibly as a sulphide, in the showings but a complex distribution in the Alaskitic granite. Zn shows the reverse tendency, a complex distribution in the showings and a correlation with Sr and Ba, two elements whose distributions are tied to feldspars, in the alaskitic granite, suggesting it may also be accommodated in these minerals. Correlations of Cu also indicate a complex distribution in the showings, probably as a sulphide, in pyrites, and biotites and a simple one in the alaskitic granite, probably in biotites. The distribution of Bi is difficult to explain, for it is very closely tied to Cr, an element with which it has an almost perfect correlation. Possibly the two elements are present as impurities in an oxide phase such as magnetite or in pyrite. Uranium, although it shows a

complex number of correlations, is probably present in zircons, sphenes and as seperate minerals (eg. pitchblende) in which Nb and Y are also concentrated. It is notable that the correlations of all these elements are different in the drill core samples from Wylie Hill, a fact which suggests that the distribution of elements varies between the showings.

5.3.8 Geochemistry of Muscovite Alteration

One of the showings, the Ackley City, not only had extensive silicification but also muscovite alteration associated with mineralization. The nature of the chemical changes involved in this alteration were examined by analyzing three closely spaced samples across a patch of muscovite alteration (Table 15). The first sample at the edge of the alteration had only slight sericitic alteration of feldspars, the second from the outer part of the zone had all feldspars completely replaced by muscovite with augmentation of primary quartz, while the third sample from the middle of the zone consisted of massive coarse grained (1 cm) muscovite.

The difference between the slightly altered granite and the quartz-sericite rock is very slight, consisting essentially of an increase in Fe_2O_3 (total) and H_2O, a one percent drop in Na_2O and K_2O, with the trace elements remaining essentially the same. An increase

Table 15

Ackley City Showing
Increasing Degree of Muscovite Alteration of Mg. Granite

Element	Minor Quartz-Sericite Alteration	Pervasive Quartz-Sericite Alteration	Massive Cg. Muscovite Alteration
SiO_2	78.22	78.00	51.00
TiO_2	.05	.15	.38
Al_2O_3	10.43	10.60	26.90
Fe_2O_3	.89	4.30	4.93
MnO	.04	.19	.27
MgO	.06	.09	.84
CaO	.28	.04	.36
Na_2O	1.96	.49	1.50
K_2O	5.33	3.48	8.84
H_2O	.85	2.66	5.11
Total	98.11	100.00	100.13
Zr	73	73	89
Sr	8	1	11
Rb	471	547	304
Zn	224	176	175
Cu	53	46	77
Ba	45	46	77
U	12	7	13
Mo	36	33	114
Nb	32	25	52
Bi	17	34	21
Pb	51	54	37
Ni	8	6	18
Y	29	22	34
Cr	14	13	38
Ti	586	673	1724
S	540	700	270
K/Rb	9.39	5.28	24.14
Ba/Rb	.10	.08	.25
Ca/Sr	25.01	28.59	23.39
Ba/Sr	5.62	46.00	7.00
Rb/Sr	58.88	547.00	27.64

in alteration to a massive muscovite rock is marked by a large drop in SiO_2, and major increases in Al_2O_3, K_2O and H_2O. The trace elements remain relatively unchanged except for a drop in Rb and an increase in Ti. The changes in the composition of the rock seem, therefore, to be slight in comparison to the major lithological changes, the constancy of the trace elements being especially remarkable.

Apparently the early stage of muscovite alteration can almost be considered as taking place in a closed system. If the alteration reaction goes to completion, with complete replacement by muscovite, there is removal of silica, probably that which was present as free quartz. This suggestion is supported by the vuggy porous nature of the massive muscovite rock, a fact which indicates a volume-density change. Removal of silica would result in a residual increase in the other oxides, a process which could explain the major increase of Al_2O_3 and K_2O. The removal of silica, which formerly existed as quartz, would not affect trace elements greatly since they are accommodated in the other rock forming minerals. It is evident that the muscovite alteration process at the Ackley City showing is not accomplished by major transport of materials, and can most simply be explained by replacement of all but quartz by muscovite accompanied closely

by leaching of the quartz by the altering solutions. If this silica is deposited nearby it could account for some of the major silicification at the Ackley City showing, however, the observed volume of secondary quartz greatly exceeds the volume of rock replaced by muscovite.

5.4 Petrogenesis

5.4.1 Introduction

The preceeding sections on the molybdenite deposits and their host intrusives strongly suggest that the molybdenite is closely genetically related to the intrusive rocks. A close relationship to the aplite-pegmatite phases which are spatially related to the intrusive contact of the granite with the Belle Bay Formation is also important in the origin of the deposits. In view of these apparent close ties between mineralization and intrusives, the conditions of crystallization and origin of the latter must be explained prior to discussion of the former.

5.4.2 Origin of Associated Intrusives

The question of whether the granite has a crustal or mantle origin is a difficult problem. Although the initial $^{87}Sr/^{86}Sr$ ratios are low (.705, Bell and Blenkinsop, 1975), the Rb/Sr ratios are higher than those of the Sierra Nevada Batholith (Fig. 14) and the K/Rb ratios are rather low (Fig. 13), both suggesting a crustal origin. All of these

features suggest some crustal involvement but none are conclusive indication of a crustal origin and the true origin of the granite remains unresolved.

Some approximation of the conditions of crystallization of the magma can be obtained by a consideration of normative Q:Ab:Or proportions of the intrusive units for the different showings and the average alaskitic granite (Fig. 34). Superimposed on these plots are the positions of the ternary minima and eutectic at various water pressures (.5 to 3.0 kbars). Most of the intrusive units plot close to the ternary minimum at 0.5 Kbars or slightly below and to the right (therefore more Or). The intrusive units which plot well above it have undergone secondary silicification. The unusual positions of the quartz-feldspar porphyry can be attributed to the high quartz and K-feldspar phenocryst content. All intrusive units have very low An contents, a fact which is emphasized by Figure 35 in which Or:Ab:An proportions are plotted, for even though An content is artifically exaggerated in this diagram, it still appears to be low. The fact that P_2O_5 was not analyzed for, and therefore the contribution of apatite to total CaO has not been accounted for in Tables 6, 7, 8, 9 and 10 suggests An content of the intrusives is even lower. If the general effect of a trace of An in the system

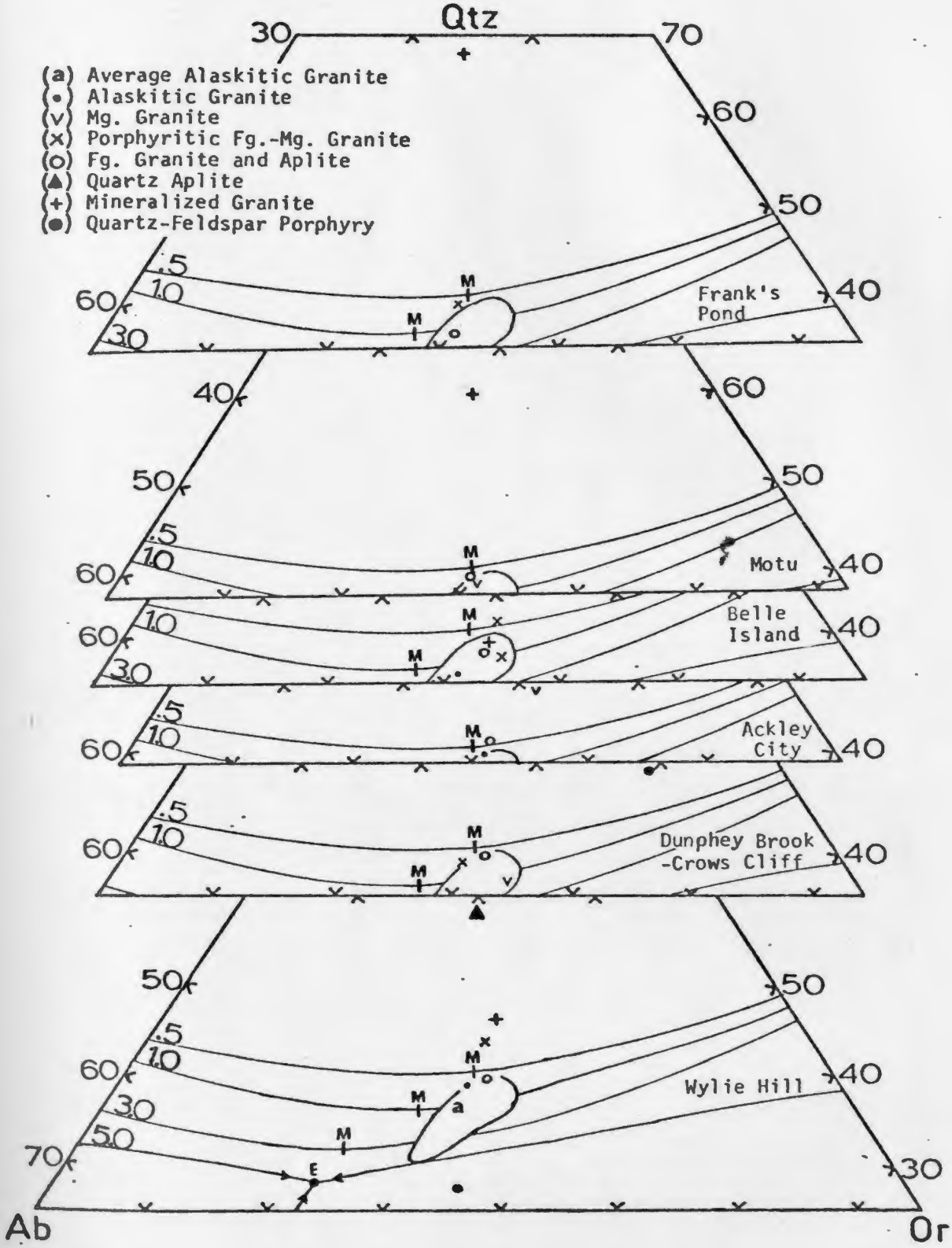

Figure 34. Plots of average intrusive unit compositions for the different molybdenite showings in the quartz-albite-orthoclase system; curves for water saturated liquidi at indicated confining pressures (.5, 1.0, 3.0 and 5.0 Kilobars), isobaric minima (M), ternary eutectic (E) and area of concentration of analyzed granites (oval area) after Tuttle and Bowen (1958).

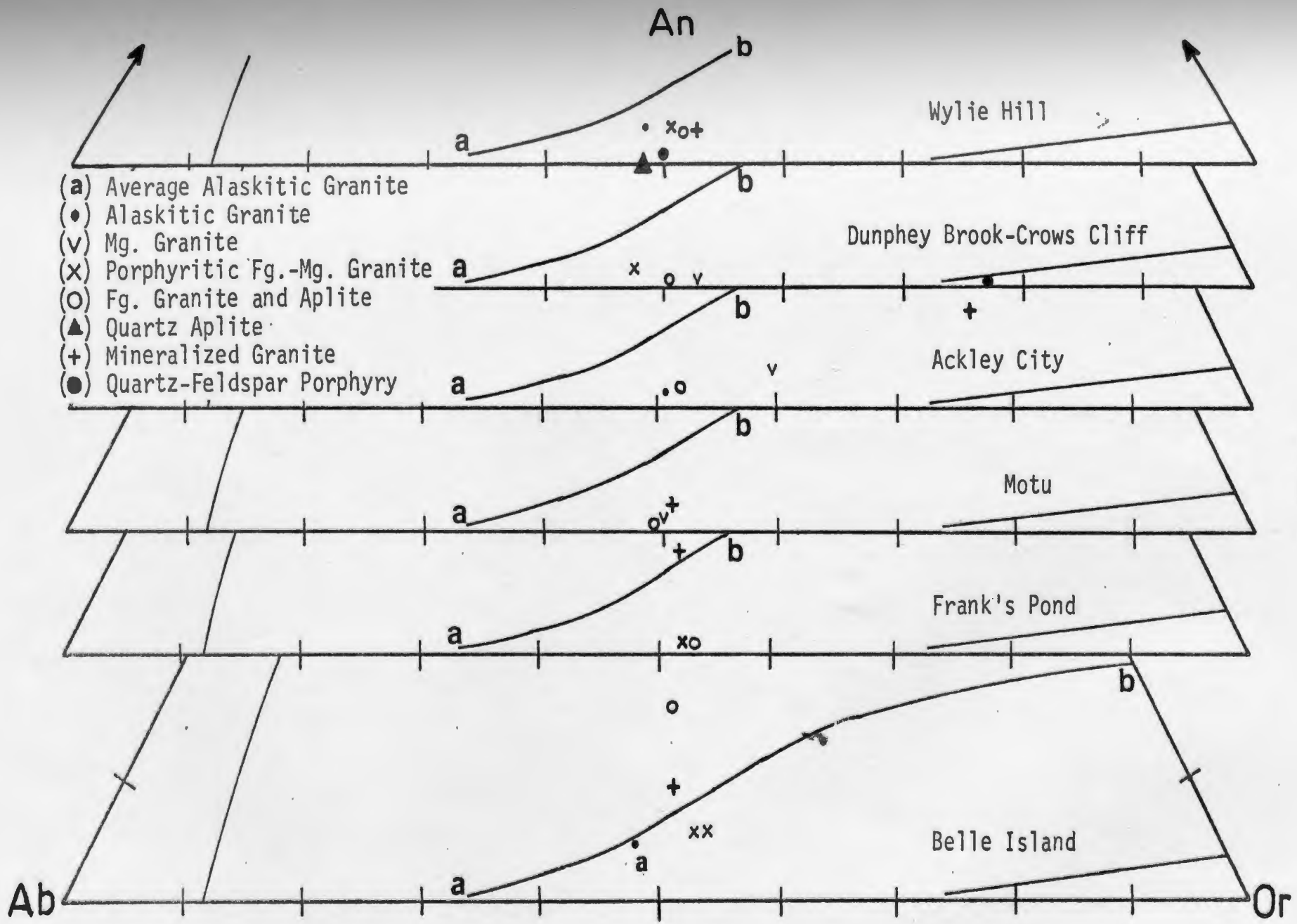

Figure 35. Plot of normative Ab-Or-An for the different molybdenite showings. a-b is the univariant liquidus curve (after Presnall and Batemen, 1973). Other solid lines represent the plagioclase and orthoclase solidus fields.

would be to shift the eutectic towards Or, as found by James and Hamilton (1969) at 1 kb P_{H_2O}, then the intrusives should plot even closer to the .5 kb ternary minimum. Pressure of crystallization is, therefore suggested to be about .5 kb P_{H_2O} for the fine grained intrusive phases with a slightly greater pressure for the average alaskitic granite. Such pressures would be equivalent to a depth of 4 km or less.

The Q:Ab:Or plot suggests a high level of emplacement for granite, but other major features of the granite are at variance with this interpretation. A number of characteristics of the mineralogy, geochemistry, textures, rock associations and depth of emplacement typify the hypersolvus and subsolvus end-members of Tuttle and Bowen's (1958) modal-chemical classification of low-calcium granites (Table 16). According to Table 16 the presence of pegmatite and aplite, especially in the volume of the Ackley showings, is inconsistent with a high level of emplacement. Other features, however, such as extensive granophyre, abundant miarolitic cavities, tuffisites and depletion in Ba, Sr and Cr are compatible with it being a high level hypersolvus granite. An important feature, the occurrance of sodic feldspar within perthite, is present in the pegmatites, but, in the other intrusive phases sodic feldspar occurs as discrete grains

Table 16

Some Characteristics of the Mineralogy, Chemistry, Texture, and Rock Associations of Hypersolvus and Subsolvus Granites

Subsolvus	Hypersolvus	Reference
	Chemistry	
Relative enrichment in V, Sc, Cr, Ba, Sr	Relative enrichment in Be, Yb, Y	Durisek (1964)
	Mineralogy	
Alkali feldspar is always in the ordered, "low-temperature" form.	Alkali feldspar may occur in the disordered, "high temperature" form.	Tuttle and Bowen (1958)
Sodic plagioclase occurs as discrete grains.	Sodic feldspar occurs within perthite.	Tuttle and Bowen (1958)
	Texture	
Miarolitic cavities are rare or absent.	Miarolitic cavities are common.	Tuttle, Luth and Jahns, (1964)
	Rock Associations	
Pegmatite, aplite	Granophyre, rhyolite, rapakiui granite	Tuttle, Luth and Jahns (1964) Jahns and Tuttle (1963) Martin (1970)
	Explosion breccia, intrusive tuff breccia	Hughes (1960), (1971) Reynolds (1954)
	Level of Emplacement	
Mesozone	Epizone	Tuttle and Bowen (1958)

of plagioclase as well as within perthite. The structural state of the alkali feldspars of the pegmatites (Fig. 21) is close to that of orthoclase, not maximum microcline, as would be expected of pegmatite. Although separated feldspars were not studied from the other intrusive phases, the XRD modal analysis method of Bradshaw (1963) included a determination of orthoclase-microcline ratios, and, the microcline III peak was not observed in any samples, nor was the characteristic patchwork twinning observed in thin section. This suggests the alkali feldspars are not in the maximum ordered "low-temperature" form but probably are in an intermediate disordered state such as orthoclase.

Many of the characteristics of a high level hypersolvus granite, therefore, correspond to those of the Ackley alaskitic granite, the major inconsistency being the aplites, pegmatites and the presence of plagioclase. These features according to Jahns and Tuttle (1963), depend to a large extent on the water content of the magma. The hypersolvus granites represent magmas initially low in water, or magmas that lost much of their water before consolidation as a result of near-surface crystallization where the overburden is not great enough to permit large amounts of water to remain in solution. The subsolvus granites, on the other hand, may carry large amounts of

pegmatitic and aplitic material or none at all again depending on the cooling history of the intrusive. The main requirement, therefore, to form the observed pegmatite and aplite at a high level would be a high water content of the magma.

An association of aplite-pegmatite-granophyre-tuffisite at Duffs, Avalon Peninsula, described by Hughes (1971) is lithologically indistinguishable from the Ackley granite association, except the later is of much greater extent. The Duffs occurrence was interpreted by Hughes (1971) to represent the upper levels of ring-dyke intrusions into comagmatic lavas, depth of intrusion being no more than 2,000 m, its origin being explained as:

> Initial crystallization of water-rich magma close to ternary eutectic composition resulted in textures grading from granophyric to microgranite. Eventual entrapment of water rich pockets resulted in crystallization form a silicate liquid and a hydrothermal liquid simultaneously, probably at magmatic overpressure, to form isolated bodies of pegmatite containing giant euhedral quartz crystals. Later aplite, rhyolite, rhyolite breccia, and tuffisite veins reflect the escape of magma and magmatic gas through the congealed parts of the intrusion, at first permissively, but later with increasingly explosive effects.

This hypothesis can be applied directly to the identical occurrences of the Ackley granite. A sealing in of volatiles at such a high level of intrusion thus facilitating the attainment of magmatic overpressures, could be related to the impermeable volcanic host rocks, a suggestion which is supported by their distribution in the area of the showings.

The above explanation reconciles the high level of emplacement of the Ackley granite with the presence of aplite and pegmatite, although the major feature which seems to control the distribution of mineralization, the distribution of the pegmatite and fine grained intrusive phases is yet to be explained. The aplite, pegmatite, fine grained granite and porphyritic granite with the associated molybdenite mineralization are located in embayments of the intrusive into the rhyolite. The fact that the coarse grained alaskitic granite phase is in sharp contact with rhyolite between the showings, and that the fine grained intrusive phases extend beyond the contact to well within the alaskitic granite at Frank's Pond, rules out a chilled contact zone origin for the fine grained intrusive phases. The most reasonable explanation is that these phases are preserved remnants of a once extensive roof zone to the alaskitic granite. The distribution supports this, for in the area of the embayments the rhyolite-intrusive contact is almost flat-lying, while elsewhere the alaskitic granite-rhyolite contacts are steep. Frank's Pond would represent an area where the rhyolite roof has also been recently removed. A sequence of alaskitic granite-porphyritic granite-aplite-pegmatite-rhyolite as the contact is approached is approximately the same in the different showings along the contact and apparently represents a layered sequence dipping parallel to the intrusive-

rhyolite contact. This is supported by diamond drill core data at Motu, Ackley City and Wylie Hill showings, observed dip of contacts, and vertical relief exposure at the Dunphey Brook-Crow's Cliff showing.

If the roof zone hypothesis is to be acceptable, a reasonable explanation for its formation must be suggested. The chemical variation of the alaskitic granite phase suggests its degree of differentiation increases toward the rhyolite contact and the fine grained intrusive phases are chemically more differentiated then the alaskitic granite. The chemistry, therefore, suggests a differentiated sequence with the roof zone being the top of the sequence. The gradational change in composition suggests differentiation in situ or as the magma rose. The rare observed sharp contacts between the different granitic phases however suggest intrusion of the roof zone complex as sills. The roof zone was an area of great concentration of volatiles, as evidenced by the pegmatites. Such concentrations could have been derived by rise of aqueous-phase bubbles from underlying magma (Burnham, 1967) or by a process of fractional crystallization, extraction of water saturated residue and concentration of the residue in the roof zone (Jahns and Burnham, 1969). A combination of these two processes is most likely to give the more highly fractionated magmas of the roof zone, as well as the large volume of volatiles. Retention of

this magmatic water in the roof zone would lead to separation of an aqueous phase, generation of magmatic overpressures, reduction of liquidus temperatures, concomitant crystallization of pegmatite, granophyre and aplite, vapor transport and crystallization of quartz, and release of pressure to form further aplite and tuffisites.

A similar but unmineralized roof complex has been described by Stone (1975) in the Tregonning-Godolphin granite, Cornwall. This complex of banded aplite-pegmatite-leucogranite (Fig. 36) is better geologically documented due to better vertical relief and preservation. Stone proposed a process of in situ differentiation, accumulation of volatiles in the roof, local partial remelting of granite and remobilization in situ to give the several intrusive phases that form the Roof Zone. Tilting of this granite (Fig. 36) by about 30° and erosion down to sea level would result in a situation similar to the Ackley intrusive complex, for the roof zone would be preserved in embayments or patches within the intrusive. The variation in thickness of the roof zone would also be realistic in view of the difference in its thickness between the Motu and Dumphey Brook-Crow's Cliff showings.

5.4.3 Genesis of the Mineralization

The different molybdenite showings, as described above vary in the mode of occurrence of mineralization and

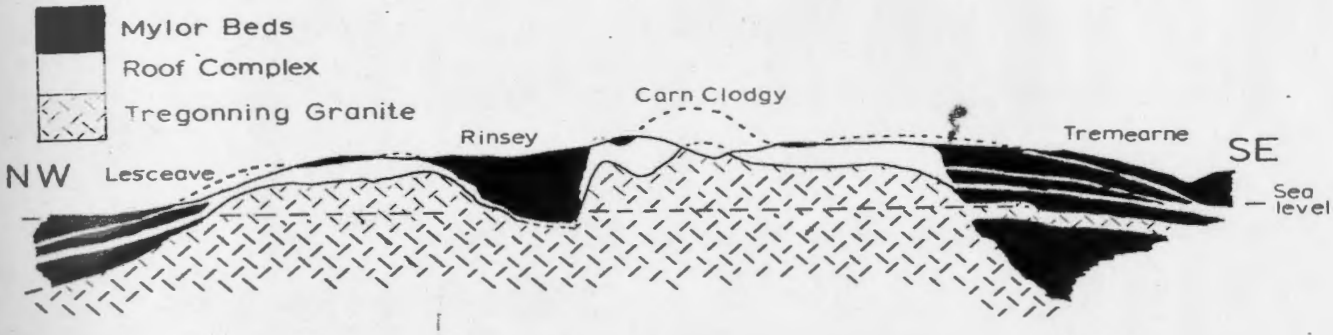

Figure 36. Diagrammatic section across the Tregonning-Godolphin granite based on the fully exposed coast section, Cornwall. Length of section about 3 km. Height of cliffs about 35 m. From Stone (1975).

nature of associated alteration. In terms of classifications of molybdenite deposits discussed in section 2.3 the different showings would be classified differently (Table 17). The mineralization at the Dunphey Brook-Crow's Cliff showing is of syngenetic pegmatite type. The large rosettes of molybdenite in aplite at Motu, characterized by lack of associated alteration could be considered also as syngenetic. The Wylie Hill and Ackley City showings are characterized by features such as disseminated mineralization which could be interpreted as syngenetic and fracture filling mineralization with associated alteration which is epigenetic with porphyry Mo type affinities. The Belle Island showing is similar to the fracture-related Mo-Cu mineralization and alteration of porphyry type deposits. The Frank's Pond showing is of quartz vein type, but the associated fracture-related quartz-sericite alteration is similar to that of porphyry type deposits. Although the classification of such mineralization as of porphyry type or affinity may be questionable, it is apparent that there are both syngenetic and epigenetic showings, as well as a gradation and overlap of characteristics of these types as indicated in Table 17, indicating a transition from a magmatic to hydrothermal origin.

All showings, other then the Belle Island showing, are related to the intrusive phases of the Ackley alaskitic granite's roof zone complex. The mineralization, like

Table 17

Classification of Ackley Molybdenite Showings

Type	Characteristics	Affinities	Showing
Syngenetic or Magmatic	disseminated mineralization large MoS_2 rosettes and pegmatite	Porphyry Type Affinities: Pegmatite	Dunphey Brook-Crow's Cliff
		Aplite	Motu
		Mo	Wylie Hill
			Ackley City
Epigenetic or Hydrothermal	fracture filling mineralization + associated alteration	Mo-Cu	Belle Island
		Quartz vein	Frank's Pond

its host rocks, has a sheet or sill-like form at Motu, Ackley City and Wylie Hill showings, dipping approximately parallel to the intrusive-rhyolite contact. Grade of mineralization reaches a peak near this contact then drops rapidly away from the contact and the sheet of mineralization fingers out quickly down dip. Apparently not only volatiles but Mo, possibly as $(MoO_4)^{2-}$ complexes (Ringwood, 1955), S and small amounts of other metals were concentrated in the roof zone complex, probably at the same time and by the same processes as the volatiles. Variation in the conditions of crystallization of the magma may be responsible for the deposition of the Mo syngenetically or epigenetically.. As already discussed the pegmatite appears to have formed under conditions of magmatic overpressure from an immiscible aqueous phase, into which not only quartz and K-feldspar but also Mo was strongly partitioned. The large rosettes at Motu may be the result of extended precipitation of Mo around scattered points or nuclei as the host aplite crystallized. Mineralization of the other showings is epigenetic, but discussion of their formation is difficult in view of lack of any detailed study of mineralization and alteration. The difference between the showings appear to be differences in retention of the volatiles within the magma, with precipitation of molybdenite as the magma crystallized for the syngenetic showings, as opposed

to release of volatiles, possibly by fracturing for the epigenetic showings. The formation process of the latter would be similar to the orthomagmatic model described in section 2.2.

CHAPTER 6

SUMMARY AND POSSIBLE EXPLORATION APPLICATIONS

6.1 Summary

The following is a brief summary of the findings of this study:

(1) The Ackley Batholith is a composite intrusion consisting of K-feldspar megacrystic granite in the north and east and alaskitic granite in the southeast.

(2) The K-feldspar megacrystic granite is composed of perthite, plagioclase, biotite, magnetite, zircon, sphene and rare tourmaline; the alaskitic granite has the same mineralogy and also rare fluorite.

(3) Major and trace element geochemistry are compatible with the different phases being related, the alaskitic granite being the younger more differentiated phase.

(4) K/Rb ratios indicate the alaskitic granite is a "late stage" granite, but not the K-feldspar megacrystic granite.

(5) The megacrystic granite is alkaline while the alaskitic granite is strongly alkaline.

(6) The Ackley granite is of a composition with geochemical affinities to the Pass Island, Red Island, Tack's Beach, Belleoram and St. Lawrence granites, although the latter two are apparently younger.

(7) All the showings of the Ackley granite (Motu, Ackley City, Dunphey Brook-Crow's Cliff, Wylie Hill and Frank's Pond) are spatially related to separate fine grained granitic and pegmatitic intrusive phases which occur in embayments of the intrusive contact and well within the alaskitic granite phase.

(8) Molybdenite of the showings is of the common $2H_1$ polytype.

(9) The alkali feldspar of the pegmatites is perthite of an orthoclase structural state characterized by anomalous cell parameters.

(10) The Motu showing is within medium grained granite and porphyritic aplite intrusive phases, occurs adjacent to their contact with rhyolite in the form of large molybdenite rosettes without associated alteration.

(11) The Ackley City showing is associated with pegmatite, fine grained granite, and aplite intrusive phases, is in the form of disseminated and fracture filling mineralization, and has extensive associated silicification, muscovite alteration and other forms of alteration.

(12) The Dunphey Brook-Crow's Cliff showing consists of coarse grained molybdenite within pegmatite that is associated with fine grained porphyritic granite, aplite and tuffisite.

(13) The Wylie Hill showing is associated with pegmatite, aplite and porphyritic granite intrusive phases, is in the form of disseminated and fracture filling molybdenite with extensive associated pyrite.

(14) The Frank's Pond showing is quartz-molybdenite veins associated with porphyritic granite and aplite intrusive phases and has associated quartz-sericite alteration near veins.

(15) The Belle Island showing is fracture filling quartz-molybdenite-chalcopyrite mineralization having extensive associated alteration within a plug of alaskitic granite.

(16) The intrusive phases associated with mineralization are all highly differentiated with silica content of 75-80% and differentiation index of 95-100 such that major and trace elements show little variation.

(17) Zn, Pb, Ti, Zr, Y, Ba, Rb, K/Rb, Ba/Rb, Rb/Sr, Ca/Sr, and Ba/Sr values indicate that the fine grained intrusive phases associated with mineralization are more highly differentiated then the alaskitic granite phase.

(18) The alaskitic granite phase shows a regional variation in major and trace elements indicating that its degree of differentiation increases gradationally toward the intrusive-rhyolite contact.

(19) Major and trace element data variation within the Wylie Hill showing indicates there has been no assimilation of rhyolite by the intrusive, and that the degree of differentiation of the intrusive decreases away from the contact.

(20) Correlation matrices indicate the major and most trace elements exhibit behavior which would be expected on standard petrological grounds.

(21) Trace element analyses for a large number of elements usually associated with Mo (Pb, Bi, U, Cu, Zn, W and Sn) indicate Mo is the only economically important element in the showings, although the content of the above elements varies between showings.

(22) Mo shows no significant correlation with any elements other than U and Nb in the showings, while its correlation with Pb and Cu in the alaskite granite indicates its probable accommodation in biotite. The other metals also vary in their correlations and therefore associations and distribution between the showings and alaskitic granite.

(23) The muscovite alteration of the Ackley City showing is, as indicated by geochemical data, not the result of major transport of elements but rather is explicable by closed system alteration followed by leaching of primary rock quartz.

(24) The Ackley alaskitic granite and its associated intrusive phases appear to have crystallized under low water pressures between .5 and 1 Kb, corresponding to a depth of about 4 km or less.

(25) The Ackley granite resembles a hypersolvus granite in most of its characteristics and the presence of aplite and pegmatite, is reconciliable with such a classification.

(26) The fine grained and pegmatite intrusive phases are explicable as erosional remnants of a once extensive roof zone complex in which volatiles were concentrated.

(27) The roof zone complex is probably the result of differentiation of the alaskitic granite as it rose through the crust and in situ as well by injection of sills of volatile rich, more differentiated magma.

(28) The mineralization exhibits characteristics indicating it can be classified as representing a gradation between true magmatic and hydrothermal deposits, there being both pegmatite and porphyry affinity showings as well as showings with composite affinities.

(29) The origin of this mineralization, which is localized in the roof zone complex, is closely related to the formation of the roof zone as the result of concentration of Mo, S and minor amounts of other metals in the volatiles of highly fractionated magma.

(3) Variation in the conditions of crystallization of the magma is probably responsible for the deposition of Mo syngenetically or epigenetically, the most important factor being the behavior of volatiles.

6.2 Possible Exploration Applications

On the basis of the present study further evaluation work on these showings is not justified, for contrary to previous interpretations, mineralization can not be expected to improve or continue at depth.

The concentration and distribution of molybdenite mineralization within the roof zone indicate that the fine grained aplite or pegmatite, not the intrusive-rhyolite contact, is the most important exploration target. Potential for mineralization is, therefore, good along the margins of the alaskitic granite phase as well as within it due to possible irregularities in the roof of the intrusion, the best method for evaluating this being a regional stream geochemical survey. The close genetic tie of this mineralization to the highly differentiated, high level, alkaline alaskitic granite indicates potential is good in intrusives of similar composition, setting and age, not only in Newfoundland but elsewhere in the Appalachians. The close affinity of some of the showings to porphyry type mineralization and the high level nature of the intrusive indicates that models of absence of

porphyry type deposits in pre-Mesozoic-Cenozoic orogenic belts due to erosional level (eg. Sillitoe, 1972b) are not valid, and therefore potential for such mineralization may exist in the Appalachians. An alternate explanation may be that base metal concentration in various types of deposits is in part a function of crustal evolution and that although features characteristic of porphyry-type deposits appear in the Precambrian and Paleozoic rocks, or even culminate in a mineable deposit as at the Copper Mountain orebody, Gaspe Copper (Whalen and Hodder, in prep.), this type of metal concentration in the plutonic phase of igneous activity in orogenic belts does not become dominant until late Mesozoic.

REFERENCES

Alcock , J.B., 1974. Gaspe Copper - a Devonian skarn porphyry copper complex: Geol. Soc. Amer. abs., V. 6, No. 7, pp. 632.

Anderson, F.D., 1965. Belleoram map-sheet, Newfoundland: Geol. Sur. Can., Map 8-1965.

_____, and Williams, H., 1970. Gander Lake (west half) map-area: Geol. Sur. Can., Map 1195A.

Atwater, T., 1970. Implications of plate tectonics for the Cenozoic tectonic evolution of North America: Geol. Soc. Amer. Bull., V. 81, pp. 3513-3536.

Ayres, D., 1974. Distribution and occurrance of some naturally-occurring polytypes of molybdenite in Australia and Papua, New Guinea: J. Geol. Soc. Aust., V. 21, Pt. 3, pp. 273-278.

Barth, T.F.W., 1962. A final proposal for calculating the mesonorm of metamorphic rocks. J. Geol., V. 70, pp. 497-498.

Barsukov, V.L., 1966. Metallogenic specialization of granitoid intrusions: in Geochemistry of the Earth's Crust, V. 2, pp. 211-231.

Bell, K. and Blenkinsop, J., 1975. Geochronology of eastern Newfoundland: Nature, V. 254, pp. 410-411.

Billings, M.P., 1972. Structural Geology: Prentice-Hall, Toronto, 606 p.

Bowen, N.L., 1933. The broader story magmatic differentiation, briefly told, in Ore Deposits of the Western States (Lindgren Vol.): New York, A.I.M.M.E., pp. 106-128.

Bradley, D.A., 1955. Report on the molybdenite deposits of the Rencontre East area, Fortune Bay, Newfoundland: unpubl. rep. 162, Javelin House, St. John's, 37 p.

Bradley, D.A., 1962. Gisborne Lake and Terrenceville map-areas, Newfoundland: Geol. Surv. Can., Mem. 321, 56 p.

Burnham, C.W., 1967. Hydrothermal fluids at the magmatic stage, in Geochemistry of Hydrothermal Ore Deposits, ed. H.L. Barnes: Holt, Rinehart and Winston Inc., New York, pp. 34-76.

Butler, J.R., Bowder, P. and Smith, A.Z., 1962. K/Rb in the evolution of the younger granites of Northern Nigeria: Geochim. et Cosmochim. Acta, V. 26, pp. 89-100.

Calcutt, M., 1974. The stratigraphy and sedimentology of the Cinq Isles Formation, Fortune Bay, Newfoundland: unpubl. M.Sc. thesis, Memorial Univ., 104 p.

Chao, E.C.T. and Fleischer, M., 1960. Abundance of zirconium in igneous rocks: Rep. Int. Geol. Congr. XXI Session (Norden) I, pp. 106-131.

Christiansen, R.L. and Lipman, P.W., 1962. Cenozoic volcanism and plate-tectonic evolution of the western United States: II Late Cenozoic: Phil. Trans. R. Soc. Lond., A 271, pp. 241-284.

Chukrov, F.V., Zvagin, B.B., Yermilova, L.P., Soboleva, S.V., and Khitrov, V.G., 1970. Polytypes of Molybdenite and their occurrance in ores: Int. Geol. Rev., V. 12(1), pp. 74-86.

Churkin, M. and McKee, E.H., 1974. Thin and layered subcontinental crust of the great basin Western North America inherited from Paleozoic marginal ocean basins?: Tectonophysics, V. 23, pp. 1-15.

Clark, A.H., Caelles, J.C., Farrar, E., Haynes, S.J., Lortie, R.B., McBride, S.L., Quirt, G.S., Robertson, R.C.R., and Zentilli, M., 1976. Longitudinal variations in the metallogenic evolution of the Central Andes: in Strong, D.F. ed., Metallogeny and Plate Tectonics, Geol. Assoc. Can., Spec. Paper 14, (in press).

Clark, K.F., 1972. Stockwork molybdenum deposits in the Western Cordillera of North America: Econ. Geol., V. 67, pp. 731-758.

Cooper, G.E. and Steward, K.J., 1956. Evaluation of the Ackley City molybdenite deposits: unpubl. rep. no. 74, Javelin House, 2 p.

Cronan, D.S., 1972. Regional geochemistry of ferromanganese nodules in the world's oceans: in Horn, D.R. ed., Ferromanganese Deposits on the Ocean Floor, Washington, D.C., Nat. Sci. Foundation, Office Internat. Dept. Ocean Expl., pp. 19-30.

DeGeoffroy, J. and Wignall, T.K., 1972. A statistical study of geological characteristics of porphyry Cu-Mo deposits in the Cordilleran belt-application to the rating of porphyry prospects: Econ. Geol., V. 67, pp. 656-665.

Dunlop, W.B., 1955. Compilation on Rencontre molybdenum deposits: unpubl. rep. no. 181, Javelin House, 17 p.

Durisek, E.J., 1964. Trace element study of some hypersolvus and subsolvus granites (abs.): Geol. Soc. Amer. Spec. Paper 82, 51 p.

Ellgring, F.H., 1959. Motu diamond drilling: unpubl. rep. no. 392, Javelin House, 38 p.

Emmons, W.H., 1933. Relations of the disseminated copper ores in porphyry to igneous intrusions: Am. Inst. Min. Met. Eng. Trans., V. 75, pp. 797-815.

Enzman, R.D., 1972. Molybdenum: element and geochemistry: in Fairbridge, R.W. ed., The Encyclopedia of Geochemistry and Environmental Sciences: van Nostrand Reinhold Corp., New York, pp. 753-758.

Ermanovics, I.F., Edgar, A.D. and Currie, K.L., 1967. Evidence bearing on the origin of the Belleoram Stock, southern Newfoundland: Can. J. Earth Sci., V. 4, pp. 413-431.

Fisher, R.A. and Yates, F., 1963. Statistical Table for Biological, Agricultural, and Medical Research: Oliver and Boyd Ltd., Edinburgh, 126 p.

Fogwill, W.D., 1965. Report on a 2 day visit to Rencontre East molybdenum occurrances: unpubl. rep. no. 210, Javelin House, 13 p.

_____, 1966. Further notes on Rencontre molybdenum: unpubl. rep. no. 357, Javelin House, 8 p.

_____, 1967. Molybdenum prospects of Rencontre East: unpubl. rep. no. 408, Javelin House, 9 p.

_____, 1968a. Ackley (or Rencontre) molybdenite prospect - recommended drill program layout for Norlex Mines Ltd.: unpubl. rep. no. 480, Javelin House, 8 p.

_____, 1968b. Wylie Hill molybdenite prospect - recommended drill program for Norlex Mines Ltd.: unpubl. rep. no. 482, Javelin House, 4 p.

Frondel, J.W. and Wickman, F.E., 1970. Molybdenite polytypes in theory and occurrance: II some naturally occurring polytypes of molybdenite: Amer. Min., V. 55, pp. 1857-1875.

Giles, D.L. and Schilling, J.H., 1972. Variation in rhenium content of molybdenite: Int. Geol. Congr. 24, Sec. 10, pp. 145-152.

Godwin, C.I., 1975. Imbricate subduction zones and their relationship with Upper Cretaceous to Tertiary porphyry deposits in the Canadian Cordillera: Can. J. Earth Sci., V. 12, pp. 1362-1378.

Goldschmidt, V.M., 1954. Geochemistry: Oxford Univ. Press, Fair Lawn, N.J., 730 p.

Greene, B.A. and O'Driscoll, C.F., 1976. Gaultois map-area: in Rep. Activities, 1975, Min. Dev. Div. Rep. 76-1, Prov. Nfld. Dept. Min. Ener., pp. 56-63.

Guild, F.N., 1971. Metallogeny: a key to exploration: Min. Eng., V. 23, pp. 69-72.

Hall, E.N., Friedman, I. and Nash, J.T., 1974. Fluid-inclusion and light-stable-isotope study of the Climax molybdenum deposits, Colorado: Econ. Geol., V. 69, pp. 884-901.

Heinrich, E. Wm., 1958. Mineralogy and Geology of Radioactive Raw Materials: McGraw-Hill Book Co. Inc., Toronto, 654 p.

Hodder, R.W., 1974. Types of porphyry copper deposits at destructive plate margins and their metallogenic implications: Geol. Assoc. Can., prog. abs., pp. 42.

Hollister, V.F., 1973. Regional characteristics of porphyry copper deposits of South America: A.I.M.M.E. annual meeting, Chicago, preprint 73-12.

_____, Potter, R.R. and Barker, A.L., 1974. Porphyry copper type mineralization of the Appalachian orogen: Econ. Geol., V. 69, pp. 618-630.

Howley, J.P., 1888. Geological Survey of Newfoundland - Report for 1887.

Hughes, C.J., 1960. The Southern Mountains igneous complex, Isle of Rhum: Quart. Jour. Geol. Soc. London, V. 116, pp. 111-138.

_____, 1971. Anatomy of a granophyre intrusion: Lithos, V. 4, pp. 403-405.

Hutchinson, R.D., 1962. Cambrian stratigraphy and trilobite faunas of southeastern Newfoundland: Geol. Surv. Can., Bull. 88, 156 p.

Ishihara, S., 1973. Molybdenum and Tungsten Provinces in the Japanese Islands and North American Cordillera: an example of a symmetrical metal zoning in Pacific type orogeny: in Fisher, N.H. ed., Metallogenic Provinces and Mineral Deposits in the Southwestern Pacific, Aust. Gov. Publ. Ser., Bull. 141, pp. 173-189.

Jahns, R.H. and Tuttle, O.F., 1963. Layered pegmatite-aplite intrusives: Miner. Soc. Amer. Spec. Paper 1, pp. 78-92.

_____, and Burnham, C.W., 1969. Experimental studies of pegmatite genesis: I a model for the derivation and crystallization of granitic pegmatites: Econ. Geol., V. 64, pp. 843-864.

James, A.D., 1971. Hypothetical diagrams of several porphyry copper deposits: Econ. Geol. V. 66, pp. 43-47.

James, D.E., 1971. Plate tectonic model for the evolution of the central Andes: Geol. Soc. Amer. Bull., V. 82, pp. 3325-3346.

James, R.S. and Hamilton, D.L., 1969. Phase relations in the system $NaAlSi_3O_8$ - $KAlSi_3O_8$ - $CaAl_2Si_2O_8$ - SiO_2 at 1 kilobar water pressure: Contr. Min. Pet., V. 21, pp. 111-141.

Jenness, S.E., 1963. Terra Nova and Bonavista Map-Areas, Newfoundland (2 DE½ and 2C): Geol. Surv. Can., Mem. 327, 184 p.

Kazitsin, Yu.V., 1962. Indication of molybdenum-bearing intrusions in Northeast Transbaikalia: Gosgeoltekhizdat.

Kennedy, M.J. and McGonigal, M.H., 1972. The Gander Lake and Davidsville Groups of northeastern Newfoundland: new data and geotectonic implications: Can. J. Earth Sci., V. 9, pp. 452-459.

Kesler, S.E., 1973. Copper, molybdenum, and gold abundances in porphyry copper deposits: Econ. Geol., V. 68, pp. 106-111.

Khitarov, N.L., Arutyunyar, L.A. and Lebedev, E.B., 1967. Experimental study of separation of molybdenum from granitic melts at water vapour pressures up to 3000 atmospheres: Geochem. Inter., V. 4, pp. 730-737.

Khurshudyar, E.B., Arutyunyan, L.A. and Meliksetyan, B.M., 1969. Origin of the polytypes of molybdenite: Geochem. Int., V. 6, pp. 942-949.

Kirkham, R.V., 1971a. Intermineral intrusions and their bearing on the origin of porphyry copper and molybdenum deposits, Econ. Geol., V. 66, pp. 1244-1249.

_____, 1971b. Geology of copper and molybdenum deposits: in Report of Activities, Pt. A, Geol. Surv. Can. Paper 72-1, pp. 82-87.

_____, and Soregaroli, A.E., 1975. Preliminary assessment of porphyry deposits in the Canadian Appalachians: in Report of Activities, Pt. A, Geol. Surv. Can., Paper 75-1, pp. 249-252.

Kistler, R.W. and Peterman, Z.E., 1973. Variations in the Sr, Rb, K, Na, and initial Sr^{87}/Sr^{86} in Mesozoic granitic rocks and intruded wall rocks in central California: Geol. Soc. Amer. Bull., V. 84, pp. 3489-3512.

Knight, F.C., 1968. Report on the Rencontre Lake molybdenite prospects in the Fortune district, Province of Newfoundland: unpublished rep. no. 514, Javelin House, 18p.

Lindgren, W., 1937. Succession of minerals and temperatures of formation in ore deposits of magmatic affiliation: A.I.M.M.E. Trans., V. 126, pp. 356-376.

Lowell, J.D., 1973. Regional characteristics of southwestern North America porphyry copper deposits: A.I.M.M.E. Annual Meeting, Chicago, Preprint 73-3-12.

_____, 1974. Plate tectonics and foreland basement deformation: Geology, V. 2, No. 6, pp. 275-278.

_____, and Guilbert, J.H., 1970. Lateral and vertical alteration - mineralization zoning in porphyry ore deposits: Econ. Geol. V. 65, pp. 373-408.

Mandarino, J.A. and Gait, R.I., 1970. Molybdenite polytypes in the Royal Ontario Museum: Can.Miner., V. 10, pp. 723-729.

Martin, R.F., 1970. Petrogenetic and tectonic implications of two contrasting Devonian batholithic associations in New Brunswick, Canada, Am. J. Sci., V. 268, pp. 309-321.

McInnis, W., 1957. Molybdenum, a materials survey: U.S. Bur. Mines Info. Circ. 7784.

McKenzie, D.P. and Morgan, W.J., 1969. Evolution of triple junctions: Nature, V. 224, pp. 125-133.

McKinstry, H.E., 1938. Report on examination of the Rencontre molybdenite deposits: unpubl. rep. no. 163, Javelin House, 15 p.

McNeil, M.J., 1959. Motu-diamond drilling by Caledon Minerals: unpubl. rep. no. 392, Javelin House, 38 p.

Mitchell, A.H.G. and Garson, M.S., 1972. Relationships of porphyry copper and circum-Pacific tin deposits to paleo-Beniof zones: Inst. Min. Met. Trans., Sec. B, V. 81, pp. 310-325.

Moorhouse, W.W., 1957. The Study of Rocks in Thin Section: Harper and Row, New York, 514 p.

Morris, D.F.C. and Short, E.L., 1969. Rhenium: in Wedepohl, K.H. ed, Handbook of Geochemistry, Springer-Verlag, pp. 607-688.

Nielsen, R.L., 1968. Hypogene texture and mineral zoning in a copper-bearing granodiorite stock, Santa Rita, New Mexico: Econ. Geol., V. 63, pp. 37-50.

Nockolds, S.R. and Allen, R., 1953. The geochemistry of igneous rock series: Geochim, et Cosmochim. Acta, V. 4, pp. 105-142.

Norton, D.L. and Cathles, L.M., 1973. Breccia pipes - product of exsolved vapour from magmas: Econ. Geol. V. 68, pp. 540-546.

O'Driscoll, C.F., 1973. Geology and Petrochemistry of the Swift Current Granite, Newfoundland: unpubl. B.Sc. (Hon.) thesis, Memorial Univ. of Newfoundland, 84 p.

Pereira, J. and Dixon, C.J., 1971. Mineralization and plate tectonics: Miner. Deposita, V. 6, pp. 404-405.

Pokalov, V.T. and Pastukhova, E.S., 1961. Age and genetic features of the Sor molybdenum deposit: Sov. Geologiya, No. 7.

_____ and Zilov, A.R., 1962. Molybdenum mineralization in the Uda-Vitim Zone of Transbaikalia: Mineral'nce Syr'e, No. 5.

Quinn, H.A., 1944. Report on diamond drilling done by Geological Survey of Newfoundland at Rencontre East: unpubl. rep. no. 135, Javelin House, 10 p.

Ramsey, J.G., 1967. Folding and Fracturing of Rocks: McGraw-Hill Co., Toronto, 568 p.

Reynolds, D.L., 1954. Fluidization as a geological process, and its bearing on the problems of intrusive granites: Am. J. Sci., V. 252, pp. 577-613.

Ringwood, A.E., 1955. The principles governing trace element behavior during magmatic crystallization, Part II: The role of complex formation: Geochim. et Cosmochim. Acta, V. 7 (5/6), pp. 242-254.

Rose, A.W., 1970. Zonal relations of wall rock alteration and sulfide distribution at porphyry copper deposits: Econ. Geol., V. 65, pp. 920-936.

Sandell, E.B. and Kuroda, P.K., 1954. Geochemistry of molybdenum: Geochim. et Cosmochim. Acta, V. 6, pp. 35-63.

Sawkins, F.J., 1972. Sulphide ore deposits in relation to plate tectonics: Jour. Geol., V. 80, pp. 377-397.

Scholz, C.H., Barazangi, M. and Shar, M.L., 1971. Late Cenozoic evolution of the Great Basin, Western United States, as an ensialic interarc basin: Geol. Soc. Amer. Bull., V. 82, pp. 2979-2990.

Sewell, D.L., 1972. Mode of occurrence of the cupriferous pyritic deposits of Cyprus: Trans. Sec. B, Inst. Min. Met., V. 81, pp. B189-B197.

Sheppard, S.M.F., Nielsen, R.L. and Taylor, H.P., 1971. Hydrogen and oxygen isotope ratios in minerals from porphyry copper deposits: Econ. Geol., V. 66, pp. 515-542.

Sillitoe, R.H., 1972a. Relation of metal provinces in Western America to subduction of oceanic lithosphere: Geol. Soc. Amer. Bull., V. 83, pp. 813-818.

_____, 1972b. A plate tectonic model for the origin of porphyry copper deposits: Econ. Geol., V. 67, pp. 184-197.

_____, 1972c. Formation of certain massive sulphide deposits at sites of sea-floor spreading: Trans. Sec. B, Inst. Min. Met., V. 81, pp. 141-148.

_____, 1973. Tops and bottoms of porphyry copper deposits: Econ. Geol., V. 68, pp. 1107-1116.

_____, 1976. Andean mineralization: a model for the metallogeny of convergent plate margins: in Strong, D.R., ed, Metallogeny and Plate Tectonics, Geol. Assoc. Can. Spec. Paper no. 14 (in press).

Smith, B.L., 1936. Rencontre molybdenite, report to Dana Co. Ltd.: unpubl. rep. no. 37, Javelin House, 20 p.

_____, 1953. Fluorite deposits of Long Harbour, Fortune Bay: Geol. Sur. Nfld., Rept. No. 2, 19 p.

_____, and White, D.E., 1954. Geology of the Rencontre East area: Geol. Sur. Can., unpubl. rep., 46 p.

Snedecor, G.W. and Cockran, W.G., 1967. Statistical Methods: The Iowa State Univ. Press, Ames, Iowa, 593 p.

Somina, M., 1966. Trigonal molybdenite East Siberia: Acad. Sci., U.S.S.R. Earth Sci., V. 167, pp. 898-901.

Soregaroli, A.E., 1975. The geology of molybdenum and copper deposits in Canada: in Report Activities Pt. A, Geol. Surv. Can., Paper 75-1, pp. 243-244.

Spurr, J.E., 1923. The Ore Magmas: McGraw-Hill, New York, 458 p.

Stevenson, J.S., 1940. Molybdenum deposits of British Columbia: B.C. Dept. Mines, Bull. 9.

Stone, M., 1975. Structure and petrology of the Tregonning-Godolphin granite, Cornwall: Proc. Geol. Assoc., V. 86, Pt. 2, pp. 155-170.

Streckeisen, A.L., 1967. Classification and nomenclature of igneous rocks: N. Jb. Miner. Abh., V. 107, pp. 144-214.

Strong, D.F., 1974. Plate tectonic setting of Newfoundland mineral deposits: Field trip guidebook for NATO Advanced Studies Inst. on Metallogeny and Plate Tectonics, St. John's, Nfld. 169 p.

_____, Dickson, W.L., O'Driscoll, C.F., and Kean, B.F., 1974. Geochemistry of eastern Newfoundland granitoid rocks: Prov. Nfld. and Lab. Dept. Min. and Energy Mineral Dev. Div. Rept. 74-3, 140 p.

Sutherland Brown, A., 1969. Mineralization in British Columbia and the copper and molybdenum deposits: Can. Min. Metall. Bull., V. 62, pp. 26-40.

Sutulov, A., 1963. LPT process: Univ. of Concepcion Press, Chile.

_____, 1970. Molybdenum and Rhenium Recovery from Porphyry Coppers: Univ. of Concepcion Press, Chile, 200 p.

_____, 1974. Copper Porphyries: Univ. Utah Press, Salt Lake City, 200 p.

Takeuchi, Y. and Nowachi, W., 1963. Detailed rhombohedral MoS_2 and systematic deduction of possible polytypes of molybdenite: Schweiz. Miner. Petrol. Mitt., V. 344, pp. 105-120.

Tausen, L.V. and Petrovskaya, S.G., 1971. Endogenic halo types of hydrothermal molybdenum deposits: in Geochemical Exploration, Can. Min. Metall. Spec. V. 11, pp. 394-396.

Taylor, H.P. Jr., 1974. Problems of hydrothermal alteration and ore deposits: Econ. Geol., V. 69, pp. 843-883.

Taylor, S.R., 1964. Abundance of chemical elements in the continental crust: Geochim. et Cosmochim. Acta, V. 28, pp. 1280-1281.

_____, 1965. The application of trace elements to problems in petrology: Physics and Chemistry of the Earth, V. 6, pp. 133-213.

Teng, H.C., 1974. A Lithogeochemical Study of the St. Lawrence Granite, Newfoundland: unpubl. M.Sc. thesis, Memorial Univ. of Newfoundland, 194 p.

Terada, K., Osaki, S., Ishihara, S. and Kiba, T., 1971. Distribution of rhenium in molybdenites in Japan: Geochem. J., V. 4, pp. 123-141.

Thornton, C.P. and Tuttle, O.F., 1960. Chemistry of igneous rocks, differentiation index: Am. J. Sci., V. 258, pp. 664-684.

Turekian, K.K. and Wedepohl, K.H., 1961. Distribution of the elements in some major units of the earth's crust: Geol. Soc. Amer. Bull., V. 72, pp. 175-192.

Tuttle, O.F. and Bowen, N.L., 1958. Origin of granite in the light of experimental studies in the system $NaAlSi_3O_8$ - $KAlSi_3O_8$ - SiO_2 - H_2O: Geol. Soc. Amer. Mem. 74, 153 p.

_____, Luth, W.C. and Jahns, R.H., 1964. The hypersolvus granite-granophyre-rhyolite association (abs): Amer. Geophys. Union Trans., V. 45, pp. 124.

Tuyarinov, A.I., Khadakovskiy and Zhidikova, A.P., 1973. Physicochemical conditions for molybdenite production in hydrothermal uranium-molybdenum deposits: Geochem. Inter., V. 10, pp. 731-739.

Twenhofel, W.H., 1947. The Silurian strata of eastern Newfoundland with some data relating to physiography and Wisconsin glaciation of Newfoundland: Am. J. Sci., V. 245, pp. 65-122.

Vandervilt, J.W., 1933. Molybdenite deposits: in Ore Deposits of the Western States (Lindgren Vol.), A.I.M.M.E., pp. 579-573.

Vinogradov, A.P., 1962. The average contents of the chemical elements in the principle types of igneous rocks of the earth's crust: Geokhimiya, No. 7.

Vokes, F.M., 1963. Molybdenum deposits of Canada: Geol. Surv. Can. Econ. Geol. Rep. No. 20, 332 p.

Vorma, A., Kallio, P. and Merilainem, K., 1966. Molybdenite - 3R from Inari, Finnish Lapland: Bull. Comm. Geol. Finl., V. 222.

Wanless, R.K., Stevens, R.D., Lachance, G.R. and Edmonds, C. M., 1967. Age determinations and geological studies: Geol. Surv. Can., Paper 66-17.

_____, _____, _____ and Rimsaite, R.Y.H., 1965. Age determinations and geological studies: Geol. Surv. Can., Paper 64-17.

Weaver, D.F., 1967. A geological interpretation of the Bouguer anomaly field of Newfoundland: Publ. of Dom. Obser. V. 35, No. 5.

White, D.E., 1939. Geology and Molybdenite Deposits of the Rencontre East Area, Fortune Bay, Newfoundland: unpubl. Ph.D. thesis, Princeton Univ., 119 p.

_____, 1940. The molybdenite deposits of the Rencontre East area, Newfoundland: Econ. Geol., V. 35, pp. 967-995.

Whitney, J.A., 1975. Vapour generation in a quartz monzonite magma: a synthetic model with application to porphyry copper deposits: Econ. Geol., V. 70, pp. 346-358.

Wickham, F.E. and Smith, D.K., 1970. Molybdenite polytypes in theory and occurrence, I theoretical considerations of polytypism in molybdenite: Amer. Miner., V. 55, pp. 1843-1856.

Widmer, K., 1950. The geology of the Hermitage Bay Area, Newfoundland: unpubl. Ph.D. dissertation, Princeton Univ., 439 p.

Williams, H., 1967. Silurian rocks of Newfoundland: in Neale, E.R.W. and Williams, H., eds., Geology of the Atlantic Region, Geol. Assoc. Can. Spec. Paper No. 4, pp. 93-137.

_____, 1968. Wesleyville, Newfoundland: Geol. Surv. Can., Map 1227A.

_____, 1971. Geology of Belleoram map-area, Newfoundland: Geol. Surv. Can. Paper 70-65, 39 p.

_____, Kennedy, M.J., and Neale, E.R.W., 1972. The Appalachian structural province: in Price, R.A., and Douglas, R.J.W., eds. Variations in tectonic styles in Canada, Geol. Assoc. Can. Spec. Paper No. 11, pp. 181-261.

_____, _____, _____, 1974. The northeastward termination of the Appalachian orogen: in Nairn, A.E.M. and Stehi, F.G., eds., The Ocean Basins and Margins, V. 2, Plenum Publ. Corp., New York, pp. 79-123.

Wright, J.B., 1969. A simple alkalinity ratio and its application to questions of non-orogenic granite genesis: Geol. Mag., V. 106, pp. 370-384.

Wright, T.L. and Steward, D.B., 1968. X-ray and optical study of alkali feldspars: II determination of composition and structural state from refined unit-cell parameters and 2V: Amer. Min., V. 53, pp. 38-87.

Yskimore, T., 1951. Molybdenum content in Japanese volcanic rocks: Bull. Chem. Soc. Japan, V. 24, pp. 251-260.

Zelikman, A.N., Indendaum, G.V., Teslitskaya, M.V. and Shalankova, V.F., 1969. Structural transformations in synthetic MoS_2: Soviet Physics-Crystallography, V. 14, pp. 687-691.

Zurowski, M., 1968. Report on the exploration activities of Norlex Mines Ltd. on their Rencontre Lake molybdenite prospect, Fortune Bay area, Province of Newfoundland: unpubl. rep. no. 496, Javelin House, 5 p.

APPENDIX A

SAMPLING AND ANALYTICAL METHODS

1.1 Sample Collection and Preparation

The sampling program was designed to access the composition and geochemical variability of different mapped intrusive units, and their mineralized and altered equivalents.

At each location an eight pound sledge hammer was used to collect in plastic sample bags single 2 kg rock samples consisting of unweathered 2 to 3 cm chips and a slab for thin sectioning.

Samples were washed prior to the following crushing procedure:

(1) All the collected chips were crushed to slightly smaller size (1-2 cm or smaller) in a Denver steel jaw crusher.

(2) A representative sample of these pieces was crushed in a tungsten carbide Siebtechnik swing mill for three minutes, producing a rock powder of -100 mesh, as determined by random sieving checks.

1.2 Analytical Procedures

1.2.1 Major Element Analysis

Nine major elements (Fe_2O_3 (total), TiO_2, SiO_2, CaO, K_2O, MgO, Al_2O_3, Na_2O, MnO) were determined by a Perkin Elmer 303 Atomic Absorption Spectrometer using solutions prepared by the following method:

(1) .1000 g of rock powder was weighed into a digestion flask (Nalgene Catalogue #5122 polycarbonate centrifuge bottle).

(2) 5 ml conc. HF acid was added by a automatic pipette, the screw top was tightened, and the bottle was placed for 5 minutes on a steam bath. If any remaining residue was black rather than white (soluble in boric acid), the original sample was weighed out and 1 ml HCl and 1 ml HNO_3 along with the HF was added and treated as above.

(3) After being removed from the heat and let cool 5 ml of saturated boric acid solution was added by pipette and the bottle again placed on a steam bath until the solution was clear.

(4) After being let cool the solution was made up to a 250 ml volume by addition of distilled water from a precise volume dispenser. This solution was than stored in polyethylene bottles and used for all analyses.

All elements except CaO and MgO, which need further dilution, were analyzed on the solutions by comparison to a range of standards 90%, 80%, 70% ....10% prepared from a standard granite stock solution employing the settings given in the A.A.S. instrument book for each element. CaO and MgO were determined on solutions prepared by pipetting 5 ml of sample solution

into a 50 ml volumetric flask, adding 5 ml conc. HCl, 10 ml of lanthanum oxide solution and making the solution up to 50 ml with distilled water. Standard solutions were treated in the same manner.

A granite rock standard (G-1) was analyzed four times in the above manner to determine the accuracy and precision of the major element analysis (Table 18).

1.2.2 Trace Element Analysis

Fifteen trace elements (Zr, Sr, Rb, Zn, Cu, Ba, Mo, Nb, Bi, Pb, Ni, Y, Cr, and Ti) were determined on pressed powder discs using a Philips PW 1450 Automatic Hardware Programmed System (AHP) X-Ray Spectrometer at the University of Western Ontario.

The sample discs were prepared in the following manner:

(1) 2.5 g of rock powder were thoroughly mixed with three to four drops of N-30-88 Mowial binding agent until the colour was uniform.

(2) Using industrial grade boric acid backing, this powder was pressed into a disc for one minute at 15 tons per sq. in.

The 2θ positions of the peaks and backgrounds for the different trace elements and the count times on the XRF are given in Table 19. Samples were run with a window setting of 150 LL, at 60 kV, and 45 MA (except Ba

Table 18. Precision of A.A.S. Analysis for Major Elements (n = 4)

Standard Sample G-2

Element	Accepted+ Value	$\bar{x}$	σ	$\frac{\sigma \times 100}{\bar{x}}$	Range Low	Range High
SiO_2	69.11	68.50	.58	.85	68.01	69.95
Al_2O_3	15.40	15.20	.25	1.64	14.95	15.60
Fe_2O_3	2.65	2.70	.02	.37	2.65	2.73
MgO	.76	.80	.05	6.25	.75	.83
CaO	1.94	2.00	.10	5.00	1.93	2.15
Na_2O	4.07	4.20	.02	.48	4.07	4.22
K_2O	4.51	4.55	.02	.44	4.50	4.58
TiO_2	.50	.50	.01	2.00	.48	.52
MnO	.03	.03	.00	0.00	—	—
Total	98.97	98.48				

+ according to Flanagan (1970)

Table 19. 2θ Positions and Count Time For Trace Element XRF Analyses

Element	2θ	Count Time (Sec)	Element	2θ	Count Time (sec)
Cr(P)	16.94	20	Pb(P)	28.82	20
Cr(B)	17.05	"	Pb(B)	28.80	"
Ba(P)	18.72	40	Bi(B)	32.70	40
Ba(B)	19.02	"	Bi(P)	33.02	"
Ni(P)	48.67	20	Bi(B)	33.60	"
Ni(B)	49.67	"	Mo(B)	19.50	"
Nb(P)	21.44	"	Mo(P)	20.33	"
Nb(B)	21.87	"	Zn(P)	41.80	20
Zr(P)	22.57	"	Zn(B)	42.40	"
Zr(B)	23.31	"	Cu(B)	44.65	40
Y(P)	23.82	"	Cu(P)	45.03	"
Y(B)	24.72	"	Cu(B)	45.70	"
Sr(P)	25.17	"	U(B)	25.70	"
Sr(B)	25.77	"	U(P)	26.17	"
Rb(P)	26.66	"	U(B)	27.00	"
Rb(B)	27.77	"			

(P) - peak

(B) - background

at 10 mA), mode/filter setting of X/O, using a LIF 200 crystal and a W target. Samples and standard rock samples were run four at a time, the count data being automatically typed out on paper and punched on paper tape by an on-line teletypewriter. Computer cards were generated from the paper tape by remote terminal programming of a Cyber 10 computer.

A program, "Tratio", written by R.C.O. Gill was used to process the count data. The information required for the operation of the program is chemical symbol, method, 20 positions, blank correction, interference correction, calibration slope factor, lower limit of linear calibration and upper limit of linear calibration (Table 20). A choice is made between using net peak intensity (Ip - Ip in counts) or a net peak counts divided by the background counts (Ip/Ib-1, a dimensionless ratio). The net peak intensity method was used for all elements. A blank correction was obtained by running silica blank pellets and also from the calibration intercept position. A K-beta interference correction from appropriate elements was obtained for Mo (.0975), Ba (.0035), Nb (.0041), Zr (.0412), and Y (.1843) by running interference standards and making appropriate calculations. It was necessary to run the program twice for the set of data. In the first run the program calculated the intensity functions upon which the calibration is based,

Table 20

Information punched on cards for trace element calculation by computer program "Tratio"

	'ZR, SR, RB AND CU IN DOLERITES'				Title describing specimens under analysis-for user reference
'ZR'	'RATIO'	30.95	32.09	33.05	For each element the following are given:
		-0.01	0.547		1. Chemical symbol
		133.0	4.0	3000.0	2. Method: 'COUNTS' for (P-B)
					'RATIO' for P/B-1
'SR'	'RATIO'	34.85	35.84	36.85*	
		0.009	0.00		
		89.0	3.0	900.0	3. (a) Low 2θ background position
					(b) Peak 2θ position
'RB'	'COUNTS'	36.85*	37.96	0.00+	(c) High 2θ background position
		-0.001	0.00		
		0.00356	3.0	600.0	4. (a) Blank correction (calibration intercept)
					(b) Interference correction (proportion of k intensity of interfering element which is to be subtracted from intensity of interfered element line)
'CUB'	'RATIO'				
		0.30	0.00		
		83.0	2.0	500.0	5. (a) Calibration slope factor
					(b) Lower limit of linear calibration
					(c) Upper limit of linear calibration

* Sharing of background position is recognised by equality of appropriate 2θ values. In such a case, the count for this channel is read only once per specimen.

\+ If only one background reading is used, enter a zero in place of the position not used.

the calibration constants were replaced by zeros with the result that the concentration listing was suppressed. The slope factor was obtained by drawing a calibration curve for each element of counts versus concentration for standard rock samples. The calculation program was repeated with calibration data supplied and the concentrations were printed out.

A number of rock standards (BCR-1, DR-1 and [illegible]-1) were run numerous times to give a measure of the precision and accuracy of trace element analysis (Table [illegible] a, [illegible], [illegible]).

1.2.3 Loss on Ignition

Loss on ignition was calculated by measuring a known amount of powder into a porcelain crucible, heating at 1050° C for two hours, weighing again and expressing the difference in percent.

1.2.4 Other Analytical Procedures

Analysis for S on the samples was made using a Leco Induction Furnace Analyser following the manual instructions and using between .1 and .5 g, depending on S content.

Feldspar structural state was determined on hand picked pegmatite feldspar following the method of Wright and Steward (1968), using two complete X-ray

Table 21 a

Standard Sample J6-1
(N - 16)

Element	Accepted Value	$\bar{x}$	σ	$\frac{\sigma \times 100}{\bar{x}}$	Range Low	Range High
Zr	——	133	3	2.3	130	141
Sr	183	261	5	1.9	255	273
Rb	186	198	3	1.5	195	206
Zn	36	26	8	30.8	21	49
Cu	——	7	2	28.6	4	11
Ba	450	397	16	4.0	386	452
Mo	——	14	3	21.4	3	17
Nb	——	18	2	11.1	16	21
Pb	24	37	3	8.1	33	43
Ni	——	12	3	25.0	8	19
Y	——	43	11	25.6	44	49
Cr	——	54	3	5.6	50	60
Ti	1690	1927	483	25.1	1812	2082

σ = standard deviation

$\bar{x}$ = mean

$\frac{\sigma \times 100}{\bar{x}}$ = coefficient of variation

Table 21 b

Standard Sample BCR - 1
N = 17

Element	Accepted Value	$\bar{x}$	σ	$\frac{\sigma \times 100}{\bar{x}}$	Range Low	Range High
Zr	180	144	35	24.3	148	157
Sr	335	282	69	24.5	291	303
Rb	48	31	8	25.8	31	35
Zn	115	61	16	26.2	59	85
Cu	22	25	7	28.0	17	30
Ba	650	585	144	24.6	591	697
Mo	—	26	7	26.9	20	31
Nb	10	8	2	25.0	7	11
Pb	5	9	3	33.3	7	14
Ni	—	3	2	66.7	1	10
Y	33	34	1	2.9	32	36
Cr	11	19	7	36.8	9	31
Ti	13440	13121	3214	24.5	12305	14122

Table 21 c

Standard Sample JB - 1
(N = 25)

Element	Accepted Value	$\bar{x}$	σ	$\frac{\sigma}{\bar{x}} \times 100$	Range Low	Range High
Zr	———	121	24	19.8	123	134
Sr	448	439	88	20.0	451	475
Rb	41	30	6	20.0	30	35
Zn	83	42	11	26.2	40	57
Cu	———	72	15	20.8	68	83
Ba	———	416	85	20.4	419	489
Mo	———	48	10	20.8	41	51
Nb	———	29	6	20.7	26	32
Pb	13	6	4	66.7	2	12
Ni	139	124	25	20.2	126	135
Y	———	24	5	20.8	22	28
Cr	420	342	69	20.2	346	369
Ti	8040	7796	1570	20.1	7316	8214

diffraction scans. Polytypes of molybdenite were determined by X-ray diffraction employing the method described by Frondel and Wickman (1970).

1.2.5 Estimation of Mode

Modal analyses were carried out by two methods. The first was by point counting greater than 1500 points on thin sections which had been stained for K-feldspar. The second method was the X-ray diffraction method described by Bradshaw (1963) which employs the intensity of quartz 100, orthoclase $\bar{2}01$, $20\bar{2}$, and 111, and microcline 111 peaks to determine the K-feldspar, oligoclase and quartz percentages of granites. Three separately prepared powder mounts were run for each sample and the results averaged.

A number of samples were run by both these methods, the results being closely comparable (Fig. 37).

1.3 Statistical Procedures and Methods of Data Presentation

Upon completion of the analytical work, the major and trace element results were punched on computer cards according to the format in Fig. 38. Barth molecular norms and correlation matrices were calculated using computer programs prepared by Dr. R.G. Cawthorne. Statistical treatment and plotting of variation diagrams for the geochemical data were performed using a Hewlett-Packard Model 20 desk computer-plotter with card-reader.

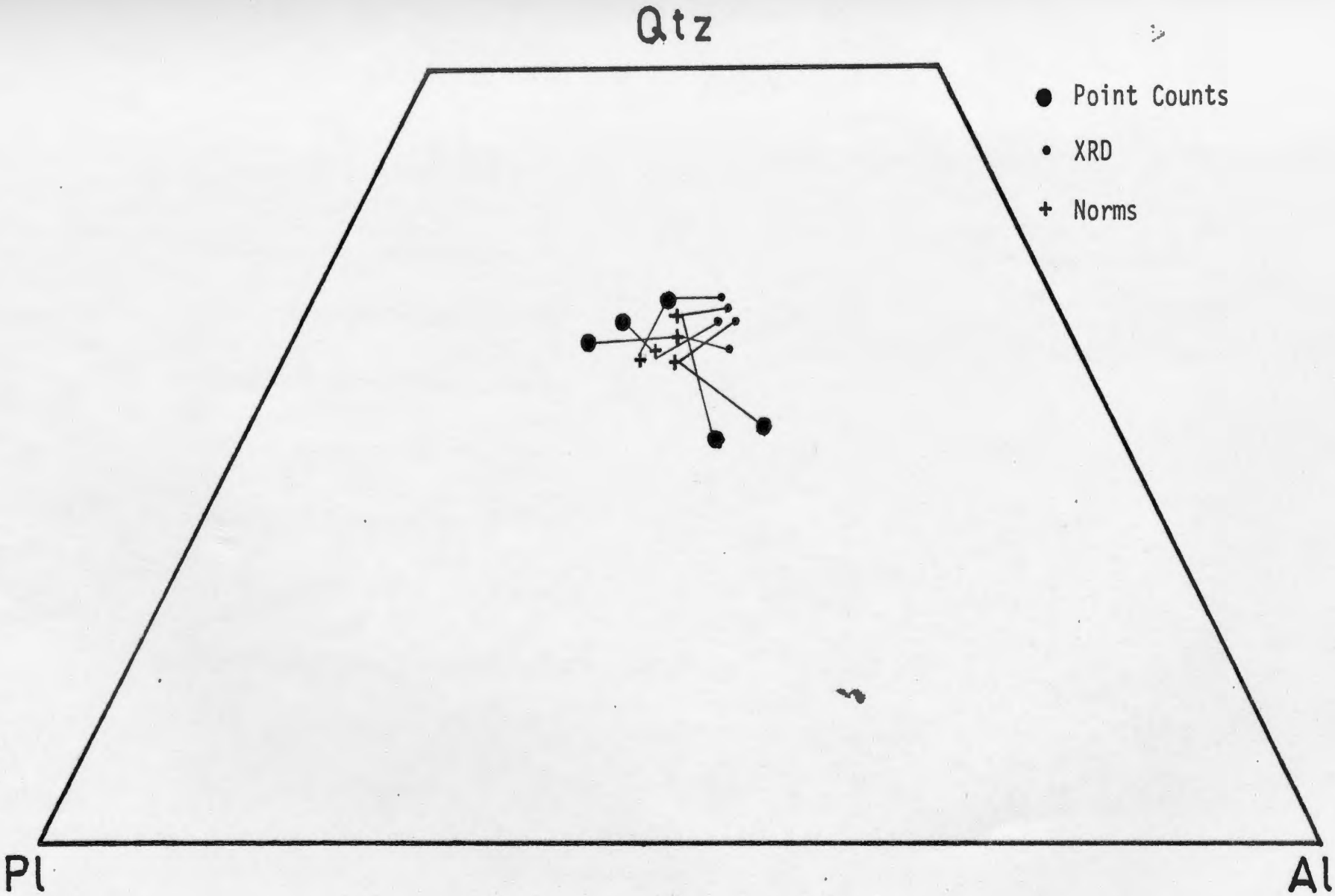

Figure 37. Comparison of modes by XRD and point counting methods and norms; results from the same sample joined by tie lines.

(a)

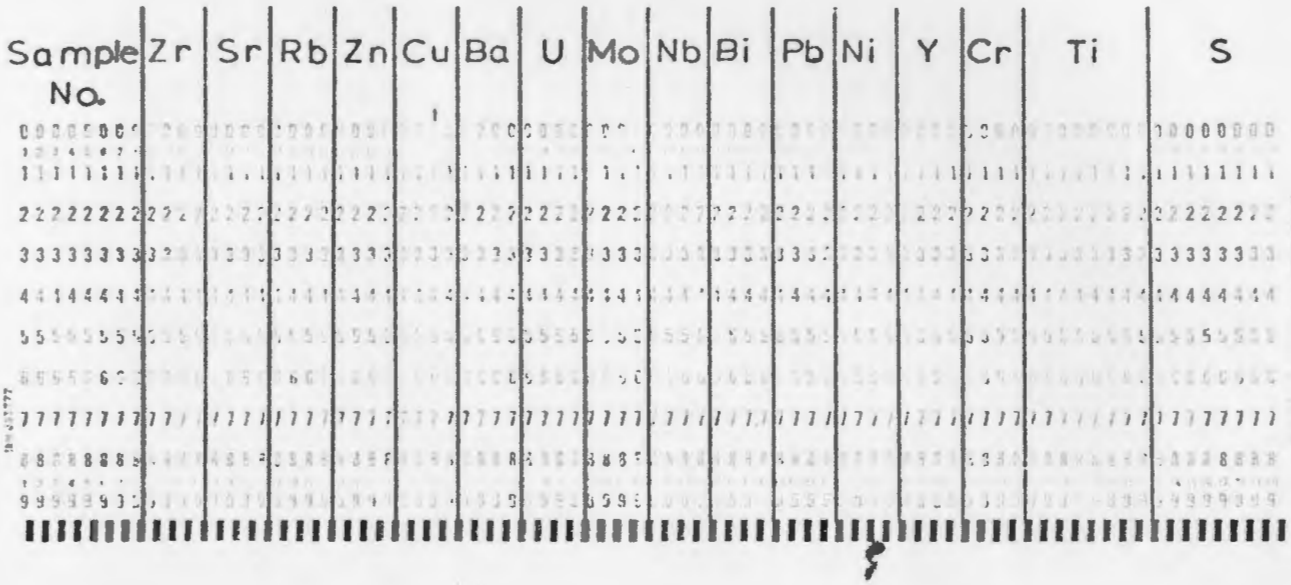

(b)

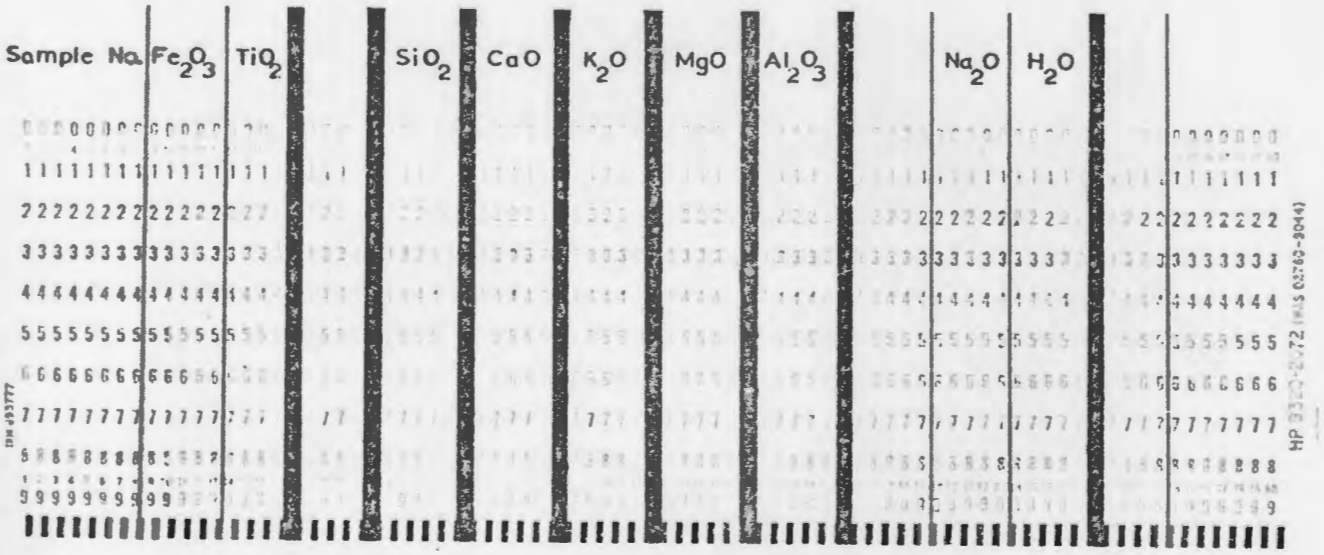

Figure 38

Format of computer cards for trace (a) and major (b) element data

APPENDIX B

MODAL ANALYSES DATA

Representative modal and corresponding normative analysis

Ackley Batholith Alaskitic Phase

Sample No. Modes (Vol. %)	CD-334	CD-335	CD-346	CD-347	CD-348	CD-349	CD-354
Qtz.	50.0	36.2	40.3	49.3	43.1	34.0	29.9
K-feld.	30.6	37.0	43.7	26.7	40.8	46.2	35.6
Plag.	17.6	25.6	14.4	17.8	13.8	17.0	31.5
Biot.	.6	1.2	1.4	5.3	1.9	1.8	3.1
Op.	.6	.2	.2	.2	.2	.6	.2
Others	.6	.2	.2	1.0	.3	.5	.1
Barth (1961) Mesonorm (Wt. %)							
Q	40.41	38.07	39.22	39.65	39.45	38.33	38.88
Or	31.30	31.88	28.27	27.80	27.47	28.88	25.96
Ab	24.95	25.06	28.33	28.18	28.31	27.88	30.97
An	—	.11	—	—	.11	.31	.67
C	1.53	2.51	1.61	1.66	2.34	1.35	.87
Mg Biot	1.78	2.26	2.62	2.69	3.12	3.02	2.52
Fe Biot	.02	.02	.02	.14	.15	.12	.10
Sp	.12	.10	.24	.22	.25	.21	.05

Motu Showing

Rock Type	Alaskite	Mg. Granite	Porphyritic Aplite		
Sample No	JW-75-94	JW-96	JW-93	JW-97	JW-98
Modes (Vol %) (Point Counts)					
Qtz.	39.5	37.4	42.0	31.0	32.0
K-feld	24.4	22.5	27.2	36.6	39.6
Plag.	33.6	36.5	29.6	31.4	27.6
Biot.	2.4	3.6	1.3	.5	.1
Op.	.1	—	—	—	—
Others	—	—	—	—	—
Mode (Vol %) (XRD)					
Qtz.	40.6	38.5	42.5	41.7	40.7
K-feld.	32.4	34.7	31.9	32.7	33.8
Plag.	27.0	26.8	25.7	25.6	25.5
Barth (1961) Mesonorm (wt. %)					
Q	37.98	39.11	37.56	40.26	37.10
Or	28.56	29.77	27.77	28.55	30.23
Ab	31.77	29.53	32.59	29.21	31.47
An	.69	.55	.81	.48	.52
C	.67	.62	.91	1.21	.33
Mg Biot	.07	.14	.07	.00	.00
Fe Biot	.05	.05	.05	.00	.10
Sp	.22	.25	.25	.30	.28

Wylie Hill Showing

Rock Type	Alaskite	Mg. Porphyritic Granite	Fg. Granite	Quartz Aplite	Porphyritic Aplite (Belle Island Showing)
Sample No.	69-9-309	69-11-506	69-7-290	JW-210	JW-7
Modes (Vol. %)					
Qtz.	39.3	41.9	35.4	57.8	31.8
K-feld	36.5	34.2	32.2	27.8	29.8
Plag.	22.9	20.5	31.9	14.1	34.0
Biot.	1.0	2.7	.5	—	2.4
Op.	1.0	.6	—	—	—
Others	.2	.1	—	—	1.7
Barth (1961) Mesonorm (wt. %)					
Q	41.11	34.84	36.76	57.83	33.20
Or	27.09	28.72	29.62	20.37	28.55
Ab	28.35	29.99	31.26	20.76	31.20
An	2.38	4.58	1.83	.36	3.11
C	.44	.00	.05	.54	1.41
Mg Biot	.49	.00	.28	.04	1.89
Fe Biot	.02	.00	.07	.00	.10
Sp	.12	.45	.12	.10	.56

Dunphey Brook - Crows Cliff Showing

Rock Type	Alaskite	Porphyritic Fg Granite		Aplite		
Sample No.	JW-109	JW-107a	JW-123	JW-115	JW-121	JW-131
Modes (Vol. %) (Point Counting)						
Qtz.	47.4	40.1	29.8	33.1	38.3	33.1
K-feld.	29.4	37.6	39.3	39.0	36.5	34.9
Plag.	22.3	21.1	26.9	26.8	23.6	30.0
Biot.	1.0	1.0	4.0	.9	.1	2.0
Op.	.1	.1	—	—	—	—
Others	—	—	.1	.1	.1	—
Mode (Vol.%) (XRD)						
Qtz.		41.8		42.1		
K-feld.		33.3		33.3		
Plag.		24.9		24.7		
Barth (1961) Mesonorms (wt. %)						
Q	40.81	37.01	38.15	35.32	36.71	38.03
Or	28.74	30.52	29.28	33.61	30.12	28.43
Ab	29.32	30.06	31.32	29.99	32.12	32.15
An	1.52	.40	.00	.74	.16	.90
C	.00	1.40	.90	.17	.50	.35
Mg Biot	.00	.21	.07	.00	.00	.03
Fe Biot	.00	.07	.10	.05	.05	.05
Sp	.10	.33	.37	.13	.35	.07
Act	.34	—	—	—	—	—

Ackley City Showing

Rock Type	Alaskite	Mg. Granite	Aplite		Mineralized Mg. Granite	
Sample No.	JW-132	ACD-19	ACD-22	JW-239	ACC-29	ACD-43
Modes (Vol. %)						
Qtz.	61.0	41.4	32.6	32.1	1.8	31.9
K-feld.	16.9	37.7	27.9	36.3	42.4	45.6
Plag.	21.4	19.3	37.8	30.8	35.8	7.2
Biot.	.7	.4	1.1	.8	1.6	1.0
Fl.	—	—	—	—	13.7	—
MoS_2	.1	—	—	—	—	11.6
Others	—	1.1	.2	—	4.7	2.7
Mode (Vol.%) (XRD)						
Qtz.		33.4	33.7	43.5		
K-feld		37.4	35.3	32.3		
Plag.		29.2	31.0	24.2		
Barth (1961) Mesonorms (wt. %)						
Q	37.65	41.23	37.85	35.88	N.A.	N.A.
Or	29.57	34.75	28.39	26.78		
Ab	31.01	21.04	31.35	35.12		
An	.64	1.69	1.33	.41		
C	.54	.51	.63	1.07		
Mg Biot	.26	.32	.07	.11		
Fe Biot	.05	.12	.05	.04		
Sp	.29	.35	.35	.60		

Wylie Hill Showing

Rock Type	Porphyritic Aplite		Granophyre	Aplite
Sample No.	69-8-171	69-2-117	69-2-139	JW-211
Modes (Vol.%)				
Qtz.	35.8	31.9	37.2	40.9
K-feld.	38.9	46.3	32.6	29.6
Plag.	24.9	20.3	29.4	29.3
Biot.	.5	.8	.8	—
Op.	—	—	—	—
Others	—	—	—	—

Modal Analysis of Samples by XRD
Alaskitic Granite (near Showings)

Sample No	JW-140	JW-143	JW-147	JW-152	JW-154	JW-220
Qtz.	35.8	40.5	38.6	42.5	44.2	42.6
Plag.	28.5	25.8	27.4	24.6	23.2	24.2
K-feld.	35.7	33.7	34.0	32.9	32.6	33.3

Sample No	JW-224	JW-225	JW-227	JW-228
Qtz.	37.5	42.5	42.00	40.5
Plag.	27.6	24.6	25.0	26.0
K-feld.	34.9	32.8	33.0	33.6

Location	Motu		Wylie Hill			
Rock Type	Mg. Granite	Mg. Granite	Aplite	Fg. Porphyritic Granite		
Sample No.	JW-99	JW-200	JW-202	JW-203	JW-204	JW-206
Qtz.	40.8	36.3	42.5	40.5	42.4	41.4
Plag.	25.4	30.0	24.7	26.0	24.4	24.6
K-feld.	33.8	33.7	32.8	33.5	33.2	33.9

Location	Dunphey Brook-Crows Cliff Showing					
Rock Type	Porphyritic Granite		Aplite			
Sample No.	JW-110	JW-112	JW-111	JW-113	JW-117	JW-122
Qtz.	42.0	42.5	41.8	31.0	42.7	41.8
Plag.	24.7	24.5	25.2	30.6	23.9	24.9
K-feld.	33.3	33.0	33.0	38.4	33.4	33.2

	Ackley City Showing-Aplite			
Sample No.	JW-238	JW-241	ACD-6a	ACD-21
Qtz.	46.0	41.9	40.0	32.6
Plag.	20.8	24.2	25.2	30.1
K-feld.	33.2	33.8	34.7	37.3

Location	Frank's Pond Showing		Belle Island Showing		
Rock Type	Mg. Granite	Porphyritic Granite	Aplite	Porphyritic Granite	
Sample No.	JW-125	JW-126	JW-8	JW-6	JW-90
Qtz.	38.6	41.2	38.5	41.8	39.2
Plag.	27.4	25.7	27.7	25.1	26.8
K-feld.	34.1	33.0	33.8	33.0	34.0

APPENDIX C

PLOTS OF ANALYSES OF DIAMOND DRILL CORE, WYLIE HILL SHOWING

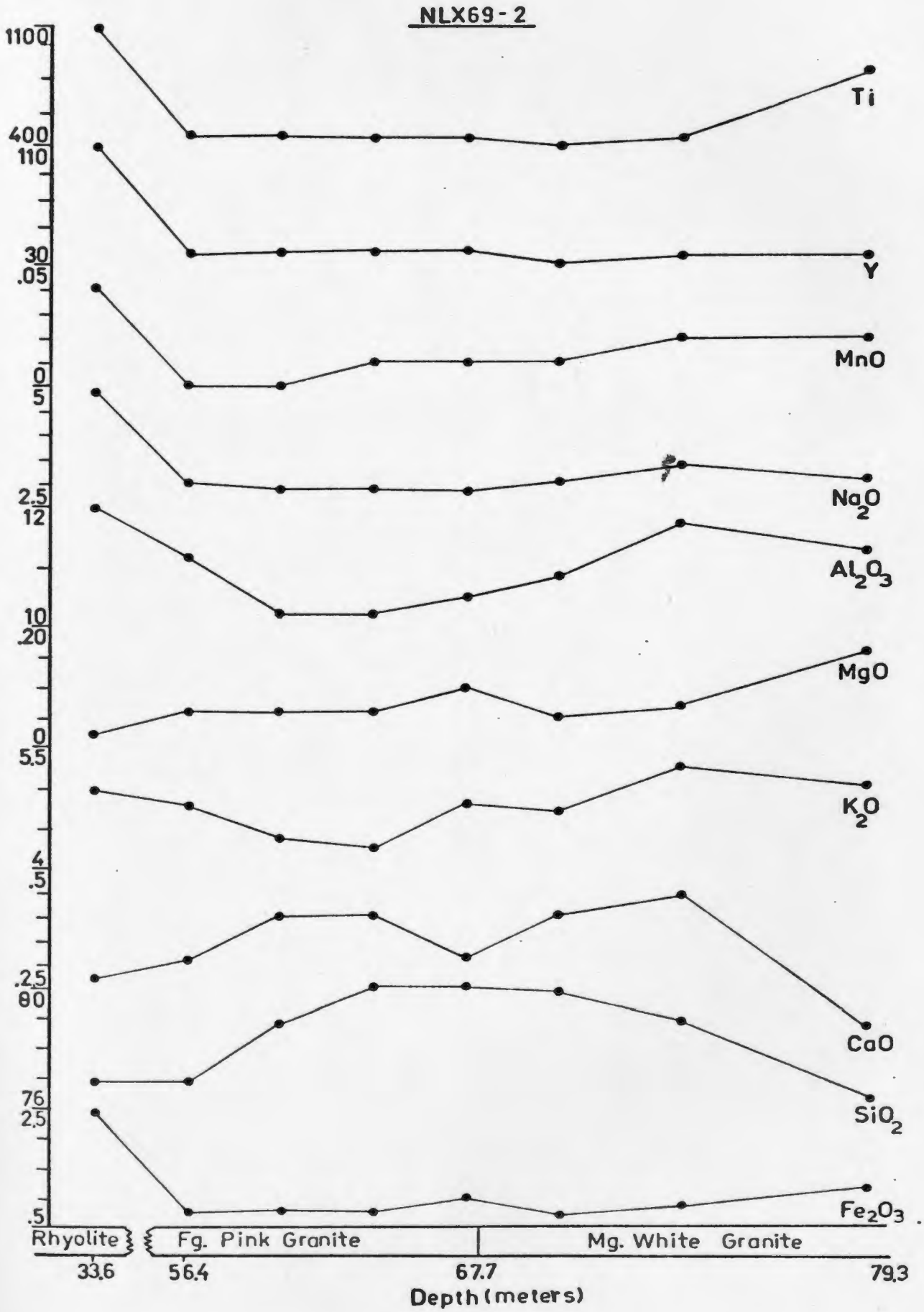
NLX69-2
1100
400
110
30
.05
0
5
2.5
12
10
.20
0
5.5
4
.5
.25
80
76
2.5
.5
Ti
Y
MnO
Na_2O
Al_2O_3
MgO
K_2O
CaO
SiO_2
Fe_2O_3
Rhyolite
Fg. Pink Granite
Mg. White Granite
33.6
56.4
67.7
79.3
Depth (meters)

NLX69-2

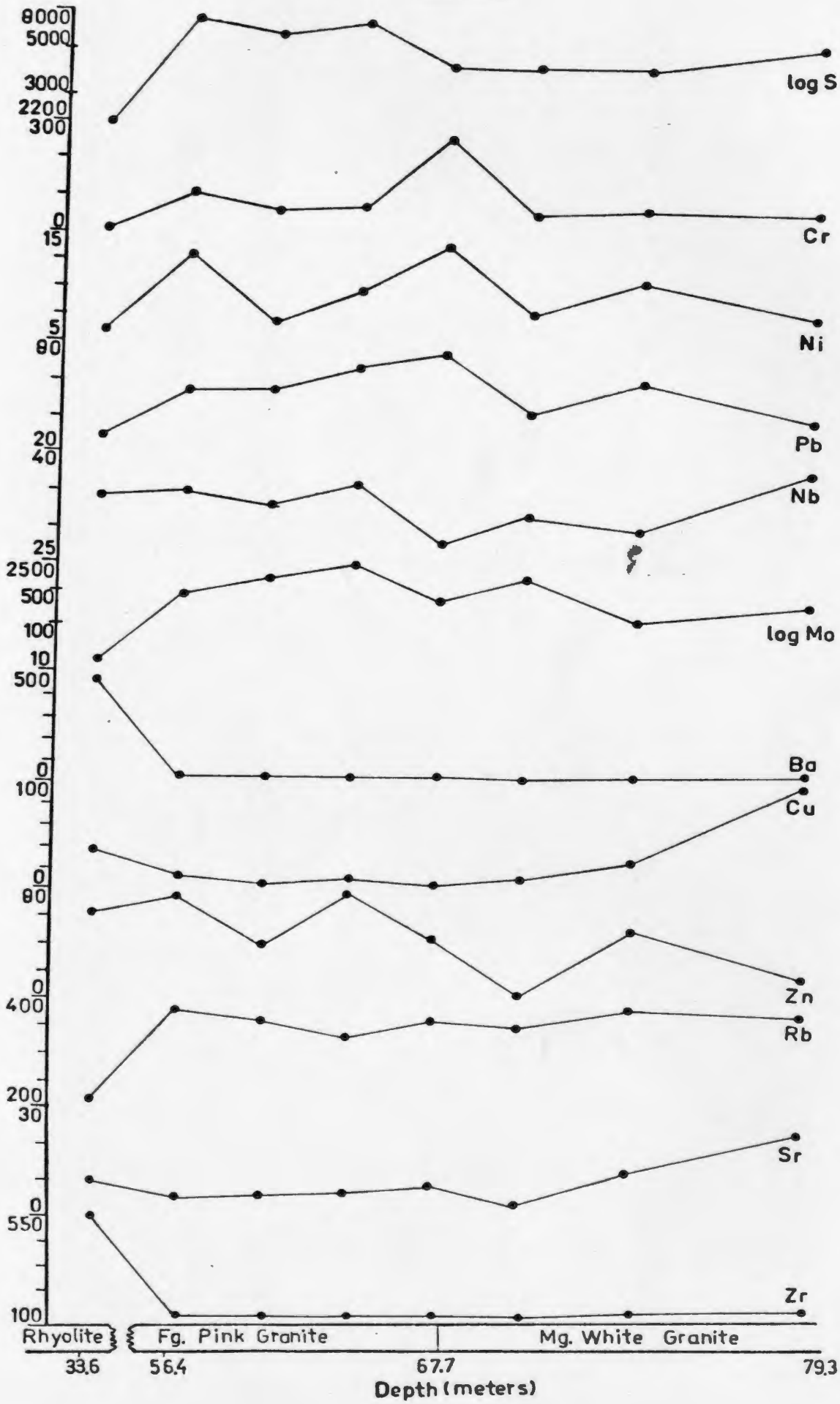
8000
5000
3000
2200
300
log S
0
15
Cr
5
80
Ni
20
40
Pb
Nb
25
2500
500
100
log Mo
10
500
Ba
0
100
Cu
0
80
0
400
Zn
Rb
200
30
Sr
0
550
Zr
100
Rhyolite
Fg. Pink Granite
Mg. White Granite
33.6
56.4
67.7
79.3
Depth (meters)

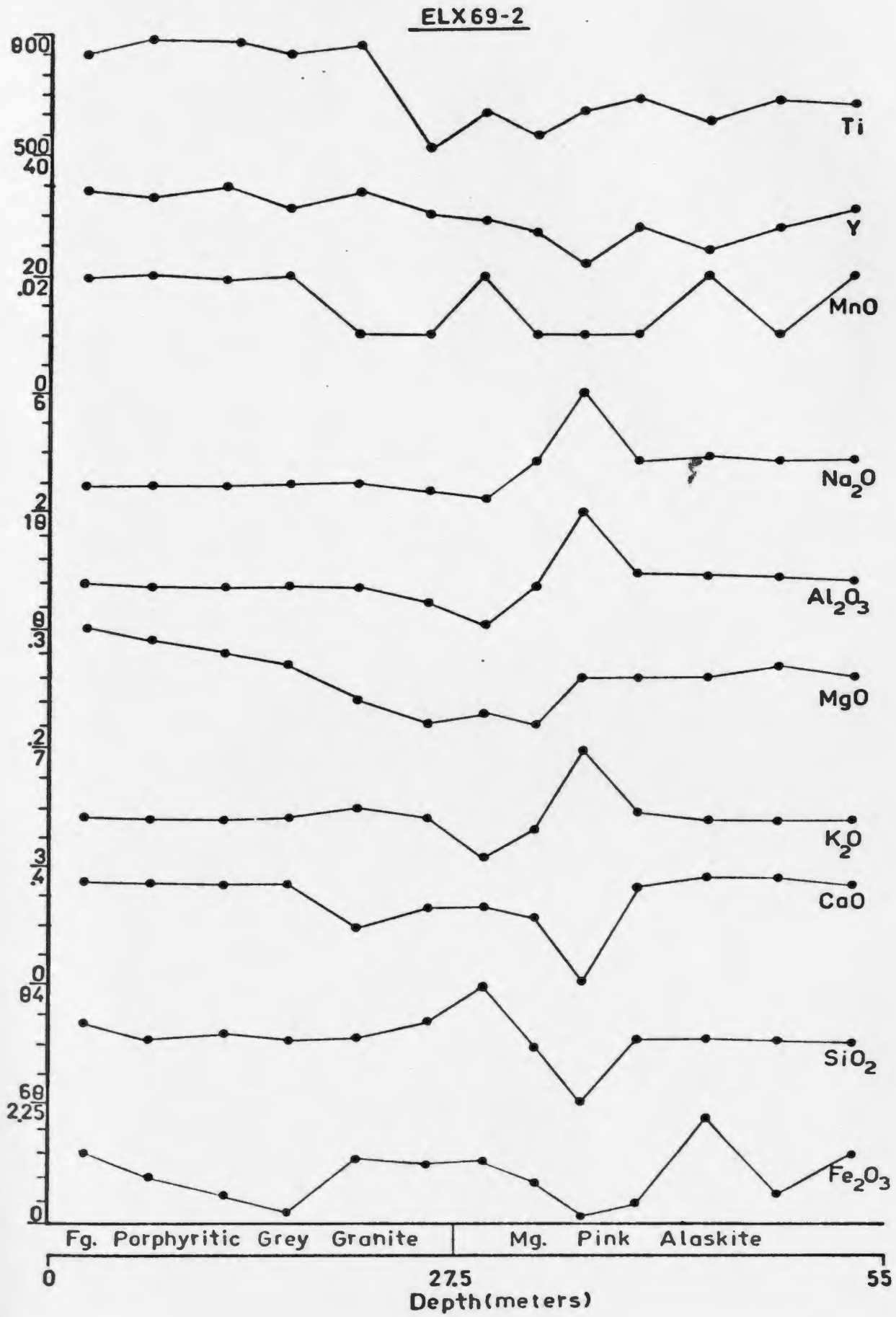
ELX69-2
800
500
40
20
.02
0
6
2
10
8
.3
.2
7
3
.4
0
84
68
2.25
0
Ti
Y
MnO
Na2O
Al2O3
MgO
K2O
CaO
SiO2
Fe2O3
Fg. Porphyritic Grey Granite
Mg. Pink Alaskite
0
27.5
55
Depth(meters)

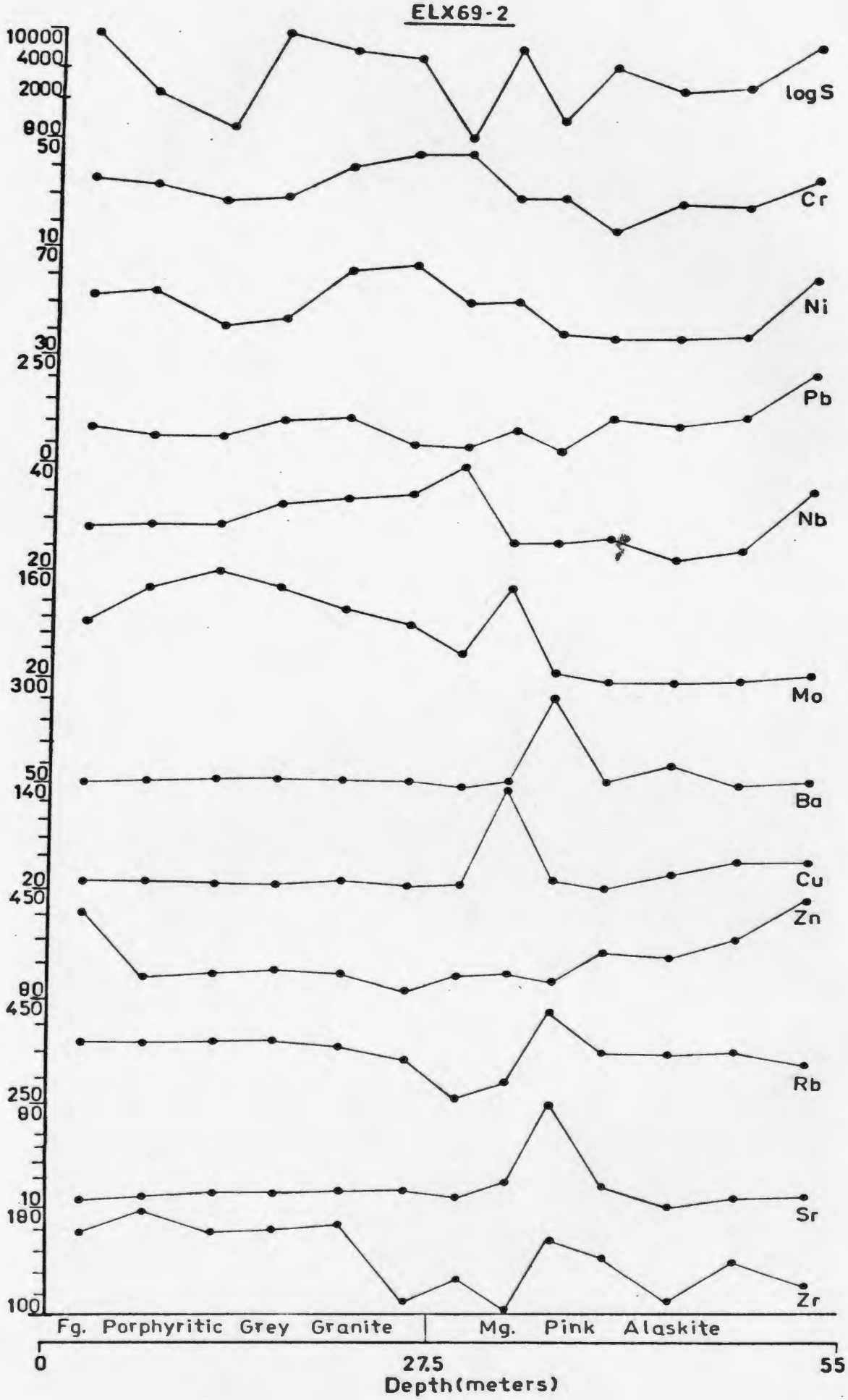
ELX69-2
10000
4000
2000
800
logS
50
Cr
10
70
Ni
30
250
Pb
0
40
Nb
20
160
20
300
Mo
50
140
Ba
20
450
Cu
Zn
80
450
Rb
250
80
10
180
Sr
100
Zr
Fg. Porphyritic Grey Granite
Mg. Pink Alaskite
0
27.5
55
Depth(meters)

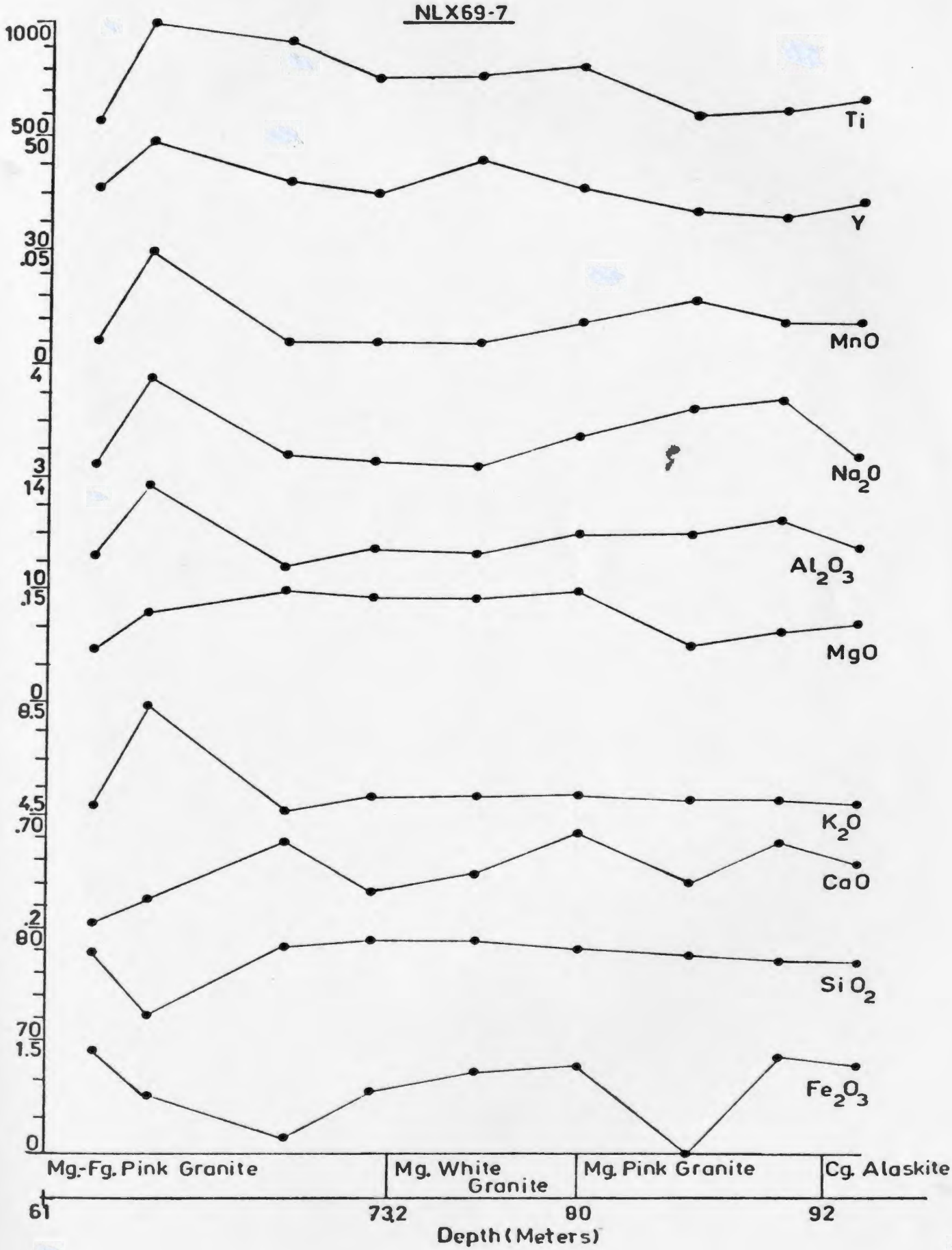
NLX69-7
1000
500
Ti
50
30
Y
.05
0
MnO
4
3
Na_2O
14
10
Al_2O_3
.15
0
MgO
8.5
4.5
.70
K_2O
CaO
.2
80
70
SiO_2
1.5
0
Fe_2O_3
Mg.-Fg. Pink Granite
Mg. White Granite
Mg. Pink Granite
Cg. Alaskite
61
73.2
80
92
Depth (Meters)

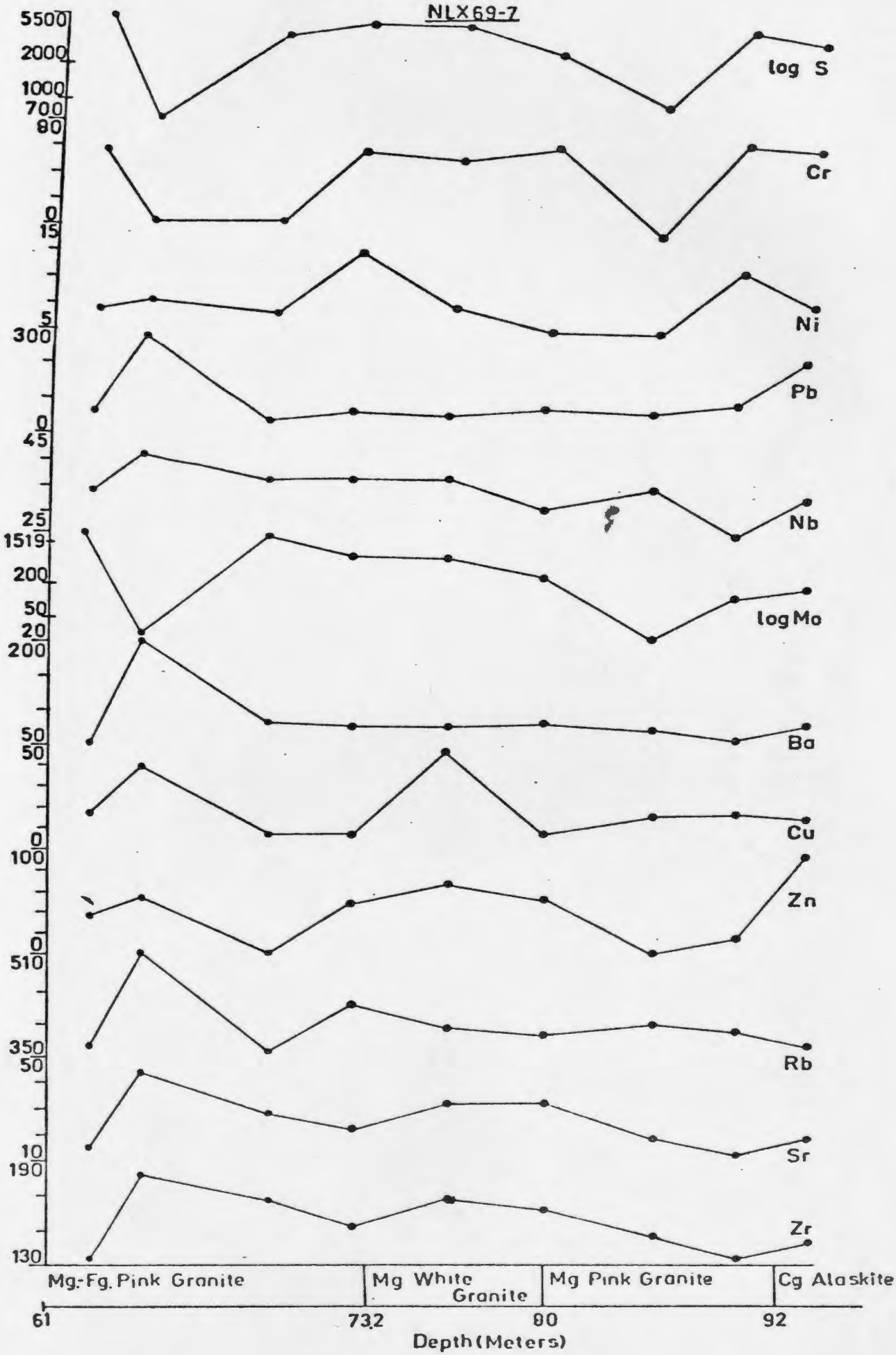
NLX69-7
5500
2000
1000
700
80
log S
0
15
Cr
5
300
Ni
0
45
Pb
25
1519
Nb
200
50
20
200
log Mo
50
50
Ba
0
100
Cu
0
510
Zn
350
50
Rb
10
190
Sr
130
Zr
Mg-Fg. Pink Granite
Mg White Granite
Mg Pink Granite
Cg Alaskite
61
73.2
80
92
Depth (Meters)

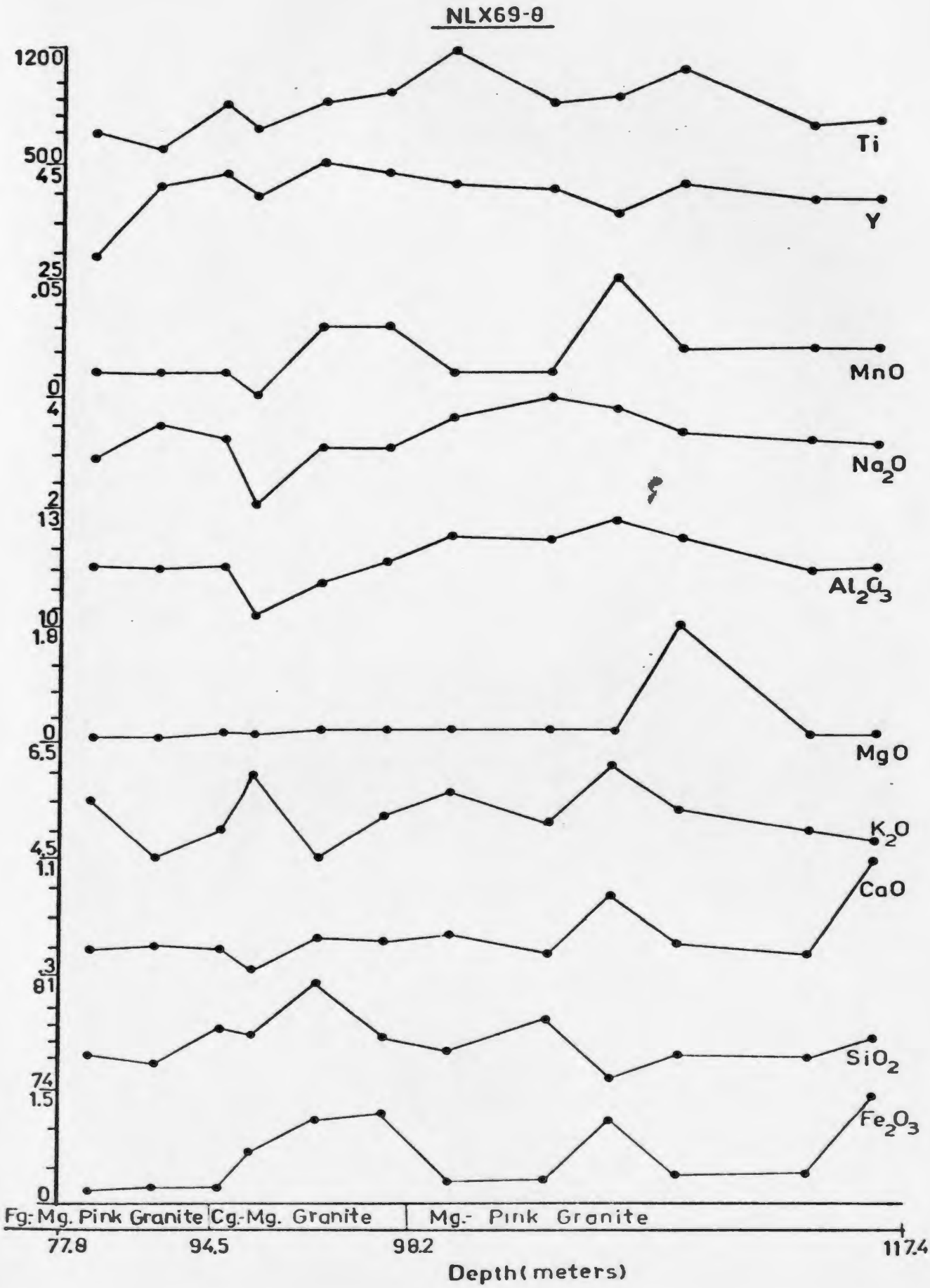
NLX69-8
1200
500
Ti
45
25
Y
.05
0
MnO
4
2
Na2O
13
10
Al2O3
1.8
0
MgO
6.5
4.5
K2O
1.1
CaO
3
81
74
SiO2
1.5
0
Fe2O3
Fg:-Mg. Pink Granite
Cg.-Mg. Granite
Mg.- Pink Granite
77.8
94.5
98.2
117.4
Depth(meters)

NLX69-8

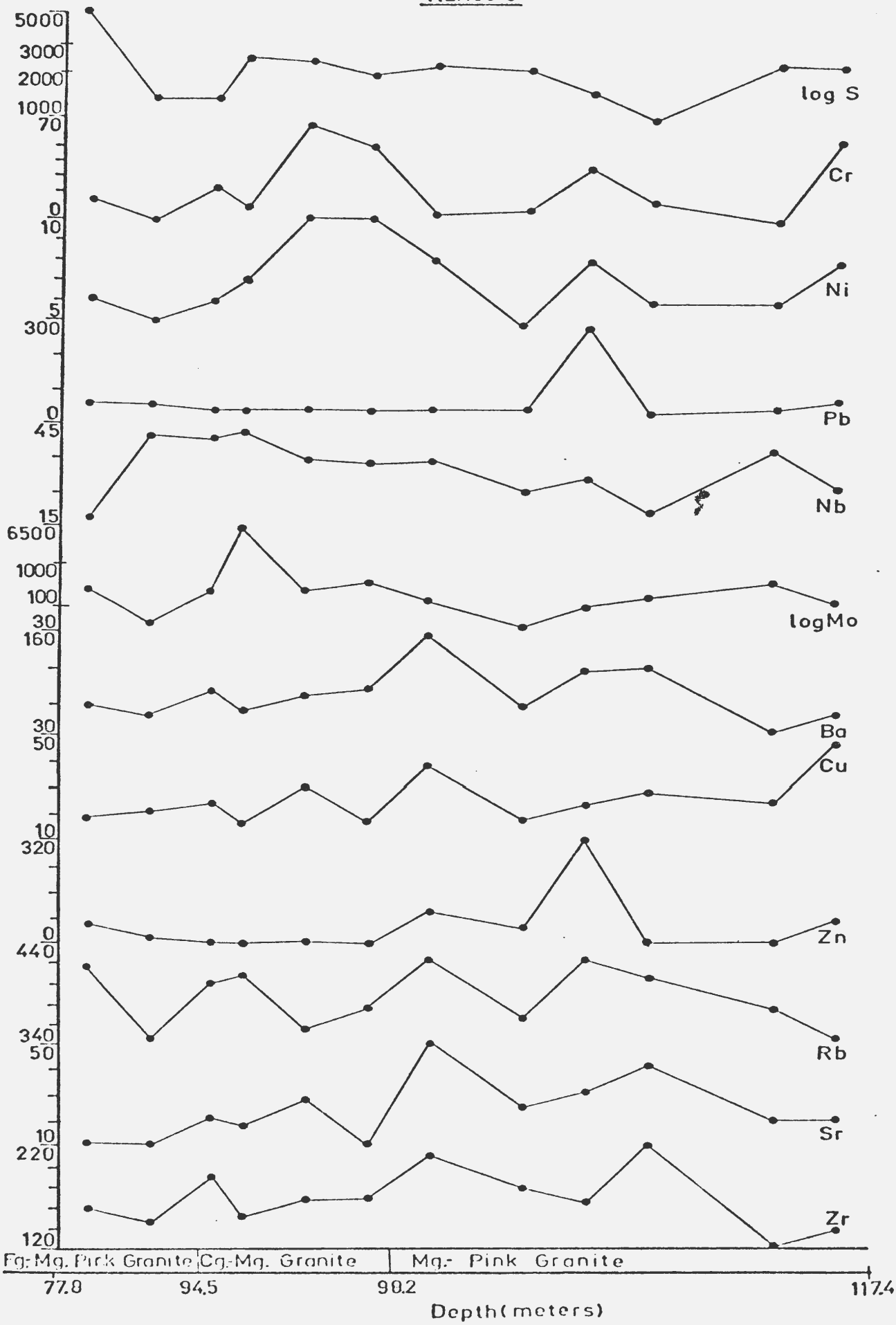
5000
3000
2000
1000
log S
70
Cr
0
10
Ni
5
300
Pb
0
45
Nb
15
6500
1000
100
logMo
30
160
Ba
30
50
Cu
10
320
Zn
0
440
Rb
340
50
Sr
10
220
Zr
120
Fg-Mg. Pink Granite
Cg-Mg. Granite
Mg- Pink Granite
77.8
94.5
98.2
117.4
Depth(meters)

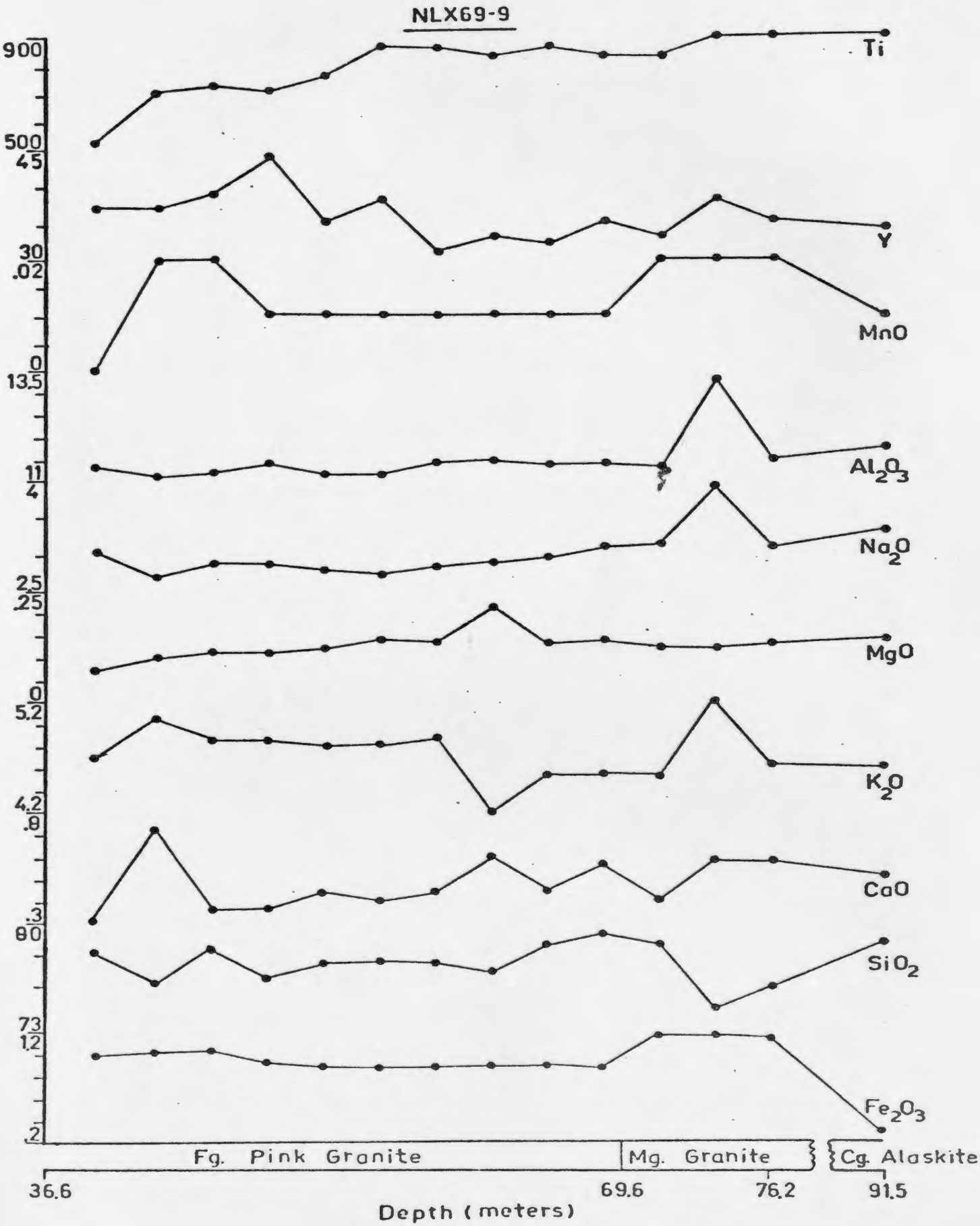
NLX69-9
900
500
45
30
.02
0
13.5
11
4
2.5
.25
0
5.2
4.2
.8
.3
80
73
1.2
.2
Ti
Y
MnO
Al_2O_3
Na_2O
MgO
K_2O
CaO
SiO_2
Fe_2O_3
Fg. Pink Granite
Mg. Granite
Cg. Alaskite
36.6
69.6
76.2
91.5
Depth (meters)

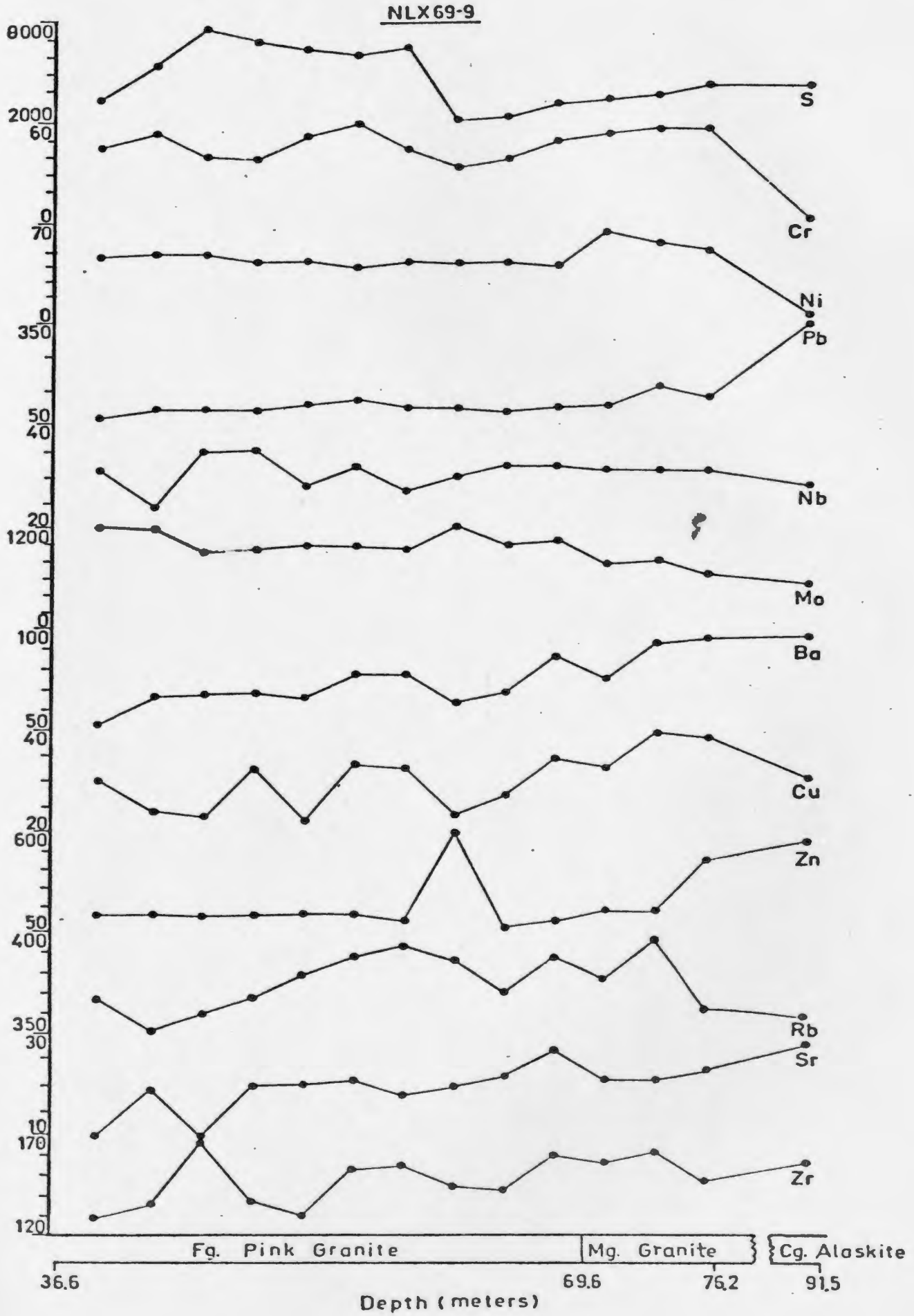
NLX69-9
8000
2000
60
0
70
0
350
50
40
20
1200
0
100
50
40
20
600
50
400
350
30
10
170
120
S
Cr
Ni
Pb
Nb
Mo
Ba
Cu
Zn
Rb
Sr
Zr
Fg. Pink Granite
Mg. Granite
Cg. Alaskite
36.6
69.6
76.2
91.5
Depth (meters)

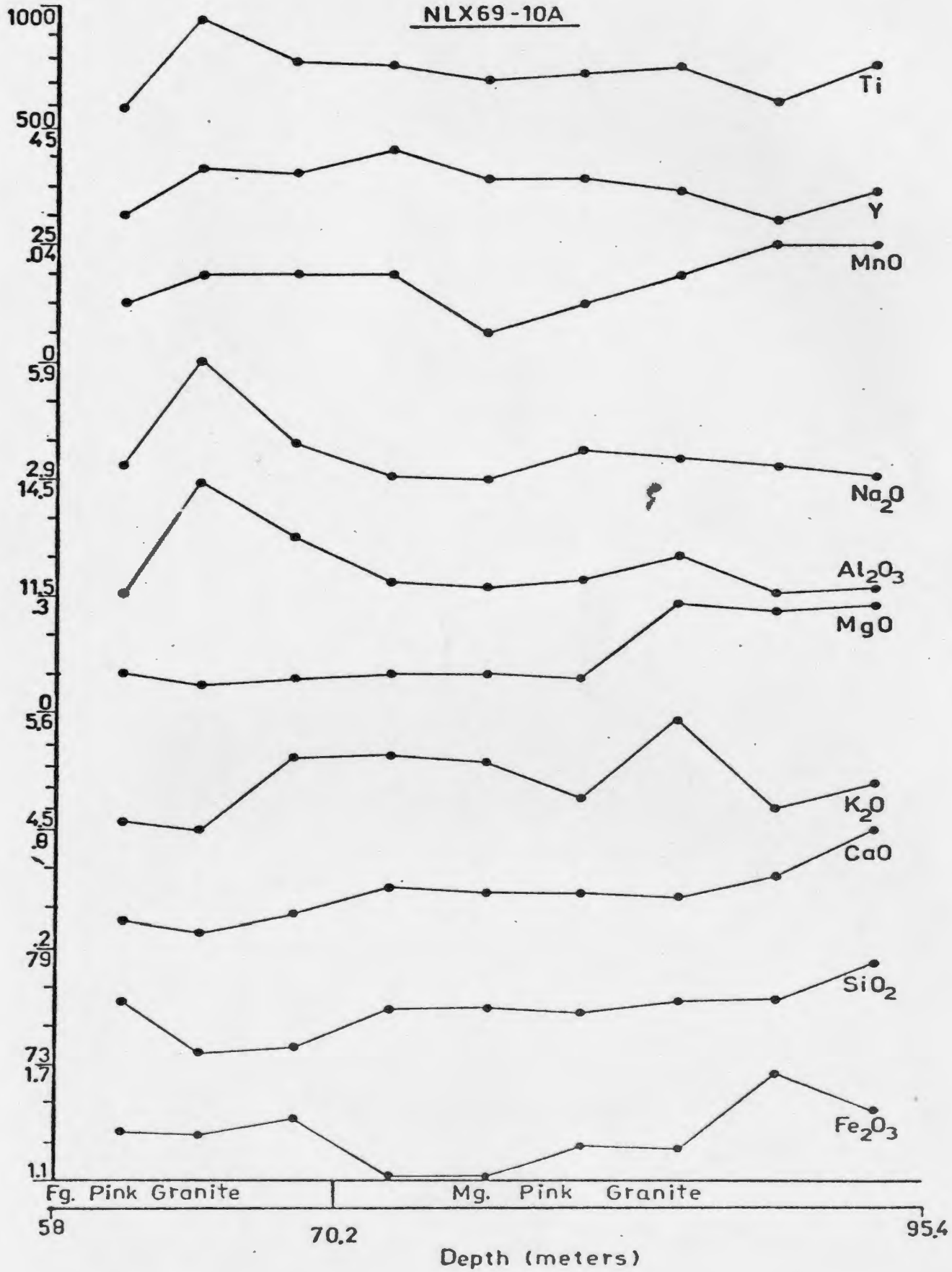
NLX69-10A
1000
500
45
25
.04
0
5.9
2.9
14.5
11.5
.3
0
5.6
4.5
.8
.2
79
73
1.7
1.1
Ti
Y
MnO
Na_2O
Al_2O_3
MgO
K_2O
CaO
SiO_2
Fe_2O_3
Fg. Pink Granite
Mg. Pink Granite
58
70.2
95.4
Depth (meters)

NLX69-10A

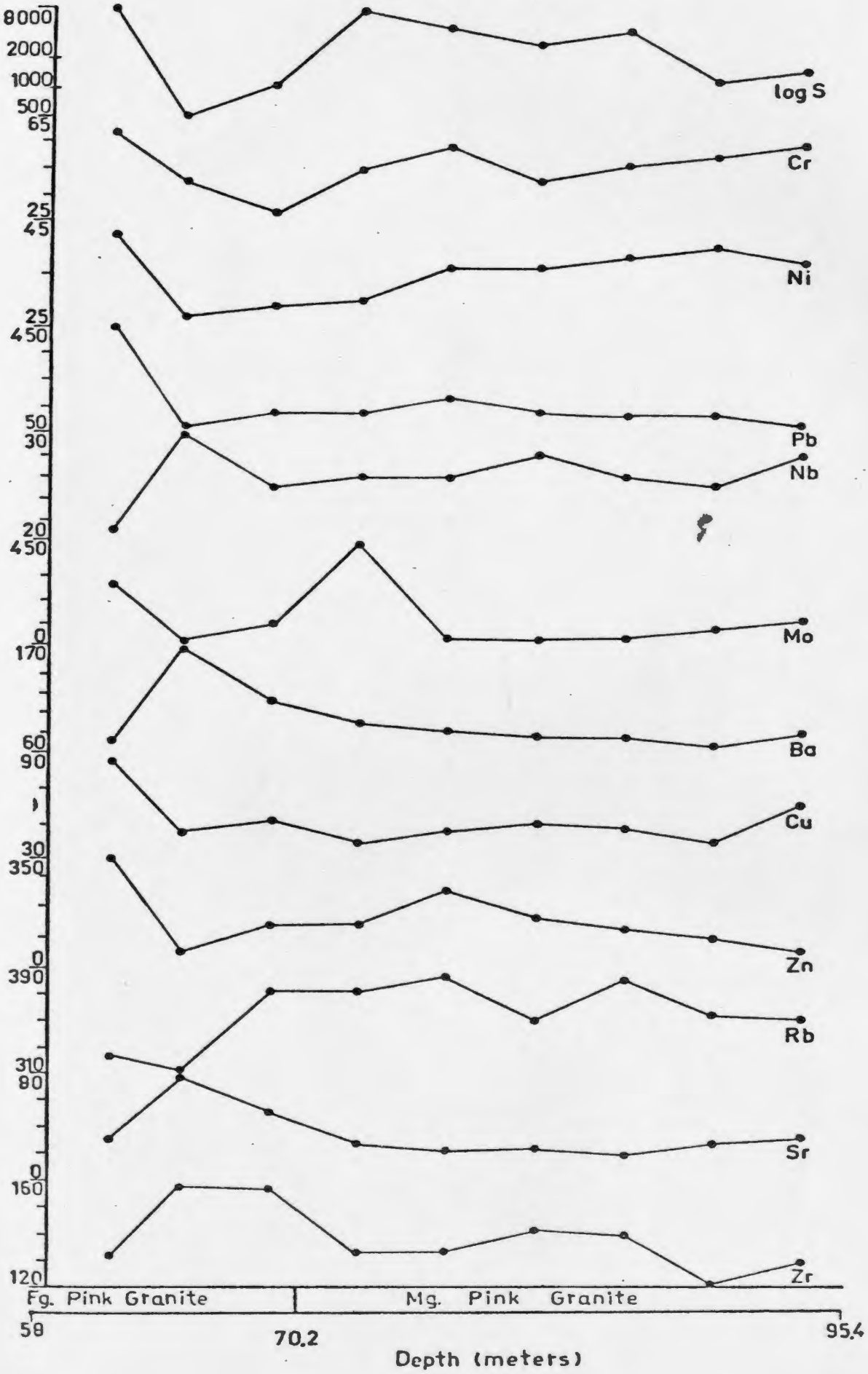
8000
2000
1000
500
log S
65
Cr
25
45
Ni
25
450
50
30
Pb
Nb
20
450
0
170
Mo
60
90
Ba
Cu
30
350
Zn
0
390
Rb
310
80
Sr
0
160
120
Zr
Fg. Pink Granite
Mg. Pink Granite
58
70.2
95.4
Depth (meters)

APPENDIX D

GEOCHEMICAL DATA

Note: Major elements in weight percent
Trace elements in ppm.
Barth (1962) molecular norms included

Abbreviations

LOI = loss on ignition
Q = quartz
AB = albite
AN = anorthite
COR = corundum
MG BI = Mg biotite
FE BI = Fe biotite
SPH = sphene
DI = diopside
WO = wollastonite
ACT = actinolite
RIEB = riebeckite

FG = fine grained
MG = medium grained
CG = coarse grained
MED = medium
DK = dark
LT = light

PK = pink
EQ = equigranular
PORP = porphyritic
MIOR = miorolitic
DISS = disseminated
SEG = segregation
PERV = pervaissive
MINER = mineralized
ALTER = alteration
ROS = rosettes
PEG = pegmatite

CHL = chlorite
MUSC = muscovite
MAG = magnetite
F = feldspar
PY = pyrite
K-F = K-feldspar

REGIONAL GRANITE

SAMPLE	JW75-135	JW75-136	JW75-137	JW75-138	JW75-139	JW75-140	JW75-141
SIO2	78.00	78.97	77.16	77.25	78.75	78.50	79.00
AL2O3	11.49	11.14	12.02	12.25	11.72	11.48	11.75
FE2O3	0.60	0.74	0.65	1.12	0.69	0.64	0.68
MGO	0.0	0.03	0.03	0.17	0.0	0.01	0.04
CAO	0.14	0.17	0.23	0.78	0.20	0.20	0.18
NA2O	3.45	3.29	3.44	3.85	3.43	3.30	3.54
K2O	4.74	4.76	5.32	4.60	5.06	4.93	4.85
TIO2	0.07	0.08	0.07	0.22	0.11	0.12	0.13
MNO	0.03	0.02	0.03	0.05	0.02	0.01	0.03
LOI	0.62	0.66	0.57	0.57	0.40	0.63	0.50
TOTAL	99.14	99.86	99.52	100.86	100.38	99.82	100.70
ZR	147	144	143	199	527	119	125
SR	1	1	8	46	233	1	16
RB	472	447	404	365	157	417	389
ZN	0	0	11	0	58	0	0
CU	0	0	27	5	13	0	3
BA	26	32	31	112	709	50	30
U	8	8	9	8	3	8	6
MO	12	14	13	13	14	11	13
NB	47	42	34	32	27	40	35
BI	11	14	13	15	20	15	10
PB	44	43	43	39	29	45	49
NI	11	16	14	16	8	8	12
Y	106	118	75	105	95	69	61
CR	0	19	8	9	11	4	0
TI	750	742	649	1104	3956	672	733
S	170	250	200	210	210	150	180
Q	40.39	41.96	36.98	35.80	39.37	40.69	39.75
OR	28.57	28.48	31.88	27.41	30.09	29.53	28.67
AB	29.82	28.28	29.61	32.85	29.23	28.34	30.10
AN	0.46	0.57	0.91	2.58	0.61	0.58	0.44
COR	0.53	0.37	0.28	0.0	0.38	0.51	0.52
MG BI	0.0	0.11	0.11	0.0	0.0	0.04	0.14
FE BI	0.07	0.05	0.07	0.0	0.05	0.02	0.07
SPH	0.18	0.20	0.17	0.54	0.27	0.30	0.32
DI	0.0	0.0	0.0	0.0	0.0	0.0	0.0
WO	0.0	0.0	0.0	0.0	0.0	0.0	0.0
ACT	0.0	0.0	0.0	0.0	0.0	0.0	0.0
RIEB	0.0	0.0	0.0	0.0	0.0	0.0	0.0

JW75 135 REGIONAL GRANITE : MG , MED PK , EQ , ALASKITE GRANITE
JW75 136 REGIONAL GRANITE : CG , MED PK , EQ , ALASKITE GRANITE
JW75 137 REGIONAL GRANITE : MG TO PATCHY CG , DK PK , GRANITE
JW75 138 REGIONAL GRANITE : MG , MED PK , EQ , ALASKITE GRANITE
JW75 139 REGIONAL GRANITE : PATCHY FG TO CG , MED RED , GRANITE
JW75 140 REGIONAL GRANITE : MG , MED PK , EQ , ALASKITE GRANITE
JW75 141 REGIONAL GRANITE : CG , MED PK , EQ , ALASKITE GRANITE

REGIONAL GRANITE

SAMPLE	JW75-142	JW75-143	JW75-144	JW75-145	JW75-146	JW75-147	JW75-149
SIO2	77.25	79.23	77.94	75.66	76.65	74.67	74.75
AL2O3	12.02	11.35	11.23	12.45	12.36	12.37	12.87
FE2O3	1.34	0.88	0.85	1.22	1.50	1.20	1.67
MGO	0.15	0.06	0.06	0.19	0.33	0.17	0.35
CAO	0.25	0.15	0.20	0.32	0.35	0.20	0.60
NA2O	3.53	3.40	3.39	3.72	3.57	3.79	3.62
K2O	4.70	4.93	4.63	4.77	4.87	4.85	5.08
TIO2	0.24	0.09	0.09	0.14	0.32	0.19	0.31
MNO	0.05	0.02	0.04	0.05	0.08	0.05	0.07
LOI	0.58	0.51	0.41	0.61	0.59	0.48	0.58
TOTAL	100.11	100.62	98.84	99.13	100.62	97.97	99.90
ZR	189	155	114	195	227	171	248
SR	57	15	14	49	84	47	130
RB	280	391	361	326	266	296	256
ZN	0	13	0	19	16	11	36
CU	3	8	0	2	2	4	5
BA	112	51	36	108	191	148	293
U	7	8	9	10	6	8	6
MO	13	9	15	17	14	19	15
NB	28	44	54	32	27	33	28
BI	0	11	15	16	18	17	17
PB	27	50	38	44	27	32	59
NI	7	12	11	10	7	8	8
Y	60	78	95	103	54	65	69
CR	6	16	3	63	6	0	13
TI	1396	983	751	1313	1761	1272	1872
S	180	130	100	130	150	110	130
Q	39.08	40.64	41.14	36.15	37.27	35.07	33.99
OR	27.87	29.20	27.85	28.45	28.33	29.29	29.82
AB	30.42	28.99	29.40	32.35	30.65	33.30	31.36
AN	0.41	0.43	0.70	1.13	0.63	0.34	1.94
COR	1.00	0.26	0.40	0.79	1.00	0.79	0.74
MG BI	0.53	0.21	0.21	0.67	1.16	0.61	1.24
FE BI	0.12	0.05	0.10	0.11	0.20	0.13	0.17
SPH	0.60	0.27	0.23	0.35	0.80	0.48	0.78
DI	0.0	0.0	0.0	0.0	0.0	0.0	0.0
WO	0.0	0.0	0.0	0.0	0.0	0.0	0.0
ACT	0.0	0.0	0.0	0.0	0.0	0.0	0.0
RIEB	0.0	0.0	0.0	0.0	0.0	0.0	0.0

JW75 142 REGIONAL GRANITE : CG , MED PK . EQ . ALASKITE GRANITE
JW75 143 REGIONAL GRANITE : CG , MED PK . EQ . ALASKITE GRANITE
JW75 144 REGIONAL GRANITE : MG , MED PK . EQ . ALASKITE GRANITE
JW75 145 REGIONAL GRANITE : PORP (Q-PK F) . MED RED . GRANITE
JW75 146 REGIONAL GRANITE : CG , MED PK . EQ . ALASKITE GRANITE
JW75 147 REGIONAL GRANITE : CG , MED PK . EQ . ALASKITE GRANITE
JW75 149 REGIONAL GRANITE : CG , MED PK . EQ . ALASKITE GRANITE

REGIONAL GRANITE

SAMPLE	JW75-150	JW75-151	JW75-152	JW75-153	JW75-154	JW75-155	JW75-156
SIO2	73.70	78.00	74.84	76.65	75.39	77.68	74.00
AL2O3	13.37	11.11	12.99	12.63	12.65	12.21	13.15
FE2O3	1.69	1.66	0.61	1.70	1.58	0.91	1.73
MGO	0.36	0.03	0.35	0.34	0.31	0.12	0.36
CAO	0.70	0.17	0.52	0.48	0.65	0.34	0.64
NA2O	3.89	3.32	3.75	3.73	3.84	3.54	3.76
K2O	5.02	4.80	4.98	4.78	4.59	5.10	4.79
TIO2	0.32	0.09	0.24	0.34	0.30	0.15	0.33
MNO	0.07	0.02	0.05	0.07	0.05	0.03	0.07
LOI	0.63	0.39	0.71	0.68	0.65	0.61	0.71
TOTAL	99.75	99.59	99.04	101.40	100.01	100.69	99.54
ZR	257	127	231	252	234	108	254
SR	139	12	85	129	107	47	101
RB	268	355	240	242	238	306	249
ZN	34	0	19	17	16	12	33
CU	6	4	1	0	6	0	6
BA	285	44	227	257	221	129	323
U	5	6	6	7	7	8	6
MO	17	11	14	15	14	18	15
NB	25	35	27	32	30	29	27
BI	0	14	17	22	21	21	18
PB	30	41	32	36	32	34	37
NI	9	9	9	7	8	9	7
Y	67	56	69	75	56	84	65
CR	3	20	5	13	11	9	7
TI	1933	624	1846	1817	1758	974	2075
S	110	180	290	250	280	170	190
Q	31.40	41.03	33.79	36.23	35.09	37.26	33.64
OR	29.50	28.99	29.22	27.64	26.94	30.07	28.20
AB	33.78	28.80	32.46	31.87	33.22	30.20	32.76
AN	2.42	0.54	1.78	1.21	2.23	1.17	2.09
COR	0.69	0.27	0.81	0.89	0.58	0.44	1.07
MG BI	1.27	0.11	1.24	1.18	1.09	0.42	1.28
FE BI	0.17	0.05	0.12	0.17	0.12	0.07	0.17
SPH	0.81	0.23	0.60	0.84	0.75	0.37	0.83
DI	0.0	0.0	0.0	0.0	0.0	0.0	0.0
WO	0.0	0.0	0.0	0.0	0.0	0.0	0.0
ACT	0.0	0.0	0.0	0.0	0.0	0.0	0.0
RIEB	0.0	0.0	0.0	0.0	0.0	0.0	0.0

JW75 150 REGIONAL GRANITE : CG , MED PK , EQ , ALASKITE GRANITE
JW75 151 REGIONAL GRANITE : MG , MED PK , EQ , ALASKITE GRANITE
JW75 152 REGIONAL GRANITE :VCG , MED PK , EQ , ALASKITE GRANITE
JW75 153 REGIONAL GRANITE : CG , MED PK , EQ , ALASKITE GRANITE
JW75 154 REGIONAL GRANITE : CG , MED PK , EQ , ALASKITE GRANITE
JW75 155 REGIONAL GRANITE : CG , MED PK , EQ , ALASKITE GRANITE
JW75 156 REGIONAL GRANITE : CG , MED PK , EQ , ALASKITE GRANITE

REGIONAL GRANITE

SAMPLE	JW75-157	JW75-216	JW75-217	JW75-218	JW75-219	JW75-220	JW75-221
SIO2	75.39	76.74	76.15	75.35	73.38	75.62	80.67
AL2O3	12.59	11.88	12.48	12.57	12.78	12.23	10.72
FE2O3	1.61	0.95	0.80	1.13	1.17	0.85	0.47
MGO	0.27	0.11	0.07	0.18	0.45	0.14	0.17
CAO	0.52	0.34	0.15	0.49	0.62	0.43	0.35
NA2O	3.61	2.99	2.97	3.51	3.57	3.21	2.77
K2O	5.08	4.71	5.85	4.71	5.03	4.80	4.39
TIO2	0.28	0.13	0.16	0.16	0.20	0.13	0.11
MNO	0.07	0.04	0.03	0.08	0.10	0.04	0.03
LOI	0.77	0.60	0.65	0.62	0.90	0.61	0.69
TOTAL	100.17	98.49	99.31	98.80	98.20	98.06	100.37
ZR	230	170	110	169	0	126	0
SR	61	17	1	57	0	47	0
RB	269	278	342	317	0	332	0
ZN	29	0	0	0	0	133	0
CU	4	0	0	1	0	0	0
BA	232	30	28	93	0	110	0
U	7	7	6	10	0	6	0
MO	14	24	13	22	0	17	0
NB	29	17	31	19	0	20	0
BI	16	16	15	13	0	12	0
PB	32	51	39	34	0	37	0
NI	7	7	7	5	0	4	0
V	75	56	57	27	0	37	0
CR	11	19	10	8	0	7	0
TI	2037	1090	905	1339	0	1112	0
S	190	370	170	270	0	50	0
Q	34.88	41.87	37.07	37.07	33.47	39.08	47.46
OR	30.03	28.40	35.12	28.15	29.70	28.98	25.71
AB	31.23	26.10	25.68	30.60	31.42	28.12	23.62
AN	1.44	1.27	0.19	1.93	2.47	1.74	1.36
COR	0.60	1.46	1.22	1.04	0.61	1.18	0.92
MG BI	0.95	0.39	0.25	0.64	1.61	0.50	0.59
FE BI	0.17	0.10	0.07	0.20	0.25	0.10	0.07
SPH	0.73	0.33	0.40	0.40	0.51	0.33	0.27
DI	0.0	0.0	0.0	0.0	0.0	0.0	0.0
WO	0.0	0.0	0.0	0.0	0.0	0.0	0.0
ACT	0.0	0.0	0.0	0.0	0.0	0.0	0.0
RIEB	0.0	0.0	0.0	0.0	0.0	0.0	0.0

JW75 157 REGIONAL GRANITE : CG , MED PK . EQ . ALASKITE GRANITE
JW75 216 REGIONAL GRANITE : CG , MED PK . EQ . ALASKITE GRANITE
JW75 217 REGIONAL GRANITE : FG TO PATCHY MG , MED RED . MIOR . APLITE GRANITE
JW75 218 REGIONAL GRANITE : MG PORP(Q) , MED PK , GRANITE
JW75 219 REGIONAL GRANITE : CG , MED PK . EQ . ALASKITE GRANITE
JW75 220 REGIONAL GRANITE : CG , MED PK . EQ . ALASKITE GRANITE
JW75 221 REGIONAL GRANITE : CG , MED PK . EQ . ALASKITE GRANITE

REGIONAL GRANITE

SAMPLE	JW75-223	JW75-224	JW75-225	JW75-226	JW75-227	JW75-228	JW75-229
SIO2	76.00	77.12	77.94	77.79	74.55	74.67	76.97
AL2O3	12.78	11.76	13.13	12.36	12.76	12.60	12.69
FE2O3	1.09	0.98	1.59	1.04	1.10	1.14	0.80
MGO	0.23	0.10	0.28	0.18	0.24	0.22	0.13
CAO	0.48	0.43	0.79	0.45	0.56	0.43	0.37
NA2O	3.46	3.23	1.37	3.33	3.63	3.67	3.56
K2O	4.85	4.66	4.74	4.72	4.69	4.71	4.79
TIO2	0.37	0.14	0.30	0.11	0.37	0.34	0.17
MNO	0.09	0.05	0.05	0.06	0.08	0.06	0.06
LOI	0.79	0.65	0.64	0.66	0.73	0.76	0.68
TOTAL	100.24	99.12	100.83	100.70	98.71	98.60	100.22
SR	175	145	217	130	162	156	111
RB	85	32	84	71	98	93	85
BA	301	320	231	290	303	309	336
ZN	9	2	11	23	22	0	43
CU	7	1	3	1	0	65	0
BA	186	76	224	130	142	159	158
U	5	16	8	6	6	7	8
NO	21	8	12	12	19	47	21
NB	24	35	31	21	26	29	25
SN	16	8	18	12	21	16	16
PB	51	36	33	47	39	41	57
MO	4	3	7	3	4	8	5
W	45	39	63	37	43	44	28
CR	27	11	13	19	28	14	30
TI	1278	1009	1675	1179	1248	1230	785
B	60	140	200	500	2010	180	0
Q	36.78	40.70	31.06	39.87	35.67	35.81	37.74
OR	29.06	27.95	27.68	27.48	27.93	28.18	28.29
AB	29.78	28.04	11.75	28.46	31.70	32.11	30.51
AN	1.14	1.69	2.91	1.87	1.54	0.98	1.26
COR	1.35	0.82	4.76	1.11	1.20	1.15	1.21
MG SI	0.81	0.35	0.98	0.63	0.85	0.78	0.45
FE SI	0.22	0.12	0.12	0.14	0.19	0.15	0.14
SPH	0.92	0.35	0.75	0.27	0.94	0.86	0.42
DI	0.0	0.0	0.0	0.0	0.0	0.0	0.0
NO	0.0	0.0	0.0	0.0	0.0	0.0	0.0
ACT	0.0	0.0	0.0	0.0	0.0	0.0	0.0
RIEB	0.0	0.0	0.0	0.0	0.0	0.0	0.0

JW75 223	REGIONAL GRANITE	CG	MED PK	EQ	ALASKITE GRANITE
JW75 224	REGIONAL GRANITE	CG	MED PK	EQ	ALASKITE GRANITE
JW75 225	REGIONAL GRANITE	VCG	MED PK	EQ	ALASKITE GRANITE
JW75 226	REGIONAL GRANITE	CG	MED PK	EQ	ALASKITE GRANITE
JW75 227	REGIONAL GRANITE	CG	MED PK	EQ	ALASKITE GRANITE
JW75 228	REGIONAL GRANITE	CG	MED PK	EQ	ALASKITE GRANITE
JW75 229	REGIONAL GRANITE	CG	MED PK	EQ	ALASKITE GRANITE

REGIONAL GRANITE

SAMPLE	JW75-230	JW75-231
SIO2	75.13	72.26
AL2O3	12.84	13.00
FE2O3	0.82	2.23
MGO	0.05	0.41
CAO	0.22	0.76
NA2O	3.67	3.56
K2O	5.02	4.70
TIO2	0.17	0.60
MNO	0.04	0.08
LOI	0.46	0.75
TOTAL	98.42	98.35
ZR	127	299
SR	10	93
RB	257	245
ZN	32	26
CU	4	3
BA	16	213
U	7	5
MO	26	20
NB	16	31
BI	8	21
PB	52	29
NI	5	8
Y	43	82
CR	10	10
TI	738	2708
S	240	410
Q	35.23	33.95
OR	30.37	28.02
AB	31.97	31.58
AN	0.51	1.76
COR	1.22	1.51
MG BI	0.18	1.48
FE BI	0.10	0.20
SPH	0.43	1.54
DI	0.0	0.0
WO	0.0	0.0
ACT	0.0	0.0
RIEB	0.0	0.0

JW75 230 REGIONAL GRANITE : FG TO PATCHY MG , MED PK , MIOR , GRANITE
JW75 231 REGIONAL GRANITE :VCG , MED PK , EQ , ALASKITE GRANITE

MOTU SHOWING

SAMPLE	JW75- 93	JW75- 94	JW75- 96	JW75- 97	JW75- 98	JW75- 99	JW75-101
SIO2	76.57	78.00	78.18	78.62	77.20	76.21	78.00
AL2O3	12.34	12.23	11.90	12.21	11.96	12.18	12.90
FE2O3	0.70	0.69	0.52	0.32	0.31	0.50	0.68
MGO	0.02	0.02	0.04	0.0	0.0	0.05	0.04
CAO	0.23	0.20	0.18	0.18	0.18	0.23	0.29
NA2O	3.76	3.72	3.45	3.43	3.65	3.25	3.80
K2O	4.60	4.80	5.00	4.80	5.03	5.51	4.69
TIO2	0.10	0.09	0.10	0.12	0.11	0.03	0.11
MNO	0.02	0.02	0.02	0.0	0.04	0.03	0.03
LOI	0.77	0.54	0.60	0.65	0.48	2.38	0.49
TOTAL	99.11	100.31	99.99	100.33	98.96	100.37	101.03
ZR	227	137	98	142	138	119	110
SR	212	1	5	1	10	9	1
RB	274	462	436	454	460	481	425
[illegible]	0	0	7	0	48	104	11
CU	11	12	10	5	19	11	3
BA	608	20	32	9	30	32	25
U	4	9	6	8	9	9	10
MO	39	12	13	11	14	17	6
NB	22	51	33	47	40	37	44
BI	22	16	30	10	15	13	13
PB	22	47	65	49	120	85	54
NI	13	10	9	8	12	11	13
Y	45	95	36	57	102	54	83
CR	22	7	9	6	6	7	13
TI	1783	705	724	632	818	806	646
S	341	150	150	290	520	270	150
Q	37.56	37.98	39.11	40.26	37.10	36.67	37.46
OR	27.77	28.56	29.77	28.55	30.23	33.24	27.63
AB	32.59	31.77	29.53	29.21	31.47	28.21	32.20
AN	0.81	0.69	0.55	0.48	0.52	1.06	1.06
COR	0.91	0.67	0.62	1.21	0.33	0.50	1.19
MG BI	0.07	0.07	0.14	0.0	0.0	0.18	0.14
FE BI	0.05	0.05	0.05	0.0	0.10	0.07	0.07
SPH	0.25	0.22	0.25	0.30	0.28	0.08	0.27
DI	0.0	0.0	0.0	0.0	0.0	0.0	0.0
WO	0.0	0.0	0.0	0.0	0.0	0.0	0.0
ACT	0.0	0.0	0.0	0.0	0.0	0.0	0.0
RIEB	0.0	0.0	0.0	0.0	0.0	0.0	0.0

JW75 93 MOTU SHOWING :FG.MED PK.PORP(Q-F).APLITE
JW75 94 MOTU SHOWING :MG.EQ.MED PK.ALASKITE GRANITE
JW75 96 MOTU SHOWING :MG.EQ.LT PK.GRANITE
JW75 97 MOTU SHOWING:LT PK.FG.PORP(Q+F).MIOR.APLITE
JW75 98 MOTU SHOWING :FG.LT PK.PORP(Q).MIOR.APLITE;DISS MOS2
JW75 99 MOTU SHOWING :MG.MED PK.GRANITE ; CHL ALTER OF BIOT
JW75 101 MOTU SHOWING :MG.MED PK.GRANITE ; 4 CM FROM RHYOLITE CONTACT

MOTU SHOWING

SAMPLE	JW75-102	JW75-103	JW75-104	JW75-105	JW75-107
SIO2	84.75	82.84	82.89	80.52	81.89
AL2O3	7.46	8.58	9.80	9.81	6.69
FE2O3	0.56	0.32	0.35	0.75	0.27
MGO	0.0	0.05	0.04	0.0	0.04
CAO	0.0	0.31	0.37	0.13	0.28
NA2O	1.42	2.31	2.77	2.68	1.90
K2O	3.60	3.57	3.51	3.86	1.79
TIO2	0.09	0.13	0.02	0.09	0.07
MNO	0.02	0.03	0.02	0.03	0.01
LOI	0.96	1.31	0.62	1.36	5.13
TOTAL	98.86	99.45	100.39	99.23	98.07
ZR	113	97	120	106	65
SR	1	1	2	8	3
RB	376	349	344	400	194
ZN	31	10	11	40	116
CU	23	1	6	19	9
BA	11	10	13	19	1
U	8	9	7	7	8
MO	3734	6053	2548	1208	2807
NB	31	53	41	64	95
BI	7	14	13	67	24
PB	40	40	48	37	28
NI	7	9	7	4	3
Y	31	66	25	46	17
CR	2	23	21	19	27
TI	698	646	744	840	633
S	2780	6010	2520	2560	43310
Q	64.50	56.40	52.87	51.43	68.45
OR	21.83	21.41	20.75	23.45	11.30
AB	12.35	10.98	23.58	23.35	17.35
AN	0.0	1.11	1.78	0.34	1.24
COR	1.38	0.53	0.80	1.13	1.30
MG BI	0.0	0.18	0.14	0.0	0.15
FE BI	0.05	0.07	0.05	0.07	0.02
SPH	0.23	0.33	0.05	0.23	0.19
DI	0.0	0.0	0.0	0.0	0.0
WO	0.0	0.0	0.0	0.0	0.0
ACT	0.0	0.0	0.0	0.0	0.0
RIEB	0.0	0.0	0.0	0.0	0.0

JW75 102 MOTU SHOWING:MG.MED PK.Q FLOODED.GRANITE:MOS2 ROS.Q SEG.MUSC ALTER
JW75 103 MOTU SHOWING :MG.LT PK.Q FLOODED.GRANITE:MOS2 ROS
JW75 104 MOTU SHOWING :FG.LT PK.Q FLOODED.PORP(Q).APLITE:CG MOS2 ROS
JW75 105 MOTU SHOWING :MG.LT PK.Q FLOODED.PORP(Q).GRANITE:MOS2 ROS.MUSC ALTER
JW75 107 MOTU SHOWING :FG.LT PK.Q FLOODED.PORP(Q).APLITE:CG MOS2 ROS

ACKLEY CITY SHOWING

SAMPLE	JW75-132	JW75-236	JW75-237	JW75-238	JW75-239	JW75-240	JW75-241
SIO2	74.44	68.17	76.27	73.30	76.65	76.39	80.00
AL2O3	11.61	13.88	11.95	11.39	12.78	12.31	10.09
FE2O3	0.77	6.14	0.69	0.67	0.60	0.76	0.64
MGO	0.07	0.10	0.10	0.02	0.03	0.05	0.04
CAO	0.20	0.04	0.25	0.18	0.25	0.36	0.11
NA2O	3.47	0.48	3.40	3.27	4.09	3.69	1.99
K2O	4.77	11.08	4.73	4.30	4.48	4.94	4.96
TIO2	0.11	0.15	0.13	0.04	0.24	0.16	0.15
MNO	0.02	0.08	0.02	0.02	0.02	0.04	0.02
LOI	0.56	0.67	0.57	0.67	0.52	0.57	0.60
TOTAL	96.02	100.79	98.11	93.86	99.66	99.27	98.60
ZR	133	106	108	96	100	122	131
SR	22	56	16	1	1	4	12
RB	384	670	431	368	476	458	434
ZN	0	16	0	0	15	0	0
CU	7	2	2	7	5	0	10
BA	51	129	46	25	13	28	34
U	5	5	5	6	11	9	7
MO	13	33	19	18	22	17	67
NB	28	21	30	43	44	32	34
BI	20	27	22	17	13	19	25
PB	44	57	47	48	83	39	86
NI	7	9	5	5	9	9	11
Y	46	44	53	37	53	89	68
CR	16	5	25	13	65	11	18
TI	973	727	907	425	504	672	916
S	230	750	430	150	180	240	700
Q	37.65	24.47	39.18	40.49	35.88	36.11	50.65
OR	29.57	69.33	28.60	27.39	26.78	29.64	29.99
AB	31.01	4.39	29.70	29.91	35.12	31.88	17.30
AN	0.64	0.0	0.81	0.81	0.41	1.25	0.02
COR	0.54	1.29	0.98	1.17	1.07	0.45	1.48
MG BI	0.26	0.37	0.36	0.07	0.11	0.18	0.14
FE BI	0.05	0.20	0.05	0.05	0.04	0.10	0.05
SPH	0.29	0.39	0.33	0.11	0.60	0.40	0.38
DI	0.0	0.0	0.0	0.0	0.0	0.0	0.0
WO	0.0	0.0	0.0	0.0	0.0	0.0	0.0
ACT	0.0	0.0	0.0	0.0	0.0	0.0	0.0
RIEB	0.0	0.0	0.0	0.0	0.0	0.0	0.0

JW75 132 ACKLEY SHOWING,CG,MED RED,ALASKITE GRANITE
JW75 236 ACKLEY SHOWING,CG,ALASKITE GRANITE,DK GREY PERV SER&CHL&FE2O3 ALTER
JW75 237 ACKLEY SHOWING,MG,MED PK,ALASKITE GRANITE,CHL ALTER OF BIOT
JW75 238 ACKLEY SHOWING,FG,DK PK,APLITE
JW75 239 ACKLEY SHOWING,FG,MED PK,MIOR,APLITE(MG PATCHES)
JW75 240 ACKLEY SHOWING,MG,MED PK,ALASKITE GRANITE,CHL ALTER MAFICS
JW75 241 ACKLEY SHOWING;FG TO MG,LT PK,APLITE GRANITE;CHL ALTER

ACKLEY CITY SHOWING

SAMPLE	JWM5-242	JW75-243	JW75-AD1	JW75AD3A	JW75AD3B	JW75AD6A	JW75AD6B
SIO2	88.00	79.36	51.00	78.00	78.22	76.60	66.90
AL2O3	4.58	4.99	26.90	10.60	10.43	12.07	17.28
FE2O3	1.20	11.90	4.93	4.30	0.89	0.82	0.44
MGO	0.17	0.05	0.84	0.09	0.06	0.04	0.06
CAO	0.73	0.15	0.36	0.04	0.28	0.32	0.20
NA2O	1.38	0.23	1.50	0.49	1.96	3.04	3.63
K2O	0.70	2.08	8.84	3.48	5.33	5.58	10.42
TIO2	0.04	0.08	0.38	0.15	0.05	0.02	0.14
MNO	0.14	0.06	0.27	0.19	0.04	0.04	0.02
LOI	1.07	1.99	5.11	2.66	0.85	1.54	1.68
TOTAL	98.01	100.89	100.13	100.00	98.11	100.07	100.77
ZR	99	118	89	73	73	81	89
SR	32	1	1	1	8	1	8
RB	45	251	1304	547	471	567	600
ZN	174	2	175	176	224	222	10
CU	195	244	77	46	53	64	35
BA	34	25	77	46	45	44	55
U	5	0	13	7	12	6	6
MO	24	53	114	33	36	37	23
NB	18	8	52	25	32	27	14
BI	131	6275	21	34	17	15	23
PB	2603	197	37	54	51	58	66
NI	0	0	18	6	8	6	10
Y	26	2	34	22	29	29	27
CR	44	567	38	13	14	11	1
TI	934	818	1724	673	586	701	259
S	1160	1040	270	700	540	580	170
Q	79.14	80.15	8.83	66.52	47.58	37.76	6.08
OR	3.73	13.95	55.43	21.63	32.49	33.60	62.62
AB	12.20	2.23	14.08	4.46	17.21	26.33	31.24
AN	3.64	0.53	0.51	0.0	1.26	1.55	0.08
COR	0.29	2.51	16.30	6.61	1.03	0.48	0.0
MG BI	0.61	0.20	3.22	0.33	0.21	0.14	0.0
FE BI	0.35	0.06	0.72	0.49	0.10	0.10	0.0
SPH	0.10	0.23	1.03	0.40	0.13	0.05	0.35
DI	0.0	0.0	0.0	0.0	0.0	0.0	0.0
WO	0.0	0.0	0.0	0.0	0.0	0.0	0.0
ACT	0.0	0.0	0.0	0.0	0.0	0.0	0.0
RIEB	0.0	0.0	0.0	0.0	0.0	0.0	0.0

JW75 242 ACKLEY SHOWING,Q&SER&PY&MAG&K-F VEIN IN MG GRANITE ALASKITE AT 050/80S
JW75 243 ACKLEY SHOWING,Q&MAG&SER VEIN IN MG GRANITE ALASKITE AT 045/90
JW75 AD1 ACKLEY SHOWING,MASS.VCG,DK GREY,MUSC ALTER OF MG,MED PK,GRANITE
JW75AD3A ACKLEY SHOWING,PERV FG Q&SER,DK GREY ALTER OF AD3B GRANITE
JW75AD3B ACKLEY SHOWING,MG.DK PK,GRANITE,MINOR Q&SER ALTER
JW75AD6A ACKLEY SHOWING,FG TO PATCHY MG,DK RED,APLITE GRANITE,BORDERS SAMPLEAD6B
JW75AD6B ACKLEY SHOWING:CG PEGMATITE CLOT K-F>>Q>BIOTITE(REPLACED BY MAG)

ACKLEY CITY SHOWING

SAMPLE	JW75AD 7	JW75AD 9	JW75AD14	JW75AD15	JW75AD19	JW75AD20	JW75AD21
SIO2	61.46	82.80	77.58	81.29	77.11	77.78	77.65
AL2O3	9.11	6.95	11.66	9.56	11.33	11.00	11.48
FE2O3	5.11	1.24	0.73	0.70	0.64	0.90	0.62
MGO	0.21	0.15	0.06	0.12	0.09	0.13	0.05
CAO	1.05	0.71	0.53	0.45	0.43	0.34	0.44
NA2O	1.43	1.00	2.58	2.52	2.42	2.65	2.77
K2O	4.04	4.12	5.52	3.80	5.77	5.00	5.29
TIO2	0.08	0.12	0.13	0.13	0.14	0.19	0.14
MNO	0.21	0.06	0.05	0.06	0.05	0.10	0.02
LOI	7.46	1.94	0.53	0.64	0.63	0.72	0.64
TOTAL	90.16	99.09	99.37	99.27	98.61	98.81	99.10
ZR	52	119	106	134	117	138	98
SR	8	4	12	20	16	25	17
RB	301	373	541	377	548	458	496
ZN	328	143	502	44	227	259	329
CU	46	47	42	22	14	37	25
BA	26	42	63	50	57	53	46
U	15	21	12	12	11	11	10
MO	8313	5866	25	17	29	176	33
NB	129	54	27	34	24	29	26
RI	59	29	18	8	24	19	20
PB	63	46	58	43	63	80	58
NI	5	9	11	6	12	13	9
Y	57	74	37	45	39	50	41
CR	19	14	0	3	5	21	2
TI	465	1168	702	1000	777	892	666
S	96080	6720	1520	250	580	810	420
Q	45.76	63.75	41.19	52.30	41.23	43.88	41.35
OR	29.81	25.57	33.05	22.57	34.75	29.97	31.81
AB	15.60	8.89	22.25	21.78	21.04	23.08	23.96
AN	6.36	2.42	2.22	1.82	1.69	1.05	1.73
COR	0.75	0.0	0.66	0.66	0.51	0.88	0.59
MG BI	0.93	0.0	0.21	0.42	0.32	0.46	0.18
FE BI	0.65	0.0	0.12	0.15	0.12	0.24	0.05
SPH	0.25	0.31	0.33	0.33	0.35	0.48	0.35
DI	0.0	0.0	0.0	0.0	0.0	0.0	0.0
WO	0.0	0.0	0.0	0.0	0.0	0.0	0.0
ACT	0.0	0.48	0.0	0.0	0.0	0.0	0.0
RIEB	0.0	0.0	0.0	0.0	0.0	0.0	0.0

JW75 AD7 ACKLEY SHOWING:STRONGLY MINER(MOS2+Q+CHL).DK PK.PEGMATITIC GRANITE
JW75 AD9 ACKLEY SHOWING.MIN[illegible]MOS2.Q FLOODED.MG.LT PK.GRANITE.CHL&BIOT&SER ALTER
JW75AD14 ACKLEY SHOWING.LT PK GREY.MG.EQUI.GRANITE.DISS MOS2
JW75AD15 ACKLEY SHOWING.MED PK.STRONGLY Q FLOODED.SHEARED.MG.GRANITE
JW75AD19 ACKLEY SHOWING.LT PK.MG.EQUI.GRANITE
JW75AD20 ACKLEY SHOWING.MG.MED PK.EQUI.ALCSKITE GRANITE
JW75AD21 ACKLEY SHOWING : FG.PORP(Q-F).MED RED.GRANITE

ACKLEY CITY SHOWING

SAMPLE	JW75AD22	JW75AD24	JW75AD51	JW75AD98
SIO2	76.94	77.65	75.97	78.90
AL2O3	12.17	11.40	8.18	11.60
FE2O3	0.58	0.40	0.83	0.40
MGO	0.02	0.01	0.05	0.01
CAO	0.36	0.36	0.45	0.35
NA2O	3.63	3.58	0.68	3.57
K2O	4.72	4.43	5.79	4.41
TIO2	0.14	0.16	0.10	0.08
MNO	0.02	0.02	0.03	0.02
LOI	0.69	0.50	2.83	0.66
TOTAL	99.27	98.51	94.91	100.00
ZR	103	89	81	178
SR	7	1	1	2
RB	384	404	511	389
ZN	223	0	377	71
CU	34	29	59	17
BA	16	21	29	25
U	12	9	19	16
MO	14	21	1792	25
NB	26	30	74	24
BI	13	11	19	18
PB	56	53	67	57
NI	9	8	11	11
Y	37	28	52	55
CR	9	11	3	8
TI	577	318	644	356
S	230	350	30880	460
Q	37.85	40.18	53.66	41.00
OR	28.39	26.77	37.33	26.29
AB	31.35	31.04	6.31	30.53
AN	1.33	1.26	2.07	1.47
COR	0.63	0.27	0.11	0.42
MG BI	0.07	0.04	0.19	0.03
FE BI	0.05	0.05	0.08	0.05
SPH	0.35	0.40	0.27	0.20
DI	0.0	0.0	0.0	0.0
WO	0.0	0.0	0.0	0.0
ACT	0.0	0.0	0.0	0.0
RIEB	0.0	0.0	0.0	0.0

JW75AD22 ACKLEY SHOWING,FG.DK RED,APLITE GRANITE WITH GRANOPHYRE(K-F+Q) PATCHES
JW75AD24 ACKLEY SHOWING,CG.MED PK,FEATHERY,K-F&MINOR BIOT FROM PEG CLOT
JW75AD51 ACKLEY SHOWING,STRONGY MINER(MOS2+CHL),FG.MED PK,GRANITE
JW75AC98 ACKLEY SHOWING,FG.MED RED,APLITE GRANITE

DUNPHEY BROOK - CROW'S CLIFF SHOWING

SAMPLE	JW75106A	JW75107A	JW75-109	JW75-110	JW75-111	JW75-112	JW75-113
SIO2	77.48	75.37	78.90	75.83	76.36	75.62	79.31
AL2O3	12.02	12.60	11.37	12.29	12.30	12.47	10.56
FE2O3	0.76	0.80	0.86	0.75	0.70	1.06	0.78
MGO	0.05	0.06	0.09	0.14	0.03	0.18	0.04
CAO	0.28	0.17	0.40	0.28	0.20	0.49	0.17
NA2O	3.46	3.44	3.42	3.65	3.33	3.64	3.05
K2O	5.13	5.03	4.80	5.11	5.77	4.75	4.33
TIO2	0.09	0.13	0.04	0.09	0.08	0.25	0.02
MNO	0.03	0.03	0.02	0.05	0.03	0.04	0.02
LOI	0.72	0.62	0.80	0.65	0.90	0.71	0.37
TOTAL	100.02	98.25	100.70	98.84	99.70	99.21	98.65
ZR	116	152	152	134	110	171	117
SR	16	26	30	21	7	29	2
RB	362	379	347	363	334	380	342
ZN	0	0	36	0	0	39	0
CU	6	7	3	3	3	6	20
BA	77	108	78	78	58	72	37
U	8	6	8	8	8	8	5
MO	11	13	12	12	17	15	171
NB	35	33	27	24	23	28	11
BI	6	14	17	14	15	13	0
PB	20	77	38	42	43	40	48
NI	14	11	13	11	6	9	8
Y	80	80	83	77	54	48	19
CR	8	12	12	0	6	5	4
TI	832	785	1215	760	875	1233	569
S	130	250	570	200	140	200	290
Q	37.74	37.01	40.81	35.41	35.21	36.33	45.79
OR	30.61	30.52	28.74	30.59	34.65	28.33	26.12
AB	29.71	30.06	29.32	31.70	28.73	31.61	26.47
AN	1.09	0.40	1.52	1.10	0.73	1.60	0.79
COR	0.39	1.40	0.0	0.37	0.32	0.79	0.59
MG BI	0.18	0.21	0.0	0.50	0.11	0.64	0.14
FE BI	0.07	0.07	0.0	0.12	0.07	0.10	0.05
SPH	0.22	0.33	0.10	0.23	0.20	0.63	0.05
DI	0.0	0.0	0.0	0.0	0.0	0.0	0.0
WO	0.0	0.0	0.0	0.0	0.0	0.0	0.0
ACT	0.0	0.0	0.0	0.0	0.0	0.0	0.0
RIEB	0.0	0.0	0.0	0.0	0.0	0.0	0.0

JW75106A DUNPHEY BR - CROW.S CLIFF SHOWING:CG.MED RED.ALASKITE GRANITE
JW75107A DUNPHEY BR - CROW.S CLIFF SHOWING:PORP(Q-F).MG.MED PK.GRANITE
JW75 109 DUNPHEY BR - CROW.S CLIFF SHOWING:CG.MED RED.ALASKITE GRANITE
JW75 110 DUNPHEY BR - CROW.S CLIFF SHOWING:PORP(Q-F).MG.MED PK.GRANITE
JW75 111 DUNPHEY BR - CROW.S CLIFF SHOWING:FG.MED PK.MIOR.APLITE GRANITE:(Q-K)SE
JW75 112 DUNPHEY BR - CROW.S CLIFF SHOWING:PORP(Q-F).MG.MED PK.GRANITE
JW75 113 DUNPHEY BR - CROW.S CLIFF SHOWING:FG.PK.APLITE GRANITE;DISS MOS2

DUNPHEY BROOK - CROW'S CLIFF SHOWING

SAMPLE	JW75-115	JW75-117	JW75-118	JW75-119	JW75-120	JW75-121	JW75-122
SIO2	76.00	75.11	76.97	76.52	76.71	77.55	76.21
AL2O3	12.10	12.78	12.02	11.96	12.71	12.18	12.07
FE2O3	0.49	0.76	0.68	0.68	0.36	0.63	0.76
MGO	0.0	0.03	0.0	0.0	0.0	0.0	0.01
CAO	0.18	0.15	0.18	0.10	0.20	0.13	0.23
NA2O	3.45	3.41	3.71	3.47	3.40	2.75	3.68
K2O	5.64	5.28	4.95	5.57	4.80	5.04	4.80
TIO2	0.05	0.06	0.05	0.04	0.02	0.14	0.05
MNO	0.02	0.02	0.02	0.01	0.02	0.02	0.03
LOI	0.61	0.55	0.41	0.35	0.48	0.43	0.56
TOTAL	98.74	98.15	98.99	98.44	98.70	99.87	98.40
ZR	0	144	0	266	132	138	0
SR	0	1	0	109	1	4	0
RB	0	379	0	245	435	397	0
NB	0	21	0	62	0	18	0
CU	0	10	0	0	12	6	0
BA	0	30	0	269	22	31	0
U	0	11	0	6	8	8	0
MO	0	18	0	23	16	18	0
NB	0	19	0	22	42	47	0
[illegible]	0	12	0	13	15	15	0
[illegible]	0	12	0	33	51	38	0
[illegible]	0	1	0	5	11	12	0
[illegible]	0	87	0	64	100	104	0
CR	0	12	0	19	19	14	0
[illegible]	0	729	0	2105	685	569	0
[illegible]	18	280	0	390	230	160	0
Q	36.32	36.92	36.87	37.31	38.98	36.71	37.06
OR	33.34	32.12	29.86	33.78	28.96	30.12	29.16
AB	29.34	29.40	32.07	29.89	29.40	32.12	32.08
AN	0.85	0.85	0.74	0.37	0.94	0.16	1.00
COR	0.17	1.20	0.30	0.53	1.62	0.50	0.48
NC BI	0.0	0.11	0.0	0.0	0.0	0.0	0.04
FE BI	0.05	0.05	0.05	0.02	0.05	0.05	0.07
SPH	0.13	0.18	0.13	0.10	0.05	0.36	0.13
DI	0.0	0.0	0.0	0.0	0.0	0.0	0.0
WO	0.0	0.0	0.0	0.0	0.0	0.0	0.0
ACT	0.0	0.0	0.0	0.0	0.0	0.0	0.0
RIEB	0.0	0.0	0.0	0.0	0.0	0.0	0.0

JW75 115 DUNPHEY BR - CROW.S CLIFF SHOWING;PG.PK,APLITE GRANITE ; MIOR.(Q-K)SE
JW75 117 DUNPHEY BR - CROW.S CLIFF SHOWING;PG TO PATCHY MG,LT PK,GRANITE
JW75 118 DUNPHEY BR - CROW.S CLIFF SHOWING;PG,LT PK,GRANITE ; RARE Q AUGENS
JW75 119 DUNPHEY BR - CROW.S CLIFF SHOWING;PG TO PATCHY MG,MED PK.MIOR.GRANITE
JW75 120 DUNPHEY BR - CROW.S CLIFF SHOWING;PG.MED PK,GRANITE;NEAR Q-K-MOS2 PEG
JW75 121 DUNPHEY BR - CROW.S CLIFF SHOWING;PG.LT PK,MIOR.GRANITE;(Q-K)SE
JW75 122 DUNPHEY BR - CROW.S CLIFF SHOWING;PG,LT PK;GRANITE APLITE

DUNPHEY BROOK - CROW'S CLIFF SHOWING

SAMPLE	JW75-123	JW75-124	JW75-130	JW75-131
SIO2	77.45	77.11	78.13	78.17
AL2O3	12.10	12.04	12.15	12.02
FE2O3	0.84	0.96	0.81	0.84
MGO	0.02	0.06	0.04	0.01
CAO	0.07	0.20	0.19	0.20
NA2O	3.64	3.45	3.81	3.76
K2O	4.89	5.01	3.36	4.77
TIO2	0.15	0.11	0.02	0.03
MNO	0.04	0.03	0.02	0.02
LOI	0.60	0.72	0.44	0.38
TOTAL	99.80	99.69	98.97	100.20
ZR	164	173	148	0
SR	2	14	4	0
RB	480	366	401	0
ZN	1	24	0	0
CU	4	28	3	0
BA	25	84	33	0
U	10	8	12	0
MO	24	21	18	0
NB	15	25	20	0
SN	15	15	14	0
PB	38	65	40	0
W	12	10	12	0
Y	103	91	125	0
CR	9	0	0	0
TI	757	1004	737	0
S	130	240	200	0
Q	38.15	38.28	43.71	38.03
OR	29.28	30.03	20.20	28.43
AB	31.52	29.79	32.99	32.15
AN	0.0	0.62	0.89	0.90
COR	0.80	0.73	1.97	0.35
MG BI	0.07	0.21	0.14	0.03
FE BI	0.10	0.07	0.05	0.05
SPH	0.37	0.28	0.05	0.07
DI	0.0	0.0	0.0	0.0
WO	0.0	0.0	0.0	0.0
ACT	0.0	0.0	0.0	0.0
RIEB	0.0	0.0	0.0	0.0

JW75 123 DUNPHEY BR - CROW,S CLIFF SHOWING:FG,PORP(Q-F),MED PK.GRANITE
JW75 124 DUNPHEY BR - CROW,S CLIFF SHOWING:FG,PORP(Q-F),MED PK.GRANITE
JW75 130 DUNPHEY BR - CROW,S CLIFF SHOWING:FG,PORP(Q-F),MED PK.GRANITE
JW75 131 DUNPHEY BR - CROW,S CLIFF SHOWING:FG,LT PK,APLITE GRANITE

FRANK'S POND SHOWING

SAMPLE	JW75-125	JW75-126	JW75-FP1
SIO2	75.64	77.56	85.00
AL2O3	12.71	11.84	6.98
FE2O3	0.90	1.03	1.17
MGO	0.0	0.01	0.10
CAO	0.17	0.20	0.62
NA2O	3.78	3.59	1.86
K2O	4.80	4.67	2.48
TIO2	0.04	0.07	0.03
MNO	0.04	0.03	0.03
LOI	0.59	0.61	0.81
TOTAL	98.67	99.61	99.08
ZR	179	171	141
SR	1	7	8
RB	441	357	192
ZN	27	19	10
CU	0	1	6
BA	24	32	53
U	11	7	4
MO	16	19	3275
NB	49	37	34
BI	16	15	18
PB	57	36	35
NI	15	8	10
Y	137	111	123
CR	8	9	22
TI	305	647	878
S	160	210	2940
Q	35.96	39.23	65.27
OR	29.14	28.11	14.82
AB	32.92	31.01	16.21
AN	0.72	0.76	3.06
COR	1.07	0.62	0.15
MG BI	0.0	0.04	0.36
FE BI	0.10	0.07	0.07
SPH	0.10	0.18	0.08
DI	0.0	0.0	0.0
WO	0.0	0.0	0.0
ACT	0.0	0.0	0.0
RIEB	0.0	0.0	0.0

JW75 125FRANK,S POND SHOWING :FG,MED PK,EQ,GRANITE
JW75 126FRANK,S POND SHOWING ::MG,PORP(Q-F),MED PK,GRANITE
JW75 FP1FRANK,S POND SHOWING ::CG,MED RED,EQ,ALASKITE GRANITE;CUT BY Q-MO VEINS

BELLE ISLAND SHOWING

SAMPLE	JW75- 6	JW75- 7	JW75- 8	JW75- 11	JW75- 90
SIO2	72.00	72.91	69.71	71.29	75.03
AL2O3	13.14	13.60	13.65	13.15	13.03
FE2O3	1.00	1.36	1.56	1.34	1.00
MGO	0.30	0.53	0.48	0.59	0.0
CAO	0.76	0.76	2.13	1.27	0.74
NA2O	3.02	3.56	2.90	2.96	2.97
K2O	5.12	4.88	4.53	4.71	4.77
TIO2	0.13	0.22	0.21	0.20	0.14
MNO	0.03	0.04	0.05	0.03	0.02
LOI	2.14	2.26	3.74	2.78	2.29
TOTAL	97.64	100.12	98.96	98.32	99.99
ZR	235	125	254	218	220
SR	209	3	422	208	203
RB	253	398	259	244	251
ZN	0	0	4	0	0
CU	26	15	132	84	17
BA	501	22	748	628	501
U	4	8	5	4	7
MO	25	12	19	143	28
NB	32	36	18	22	23
BI	15	19	19	19	18
PB	25	41	23	41	26
NI	12	4	14	13	12
Y	53	33	33	42	49
CR	19	6	20	9	18
TI	1689	745	2083	1714	1684
S	60	150	300	290	300
Q	35.23	33.20	33.18	35.50	39.32
OR	31.24	28.55	27.32	28.04	29.13
AB	27.03	31.20	26.19	26.57	25.99
AN	3.51	3.11	10.50	5.94	3.79
COR	1.50	1.41	0.40	1.20	1.88
MG BI	1.09	1.89	1.77	2.16	0.0
FE BI	0.07	0.10	0.13	0.08	0.05
SPH	0.34	0.56	0.55	0.52	0.36
DI	0.0	0.0	0.0	0.0	0.0
WO	0.0	0.0	0.0	0.0	0.0
ACT	0.0	0.0	0.0	0.0	0.0
RIEB	0.0	0.0	0.0	0.0	0.0

JW75 6 BELLE ISLAND SHOWING :MG,PORP(Q-F),MED PK,GRANITE
JW75 7 BELLE ISLAND SHOWING : CG,PORP(Q-F),MED PK,GRANITE
JW75 8 BELLE ISLAND SHOWING: FG,MED PK,MIOR,APLITE GRANITE
JW75 11 BELLE ISLAND SHOWING: CG,PORP(Q-F),MED PK,GRANITE ;MOS2 ON FRACTURES
JW75 90 BELLE ISLAND SHOWING: FG,PORP(Q-F),APLITE GRANITE

WYLIE HILL SHOWING

SAMPLE	JW75-200	JW75-201	JW75-202	JW75-203	JW75-204	JW75-205	JW75-206
SIO2	78.33	75.61	77.76	75.87	76.00	75.87	79.38
AL2O3	11.57	12.76	12.54	12.98	12.13	12.63	11.09
FE2O3	0.42	1.15	0.56	0.88	0.71	1.19	0.20
MGO	0.09	0.26	0.12	0.20	0.15	0.26	0.01
CAO	0.40	0.54	0.37	0.43	0.33	0.60	0.30
NA2O	4.01	3.49	3.44	3.64	3.46	3.49	3.08
K2O	3.54	4.70	5.03	4.72	4.91	3.72	4.47
TIO2	0.29	0.31	0.19	0.20	0.17	0.13	0.13
MNO	0.04	0.09	0.02	0.07	0.03	0.08	0.0
LOI	0.55	0.56	0.60	0.69	0.73	0.68	0.42
TOTAL	99.24	99.47	100.63	99.68	98.62	98.65	99.08
ZR	97	196	135	142	134	147	124
SR	46	117	14	64	42	87	17
RB	256	356	364	319	330	371	376
ZN	27	0	232	30	18	10	0
CU	15	8	15	2	24	3	4
BA	92	252	56	211	171	238	47
U	11	5	7	9	10	5	6
MO	11	25	45	6	27	7	90
NB	25	23	25	27	27	31	30
BI	12	11	15	22	5	16	15
PB	51	28	84	35	113	35	36
NI	8	6	2	7	4	7	7
Y	16	58	23	32	25	40	31
CR	5	10	12	9	8	9	22
TI	812	1340	839	1304	992	1124	590
S	270	210	380	320	310	190	440
Q	41.53	37.23	38.04	65.55	37.56	41.47	44.49
OR	21.03	27.68	29.58	27.87	29.46	21.99	26.80
AB	34.53	30.21	29.26	31.39	30.12	30.51	26.47
AN	0.99	1.64	1.17	1.46	1.08	2.61	1.05
COR	0.80	1.38	1.01	1.38	0.76	2.00	0.82
MG BI	0.32	0.92	0.42	0.70	0.53	0.93	0.04
FE BI	0.10	0.22	0.05	0.17	0.07	0.20	0.0
SPH	0.72	0.78	0.47	0.50	0.43	0.33	0.32
DI	0.0	0.0	0.0	0.0	0.0	0.0	0.0
WO	0.0	0.0	0.0	0.0	0.0	0.0	0.0
ACT	0.0	0.0	0.0	0.0	0.0	0.0	0.0
RIEB	0.0	0.0	0.0	0.0	0.0	0.0	0.0

JW75 200 WYLIE HILL SHOWING. FG.MED RED.GRANITE
JW75 201 WYLIE HILL SHOWING. CG.LT PK.ALASKITE GRANITE
JW75 202 WYLIE HILL SHOWING. FG.LT PK TO WT.APLITE GRANITE.MIOR.DISS PY&MOS2
JW75 203 WYLIE HILL SHOWING: FG.PORP(Q+F).MED PK.GRANITE
JW75 204 WYLIE HILL SHOWING:FG.PORP(Q+F).LT PK.GRANITE;MINOR DISS PY+MOS2
JW75 205 WYLIE HILL SHOWING.FCG.MED PK.ALASKITE GRANITE.DISSPY
JW75 206 WYLIE HILL SHOWING:FG.WT.PORP(Q+PK F).GRANITE;MINOR DISS PY+MOS2

WYLIE HILL SHOWING

SAMPLE	JW75-210	JW75-212	JW75-213	JW75-214	JW75-325	69-2-110	69-2-104
SIO2	84.00	81.30	78.96	72.59	66.51	76.85	76.88
AL2O3	8.30	9.61	11.20	10.25	17.99	12.17	11.35
FE2O3	0.27	1.04	0.73	5.21	0.12	2.40	0.75
MGO	0.01	0.01	0.07	0.01	0.0	0.02	0.06
CAO	0.10	0.30	0.33	0.40	0.28	0.27	0.31
NA2O	2.41	2.44	2.91	3.31	3.77	4.85	3.00
K2O	3.39	3.59	4.64	3.30	10.24	4.95	4.77
TIO2	0.04	0.09	0.04	0.13	0.05	0.05	0.05
MNO	0.0	0.0	0.0	0.0	0.0	0.04	0.0
LOI	0.54	1.40	0.92	3.37	1.51	0.10	1.76
TOTAL	99.06	99.78	99.80	98.57	100.47	101.70	98.93
ZR	82	117	155	102	56	534	141
SR	7	4	14	4	3	10	5
RB	295	298	378	232	530	213	378
ZN	117	181	0	0	14	61	78
CU	0	0	2	0	4	36	13
BA	25	42	71	32	66	461	36
U	4	8	6	5	7	0	0
NO	72	4666	2958	3852	26	18	529
NB	22	28	44	26	13	34	35
BI	3	20	38	22	13	0	0
PB	121	155	41	67	68	29	55
NI	0	2	6	3	7	6	13
Y	21	25	37	21	12	118	40
CR	30	20	28	41	0	10	114
TI	500	492	830	595	114	1081	473
S	220	11250	8450	54300	430	2200	7450
Q	57.83	54.23	44.41	44.38	4.88	27.01	42.04
OR	20.37	21.77	27.77	21.64	61.23	28.22	29.08
AB	20.76	21.21	25.08	31.12	32.28	33.80	26.32
AN	0.36	1.21	1.53	1.70	1.23	0.0	1.41
COR	0.54	1.31	0.86	0.75	0.26	0.0	0.78
MG BI	0.04	0.04	0.25	0.04	0.0	0.0	0.21
FE BI	0.0	0.0	0.0	0.0	0.0	0.0	0.0
SPH	0.10	0.23	0.10	0.34	0.12	0.12	0.13
DI	0.0	0.0	0.0	0.0	0.0	0.37	0.0
WO	0.0	0.0	0.0	0.0	0.0	0.34	0.0
ACT	0.0	0.0	0.0	0.0	0.0	0.0	0.0
RIEB	0.0	0.0	0.0	0.0	0.0	10.30	0.0

JW75 210 WYLIE HILL SHOWING:FG.PORP(WORNY Q),LT PK.Q FLOODED ? ,APLITE
JW75 212 WYLIE HILL SHOWING:FG.PORP(Q+F).WT.APLITE GRANITE.STRONG DISS PY+MOS2
JW75 213 WYLIE HILL SHOWING:FG.PORP(Q+F).WT.APLITE GRANITE.FRAC&DISS PY+MOS2
JW75 214 WYLIE HILL SHOWING:FG.PORP(Q+F).WT.APLITE.DISS PY+MOS2.MUSC ALTER
JW75 325 WYLIE HILL SHOWING:NLX13-325:CG.MED PK.K-F+MINOR GRANOPHYRIC Q.PEGMATIT
W-692110 WYLIE HILL SHOWING:NLX69-2-110:FLOW BANDED.SPOTTY GREY.RHYOLITE:RARE PY
JW-WH104 WYLIE HILL SHOWING.NLX69-2-180.1-190.FG.PK.APLITE.DISS PY&MOS2

WYLIE HILL SHOWING

SAMPLE	69-2-105	69-2-106	69-2-107	69-2-108	69-2-109	69-2-110	69-3-116
SIO2	78.79	80.00	80.00	79.76	78.78	78.59	78.07
AL2O3	10.42	10.42	10.71	11.05	11.93	11.48	11.68
FE2O3	0.80	0.75	1.00	0.67	0.86	1.13	1.50
MGO	0.06	0.06	0.10	0.05	0.07	0.16	0.12
CAO	0.40	0.40	0.31	0.40	0.44	0.44	0.36
NA2O	2.86	2.88	2.81	3.05	3.37	3.08	3.26
K2O	4.35	4.23	4.80	4.67	5.24	4.98	4.95
TIO2	0.05	0.05	0.05	0.05	0.05	0.05	0.05
MNO	0.0	0.01	0.01	0.01	0.02	0.02	0.02
LOI	1.47	1.62	1.57	1.64	1.14	1.81	1.16
TOTAL	99.20	100.42	101.36	101.35	101.90	101.74	101.17
ZR	135	140	142	123	144	155	146
SR	7	7	10	5	14	25	18
RB	360	330	364	351	389	376	362
ZN	39	77	45	5	53	19	266
CU	7	14	8	15	32	103	102
BA	36	45	53	37	60	79	75
U	0	0	0	0	0	0	0
MO	1211	2492	420	1338	166	417	339
NB	33	36	28	32	30	38	30
BI	0	0	0	0	0	0	0
PB	56	68	76	44	62	42	260
NI	7	10	14	8	11	8	7
Y	42	43	42	33	40	43	50
CR	64	79	260	59	78	74	49
TI	465	457	470	420	479	870	791
S	6210	7299	4401	4360	4360	5720	2200
Q	46.09	47.15	45.18	43.74	40.81	41.19	40.02
OR	26.37	25.34	28.46	27.74	28.74	29.39	29.38
AB	24.96	24.85	24.05	26.06	29.32	26.37	28.00
AN	1.87	1.85	1.38	1.83	1.52	2.03	1.64
COR	0.35	0.45	0.40	0.32	0.0	0.29	0.37
MG BI	0.21	0.21	0.35	0.17	0.0	0.56	0.42
FE BI	0.0	0.01	0.0	0.01	0.0	0.04	0.04
SPH	0.13	0.13	0.12	0.12	0.10	0.12	0.12
DI	0.0	0.0	0.0	0.0	0.0	0.0	0.0
WO	0.0	0.0	0.0	0.0	0.0	0.0	0.0
ACT	0.0	0.0	0.0	0.0	0.34	0.0	0.0
RIEB	0.0	0.0	0.0	0.0	0.0	0.0	0.0

JW-WH105 WYLIE HILL SHOWING.NLX69-2-190-200.FG.PK.APLITE.DISS PY&MOS2
JW-WH106 WYLIE HILL SHOWING.NLX69-2-200-210.PK.APLITE&MG.WT.GRANITE.DISS MOS2
JW-WH107 WYLIE HILL SHOWING.NLX69-2-210-220.PK.APLITE&MG.WT.GRANITE.DISS MOS2&PY
JW-WH108 WYLIE HILL SHOWING.NLX69-2-220-230.WT.MG.GRANITE.DISS PY&MOS2
JW-WH109 WYLIE HILL SHOWING.NLX69-2-230-245.WT.MG.GRANITE.DISS PY&MOS2
JW-WH110 WYLIE HILL SHOWING.NLX69-2-245-260.WT.MG.GRANITE.DISS PY&MOS2
JW-WH116 WYLIE HILL SHOWING.NLX69-3-173-185.RED APLITE&WT.MG GRANITE.DISS PY&MOS

WYLIE HILL SHOWING

SAMPLE	69-3-117	69-6-146	69-6-147	69-7-148	69-7-149	69-7-150	69-7-151
SIO2	78.00	78.78	79.00	77.71	72.21	78.35	78.92
AL2O3	11.95	11.79	12.06	11.20	13.74	10.80	11.54
FE2O3	1.47	1.36	1.13	1.38	0.79	0.23	0.86
MGO	0.13	0.13	0.08	0.07	0.12	0.15	0.14
CAO	0.49	0.44	0.40	0.22	0.33	0.58	0.36
NA2O	3.31	3.48	3.52	3.12	3.89	3.21	3.15
K2O	5.29	4.69	4.92	4.82	8.38	4.60	5.16
TIO2	0.05	0.11	0.05	0.05	0.11	0.05	0.05
MNO	0.02	0.02	0.02	0.01	0.05	0.01	0.01
LOI	1.16	1.00	0.55	1.75	2.03	0.42	1.59
TOTAL	101.87	101.80	101.73	100.33	101.65	98.40	101.78
ZR	163	155	131	134	182	167	152
SR	23	27	6	15	44	28	22
RB	370	357	343	366	509	357	430
ZN	64	275	437	36	54	0	48
CU	49	22	21	17	39	7	7
BA	89	89	86	52	203	81	76
U	0	0	0	0	0	0	0
MO	169	111	44	1872	27	1519	648
NB	31	28	37	34	41	36	36
BI	0	0	0	0	0	0	0
PB	93	400	52	67	284	36	65
NI	9	6	7	7	8	7	13
Y	55	34	38	41	49	42	40
CR	60	60	66	58	5	8	62
TI	878	884	735	582	1015	940	781
S	1550	3810	3170	5380	770	4090	5370
Q	37.71	39.94	38.85	41.84	14.16	41.84	40.37
OR	31.28	27.54	28.84	29.13	46.96	27.81	30.36
AB	28.22	29.61	29.77	27.16	22.78	27.79	26.83
AN	2.14	1.81	1.81	0.94	0.0	1.51	1.62
COR	0.0	0.33	0.28	0.53	0.0	0.0	0.18
MG BI	0.30	0.45	0.04	0.25	0.0	0.0	0.49
FE BI	0.03	0.04	0.12	0.02	0.0	0.0	0.01
SPH	0.12	0.27	0.13	0.13	0.26	0.13	0.12
DI	0.0	0.0	0.0	0.0	0.61	0.85	0.0
WO	0.0	0.0	0.0	0.0	0.17	0.07	0.0
ACT	0.19	0.0	0.0	0.0	0.0	0.0	0.0
RIEB	0.0	0.0	0.0	0.0	15.00	0.0	0.0

JW-WH117 WYLIE HILL SHOWING.NLX69-3-185-200.MG.RED&WT.GRANITE.DISS PY&MOS2
JW-WH146 WYLIE HILL SHOWING.NLX69-6-340-355.MG.RED&WT.GRANITE
JW-WH147 WYLIE HILL SHOWING.NLX69-6-355-370.MG.RED GRANITE.PARTLY LEACHED.CARB
JW-WH148 WYLIE HILL SHOWING.NLX69-7-204-210.MG.PK.GRANITE.DISS PY&MOS2
JW-WH149 WYLIE HILL SHOWING:NLX69-7-215:MG-FG.LT PK.GRANITE.MINOR DISS PY+MOS2
JW-WH150 WYLIE HILL SHOWING:NLX69-7-235:MG-FG.LT PK.GRANITE.MINOR DISS PY+MOS2
JW-WH151 WYLIE HILL SHOWING.NLX69-7-240-255.MG.WT.GRANITE.MINOR DISS PY&MOS2

WYLIE HILL SHOWING

SAMPLE	69-7-152	69-7-153	69-7-154	69-7-155	69-7-156	69-8-167	69-8-169
SIO2	78.72	78.00	77.47	76.97	76.76	76.00	75.52
AL2O3	11.33	12.07	12.12	12.64	11.62	11.48	11.48
FE2O3	1.10	1.17	0.18	1.30	1.17	0.17	0.23
MGO	0.14	0.15	0.08	0.10	0.11	0.06	0.08
CAO	0.44	0.62	0.40	0.58	0.48	0.47	0.50
NA2O	3.11	3.39	3.65	3.73	3.21	2.99	3.59
K2O	5.10	5.18	4.99	5.03	4.84	5.48	4.50
TIO2	0.05	0.05	0.05	0.05	0.05	0.05	0.05
MNO	0.01	0.02	0.03	0.02	0.02	0.01	0.01
LOI	1.84	1.00	1.78	1.41	1.30	1.89	2.13
TOTAL	101.84	101.65	100.75	101.83	99.56	98.60	98.09
ZR	166	161	146	133	143	158	145
SR	32	32	18	12	18	12	12
RB	391	381	398	386	363	414	345
ZN	66	51	0	14	91	57	17
CU	47	7	16	17	14	18	21
BA	77	81	71	56	78	68	55
U	0	0	0	0	0	0	0
MO	580	265	21	115	163	267	47
NB	36	30	34	25	32	17	41
BI	0	0	0	0	0	0	0
PB	49	70	51	80	200	57	55
NI	8	6	6	12	9	6	5
Y	46	41	37	36	39	29	41
CR	56	68	2	74	70	13	0
TI	749	836	620	648	690	677	588
S	5170	3160	1180	5360	4250	6100	8590
Q	40.59	38.27	36.76	35.12	39.72	38.50	38.59
OR	30.23	30.92	29.62	29.72	29.17	33.65	27.87
AB	26.60	28.97	31.26	31.84	27.97	26.29	31.84
AN	1.91	2.44	1.83	2.73	2.27	1.79	2.01
COR	0.0	0.0	0.05	0.07	0.30	0.0	0.0
MG BI	0.35	0.0	0.28	0.35	0.39	0.0	0.0
FE BI	0.01	0.0	0.07	0.04	0.04	0.0	0.0
SPH	0.12	0.12	0.12	0.12	0.13	0.13	0.13
DI	0.0	0.0	0.0	0.0	0.0	0.0	0.0
WO	0.0	0.0	0.0	0.0	0.0	0.0	0.0
ACT	0.17	0.60	0.0	0.0	0.0	0.01	0.21
RIEB	0.0	0.0	0.0	0.0	0.0	0.0	0.0

JW-WH152 WYLIE HILL SHOWING.NLX69-7-255-270.MG.WT&PK.GRANITE.MINOR DISS PY&MOS2
JW-WH153 WYLIE HILL SHOWING.NLX69-7-270-285.MG.PK.GRANITE.MINOR DISS PY&MOS2
JW-WH154 WYLIE HILL SHOWING:NLX69-7-295:MG.WT.GRANITE:MINOR DISS PY+MOS2
JW-WH155 WYLIE HILL SHOWING.NLX69-7-300-315.ALTERNATING PK GRANITE&ALASKITE
JW-WH156 WYLIE HILL SHOWING.NLX69-7-315-323.ALTERNATING PK GRANITE&ALASKITE
JW-WH167 WYLIE HILL SHOWING:NLX69-8-260:FG.WT.APLITE GRANITE.MINOR DISS PY+MOS2
JW-WH169 WYLIE HILL SHOWING:NLX69-8-270:MG.PK.GRANITE.MIOR.STRONG DISS PY

WYLIE HILL SHOWING

SAMPLE	69-8-170	69-8-171	69-8-172	69-8-173	69-8-174	69-8-175	69-8-176
SIO2	77.68	77.26	80.42	77.09	76.27	78.28	74.67
AL2O3	11.54	10.26	11.11	11.67	12.32	12.21	12.71
FE2O3	0.21	0.69	1.11	1.18	0.32	0.32	1.08
MGO	0.15	0.10	0.19	0.19	0.20	0.16	0.16
CAO	0.47	0.33	0.56	0.52	0.58	0.44	0.84
NA2O	3.33	2.18	3.19	3.17	3.70	4.04	3.86
K2O	5.01	5.92	4.51	5.24	5.65	5.11	6.11
TIO2	0.05	0.05	0.05	0.05	0.05	0.10	0.05
MNO	0.01	0.0	0.03	0.03	0.01	0.01	0.05
LOI	1.78	1.84	0.54	1.27	2.07	1.20	1.90
TOTAL	100.23	98.63	101.71	100.41	101.17	101.87	101.43
ZR	188	150	167	169	210	178	164
SR	22	19	29	12	51	26	32
RB	400	407	356	376	422	366	422
ZN	0	0	7	0	99	46	319
CU	24	16	30	17	38	17	23
BA	85	61	80	89	155	66	110
U	0	9	0	0	0	0	0
MO	250	6442	245	384	137	37	107
NB	40	42	34	33	34	25	29
BI	0	26	0	0	0	0	0
PB	39	43	47	41	49	54	287
NI	6	7	10	10	8	4	8
Y	43	39	45	43	41	40	36
CR	22	9	65	50	5	9	37
TI	852	707	867	923	1179	854	896
S	1666	14840	4420	3210	4300	3770	2030
Q	38.66	42.93	43.40	38.17	32.52	34.36	27.56
OR	30.12	36.40	26.16	31.35	33.80	30.09	36.33
AB	28.68	19.20	26.97	27.38	31.70	34.07	31.56
AN	1.78	0.76	2.60	2.18	0.33	0.09	0.0
COR	0.61	0.0	0.03	0.0	0.0	0.0	0.0
MG BI	0.02	0.0	0.65	0.35	0.0	0.0	0.0
FE BI	0.0	0.0	0.06	0.03	0.0	0.0	0.0
SPH	0.12	0.13	0.12	0.13	0.12	0.24	0.12
DI	0.0	0.56	0.0	0.0	1.12	0.89	0.86
WO	0.0	0.02	0.0	0.0	0.41	0.25	1.21
ACT	0.0	0.0	0.0	0.40	0.0	0.0	0.0
RIEB	0.0	0.0	0.0	0.0	0.0	0.0	2.30

JW-WH170 WYLIE HILL SHOWING:NLX69-8-280:MG,WT,GRANITE:FRAC+DISS PY+MOS2
JW-WH171 WYLIE HILL SHOWING,NLX69-8-280-290,MG,WT,GRANITE,FRAC&DISS PY&MOS2
JW-WH172 WYLIE HILL SHOWING,NLX69-8-290-300,MG,WT,GRANITE,FRAC&DISS PY&MOS2
JW-WH173 WYLIE HILL SHOWING,NLX69-8-300-310,MG,WT,GRANITE,FRAC&DISS PY&MOS2
JW-WH174 WYLIE HILL SHOWING:NLX69-8-315:MG,WT,GRANITE:MINOR DISS PY+MOS2
JW-WH175 WYLIE HILL SHOWING:NLX69-8-330:FG-MG,LT PK,GRANITE,MINOR DISS PY+MOS2
JW-WH176 WYLIE HILL SHOWING,NLX69-8-335-345,MG,WT,GRANITE,FRAC&DISS PY&MOS2

WYLIE HILL SHOWING

SAMPLE	69-8-177	69-8-178	69-8-179	69-9-180	69-9-181	69-9-182	69-8-183
SIO2	76.13	75.89	77.05	78.11	76.11	78.40	76.44
AL2O3	12.26	11.43	11.50	11.31	11.09	11.20	11.41
FE2O3	0.39	0.43	1.42	0.99	1.02	1.02	0.92
MGO	1.80	0.10	0.13	0.07	0.10	0.11	0.11
CAO	0.51	0.44	1.08	0.31	0.72	0.36	0.36
NA2O	3.43	3.28	3.21	3.00	2.68	2.88	2.85
K2O	5.33	4.97	4.78	4.69	5.05	4.85	4.85
TIO2	0.10	0.05	0.05	0.05	0.05	0.05	0.13
MNO	0.02	0.02	0.02	0.0	0.02	0.02	0.01
LOI	1.79	2.00	1.50	1.12	1.53	1.60	1.71
TOTAL	101.76	98.61	100.74	99.65	98.37	100.49	98.79
ZR	219	119	137	129	136	166	137
SR	42	21	21	10	19	10	20
RB	404	374	346	367	351	360	368
ZN	0	3	67	138	152	134	148
CU	28	24	46	30	24	23	32
BA	113	33	54	52	66	67	68
U	0	0	0	0	0	0	0
MO	166	335	116	1050	955	182	242
NB	19	37	26	31	24	35	35
BI	0	0	0	0	0	0	0
PB	40	57	83	68	94	89	88
NI	6	6	8	45	49	47	42
Y	41	38	38	37	37	39	44
CR	14	1	56	45	53	40	38
TI	1057	712	736	522	697	730	707
S	1060	4340	4220	3400	5440	7540	6900
Q	34.81	38.25	38.95	43.13	41.37	43.26	42.24
OR	27.37	30.46	28.88	28.24	30.95	29.00	29.53
AB	29.07	28.86	27.77	26.02	23.66	24.90	25.08
AN	2.19	1.86	2.92	1.40	3.46	1.65	1.39
COR	0.05	0.0	0.0	0.82	0.0	0.64	1.02
MG BI	6.22	0.10	0.0	0.25	0.26	0.39	0.39
FE BI	0.05	0.01	0.0	0.0	0.03	0.04	0.02
SPH	0.25	0.13	0.13	0.13	0.13	0.13	0.33
DI	0.0	0.0	0.76	0.0	0.0	0.0	0.0
WO	0.0	0.0	0.58	0.0	0.0	0.0	0.0
ACT	0.0	0.34	0.0	0.0	0.12	0.0	0.0
RIEB	0.0	0.0	0.0	0.0	0.0	0.0	0.0

JW-WH177 WYLIE HILL SHOWING:NLX69-8-350:FG.PK.GRANITE.STRONG PY+MO.PK ALTER OF F
JW-WH178 WYLIE HILL SHOWING:NLX69-8-370:FG-MG.RED.ALASKITE.MIOR.WEAK MOS2
JW-WH179 WYLIE HILL SHOWING.NLX69-8-375-386.MG.PK.GRANITE.DISS PY&MINOR MOS2
JW-WH180 WYLIE HILL SHOWING.NLX69-9-126-135.FG.PK.GRANITE
JW-WH181 WYLIE HILL SHOWING.NLX69-9-135-145.FG.PK.GRANITE
JW-WH182 WYLIE HILL SHOWING.NLX69-9-145-155.FG.PK.GRANITE
JW-WH183 WYLIE HILL SHOWING.NLX69-9-155-165.FG.PK.GRANITE

WYLIE HILL SHOWING

SAMPLE	69-9-184	69-9-185	69-8-186	69-8-187	69-8-188	69-8-189	69-8-190
SIO2	77.42	77.58	77.33	76.80	78.51	79.27	78.53
AL2O3	11.13	11.13	11.41	11.46	11.35	11.41	11.30
FE2O3	0.87	0.87	0.87	0.90	0.87	0.86	1.17
MGO	0.12	0.14	0.13	0.21	0.13	0.14	0.12
CAO	0.44	0.40	0.44	0.60	0.44	0.56	0.40
NA2O	2.77	2.71	2.82	2.88	2.94	3.09	3.12
K2O	4.80	4.80	4.87	4.19	4.54	4.55	4.52
TIO2	0.10	0.05	0.05	0.05	0.05	0.05	0.05
MNO	0.01	0.01	0.01	0.01	0.01	0.01	0.02
LOI	1.25	1.43	1.15	2.64	1.24	1.04	1.06
TOTAL	98.91	99.12	99.08	99.74	100.08	100.98	100.29
ZR	130	153	155	144	143	160	156
SR	20	21	18	20	22	27	21
RB	379	388	393	386	371	388	377
ZN	157	153	113	607	78	122	179
CU	22	33	32	23	27	34	32
BA	65	77	77	63	68	85	74
U	0	0	0	0	0	0	0
MO	314	288	224	1173	338	455	87
NB	28	32	27	30	32	32	31
BI	0	0	0	0	0	0	0
PB	107	122	94	96	84	102	103
NI	43	39	43	42	42	40	63
Y	35	38	31	33	32	35	33
CR	52	61	44	34	39	49	53
TI	762	875	857	830	869	831	836
S	6430	6050	6560	32300	2480	3270	3520
Q	43.45	44.01	42.62	44.44	44.01	43.10	43.09
OR	29.01	28.95	29.33	25.22	27.06	26.80	26.93
AB	24.21	23.68	24.58	25.32	25.39	26.38	26.92
AN	1.90	1.87	2.07	2.91	2.05	2.63	1.85
COR	0.73	0.84	0.79	1.21	0.83	0.45	0.62
MG BI	0.43	0.50	0.46	0.75	0.46	0.49	0.42
FE BI	0.02	0.01	0.02	0.02	0.02	0.02	0.04
SPH	0.25	0.13	0.13	0.13	0.13	0.12	0.13
DI	0.0	0.0	0.0	0.0	0.0	0.0	0.0
WO	0.0	0.0	0.0	0.0	0.0	0.0	0.0
ACT	0.0	0.0	0.0	0.0	0.0	0.0	0.0
RIEB	0.0	0.0	0.0	0.0	0.0	0.0	0.0

JW-WH184 WYLIE HILL SHOWING,NLX69-9-165-175,FG,PK,GRANITE
JW-WH185 WYLIE HILL SHOWING,NLX69-9-175-185,FG,PK,GRANITE
JW-WH186 WYLIE HILL SHOWING,NLX69-9-185-195,FG,PK,GRANITE
JW-WH187 WYLIE HILL SHOWING,NLX69-9-195-205,FG,PK,GRANITE
JW-WH188 WYLIE HILL SHOWING,NLX69-9-205-215,FG,PK,GRANITE
JW-WH189 WYLIE HILL SHOWING,NLX69-9-215-225,FG,PK,GRANITE
JW-WH190 WYLIE HILL SHOWING,NLX69-9-225-235,MG,PK,GRANITE,DISS PY&MOS2

WYLIE HILL SHOWING

SAMPLE	69-8-191	69-8-192	69-9-309	6910A193	6910A194	6910A195	6910A196
SIO2	74.53	75.89	78.71	76.21	73.68	73.96	75.89
AL2O3	13.27	11.48	11.74	11.54	14.40	13.00	11.85
FE2O3	1.16	1.12	0.29	1.35	1.33	1.42	1.12
MGO	0.12	0.13	0.14	0.10	0.07	0.09	0.10
CAO	0.58	0.58	0.51	0.33	0.27	0.37	0.50
NA2O	3.90	3.09	3.32	3.27	5.89	3.82	2.99
K2O	5.19	4.62	4.60	4.57	4.50	5.18	5.20
TIO2	0.10	0.05	0.05	0.05	0.12	0.11	0.05
MNO	0.02	0.02	0.01	0.02	0.03	0.03	0.03
LOI	1.11	1.25	0.83	1.47	1.01	1.03	1.40
TOTAL	99.98	98.23	100.20	98.91	101.30	99.01	99.13
ZR	161	147	156	132	157	156	133
SR	21	23	28	30	77	50	27
RB	396	362	359	323	312	371	370
ZN	170	460	557	345	46	134	137
CU	39	38	30	84	45	52	39
BA	92	94	95	71	168	112	89
U	0	0	0	0	0	0	0
MO	104	40	19	260	23	99	431
NB	31	31	28	21	30	25	26
BI	0	0	0	0	0	0	0
PB	159	127	342	433	68	120	118
NI	55	50	6	42	27	29	30
Y	38	35	34	30	38	37	41
CR	57	56	4	58	40	28	44
TI	910	920	906	589	963	786	766
S	3810	4350	14290	8030	500	1130	7640
Q	31.53	40.70	41.11	40.61	21.71	32.31	38.87
OR	31.08	28.14	27.09	27.84	26.71	31.45	31.53
AB	33.77	27.27	28.35	28.79	49.24	33.47	26.19
AN	2.59	2.82	2.38	1.52	0.0	1.50	2.39
COR	0.32	0.42	0.44	0.71	0.0	0.60	0.47
MG SI	0.42	0.47	0.49	0.34	0.0	0.32	0.36
FE SI	0.04	0.04	0.02	0.04	0.0	0.07	0.07
SPH	0.25	0.13	0.12	0.13	0.30	0.28	0.13
DI	0.0	0.0	0.0	0.0	0.38	0.0	0.0
WO	0.0	0.0	0.0	0.0	0.18	0.0	0.0
ACT	0.0	0.0	0.0	0.0	0.0	0.0	0.0
RIEB	0.0	0.0	0.0	0.0	1.40	0.0	0.0

JW-WH191 WYLIE HILL SHOWING:NLX69-9-235-245:MG,DK RED,MIOR,GRANITE;MINOR PY+MOS2
JW-WH192 WYLIE HILL SHOWING,NLX69-9-245-255,MG,GREY,GRANITE
W69-9309 WYLIE HILL SHOWING:NLX69-9-309:MG,PK,ALASKITE GRANITE;DISS PY+MOS2
JW-WH193 WYLIE HILL SHOWING,NLX69-10A-193-200,MG,PK,ALASKITE GRANITE,DISSPY&MO
JW-WH194 WYLIE HILL SHOWING,NLX69-10A-200-210,FG,RED,MIOR,GRANITE,DISS PY&MOS2
JW-WH195 WYLIE HILL SHOWING,NLX69-10A-200-210,FG,RED,MIOR,GRANITE,DISS PY&MOS2
JW-WH196 WYLIE HILL SHOWING,NLX69-10A-220-230,MG,PK,ALASKITE GRANITE,DISS PY&MO

WYLIE HILL SHOWING

SAMPLE	6910A197	6910A198	6910A199	6910A200	6910A201	E692-202	E692-203
SIO2	76.00	75.66	76.30	76.35	78.29	78.63	76.57
AL2O3	11.74	11.93	12.55	11.59	11.75	11.78	11.52
FE2O3	1.12	1.28	1.26	1.65	1.46	1.73	1.49
MGO	0.10	0.09	0.28	0.26	0.28	0.31	0.30
CAO	0.47	0.47	0.45	0.56	0.79	0.34	0.34
NA2O	2.91	3.67	3.43	3.24	3.00	2.85	2.90
K2O	5.13	4.80	5.52	4.71	4.95	4.61	4.54
TIO2	0.05	0.05	0.05	0.05	0.05	0.05	0.05
MNO	0.01	0.02	0.03	0.04	0.04	0.02	0.02
LOI	1.04	1.05	0.22	0.42	0.56	0.58	0.93
TOTAL	98.57	99.02	100.09	98.87	101.17	100.90	98.66
ZR	134	141	139	121	129	138	148
SR	21	23	17	26	31	15	18
RB	382	349	379	352	350	367	364
ZN	249	157	119	87	44	352	89
CU	46	50	47	39	61	30	32
BA	81	76	74	65	80	54	61
U	0	0	0	0	0	0	0
MO	33	25	39	81	113	92	138
NB	26	28	26	25	28	28	29
BI	0	0	0	0	0	0	0
PB	173	117	102	103	65	81	64
NI	36	38	38	40	37	52	54
Y	36	36	34	29	34	34	33
CR	53	40	46	49	54	35	33
TI	705	732	762	611	769	749	791
S	4830	3180	4760	1250	1720	9220	12290
Q	39.87	28.05	34.76	39.57	40.57	44.32	43.24
OR	31.19	29.32	32.38	28.08	28.80	26.87	27.13
AB	25.54	32.12	29.42	28.31	25.59	24.45	25.49
AN	2.24	1.97	2.09	2.69	3.78	1.53	1.57
COR	0.63	0.0	0.18	0.21	0.09	1.57	1.33
MG BI	0.36	0.02	0.98	0.93	0.97	1.08	1.07
FE BI	0.02	0.0	0.07	0.09	0.09	0.04	0.04
SPH	0.13	0.13	0.12	0.13	0.12	0.12	0.13
DI	0.0	0.0	0.0	0.0	0.0	0.0	0.0
WO	0.0	0.0	0.0	0.0	0.0	0.0	0.0
ACT	0.0	0.39	0.0	0.0	0.0	0.0	0.0
RIEB	0.0	0.0	0.0	0.0	0.0	0.0	0.0

JW-WH197 WYLIE HILL SHOWING,NLX69-10A-230-240.MG.PK.ALASKITE GRANITE.DISS PY&MO
JW-WH198 WYLIE HILL SHOWING,NLX69-10A-240-250.MG.PK.ALASKITE GRANITE.DISS PY&MO
JW-WH199 WYLIE HILL SHOWING,NLX69-10A-250-260.MG.PK.ALASKITE GRANITE.DISS PY&MO
JW-WH[illegible]0 WYLIE HILL SHOWING,NLX69-10A-260-270.MG.PK.ALASKITE GRANITE.DISS PY&MO
JW-WH201 WYLIE HILL SHOWING,NLX69-10A-270-280,MG,PK,ALASKITE GRANITE.DISS PY&MO
JW-WH202 WYLIE HILL SHOWING:ELX69-2-0-15:FG,PK,GRANITE:DISS PY+MOS2+SER
JW-WH203 WYLIE HILL SHOWING:ELX69-2-15-30:FG.PORP(Q-F).GREY.GRANITE:DISS PY+MOS2

WYLIE HILL SHOWING

SAMPLE	E692-204	E692-205	E692-206	E692-207	E692-208	E692-209	E692-210
SIO2	77.41	76.36	77.00	79.06	83.66	75.46	68.09
AL2O3	11.52	11.59	11.54	10.20	8.44	11.74	17.89
FE2O3	1.30	1.12	1.69	1.61	1.67	1.43	1.08
MGO	0.29	0.28	0.25	0.23	0.24	0.23	0.27
CAO	0.43	0.33	0.19	0.26	0.26	0.22	0.01
NA2O	2.87	2.92	3.00	2.70	2.40	3.71	6.00
K2O	4.56	4.69	4.97	4.61	3.29	4.29	6.91
TIO2	0.05	0.05	0.05	0.05	0.05	0.05	0.05
MNO	0.02	0.02	0.01	0.01	0.02	0.01	0.01
LOI	0.54	0.72	0.34	1.56	0.04	2.82	0.04
TOTAL	98.69	98.08	99.04	100.29	100.07	99.96	100.35
ZR	138	140	142	106	117	102	135
SR	20	19	22	21	16	27	77
RB	374	376	362	340	269	302	430
ZN	109	130	112	42	106	119	87
CU	29	29	34	28	32	136	37
BA	69	65	67	64	52	67	260
U	0	0	0	0	0	0	0
MO	160	138	111	90	56	142	32
NB	29	33	34	35	40	26	26
AS	0	0	0	0	0	0	0
PB	66	103	110	47	43	84	34
NI	41	44	62	64	50	51	39
V	35	31	34	30	29	27	22
CR	27	29	40	45	45	29	29
TI	891	747	777	516	608	548	612
S	10530	9420	6200	5260	810	26620	1270
Q	43.87	42.33	41.38	46.51	57.51	38.67	6.81
OR	27.04	28.09	29.66	27.49	19.18	25.92	40.50
AB	24.61	25.66	26.16	23.52	20.64	32.79	51.15
AN	1.51	1.52	0.79	1.15	1.13	0.96	0.0
COR	1.37	1.22	0.97	0.37	0.53	0.69	0.59
MG SI	1.03	1.00	0.89	0.82	0.84	0.83	0.94
FE SI	0.05	0.05	0.02	0.02	0.04	0.02	0.02
SPH	0.13	0.13	0.13	0.13	0.12	0.13	0.13
DI	0.0	0.0	0.0	0.0	0.0	0.0	0.0
WO	0.0	0.0	0.0	0.0	0.0	0.0	0.0
ACT	0.0	0.0	0.0	0.0	0.0	0.0	0.0
RIEB	0.0	0.0	0.0	0.0	0.0	0.0	0.0

JW-WH204 WYLIE HILL SHOWING:ELX69-2-30-45:FG.PORP(Q-F).GREY.GRANITE:DISS PY+MOS2
JW-WH205 WYLIE HILL SHOWING:ELX69-2-45-60:FG.PORP(Q-F).GREY.GRANITE:DISS PY+MOS2
JW-WH206 WYLIE HILL SHOWING:ELX69-2-60-75:FG.PORP(Q-F).GREY.GRANITE:DISS PY+MOS2
JW-WH207 WYLIE HILL SHOWING:ELX69-2-75-90:FG.PORP(Q-F).GREY.GRANITE:DISS PY+MOS2
JW-WH208 WYLIE HILL SHOWING:ELX69-2-90-98:MG.PALE PK.ALASKITE:DISS PY+MOS2
JW-WH209 WYLIE HILL SHOWING:ELX69-2-98-110:MG.MIOR.GRANITE:DISS PY+MOS2
JW-WH210 WYLIE HILL SHOWING:ELX69-2-110-120:MG.PALE PK.ALASKITE GRANITE:PY+MOS2

WYLIE HILL SHOWING

SAMPLE	E692-211	E692-212	E692-213	E692-214	69-17-65	69-11441	69-11215
SIO2	76.75	76.75	76.50	76.11	76.13	76.24	75.56
AL2O3	12.72	12.49	12.37	12.09	11.37	12.71	13.03
FE2O3	1.23	2.12	1.32	1.74	2.76	2.09	1.79
MGO	0.27	0.27	0.28	0.27	0.18	0.02	0.24
CAO	0.33	0.36	0.36	0.33	2.57	0.17	0.61
NA2O	3.71	3.88	3.71	3.72	2.76	4.24	3.54
K2O	4.77	4.53	4.57	4.50	5.06	4.68	5.84
TIO2	0.05	0.05	0.05	0.05	0.11	0.12	0.05
MNO	0.01	0.02	0.01	0.02	0.11	0.06	0.03
LOI	0.20	0.10	0.08	0.10	0.77	0.06	0.14
TOTAL	100.04	100.57	99.25	98.93	101.82	100.39	100.83
ZR	126	106	125	113	628	767	112
SR	23	10	17	17	19	6	20
RB	354	357	360	335	193	187	379
ZN	211	186	268	434	40	105	119
CU	27	45	60	60	40	31	49
BA	66	44	62	75	475	446	67
U	0	0	0	0	0	0	0
MO	20	21	25	33	21	27	46
NB	27	23	25	36	41	34	32
BI	0	0	0	0	0	0	0
PB	113	93	117	216	28	37	129
NI	37	38	39	60	9	10	49
Y	28	24	28	31	124	126	43
CR	17	28	26	37	3	9	45
TI	639	580	638	622	972	1097	474
S	4560	2580	2880	7220	4610	1060	2250
Q	36.74	36.70	37.48	37.66	37.45	33.99	31.50
OR	27.93	26.55	26.92	26.72	30.44	28.03	34.66
AB	31.82	33.37	32.07	32.41	23.77	36.53	30.28
AN	1.48	1.64	1.65	1.51	3.76	0.43	2.44
COR	0.93	0.62	0.75	0.58	0.0	0.52	0.64
MG SI	0.94	0.95	0.99	0.96	0.0	0.07	0.32
FE SI	0.02	0.04	0.02	0.04	0.0	0.15	0.03
SPH	0.12	0.12	0.13	0.13	0.27	0.30	0.12
DI	0.0	0.0	0.0	0.0	1.33	0.0	0.0
WO	0.0	0.0	0.0	0.0	2.98	0.0	0.0
ACT	0.0	0.0	0.0	0.0	0.0	0.0	0.0
RIEB	0.0	0.0	0.0	0.0	0.0	0.0	0.0

JW-WH211 WYLIE HILL SHOWING:ELX69-2-120-135;MG.PALE PK.ALASKITE GRANITE;PY+MOS2
JW-WH212 WYLIE HILL SHOWING:ELX69-2-135-150;MG.PALE PK.ALASKITE GRANITE;PY+MOS2
JW-WH213 WYLIE HILL SHOWING:ELX69-2-150-165;MG.PALE PK.ALASKITE GRANITE;PY+MOS2
JW-WH214 WYLIE HILL SHOWING:ELX69-2-165-182;MG.PALE PK.ALASKITE GRANITE;PY+MOS2
W69-1165 WYLIE HILL SHOWING:NLX69-11-65: GREY.FLOW BANDED.RHYOLITE
W6911441 WYLIE HILL SHOWING:NLX69-11-441:GREY.FLOW BANDED.RHYOLITE
JW-WH215 WYLIE HILL SHOWING.NLX69-11-440-450.GRANOPHYRIC.PK.GRANITE.MINOR PY&MO

WYLIE HILL SHOWING

SAMPLE	69-11216	69-11217	69-11218	69-11219	69-11220	69-11560	69-12222
SIO2	77.20	76.44	75.78	75.80	79.00	76.00	75.25
AL2O3	12.28	12.26	11.99	12.03	10.25	12.61	11.60
FE2O3	1.69	1.71	1.69	2.32	2.21	1.04	3.70
MGO	0.26	0.33	0.32	0.34	0.38	0.21	0.25
CAO	0.57	0.33	0.33	0.48	0.62	1.43	0.19
NA2O	4.04	3.38	3.30	3.42	2.38	3.50	3.57
K2O	5.68	5.00	4.80	4.82	4.08	4.80	4.68
TIO2	0.05	0.05	0.05	0.05	0.05	0.18	0.05
MNO	0.02	0.04	0.03	0.04	0.05	0.05	0.02
LOI	0.0	0.0	0.10	0.14	0.50	0.34	1.23
TOTAL	101.79	99.54	98.39	99.44	99.52	100.16	100.54
ZR	203	148	150	160	135	167	665
SR	19	38	34	42	38	111	8
RB	327	363	348	333	315	350	216
ZN	143	196	78	113	43	20	239
CU	49	59	50	69	48	50	138
BA	77	113	103	118	127	326	420
U	0	0	0	0	0	7	0
MO	169	74	40	31	36	36	37
NB	25	31	31	27	27	24	27
BI	0	0	0	0	0	29	0
PB	120	178	132	129	95	33	57
NI	46	35	39	63	54	5	45
Y	34	39	37	39	40	30	112
CR	31	24	22	40	39	21	88
TI	607	994	992	1061	961	1198	1074
S	2000	2260	1510	2140	1580	3420	2780
Q	29.74	37.78	38.85	37.59	49.81	34.84	37.85
OR	32.89	29.36	28.55	28.50	23.93	28.72	28.29
AB	30.90	29.22	28.90	29.83	20.79	29.99	31.58
AN	0.0	1.49	1.51	2.27	3.00	4.58	0.80
COR	0.0	0.77	0.86	0.39	0.88	0.0	0.40
MG BI	0.0	1.16	1.14	1.21	1.35	0.0	0.90
FE BI	0.0	0.09	0.07	0.09	0.12	0.0	0.04
SPH	0.12	0.13	0.13	0.13	0.13	0.45	0.13
DI	1.37	0.0	0.0	0.0	0.0	1.29	0.0
WO	0.35	0.0	0.0	0.0	0.0	0.13	0.0
ACT	0.0	0.0	0.0	0.0	0.0	0.0	0.0
RIEB	4.60	0.0	0.0	0.0	0.0	0.0	0.0

JW-WH216 WYLIE HILL SHOWING.NLX69- 11-450-460,FG,PK&WT.GRANITE
JW-WH217 WYLIE HILL SHOWING:NLX69-11-460-470,FG,PORP(Q+F),PK,GRANITE,MINOR PY+MO
JW-WH218 WYLIE HILL SHOWING:NLX69-11-470-480,FG,PORP(Q+F),PK,GRANITE,MINOR PY+MO
JW-WH219 WYLIE HILL SHOWING:NLX69-11-480-490,FG,PORP(Q+F),PK,GRANITE,MINOR PY+MO
JW-WH220 WYLIE HILL SHOWING:NLX69-11-490-500,FG,PORP(Q+F),PK,GRANITE,MINOR PY+MO
W6911560 WYLIE HILL SHOWING:NLX69-11-560:CG,PORP(Q-F),GREY TO PK,GRANITE:>>PY+MO
JW-WH222 WYLIE HILL SHOWING,NLX69-12-135-140,GREY-BLUE,FLOW BANDED,RHYOLITE

WYLIE HILL SHOWING

SAMPLE	69-12226	69-12228	69-12230	69-12240	69-12242	69-14245	69-14249
SIO2	76.75	77.94	76.65	78.13	78.67	78.49	77.62
AL2O3	11.45	11.52	11.63	11.46	11.22	11.62	11.22
FE2O3	1.34	1.17	1.53	1.39	1.29	2.27	1.13
MGO	0.30	0.31	0.39	0.31	0.31	0.25	0.31
CAO	0.33	0.33	0.55	0.50	0.54	0.20	0.48
NA2O	2.74	2.77	2.87	3.00	2.70	2.82	2.15
K2O	5.09	5.16	5.16	4.83	5.14	5.39	5.48
TIO2	0.05	0.05	0.05	0.05	0.05	0.10	0.05
MNO	0.02	0.02	0.02	0.02	0.03	0.04	0.02
LOI	0.67	0.63	1.10	0.69	1.10	0.37	0.72
TOTAL	98.74	99.90	99.95	100.38	101.05	101.55	99.18
ZR	154	147	141	149	146	129	154
SR	19	17	17	18	26	16	23
RB	385	389	373	369	394	363	432
ZN	211	169	242	219	274	43	99
CU	42	34	16	21	18	21	13
BA	81	84	83	86	104	74	87
U	0	0	0	0	0	0	0
MO	219	288	305	186	561	163	1131
NB	32	30	30	25	35	28	34
BI	0	0	0	0	0	0	0
PH	187	113	163	89	162	58	172
NI	28	26	113	8	0	6	11
Y	46	36	42	38	45	39	51
CR	61	55	18	62	72	55	53
TI	911	845	827	718	832	666	722
S	11260	10420	14240	8480	12910	2450	5910
Q	42.01	42.19	40.12	41.85	42.72	41.54	44.31
OR	30.35	30.32	30.37	28.28	30.02	31.56	32.50
AB	23.96	23.88	24.94	25.81	23.15	24.12	18.68
AN	1.51	1.49	2.62	2.35	2.54	0.65	2.27
COR	0.93	0.86	0.40	0.46	0.30	0.92	0.97
MG BI	1.07	1.09	1.38	1.09	1.08	0.87	1.10
FE BI	0.04	0.04	0.05	0.04	0.06	0.09	0.04
SPH	0.13	0.13	0.13	0.12	0.12	0.25	0.13
DI	0.0	0.0	0.0	0.0	0.0	0.0	0.0
WO	0.0	0.0	0.0	0.0	0.0	0.0	0.0
ACT	0.0	0.0	0.0	0.0	0.0	0.0	0.0
RIEB	0.0	0.0	0.0	0.0	0.0	0.0	0.0

JW-WH226 WYLIE HILL SHOWING.NLX69-12-170-180.MG.RED&GREY.GRANITE.DISS PY&MOS2
JW-WH228 WYLIE HILL SHOWING.NLX69-12-190-200.MG.RED&GREY.GRANITE.DISS PY&MOS2
JW-WH230 WYLIE HILL SHOWING.NLX69-12-210-220.MG.RED&GREY.GRANITE.DISS PY&MOS2
JW-WH240 WYLIE HILL SHOWING:NLX69-
JW-WH242 WYLIE HILL SHOWING:NLX69-
JW-WH245 WYLIE HILL SHOWING.NLX69-14-131-145.FG.APLITE.DISS PY&MOS2&MUSC&MAG
JW-WH249 WYLIE HILL SHOWING.NLX69-14-187-194.FG.APLITE.DISS PY&MOS2&MUSC&MAG

WYLIE HILL SHOWING

SAMPLE	69-14250	69-14251
SIO2	78.06	77.88
AL2O3	11.65	11.70
FE2O3	0.99	0.91
MGO	0.15	0.17
CAO	0.47	0.80
NA2O	2.69	2.88
K2O	4.77	4.98
TIO2	0.05	0.05
MNO	0.02	0.02
LOI	0.94	0.96
TOTAL	99.79	100.35
ZR	152	152
SR	22	20
RB	374	374
ZN	100	300
CU	14	13
BA	84	90
U	0	0
MO	308	217
NB	32	28
BI	0	0
PB	88	128
NI	9	7
Y	36	38
CR	55	41
TI	818	803
S	14550	15010
Q	44.12	41.00
OR	28.42	29.46
AB	23.25	24.74
AN	2.20	3.85
COR	1.30	0.18
MG BI	0.53	0.60
FE BI	0.04	0.04
SPH	0.13	0.12
DI	0.0	0.0
WO	0.0	0.0
ACT	0.0	0.0
RIEB	0.0	0.0

JW-WH250 WYLIE HILL SHOWING:NLX69-14-194-205:MG.GREY TO PK GRANITE:PY+MOS2
JW-WH251 WYLIE HILL SHOWING.NLX69-14-205-220,MG.GREY TO PK.GRANITE.DISS PY&MOS2

DYKE ROCKS

SAMPLE	JW75- RP	JW75- 2	JW75- 59	JW75-114	JW75-116	JW75-166	JW75-172
SIO2	77.06	77.82	77.50	74.91	78.27	76.33	75.39
AL2O3	12.00	11.35	11.09	12.01	12.45	11.81	11.93
FE2O3	1.39	1.36	1.40	1.23	1.01	1.15	1.41
MGO	0.07	0.03	0.0	0.03	0.09	0.04	0.03
CAO	0.47	0.14	0.05	0.10	0.11	0.31	0.10
NA2O	5.17	1.41	3.49	2.17	0.24	3.04	3.72
K2O	5.14	6.02	4.38	6.06	6.28	5.14	6.96
TIO2	0.05	0.15	0.14	0.12	0.03	0.13	0.12
MNO	0.02	0.05	0.03	0.03	0.03	0.04	0.05
LOI	0.53	1.04	0.38	1.26	1.33	0.70	1.17
TOTAL	101.90	99.37	98.46	98.02	99.84	98.69	100.88
ZR	247	381	327	193	200	232	217
SR	14	14	8	36	37	27	53
RB	271	303	217	454	678	356	644
BA	42	88	114	84	28	26	139
CU	27	7	8	1	0	1	3
PB	37	41	43	67	53	75	88
U	8	3	6	7	7	7	10
MO	23	18	27	8	15	20	16
NB	42	55	55	50	54	54	81
BI	14	15	19	18	17	21	20
PB	52	71	45	72	50	12	44
NI	8	12	10	15	17	11	24
S	103	130	138	118	105	119	223
CR	8	8	9	2	11	12	18
TI	812	730	537	681	555	702	426
P	320	180	240	160	190	280	4420
Q	22.48	47.85	41.83	40.84	53.97	39.66	23.76
OR	28.14	36.68	26.74	37.42	37.81	31.22	39.21
AB	30.87	12.31	30.55	19.24	2.08	26.57	21.56
AN	0.0	0.18	0.0	0.08	0.45	1.12	0.0
COR	0.0	2.53	0.72	1.94	5.23	0.88	0.0
MG SI	0.0	0.11	0.0	0.11	0.32	0.14	0.01
FE SI	0.0	0.12	0.07	0.08	0.07	0.10	0.0
SPH	0.11	0.38	0.36	0.31	0.08	0.33	0.28
DI	0.35	0.0	0.0	0.0	0.0	0.0	0.0
NO	0.46	0.0	0.0	0.0	0.0	0.0	0.0
ACT	0.0	0.0	0.0	0.0	0.0	0.0	0.11
RIEB	17.50	0.0	0.0	0.0	0.0	0.0	15.00

JW-WH-RP WYLIE HILL SHOWING:DK BROWN Q-PK FELDSPAR PORPHYRY DYKE ROCK
JW75 2 DYKE CUTTING BELLE BAY VOL:MED RED,QUARTZ-FELDSPAR PORPHYRY
JW75 59 DYKE CUTTING BELLE BAY VOL:MED BROWN,QUARTZ-FELDSPAR PORPHYRY
JW75 114 DYKE CUTTING ACKLEY FG GRANITE AT CROWS CLIFF:MED RED,QUARTZ PORPHYRY
JW75 116 DYKE CUTTING ACKLEY FG GRANITE AT CROWS CLIFF:PK TO GREEN,FG,Q-PORPHYRY
JW75 166 DYKE CUTTING BELLE BAY VOL: FG,MED RED,QUARTZ-FELDSPAR PORPHYRY
JW751726 DYKE CUTTING BELLE BAY VOL: DK RED BROWN,QUARTZ PORPHYRY